ADDIS ABABA UNIVERSITY

ADDIS ABABA INSTITUTE OF TECHNOLOGY

SCHOOL OF ELECTRICAL AND COMPUTER ENGINEERING

POTENTIAL AND FEASIBILITY STUDY OF STANDALONE SOLAR PV/WIND/BIOGAS & BIODIESEL HYBRID ELECTRIC SUPPLY SYSTEM WITH ENERGY SAVING MECHANISMS

(Case study: Jama Woreda)

A thesis Submitted to the School of Graduate Studies of

Addis Ababa Institute of Technology

In Partial Fulfillment of the Requirement for the Degree of Master of

Science in Electrical Power Engineering

By Demsew Mitiku

Advisor: Getachew Bekele (PhD)

August, 2014

ADDIS ABABA UNIVERSITY

ADDIS ABABA INSTITUTE OF TECHNOLOGY

SCHOOL OF ELECTRICAL AND COMPUTER ENGINEERING

POTENTIAL AND FEASIBILITY STUDY OF STANDALONE SOLAR PV/WIND/BIOGAS & BIODIESEL HYBRID ELECTRIC SUPPLY SYSTEM WITH ENERGY SAVING MECHANISMS

(Case study: Jama Woreda)

By Demsew Mitiku

APPROVED BY BOARD OF EXAMINERS

Chairman, School of Electrical and Computer Engineering	**Signature**
Dr. Getachew Bekele Advisor	**Signature**
Internal Examiner	**Signature**
External Examiner	**Signature**

DECLARATION

I, the undersigned, declare that this thesis is my original work, has not been presented for a degree in this or any other university, and all sources of materials used for the thesis have been acknowledged.

All examiners' comments are duly incorporated.

Demsew Mitiku

Signature: _____

Place: Addis Ababa

Date of submission: 8/12/2014

This thesis has been submitted for examination with my approval as a university advisor.

Dr. Getachew Bekele_____
Advisor's Name Signature

ACKNOWLEDGEMENT

First and foremost, I take this opportunity to give glory to the almighty God without which the completion of this work would have been impossible.

Next I would like to thank all the staffs at Addis Ababa institution of Technology involved throughout my postgraduate course and Debre Markos University for sponsoring my MSc program in the field of Electrical Power Engineering.

In particular, I would like to thank Dr. Getachew Bekele, my thesis advisor, for all his assistance, help, advice, and encouragement.

Further thanks go to Jama woreda rural development office and Kebele-8 administration office for providing helpful information to this thesis work. In particular, I would like to thank Mr. Wondye Melku, governor of Kebele-8; he provides all the required data that are relevant to my thesis work.

Finally, I would like to acknowledge the love and support given to me by my parents. Also, thanks to Mr. Sindew Nigussie and Mr. Sitotaw Gebeyehu for their assistance and being there by my side.

Lastly but certainly not the least important, I would like to thank all the people stood by my side.

Addis Ababa, August 2014

ABSTRACT

Improved stove technology and efficient collector design using KOLEKTOR 2.2 modeling tool together with hybrid electric power supply system increase the reliability, the renewable fraction and made the system more cost effective and attractive to electrify rural area.

This thesis investigates renewable energy resource potential study and feasibility analysis of biogas, solar PV, wind turbine and biodiesel for rural electrification. This is achieved through the uses of a model, HOMER, which simulates energy resources and electrical loads for a specific site, as well as various equipment configurations and financial data to create a cost-based ranking of different energy solutions based on net present cost of the system.

Under this study, the site used in the model is a rural Kebele in Jama Woreda at 10.548^{o} N, 39.33^{o} E and electrical primary loads for the community are estimated and forecasted for the project lifetime. Energy resources used in the model include Solar, Wind, Biomass, and Biodiesel. The resource potential of solar and wind resources are taken from various sources such as Meteonorm, NASA and SWERA but NASA is chosen for simulation. The common biogas feedstock considered under this study are animal slurry, human feces and jatropha byproducts where as the biodiesel is considered from jatropha seed.

Various PV, wind turbine, converter, battery, biogas and biodiesel generator, sizes and costs are considered and sensitive values, constraints, and system control mechanisms are selected to perform hybrid system optimization and sensitivity analysis. In addition to the cost of equipments, the hybrid system power distribution cost is also considered. Grid comparison against the hybrid system is analyzed to answer which alternative is economical.

Based on the resource, load, hybrid system size and component cost input data considered and running the simulation in HOMER gives optimization, sensitivity and grid comparison result. The optimization result of the simulation demonstrates that the top optimal hybrid system consists of solar PV, wind turbine, biogas generator, biodiesel generator, converter and battery under LF system control strategy. The initial capital cost for the best optimal hybrid system is $335,468, $303,199, $301,356 and $213,297, and the net present cost of the system is $837,915, $725,188, $703,213, $377,669 for Site-A, Site-B, Site-C and Site-D respectively. These costs give a levelized COE of $0.239, $0.237, $0.234 and $0.241 per kWh for Site-A, Site-B, Site-C and Site-D respectively. The model also includes a sensitivity analysis for 5 sensitivity input variables and 36 sensitivity cases. Based on the data obtained from universal electricity access program, the total capital cost of grid extension was estimated as $147,752, $104,724, $71,584, and $140,892 and the unit O&M cost in $/km/yr is 267; 349; 716 and 235 for Site-A, Site-B, Site-C and Site-D respectively.

Keywords*: Biogas digester, Break even distance, COE, Deferrable load, Green energy, Hybrid system, KOLEKTOR 2.2, Load forecast, Net present cost, Primary electrical load.*

Table of Contents

List of Figure

List of Table

ACRONYMS

AD	Anaerobic Digestion
BGD	Break even Grid extension Distance
COE	Cost of Energy
DM	Dry Matter
EPSS	Electric Power Supply System
FACT	Fuels from Agriculture in Communal Technology
FP	Flat Plate
GTP	Growth and Transformation Plan
HAWT	Horizontal Axis Wind Turbine
HES	Hybrid Energy Supply
HH	Household
HOMER	Hybrid Optimization Model for Electrical Renewable
HRT	Hydraulic Retention Time
KSG	Kisangani Smith Group
NREL	National Renewable Energy Laboratory
PDF	Probability Distribution Function
Ppm	Part Per Million
PPO	Pure Plant Oil
PV	Photo Voltaic
RE	Renewable Energy
RES	Renewable Energy Source
RET	Renewable Energy Technology
SPV	Solar Photo Voltaic
SWERA	Solar and Wind Resource Assessment
T_o	Temperature
TS	Total Solid
UEAP	Universal Electricity Acess Program
VAWT	Vertical Axis Wind Turbine
VFA	Volatile Fatty Acid
VITA	Volunteers In Technical Assistance
VS	Volatile Solid

CHAPTER 1

1. INTRODUCTION

1.1. Overview

Ethiopia is located in the eastern part of Africa between 3^o to 15^o north and 33^o to 48^o east with a surface area of 1.1 million square kilometers. It is the third largest country in Africa. It is the second most populous country in Sub Saharan Africa with an estimated population of about 82 million, which is mostly distributed in northern, central and southwestern highlands.

Ethiopian economy is predominantly based on agriculture which contributes the lion's share of about 50% to the GDP and over 80% of employment. The agriculture sector is the leading source of foreign exchange. Coffee distantly followed by hides and skins, oil seeds and recently cut-flower are the major agricultural export commodities. At present the per capita income in Ethiopia is less than USD 500 [1]. Access to electricity in Ethiopia is one of the lowest by any standard, with only 25% of households connected and 53% of electricity coverage of the country from Ethiopian Electric Power Corporation (EEPCo) in 2014 [2]. Despite the fact that 80% of the population of Ethiopia live in rural areas, electricity supply from the grid is almost entirely concentrated in urban areas. Among other things, dispersed demand and very low consumption level of electricity among rural consumers, limited grid electricity penetration to rural population is less than 4%. Based on the hitherto electricity expansion practices in the country, access to electricity does not seem to be the reality of the near future for the greater percentage of the rural population.

However, the recent government's strategy under Universal Electricity Access Program (UEAP) ambitiously increase access to electricity by connecting 5168 new towns and villages to the grid and the country managed to electrify 1700 rural towns and villages per annum. The UEAP does not only aim to increase access, but also aims to raise the level of national per capita consumption of electricity from 28 kWh in 2010 to 128 kWh by the year 2015. [2, 3]

Ethiopia, Under UEAP, follows two basic strategies in order to electrify rural area. These are:

- Grid based large and medium scale power generation and,
- Small scale renewable energy standalone/ mini-grid technology options.

70% of rural energy demand of Ethiopia is related to cooking and satisfied from fuel wood. In Ethiopia up to 7millions improved cooking stoves are distributed up to 2010 and only 16% of the rural households have access to improved/ fuel efficient cooking stoves. A total of 1,300 biogas plant for gas application and 112,500 solar technologies are installed all over rural part of Ethiopia [3]. To access a reliable, affordable, clean and sustainable energy service the government set a plan to set an energy mix power generation system.

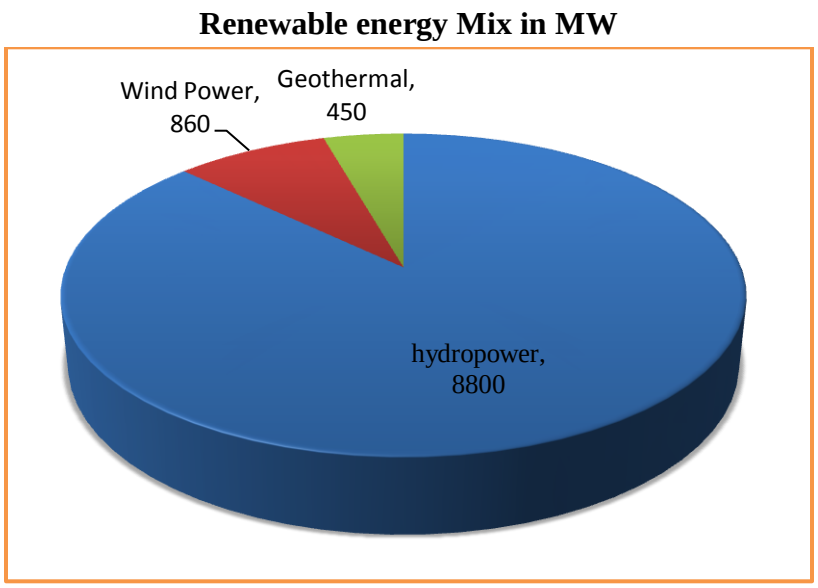

Figure 1-1: Ethiopia power generation plan from renewable energy in the year 2011-2015. [3]

The Government is aware of the fact that the national utility alone through continous grid extension cannot accelerate rural access to electricity. In the struggle to improve rural access to electricity, the government has recently streamlined its strategies and embarked upon removal of barriers and constraints to accelerated off-grid rural electrification. The Rural Electrification Strategy provides opportunities for an increasing participation of the private sector in the supply of electricity to un-electrified rural village. This has included the design of institutional and financing framework for private sector-led rural electrification, which is expected to remove barriers and facilitate private sector participation in the provision of off-grid electricity supply (generation, transmission, distribution and marketing).

1.2. Problem description and Motivation

It is known that the development of any country depends on the amount of energy consumed. Energy consumption is proportionally to the level of economic development. According to current figures only about 25% of the household is estimated to have electricity connection and the per capita energy consumption is still less than 100kWh, which is the lowest in the world and almost biomass [2, 3]. This had a direct impact on deforestation. For lighting systems, in rural areas, kerosene is used which produces emission of pollutants and have significant effect on health and economy. In spite of the huge hydroelectric potential of Ethiopia, severe power cuts in recent years have a heavy impact on the country's economy. Even it has a tremendous amount of hydro power potential, because of the high initial cost, it is able to harness no more than 5 % of its potential so far. Moreover the cyclic drought in the country was affected the hydrological situation and is causing shortage of power supply.

Urban communities of Ethiopia have yet to achieve reliable electricity services, but areas like under this study have not electricity access yet and even in the near future. The lack of

electricity supply has contributed to social issues such as poverty, poor health services, low education, and gender inequity. This thesis explores the ways of harnessing the promising sources of renewable energy in 11 clusters of the study area including biogas, wind and solar photovoltaic (PV) energies as a contribution to replace the existing biomass energy supply system. For each cluster, they have good solar and biogas resource potential and sufficient wind resource for small power generation help to develop a standalone solar PV/Wind/Biogas and Biodiesel power supply system for the community.

Hybrid energy standalone (Off-Grid) system is an excellent solution for electrification of remote rural areas where the grid extension is difficult and economically not viable. Such system incorporates a combination of one or several renewable energy sources such as solar photovoltaic and wind energy. So biogas, sun and wind energy can bring an important contribution to a sustainable and decentralize energy mix for Ethiopia. Hence the use of wind, biogas and photovoltaic systems are only worth to generate electricity for island net systems which cannot join the main grid. As of [EEPCO, 2013], the total transmission and distribution losses are around 23%. The total system losses comprise technical and nontechnical losses. Decentralized energy (Off-Grid) system also have big contribution to reduce energy losses comes to be associated with long transmission and distribution system.

1.3. Objectives of the Study

The primary objective of this study is to study the Potential and it's feasibility of Solar-PV/Wind/Biogas & Biodiesel standalone hybrid electric power supply system for Jama Woreda and to suggest energy conservation mechanisms to the community.

Specific Objectives

- Solar and wind resource assessment of Jama Woreda.
- Biogas and biodiesel feedstock Potential studies of four sites (Site-A, Site-B, Site-C and Site-D) in the districts.
- Community load estimation and load forecasting for all the sites.
- Grid extention comparison against the standalone hybrid system to all sites.
- Self contained FP-solar collector design.
- Assessment of cost effective and efficient cooking stoves.
- Feasibility studies of standalone hybrid system for all the sites.

1.4. Methodologies

Different methodologies have been applied to address each objective of this study. First the site should be identified, problems of the community is clearly stated, data required for the thesis work is collected through various data collection mechanisms and different literatures are surveyed to identify the way to do the work, to get data and to enhance academic knowledge and research skills. And following that the data collected from various sources are

analyzed using software tool and integrated to give solution for the problems and challenges raised at the start of the thesis work.

1.4.1. Site identification

The case study area is identified by directly visiting the site. But to get data's like solar and wind resources climate data, site map obtained from Google earth and Google Map is used.

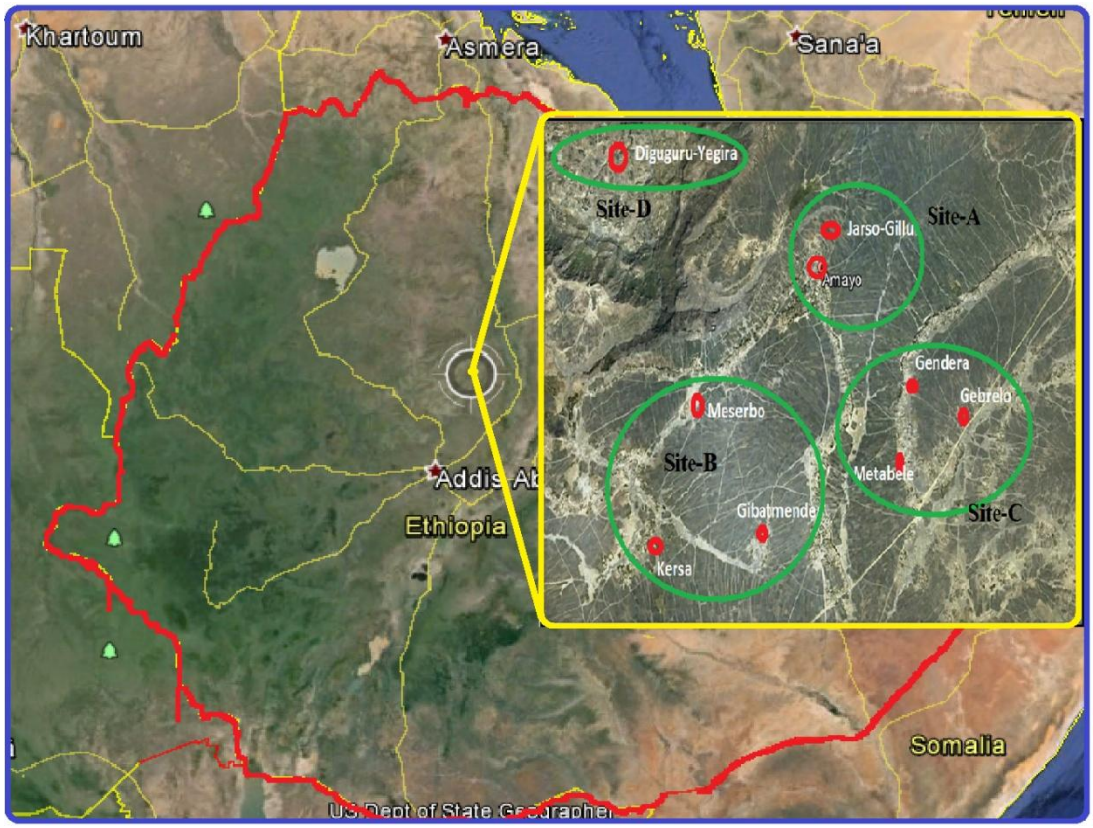

Figure 1-2: Map of study area [Site-A, Site-B, Site-C and Site-D]. ***(Source: Google Earth)***

The Study area:

- Is located at 10.548^{o} N latitude and 39.33^{o}E longitude
- Has a total of 5675 population(1135 families with 5-family member/HH)
- Has 11-cluster and is merged to four sites based on the distance between them to make hybrid system more economical, analysis & power supply simpler.
    - Site-A=390family
    - Site-B=332family
    - Site-C=313 family and
    - Site-D=100family

1.4.2. Problem Identifications

The problem identification involved a literature survey and direct observation in collecting general information about Jama woreda, Kebele-8 community, such as geography, climate, population, current energy supply sources, current energy utilization mechanism, effects of the current energy supply mechanism, and effects of traditional energy utilization mechanism. The main focus of the survey was on the renewable energy sources availability, the effect of the current biomass based energy supply on women health and the effect of fully dependent biomass based energy supply on the environment.

1.4.3. Data Collection and Literature Survey

The potential of animal livestock for biogas feedstock production, the potential of solar resource, wind resource, biodiesel feedstock data, and costs of various components of the hybrid systems are collected from surveying of various literatures and collection of primary data directly from agencies was done.

1.4.4. Data Analysis and Feasibility Study

HOMER, micro power optimization software is a computer model that was developed by NREL in the U.S.A and used for analysis and feasibility studies of the hybrid system. One of the major applications of HOMER is the design of micro power systems for the efficient evaluation of various RE power generation technologies. It compares a wide range of equipment with different constraints and sensitivities to optimize the system design. In the early phases of planning and decision making in rural electrification projects, HOMER can be of significant use for the designing of the system due to its flexibility.

The designer can input various data and compare different designs based on their technical and economic factors. HOMER also considers the effects of uncertainty in its modelling. It allows modelling of grid-connected or off-grid systems, generating electricity and heat from various combinations of SPV Modules, Wind turbines, Biomass based power generation, micro-turbines, fuel cells, batteries, hydrogen storage, and generators with various fuel options. Designing a micro power system with various design options and uncertainty issues in demand loads and fuel prices makes it a challenge. HOMER was designed to overcome these challenges and also the complexity of the RES being intermittent, seasonal, non-dispatchable and having uncertain availability.

Simulation, Optimization and Sensitivity analysis are the three major actions run by HOMER. In the simulation process, different micro power system configurations for every hour of the year are generated with their technical feasibility and NPC. In the optimization process, HOMER selects one system configuration out of all configurations generated in the simulation process that satisfies all technical constraints and has the lowest NPC. In the sensitivity analysis, multiple optimizations are performed on the selected configurations by

Homer with a range of uncertain input parameters that is assumed to affect the model inputs with time. For the different variables known to the system designer- that is, the mix of system components and their respective quantity and size - the optimization process allows to calculate the optimal value. There are, however, also unknown factors such as uncertainties or changes in the variables outside the designer's control (for example, rises in the fuel price or the average wind speed). The effects of these can be analyzed with the help of the sensitivity analysis.

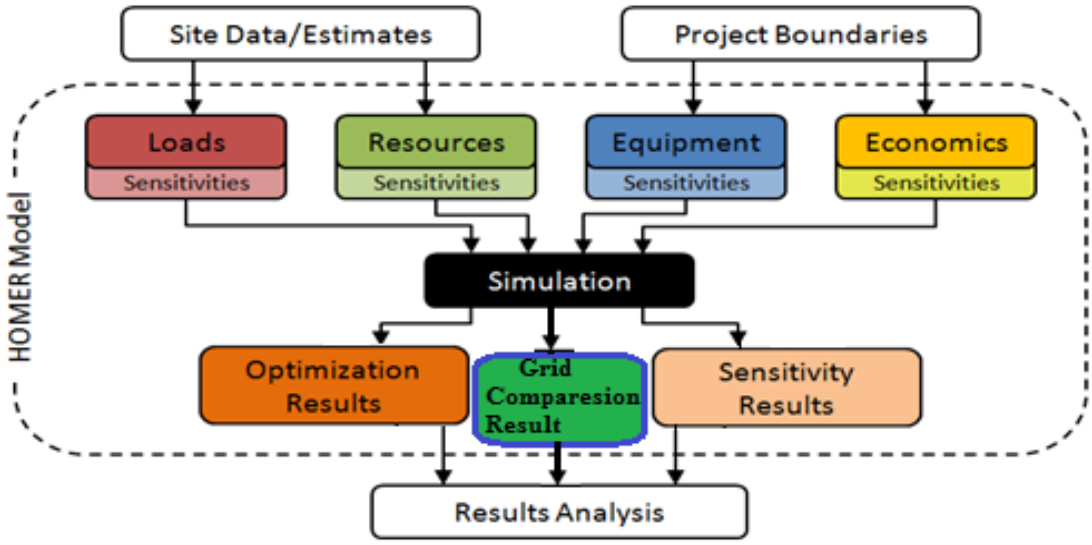

Figure 1-3: Schematics of data feeding and analysis in HOMER. [4]

1.5. Related Works

To get a better insight about the different energy sources, Solar, Wind, Biogas and Biodiesel energy potentials of Ethiopia, hybrid power generation system, and rural electrification, an elaborated literature study was essential. There have been several studies on off-grid electricity generation in Ethiopia and other developing countries among this few of them are discussed here. Different techniques and approaches have been used related to various scenarios and circumstance, including the evaluation of such as wind turbine, solar PV, biogas generator, DG's, fuel cells, BDG and various hybrids of them.

1.5.1. Reviews on related work on RETs, rural electrification and hybrid concepts

Celik, A.N. [5] conducted a techno-economic analysis based on solar and wind biased months for autonomous hybrid PV/wind energy system. He has observed that any optimum combination of the hybrid PV/wind energy system provides higher system performance than either of the single systems for the same system cost for every battery storage capacity. The author has also observed that the magnitude of the battery storage capacity has important bearing on the system performance of single photovoltaic and wind systems.

Timur Gul [6] studied on an integrated analysis of hybrid system for rural electrification in developing countries and he identifies various technologies for rural energy supply and analysis those technology from sustainability, ecological dimension and socio-economic perspectives was done. The result of his study demonstrates RET based hybrid system is more preferable than conventional energy system or a hybrid system contain conventional energy supply.

A thesis by Rohit Sen [7] on off-Grid electricity generation with renewable energy technology; with the help of HOMER simulations, the optimized sizing of Small-Hydro power (SHP), wind turbine generator, solar photovoltaic's (SPV) and Biodiesel Generator (BDG) systems is obtained. On the basis of minimized cost of energy (COE) generation obtained, HOMER then calculates the Economical Distance Limit (EDL), that is the relation between a RET system's lifecycle cost (LCC) and the cost of an extension from the existing grid allowing to determine the distance where the use of the former method is more cost-effective. The solution obtained shows that the use of decentralized RET systems at an Off-grid location is the best alternative to grid extension. HOMER results show that the solution is sustainable and techno-economically viable and environmentally sound.

1.5.2. Reviews on related work on solar and wind resource assessment

The SWERA solar resource data is the first kind of resource assessment conducted in Ethiopia. Solar resource assessment studies were also made by CESEN-ANSALDO group in the 1980s. Comparisons of the solar resource made by SWERA, CESEN-ANSALDO and NASA indicate that the estimation of the resource by SWERA is less by more than 50% of that estimated by CESEN. Estimations of CESEN and NASA provide similar figures for the sites comparisons are made for. Based on the SWERA data, the mean annual average daily radiation for the country as a whole is 3.74 kWh/m^2/day. [8]

Drake F. and Mulugeta Y. [9] studied the solar and wind potential distribution of Ethiopia. Regression coefficients of the angstrom equation (*a* and *b*) relating sunshine duration to daily solar radiation and Weibull parameters (shape factor, K, and the scale factor, c) are estimated throughout the country.

Bekele G. [10] determined solar and wind potentials of selected locations in Ethiopia and studied feasibility of Wind/PV hybrid system to electrify 200 model families using HOMER for optimization and sensitivity analysis.

1.5.3. Reviews on Biogas System

A thesis by John Furtado [4] on biomass based hybrid energy system for rural electrification in Uganda demonstrates, using gasified biogas in hybrid with solar and wind energy resource it is possible to electrify rural community and telecom loads with, optimal cost, environmentally clean, efficient and reliable electric power supply.

Kanwardeep Singh [11] studied on solar/biogas hybrid power generation and shows that a more cost effective power supply system can be created near to the rural loads like, farmer community, school community, and food processing industry and west reach area where most of the biogas feedstocks are found. He also introduce that various biogas technologies applicable for hybrid system application.

1.6. Organization of the thesis

This thesis paper includes seven chapters and two appendices, which are organized as:

Chapter 1: Introduction, overviews the rationale for this study. It includes Problem description and Motivation, objectives of the studies, methodologies, related works and the structure of the thesis.

Chapter 2: Basic theory of solar, wind, biogas and biodiesel energy potential of Ethiopia, Which comprises Introduction, distribution of wind speed, wind power density distribution, turbine Siting, wind turbine type and blade aerodynamics, assessment of wind resource potential in Ethiopia and the study area, solar photovoltaic technology, PV cell performance characteristics, PV system installation, assessment of solar energy resource of Ethiopia and the study area-Jama, the biogas production process, factor determine methane productions, biogas plant, biogas plant technology, design of biogas plant, common biomass feedstock for biogas production, jatropha plant, biogas potential assessment of the study area from jatropha plant, biodiesel potential from jatropha, biogas energy potential of the study area from animal dung, biogas energy potential of the study area from human feces, total biogas potential of the study area, monthly variation of the biogas feedstock potential by districts.

Chapter 3: Energy conservation mechanisms, which comprises design of self contained FP solar collector and suggestion of efficient cooking stoves for the community.

Chapter 4: Hybrid system feasibility study and grid comparison using Homer comprises introduction, hybrid system setup, Hybrid system load assessment, load estimation, electric demand forecasting, hybrid system resource assessment, hybrid system component assessment, HOMER Sensitivity input, grid extension system, grid extension cost analysis.

Chapter 5: Simulation Results and Discussion comprises Introduction, optimization result, sensitivity results with different sensitivity input scenarios, and grid comparison result for all sites of the study area.

Chapter 6: Conclusion and Recommendation presents conclusions that have been derived from this study, followed by recommendations for further study and for practical implementation of a proposed option. This chapter concludes with a few brief final different data tables and graphs are presented in the appendices.

CHAPTER 2

2. BASIC THEORY OF WIND, SOLAR, BIOGAS AND BIODIESEL ENERGY POTENTIAL

2.1. Introduction

Driven by its fast developing economy and population increment, Ethiopia has put a significant effort to develop its huge energy resources, basically renewable energy resources, to address the energy demand of these socio-economic changes. Its installed capacity is expected to increase to 10GW from the current 2.2GW, at the end of the GTP period. 95% of this power is harvested from its hydro resources. Although much of the electric power is derived from hydro, there is a proven and technically exploitable solar and wind energy resource. Efforts are already underway to reach out the rural society (where there is no access to the grid) through off-grid energy technology solutions, which make use of the solar and wind energy resources, to address some of the energy demands created due to the income increase and the improvement of the living standard of the farmers. However, large scale deployment of these technologies for grid-based power generations is at the early stage of its development as viewed with respect to the available potential. [12]

The current global energy supply is highly dependent on fossil sources (crude oil, hard coal, natural gas). These are fossilized remains of dead plants and animals, which have been exposed to heat and pressure in the Earth's crust over millions of years. For this reason, fossil fuels are non-renewable resources which reserves are being depleted much faster than new ones are being formed. Unlike fossil fuels, biogas and biodiesel are permanently renewable, as they are produced on biomass, which is actually a living storage of solar energy through photosynthesis. Biogas and Biodiesel will not only improve the energy balance of a country but also make an important contribution to the preservation of the natural resources and to environmental protection.

2.2. Wind Potential in Ethiopia

2.2.1. Distribution of Wind Speed

In probability theory and statistics, the Weibull distribution is a continuous probability distribution. It is named after Waloddi Weibull who described it in detail in 1951 [13]. In most locations worldwide, the distribution of wind speeds keeps fairly close to a Weibull or (simplified) Rayleigh distribution of wind speeds. The k=2 form of the Weibull PDF, f(v) commonly known as the Rayleigh density function. If the probability density is known, alternatively, the mean wind speed can be determined from: [14]

$$V_{ave}=\int_0^\infty vf(v)dv \qquad (2.1)$$

The probability density function of the Weibull distribution is given by [15],

$$f(v) = \frac{k}{c}\left(\frac{v}{c}\right)^{k-1}\exp\left[-\left(\frac{v}{c}\right)^{k}\right] \quad (2.2)$$

Where: k>1, v≥0, c>0, k is the shape factor, v is the wind speed and c is the scale parameter.

The shape factor will normally range from 1 to 4. These typical values are known from experience and multiple observations of sites where wind speed measurements have been taken. These wind types are categorized as inland, coastal, and trade wind (off-shore) sites. Table 2.1 shows typical values for the shape factor [16].

Table 2-1: Typical Shape Factor Values [16]

Types of Winds	Shape factor (k)
Inland winds	1.5-2.5
Coastal winds	2.5-3.5
Trade winds & Island	3.0-4.0

If Weibull k is not known, use k = 2 for inland sites, use 3 for coastal sites, and use 4 for island sites and trade wind regimes.

If Eq. (2-1) is solved together with Eq. (2-2) making the substitution of β= (v/c)k for v, the following is obtained for the mean wind speed, [17]

$$Vave = C\,\Gamma\left(1+\frac{1}{k}\right) \quad (2.3)$$

$$\Gamma(x) = \int_0^{\infty} \beta^{x-1}\exp(-\beta)\,d\beta \quad (2.4)$$

For k=2, the following is obtained from Eq.2-3 and Eq.2-4

$$C = \frac{2}{\sqrt{\pi}}V_{ave} \quad (2.5)$$

V_{ave}=average wind speed at 10m height which is 3.1m/s and scale factor C=3.5m/s of the study area.

For this study a Weibull shape factor of 2 (k=2) is selected since the selected districts for inland sites were used to develop probability density function (PDF) hourly profile of the wind speeds for a hypothetical year. The wind probability distribution function, PDF of the study area is shown in Figure 2-1.

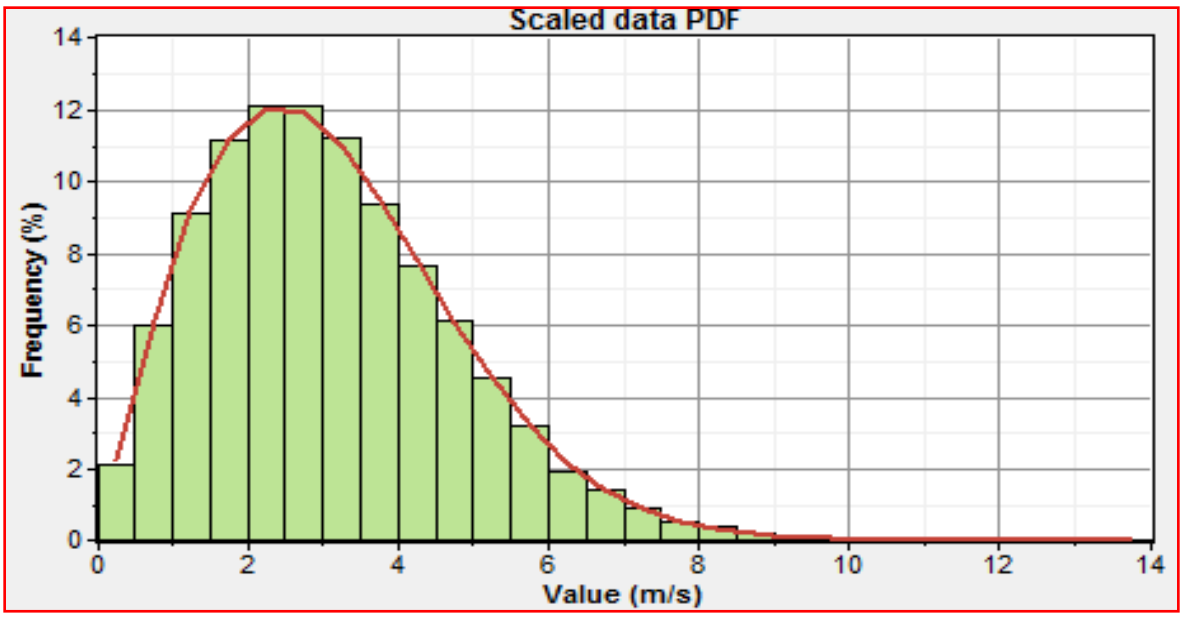

Figure 2-1: Probability density vs. wind speed at 10m for the study area

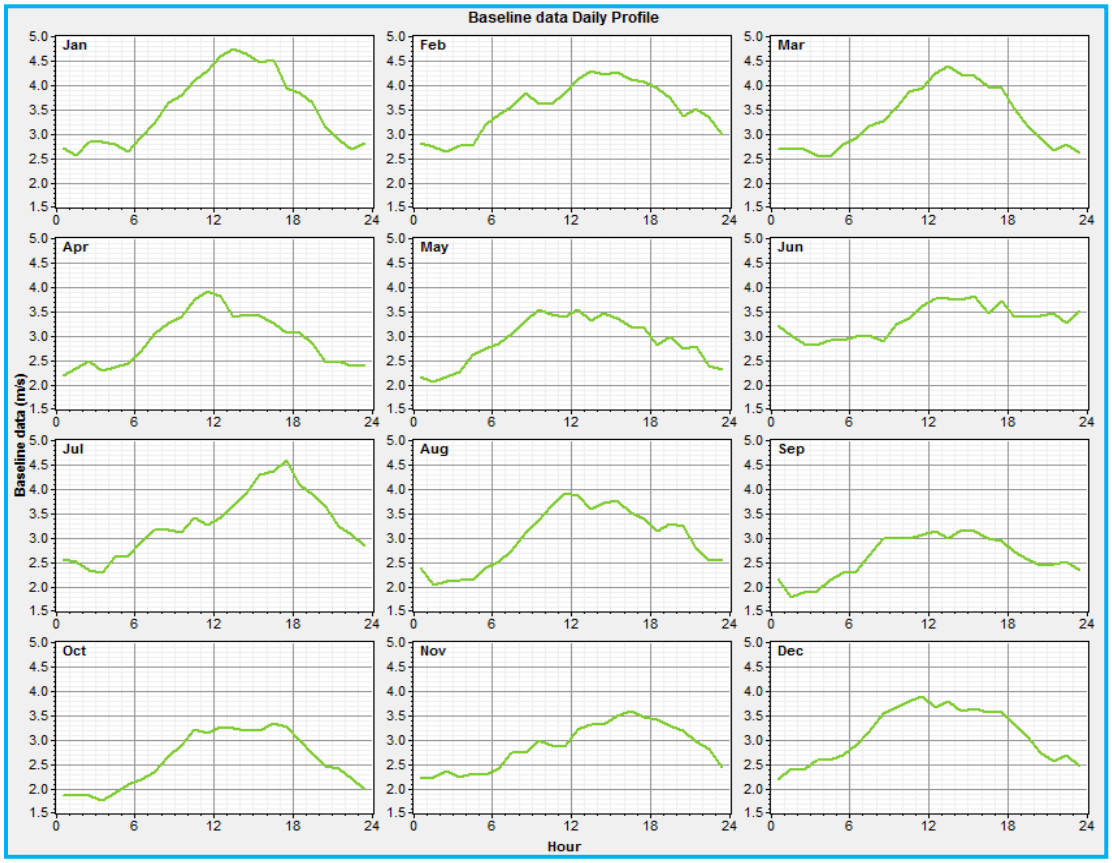

Figure 2-2: The annual hourly wind speed profile of the case study area.

The variation of wind speed with height can be expressed with Eq^{n} 2.6. [17]

$$v(z).ln\left(\frac{z_r}{z_o}\right) = v(z_r).ln\left(\frac{z}{z_o}\right) \quad (2.6)$$

Where,
Zr =Reference height (m)
Z =Height where wind speed is to be determined (m)
Z_0 =Measure of surface roughness
V(z) =Wind speed at height of Z m (m/s)
$V(z_r)$=Wind speed at the reference height (m/s)

For this work a power low coeffcient of 0.05 for crop land is suggested since the study area is more of crop land. With this coefficient, the average wind speed at 20m hub height is 3.5m/s.

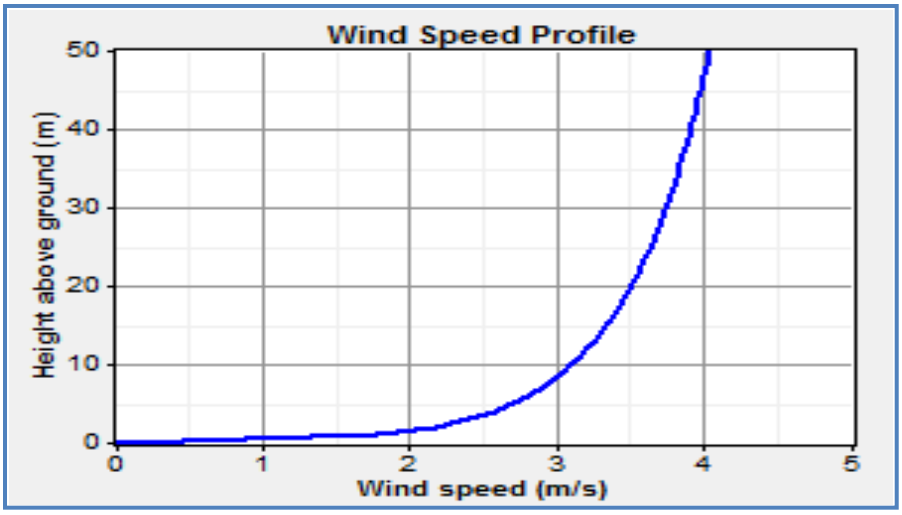

Figure 2-3: A typical wind speed profile of HY5-AD wind turbine [HOMER, Ver. 2.68 beta]

2.2.2. Wind Power Density Distribution

The power of the wind per unit area is given as:

$$P = \frac{1}{2}\rho V^3 \quad (2.7)$$

The monthly average wind speed using Weibull distributions is determined using Eq.2.3:
$Vave=C\,\Gamma(1+\frac{1}{k})$
The average power density for each month is calculated using actual probability density distribution for the specified month, which is calculated using Eq.2.8, and is given as:

$$P_{wm} = \sum_{i=1}^{n} \frac{1}{2}\rho Vmi^3 f(vi) \quad (2.8)$$

Where, the subscript m stands for the month and *n* is the number of records for the specified month.

The average power density using Weibull probability distribution is calculated as follows:

$$P_{wm} = \frac{1}{2}\rho\, C^3 \Gamma\,(1+\frac{3}{k}) \qquad (2.9)$$

For k=2,

$$C = \frac{2}{\sqrt{\pi}} V_{ave}$$

Γ is the gamma function and given as:

$$\Gamma(x) = \int_0^{\infty} \beta^{x-1} \exp(-\beta) d\beta$$

For k=2, $\Gamma(1+\frac{3}{2}) = \frac{3}{2} * \sqrt{\pi}/2 = \frac{3\sqrt{\pi}}{4}$

Finally power density for each month is calculated using Eq^{n} 2.10:

$$P_{wm} = \frac{1}{2}\rho\, C^3\, \frac{\mathbf{3\sqrt{\pi}}}{\mathbf{4}} \qquad (2.10)$$

From Eq^{n} 2.10, the wind power density values of the study area for each month is given in Table 2-2 below. The density of air varies with elevation but assuming that it is constant and taken as 1.225kg/m3.

Table 2-2: Wind Power density of the study area for all four sites

Month	Monthly average wind speed at 10m, m/s	Scale factor (C), m/s	Power density, W/m^2
January	3.510	3.96	50.60
February	3.530	3.98	51.33
March	3.300	3.72	42.00
April	2.920	3.30	29.26
May	2.900	3.27	28.47
June	3.310	3.74	42.60
July	3.290	3.71	41.60
August	2.990	3.37	31.20
September	2.600	2.93	20.50
October	2.580	2.92	20.30
November	2.860	3.23	27.44
December	3.1	3.5	34.91
Average	3.1	3.5	34.91

The power density values in Table 2-2 are calculated using Eq^{n} 2.5 and 2.10. It is clearly indicated that a figure inside Table 2.2, the power density for the case study area is not fairly constant and shows a large month to month variation. The minimum power densities occur in September and October, with 20.5 and 20.3W/m2, respectively. It is interesting to note that the highest power density values occur in January and February with the maximum value of

50.6 and 51.33 W/m2 respectively. The power densities in the remaining months are between these two groups of low and high values.

Estimation of wind power density is presented as wind class, ranging from 1 to 7. The speeds are average wind speeds over the course of a year, although the frequency distribution of wind speed can provide different power densities for the same average wind speed. See Table 2.3.

Referring Table 2-2 and 2-3, specified that the study area annual and monthly average wind speed and power density distribution are categorized in first wind class for all the sites but sufficient for a hybrid off grid electric power generation.

Table 2-3: Wind class categories by wind speed and power density

Wind class	At 10m(33ft) height		At 30m(98ft)		At 50m (164ft) height	
	Wind power density, W/m2	Wind speed, m/s	Wind power density, W/m2	Wind speed, m/s	Wind power density, W/m2	Wind Speed, m/s
1	0-100	0-4.4	0-160	0-5.1	0-200	0-5.6
2	100-150	4.4-5.1	160-240	5.1-5.9	200-300	5.6-6.4
3	150-200	5.1-5.6	240-320	5.9-6.5	300-400	6.4-7.0
4	200-250	5.6-6.0	320-400	6.5-7.0	400-500	7.0-7.5
5	250-300	6.0-6.4	400-480	7.0-7.4	500-600	7.5-8.0
6	300-400	6.4-7.0	480-640	7.4-8.2	600-800	8.0-8.8
7	400-1000	7.0-9.4	640-1600	8.2-11.0	800-2000	8.8-11.9

Sources: (United State DOE)

2.2.3. Turbine Siting

Finding a place for a wind turbine is one of the most challenging aspects of using wind energy. If located too close to homes, in addition to the uncomfortable noise it creates for surrounding families, the turbine suffers building interference. If it is too far away, then the cost of cables should not be overlooked [18].

With regard to the wind, nature itself is usually an excellent guide for finding a suitable wind turbine site. The inclination of trees and bushes reveals information about the prevailing wind of the region. However, the best guide is Meteorology data collected for more than 30 years and compiled in the form of wind rose diagrams. Nonetheless, such data are rarely available, especially in a country such as Ethiopia. It is under such circumstances that observing the surroundings gives significant clues about the wind regime of the area [19]. Furthermore, the site to be selected should be free of nearby obstacles (such as trees, small houses or other buildings). When selecting wind turbine sites, infrastructural facilities such as roads, should also be considered.

2.2.4. Wind Turbine Type and Blade Aerodynamics

A wind turbine is a machine that converts the kinetic energy from the wind into mechanical energy. If the mechanical energy is used directly by machinery, such as a pump or grinding stones, the machine is usually called a windmill. If the mechanical energy is then converted to electricity, the machine is called a wind generator [20].

There are a number of different wind turbine types available. The horizontal axis turbine, HAWT is the most common type of turbine. They come in two different types: the upwind, which face the wind (tower behind rotor) and the downwind arrangement that works away from the wind (tower in front of rotor). In HAWT, the rotor axis lies horizontally, parallel to the air flow. The blades sweep a circular (or slightly conical) plane normal to the air flow, situated upwind (in front of the tower) or downwind (behind the tower).The main advantage of HAWTs is the good aerodynamic efficiency (if blades are properly designed) and versatility of applications. Their main disadvantage is that the tower must support the rotor and all gearing and electrical generator standing on top of it, plus the necessity of yawing to face the wind.

Another kind of turbine is the vertical axis, VAWT arrangement that uses drag and lift as the driving forces; the horizontal also uses drag and lift, but in other proportions. In VAWT, the rotor axis is perpendicular to the air flow (usually vertical). The blades sweep a cylindrical, conical or elliptical plane, perpendicular to the air flow and parallel to the rotor axis. All main power train components (gearbox, generator, brakes and main bearing) are placed on the ground, allowing for easy access for maintenance and lower stress on the tower. Yaw mechanism for facing the wind is not needed as the turbine accepts wind from any direction. All these features result in a simple machine, easily scalable to large dimensions, at lower costs than a horizontal axis one. Their main disadvantage is their requirement of starting torque which may be a critical issue for stand-alone applications [21].

The modern wind turbine is a sophisticated piece of machinery with aerodynamically designed rotor and efficient power generation, transmission and regulation components. The size of these turbines ranges from a few Watts (Small Wind Turbines) to several Million Watts (Large Wind Turbines). The modern trend in the wind industry is to go for bigger units of several MW capacities in places where the wind is favorable, as the system scaling up can reduce the unit cost of wind-generated electricity. Most of today's commercial machines are horizontal axis wind turbines (HAWT) with three bladed rotors.

Wind turbine single-source systems tend to produce highly variable and therefore unreliable power supply due to the irregular wind speeds. If the wind turbine is combined with other sources of a hybrid system the produced energy can become more regular improving system performance and cost effectiveness.

The Figures below shows the various wind turbine types. (a) Upwind machine (b) down wind machines (c). Vertical axis wind turbines (VAWT) accept wind from any direction [22].

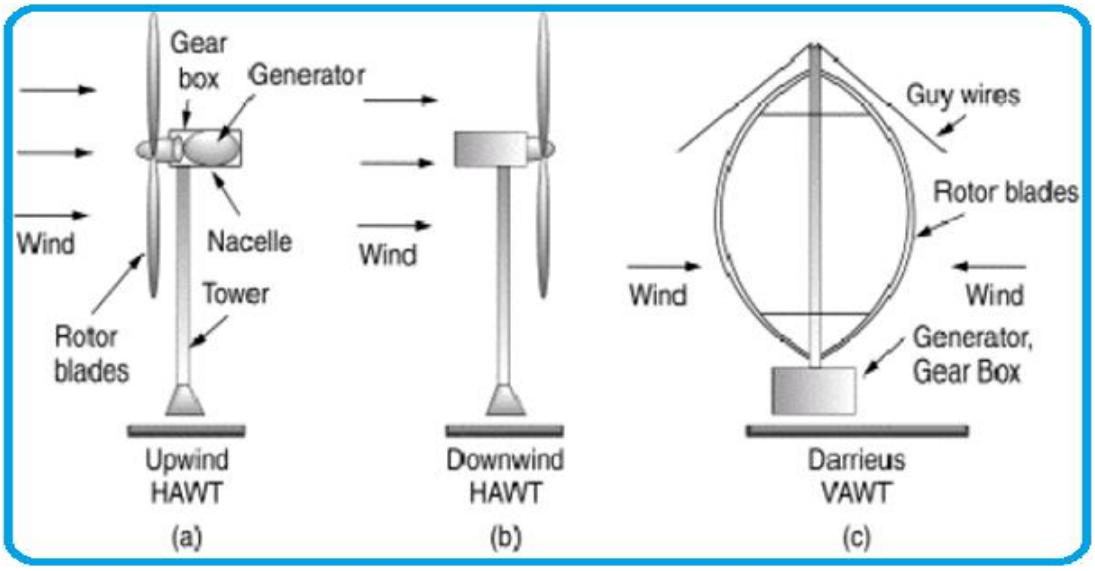

Figure 2-4: Wind turbine types and their configuration.

The turbine cross section below provides the components of a wind turbine.

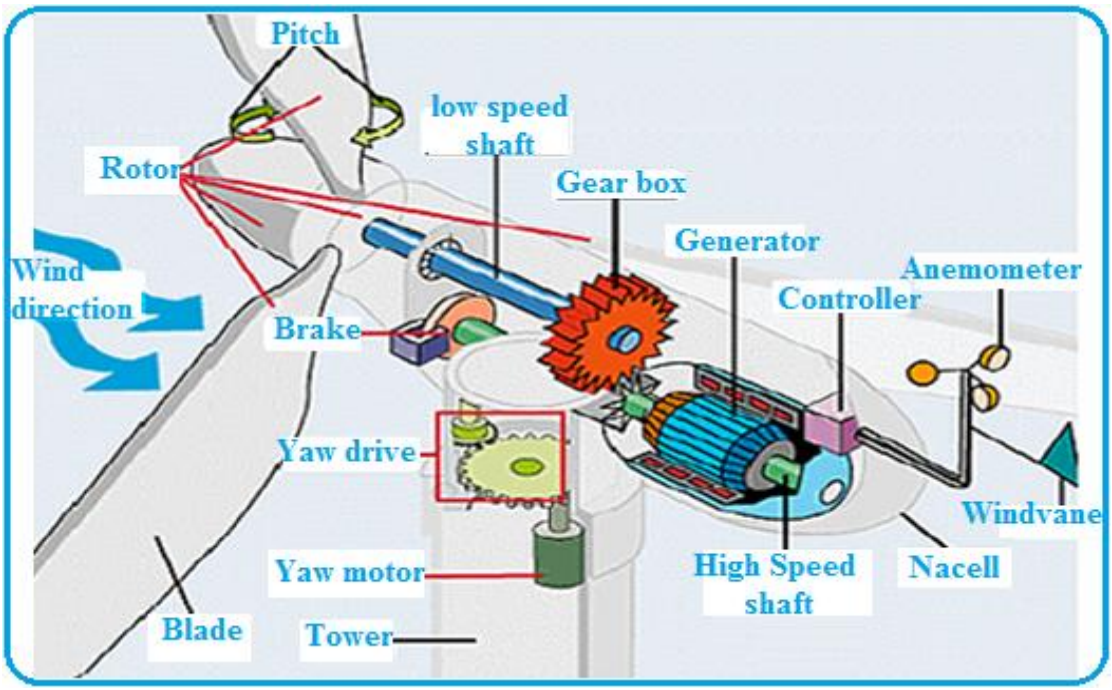

Figure 2-5: Cut-view of a wind turbine. [20]

Anemometer: Measures the wind speed and transmits wind speed data to the controller.

Blades: Most turbines have either two or three blades. Wind blowing over the blades causes the blades to "lift" and rotate.
Brake: A disc brake, which can be applied mechanically, electrically, or hydraulically to stop the rotor in emergencies.
Controller: The controller starts up the machine at a cut in wind speeds and shuts off the machine at about the turbine cutout wind speed. Turbines do not operate above the cutoff wind because they might be damaged by the high winds.
Gear box: Gears connect the low-speed shaft to the high-speed shaft and increase the rotational speeds from about 30 to 60 rotations per minute (rpm) to about 1000 to 1800 rpm, the rotational speed required by most generators to produce electricity. The gear box is a costly (and heavy) part of the wind turbine and engineers are exploring "direct-drive" generators that operate at lower rotational speeds and don't need gear boxes [20].
Generator: It usually an induction generator that produces 60/50-cycle AC electricity.
High-speed shaft: It drives the generator.
Low-speed shaft: The rotor turns the low-speed shaft at about 30 to 60 rotations per minute.
Nacelle: The nacelle sits at top of the tower and contains the gear box, low- and high-speed shafts, generator, controller, and brake. Some nacelles are large enough for a helicopter to land on.
Pitch: Blades are turned, or pitched, out of the wind to control the rotor speed and keep the rotor from turning in winds that are too high or too low to produce electricity.
Rotor: The blades and the hub together are called the rotor.
Tower: Towers are made from tubular steel, concrete, or steel lattice. Because wind speed increases with height, taller towers enable turbines to capture more energy and generate more electricity.
Wind vane: Measures wind direction and communicate with the yaw drive to orient the turbine properly with respect to the wind.
Yaw drive: Upwind turbines face into the wind; the yaw drive is used to keep the rotor facing into the wind as the wind direction changes. Downwind turbines don't require a yaw drive; the wind blows the rotor downwind [20].
Yaw motor: Powers the yaw drive.

2.2.5. Wind Turbine Generators

Wind turbine generators are a bit different from other generating units in that the input power to the generator shaft is taken from the wind turbine rotor which fluctuates greatly in terms of mechanical power (torque). The transmission system consists of the rotor shaft with bearings, brake(s), an optional gearbox, as well as a generator and optional clutches. There are two types of generator, synchronous and asynchronous. Synchronous generators are more expensive compared to asynchronous (induction) generators. Six-pole asynchronous generators are the most commonly used types. [10]

What has been discussed so far regarding wind turbine technology mainly applies to larger size wind turbines. The design principles of smaller wind turbines are somewhat different to the larger ones in that the distinctive purpose of small wind turbines is to produce power frequently over short periods, e.g. for battery charging. It is important that small turbines generate in weak winds and respond quickly when harnessable winds occur. The rapid starting of the rotor before the generator cuts in is a further requirement [23]. Small wind turbines often have direct drive generators (without a gearbox) and give out direct current. Their blades could be aero elastic types and usually use a vane to point into the wind.

2.2.6. Wind Turbines Efficiency and Power Curve

The theoretical limit of power extraction from wind was derived by the German aerodynamicist Albert Betz. Betz law, [20], states that 59.3% or less of the kinetic energy in the wind can be transformed to mechanical energy using a wind turbine. In practice, wind turbines rotors deliver much less than Betz limit. The factors that affect the efficiency of a turbine are the turbine rotor, transmission and the generator. Normally the turbine rotors have efficiencies between of 40% to 50%. Gearbox and generator efficiencies can be estimated to be around 80% to 90%. Also efficiency of a turbine is not constant. It varies with wind speeds. Many companies do not provide their wind turbine efficiencies. Instead they provide the power curve.

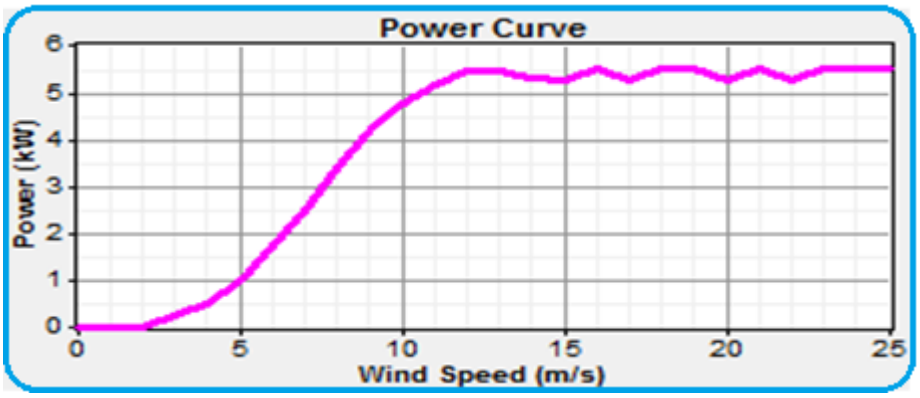

Figure 2-6: Power curve of HY5-AD5.6 wind turbine.

2.2.7. Wind power control mechanism

With regard to the power control system, the power regulation mechanisms must be implemented in such a way that power output is limited close to the rated value, as wind turbines have their highest efficiency at the wind speed they are designed for. There are three commonly used types of power control in the industry. [10]

- Stall Control
- Pitch Control
- Active stall regulation

Using stalling regulation, the aerodynamic design principle is to increase the angle at which the relative wind strikes the blades (angle of attack) and to reduce the induced lifting force at the moment the wind speed becomes too high. This happens because of turbulence created on the side of the rotor blade which is not facing the wind. Stall controlled wind turbines have their rotor blades bolted onto the hub at a fixed angle.
The Pitch control mechanism is usually hydraulically operated. An electronic controller, which depends on the output power, sends a signal to the blade pitch mechanism so as to turn the rotor blades out of the wind to the exact degree required and to keep the rotor blades at the optimum angle for maximized output at all wind speeds. In pitch control mechanism the rotor blades are rotated around their longitudinal axis. [10]

With an active stall regulation mechanism the machine is usually programmed to pitch the blades much like a pitch-controlled machine at low wind speeds, so as to get a reasonably large torque at low wind speeds. If the generator is about to be loaded, then the machine also pitches its blades to increase the angle of attack of the rotor blades forcing the blades to go into a deeper stall thus wasting the excess energy in the wind [19]. In this control mechanism the machine can be run almost exactly at rated power at all high wind speeds.

2.2.8. Assessment of Wind Resource Potential in Ethiopia

Various previous studies have given substantial results regarding the wind energy potential in Ethiopia [9] [24] by identifying the wind regimes in several areas. However, the data used in these studies is relatively old; the most recent data used in the first study is from 1968-1973 and was recorded only three times a day, at 6:00, 12:00, and 18:00. The remaining data used was also recorded three times a day at 8:00, 14:00 and 19:00 during the period 1937 – 1940. Data used in the second study was collected during the period 1979-1990 at 60 different locations across the country and recordings were made, according to the author, 4-7 times/day at a height of 2 m.

The previous studies reported Ethiopia has exploitable reserve of 10,000 MW wind energy with an average speed of 3.5 – 5.5 m/s, flowing for 6 hours/day. There are two basic zones with homogenous periodicity separated by the rift valley. In the first of these, covering most of the highland plateaus, there are two well-defined wind speed maximal occurring, respectively, between March and May and between September and November. In the second zone, covering most of the Ogaden and the eastern lowlands, average wind velocity reaches maximum values between May and August [9, 10, 25, 26, 27, 28, 29].

But a study by Hydro China Corporation in 2012 provides the country has exploitable reserve of 1.599TW wind energy. Under this study, the potential sites of wind resource are the northern highland plateaus, the rift valley region, the southern Ethiopia- Kenya border and most of the Somalia region. A maximal wind speed of 10-12m/s at 50m is found in Somalia region. [30]

2.2.9. Wind Potential Assessment in the Study Area

The two nearest metrological stations to the study area are Kombolcha (140km) and Addis Ababa (260km) North and South of it respectively. Taking data from those station leads to an error since the study area have different geographical layout and environmental condition as seen from both Kombolcha and Addis Ababa. So taking wind and solar data from secondary source is another alternative.
These data sources are from:

- NASA
- SWERA
- Meteonorm

Since the wind speed data in SWERA and NASA is the same and, Meteonorm (data base software) may consider nearby stations but its physical distance is much far from the above listed stations in order to interpolate the wind resource data, therefore, NASA is taken as a source of wind resource data for this study.

NASA has estimated the annual average wind speed of the location to be 3.1 m/s at 10 m height [31]. Generally, 10 m height is the one where most standard measurements are taken and measurements less than 10m height are error prone due to vegetation, shading and obstacles in the vicinity. This data can be extrapolated to the selected wind turbine height using Eq^{n} 2.6 [9, 26]. The value of Z_0 is taken as 0.05; Weibull parameters are estimated to be K=2 and c=3.5 m/s [32]. The following Table and Figure summarizes the wind speed at 10 m and 50m heights obtained from various sources.

Table 2-4: Wind potential comparation of the study area from three different sources.

Month	NASA (10m), m/s	Meteonorm(10m), m/s	SWERA(10m), m/s	% NASA Vs SWERA	% NASA Vs Meteonorm	% SWERA Vs Meteonorm
January	3.51	2.7	3.51	0	23%	23%
February	3.53	2.7	3.53	0	23.5%	23.5%
March	3.3	2.8	3.3	0	15.15%	15.15%
April	2.92	3.1	2.92	0	-6.2%	-6.2%
May	2.9	3.2	2.9	0	-10.3%	-10.3%
June	3.31	3.3	3.31	0	-0.3%	-0.3%
July	3.29	3.5	3.29	0	-6.4%	-6.4%
August	2.99	3.6	2.99	0	-20.4%	-20.4%
September	2.6	3.7	2.6	0	-42.3%	-42.3%
October	2.58	3.8	2.58	0	-47.3%	-47.3%
November	2.86	3.5	2.86	0	-22.4%	-22.4%
December	3.1	2.9	3.1	0	6.5%	6.5%
Average	3.1	3.23	3.1	0	-4.2%	-4.2%

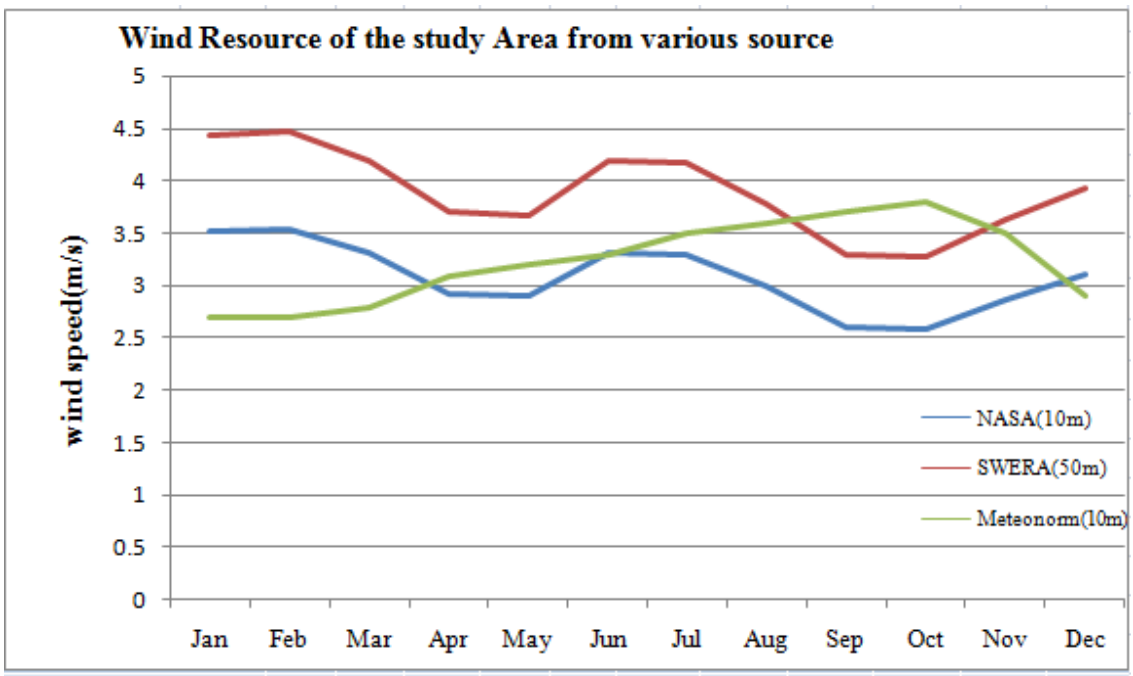

	Jan	Feb	Mar	Apr	May	Jun	Jul	Aug	Sep	Oct	Nov	Dec
NASA(10m)	3.51	3.53	3.3	2.92	2.9	3.31	3.29	2.99	2.6	2.58	2.86	3.1
SWERA(50m)	4.44	4.47	4.18	3.7	3.67	4.19	4.17	3.78	3.29	3.27	3.62	3.93
Meteonorm(10m)	2.7	2.7	2.8	3.1	3.2	3.3	3.5	3.6	3.7	3.8	3.5	2.9

Figure 2-7: Wind resource of the study area from various sources.

2.3. Solar Energy Potential in Ethiopia

2.3.1. Solar Photovoltaic Technology

Figure 2.8 shows the basic PV cell structure. Metallic contacts are provided on both sides of the junction to collect electrical current induced by the impinging photons. A thin conducting mesh of silver fibers on the top surface collects the current and lets the light through. The spacing of the conducting fibers in the mesh is a matter of compromise between maximizing the electrical conductance and minimizing the blockage of the light. Conducting-foil (solder) contact is provided over the bottom surface and on one edge of the top surface. In addition to the basic elements, several enhancement features are also included in the construction. For example, the front face of the cell has an antireflective coating to absorb as much light as possible by minimizing the reflection. The mechanical protection is provided by a cover glass applied with a transparent adhesive. PV cells are present either in single cell, in modules or in array form. This PV module consists of many PV cells wired in parallel to increase current and in series to produce a higher voltage. Use of 36 cell modules are the industry standard for large power production. Individual PV cells are typically only a few inches in diameter, but multiple cells can be connected to one another in modules, modules can be connected in arrays, and arrays can be connected in very large systems. See Figure 2.8 & 2.9.

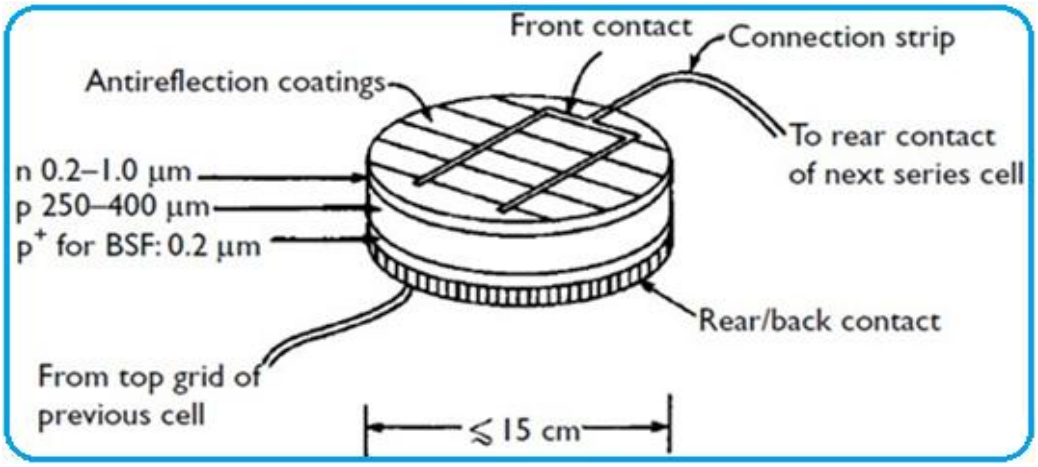

Figure 2-8: Basic structure of p-n junction PV cell [33] ***(BSF=back surface field)***

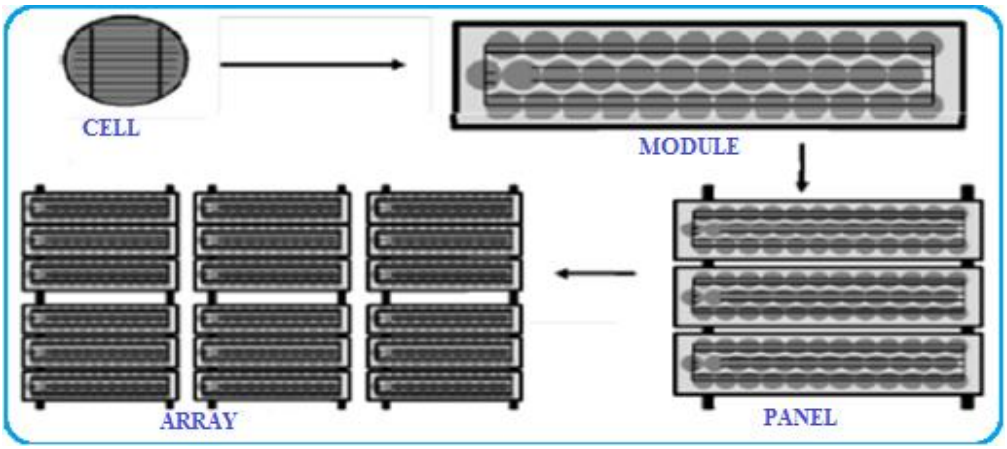

Figure 2-9: PV system diagram [20]

There are currently five commercial production technologies for PV cells:

1. **Single-Crystalline Silicon:** The basic material is mono-crystalline silicon. In order to make them, silicon is purified, melted, and crystallized into ingots. The ingots are sliced into thin wafers to make individual cells. It is the oldest and more expensive production technique, but it's also the most efficient and widely used sunlight conversion technology available. Cells efficiency oscillates between 14% and 18%. [34, 35]
2. **Polycrystalline or Multi-crystalline Silicon:** This particular cell is relatively large in size and it can be easily formed into square shape which virtually eliminates any inactive area between cells. It has a slightly lower conversion efficiency compared to single crystalline and manufacturing costs are also lower. Cells efficiency oscillates between 10% and 13%. [34, 35]
3. **String Ribbon:** This is a refinement of polycrystalline silicon production. There is less work in its production so costs are even lower. Cells efficiency averages 8% to 10%**.** [34, 35]

4. Technology which uses thin film solar cells while the total thickness of a semi conductor is about 1μm. Thin film silicon cells are solids in which the silicon atoms are much less ordered than in a crystalline form. By using multiple junctions this kind of photovoltaic cells achieve maximum efficiency which is estimated at about 13% while the installation cost is reduced. The efficiency of this cell oscillates 6% to 10%. [34, 35]
5. **Amorphous:** Made when silicon material is vaporized and deposited on glass or stainless steel. The cost is lower than any other method. Cells efficiency averages 4% to 7%, Cells efficiency decreases with increases in temperature. Crystalline cells are more sensitive to heat than thin films cells. The output of a crystalline cell decreases approximately 0.5% with every increase of one degree Celsius in cell temperature. For this reason modules should be kept as cool as possible, and in very hot condition amorphous silicon cells may be preferred because their output decreases by approximately 0.2% per degree Celsius increase. [34, 35]

The complex physics of the PV cell can be represented by the one diode equivalent electrical circuit shown in Figure 2.10 below.

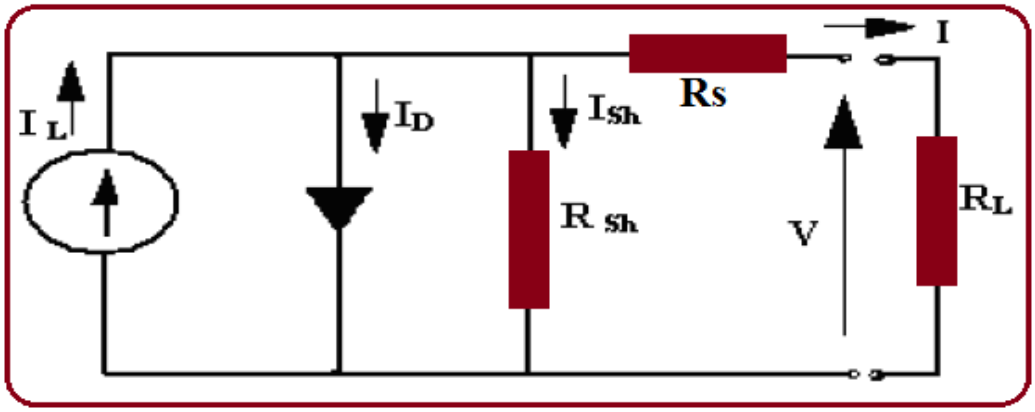

Figure 2-10: A PV cell equivalent electrical circuit [36]

The open-circuit voltage V_{oc} of the cell is obtained when the load current (I) is zero and is given by the following: [36]

$$V_{oc}=(I_L-I_D)R_{sh} \quad (2.11)$$

The diode current, I_D is given by the classical diode current expression: [36]

$$I_D=I_o\ [exp\left(\frac{q.Voc}{A.K.T}\right)-1] \quad (2.12)$$

Where I_o is the saturation current of the diode (A), q is electron charge (1.6×10^{-19} C), A is curve-fitting constant, K is Boltzmann constant (1.38×10^{-23} J/°K), T is temperature on absolute scale °K.

Thus, the load current is given by the expression: [32]

$$I=I_L-I_D-I_{sh}$$

$$I=I_L- I_o\,[exp\left(\frac{q.Voc}{A.K.T}\right)-1] - \frac{Voc}{Rsh} \quad (2.13)$$

The last term is the leakage current to the ground. In practical cells, it is negligible compared to I_L and I_o and is generally ignored.

The two most important figure of merits widely used for describing PV cell electrical performance are the open-circuit voltage V_{oc} and the short circuit current I_{sc} under full illumination. The short-circuit current is measured by shorting the output terminals and measuring the terminal current. Ignoring the small diode and ground leakage currents under zero voltage, the short-circuit current under this condition is the photocurrent I_L. The maximum photo voltage is produced under the open-circuit voltage. Again by ignoring the ground leakage current, Eq^{n}3.3 with *I=0, give* the open-circuit voltage as follows:

$$V_{oc} = \frac{A.K.T}{q}\ln(\frac{IL}{Io}+1) \quad (2.14)$$

2.3.2. PV Cell Performance Characteristics

The electrical performance characteristic of the PV cell is generally represented by the current vs. voltage (IV), power vs. voltage (PV), efficiency vs. irradiance (EI) and efficiency vs. temperature (ET) curve. The figure below depicts the electrical characteristics curve of a generic, poly crystal 60Wp PV module. Those curves show the variation of current, voltage, power and efficiency of the module when cell resistance, solar irradiance and cell temperature varies. In the I-V characteristics curve the point at which the voltage is zero is called the short-circuit current. This is the current we would measure with output terminal shorted. On the other hand the point at which current is zero is known as open-circuit voltage. This is the voltage we would measure with output terminal open. Somewhere in the middle of the two regions, the curve has a knee point. The power output of PV cell/module can be obtained from the PV cell/module current and terminal voltage from different operating condition of the module. The following equation is used to calculate the output of the PV array: [32]

$$P_{pv} = Y_{pv}.f_{pv}\,(\frac{\bar{G}_T}{\bar{G}_{T,STC}})[1+\alpha_p(T_C-T_{C,STC})] \quad (2.15)$$

Where:

Y_{pv} - is the rated capacity of the PV array, meaning its power output under standard test conditions [kW].

f_{pv} - is the PV derating factor [%]

$\bar{G}_T$ - is the solar radiation incident on the PV array in the current time step [kW/m^2]

α_p - is the temperature coefficient of power [%/°C]

$\bar{G}_{T,STC}$ - is the incident radiation at standard test conditions [1 kW/m^2]

T_c - is the PV cell temperature in the current time step [°C]
$T_{c, STC}$ - is the PV cell temperature under standard test conditions [25 °C].

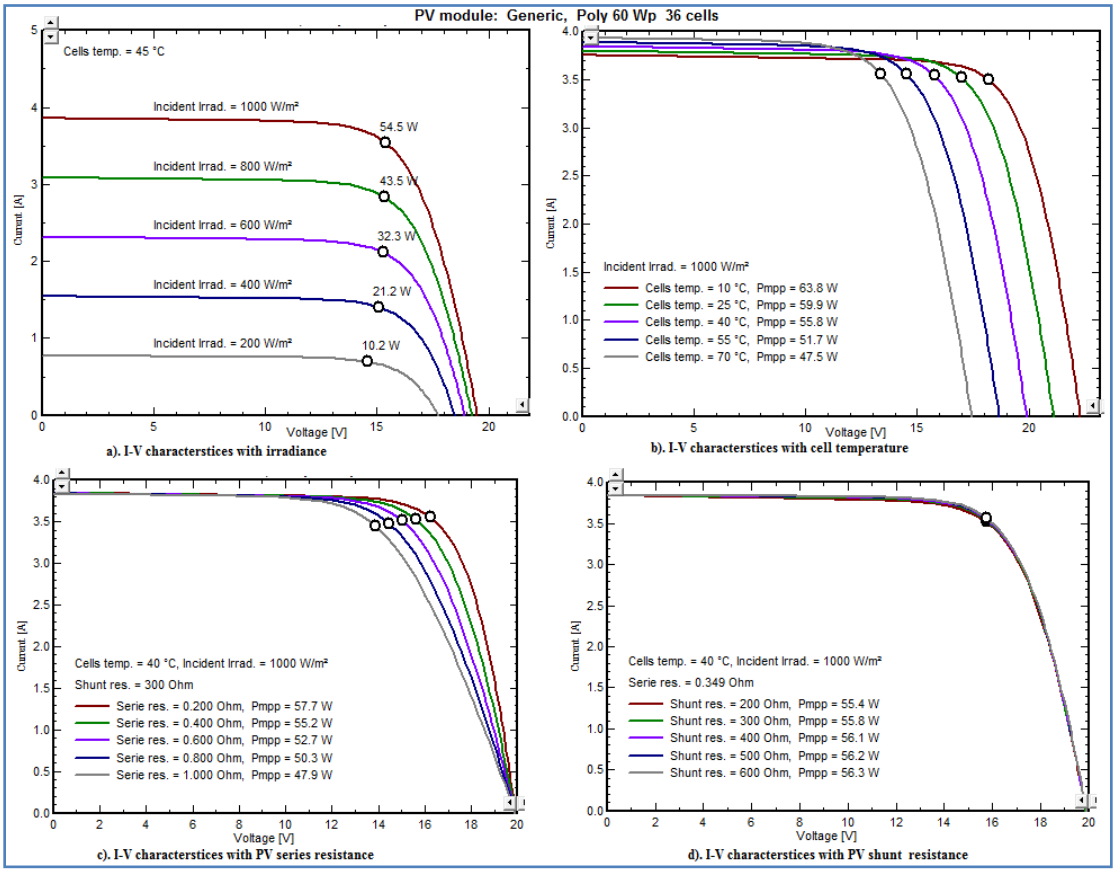

Figure 2-11: I-V curve of generic 60Wp poly crystal PV-module. [37]

PV manufacturers rate the power output of their PV modules at standard test conditions (STC), meaning a radiation of 1 kW/m^2, a cell temperature of 25°C, and no wind. Standard test conditions do not reflect typical operating conditions, since full-sun cell temperatures tend to be much higher than 25°C. The temperature coefficient of power indicates how strongly the PV array power output depends on the cell temperature, meaning the surface temperature of the PV array. It is a negative number because power output decreases with increasing cell temperature. Manufacturers of PV modules usually provide this coefficient in their product brochures, often labeled either coefficient as "power temperature coefficient in %/^{o}c". Also PV power output increase with increase of solar irradiance reached on the PV surface. [32]

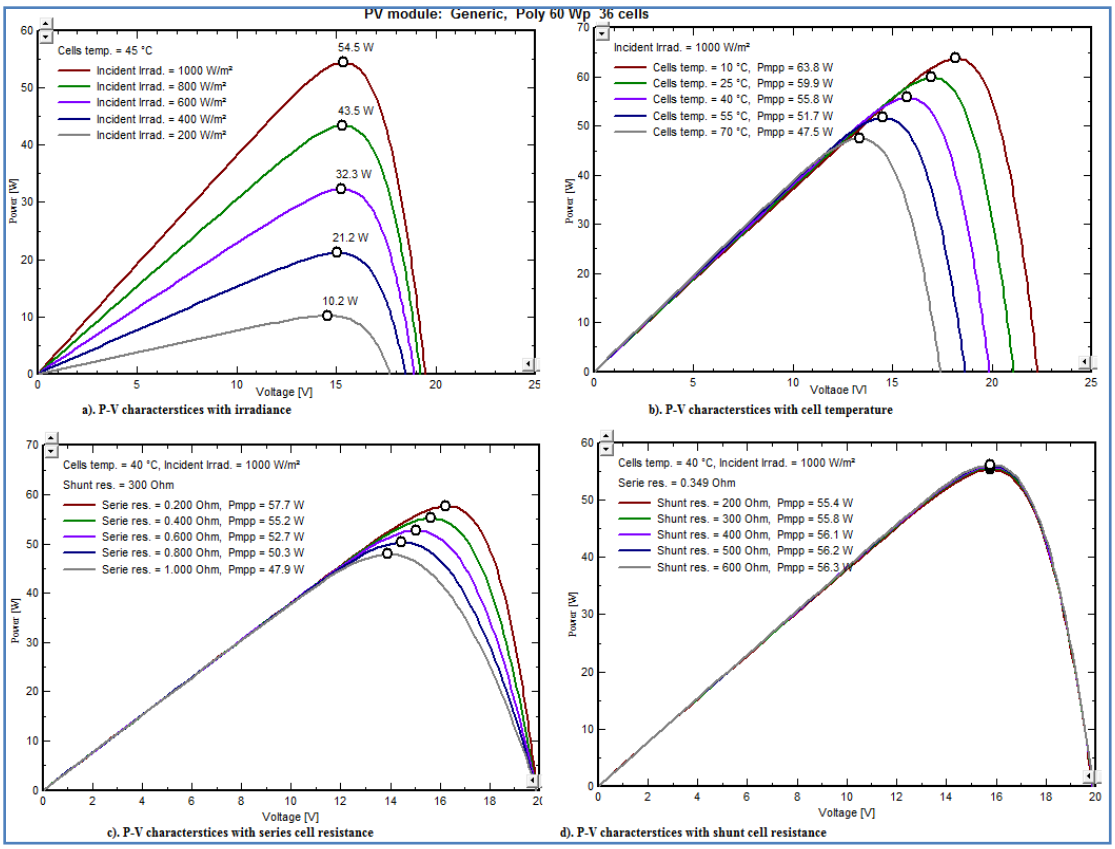

Figure 2-12: P-V curve of generic 60Wp poly crystal PV-module. [37]

The PV cell temperature is the temperature of the surface of the PV array. During the night it is the same as the ambient temperature, but in full sun the cell temperature can exceed the ambient temperature by 30°C or more [32]. The design of a PV power supply system should account the effect of PV cell temperature on PV power output. In PV based Hybrid electric power supply system HOMER will calculate the cell temperature in each time step, and use that in calculating the power output of the PV array. We start by defining an energy balance for the PV array, using Equation 2.16 [36]:

$$\tau.\alpha.G_T = \eta_C G_T + U_L(Tc-Ta) \qquad (2.16)$$

Where:

τ- is the solar transmittance of any cover over the PV array [%]

α- is the solar absorptance of the PV array [%]

G_T-is the solar radiation striking the PV array [kW/m^2]

η_c- is the electrical conversion efficiency of the PV array [%]

U_L-is the coefficient of heat transfer to the surroundings [kW/m^2°C]

Tc-is the PV cell temperature [°C]

Ta - is the ambient temperature [°C]

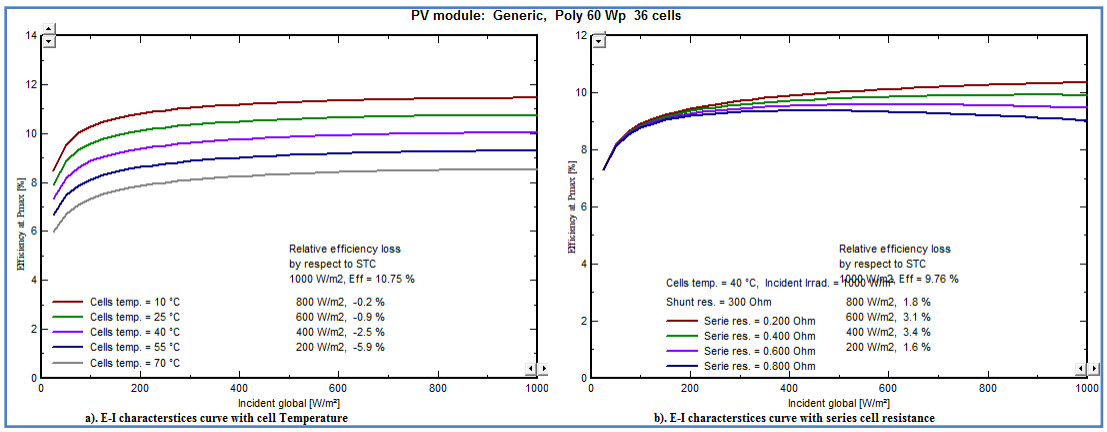

Figure 2-13: E-I curve of generic 60Wp poly crystal PV-module. [37]

The above equation states that a balance exists between, on one hand, the solar energy absorbed by the PV array, and on the other hand, the electrical output plus the heat transfer to the surroundings. We can solve that equation for cell temperature to yield:

$$T_c = T_a + G_T\left(\frac{\tau\alpha}{U_L}\right)\left(1 - \frac{\eta_c}{\tau\alpha}\right) \qquad (2.17)$$

It is difficult to measure the value of ($\tau.\alpha/ U_L$) directly, so instead manufacturers report the nominal operating cell temperature (NOCT), which is defined as the cell temperature that results at an incident radiation of 0.8 kW/m^2, an ambient temperature of 20°C, and no load operation (meaning $\eta_c = 0$).

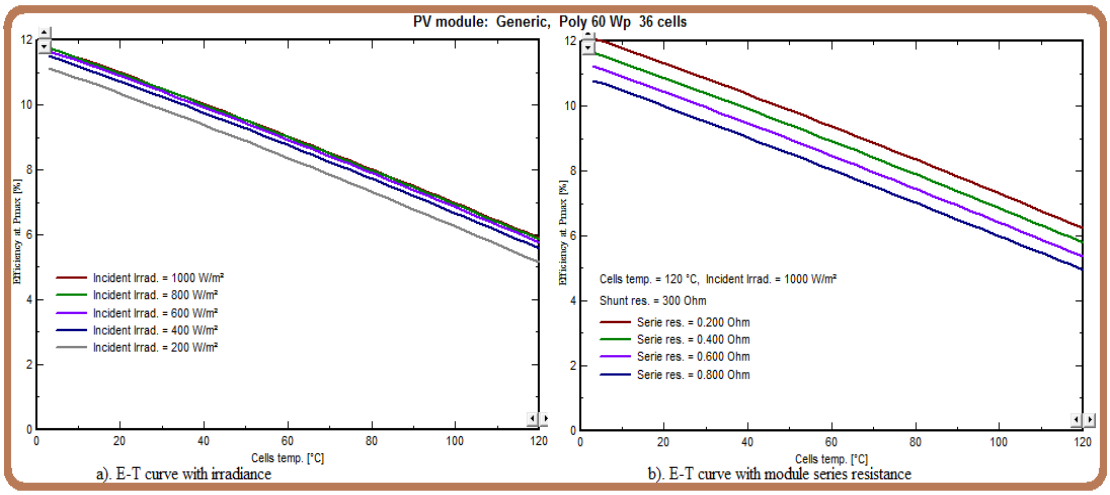

Figure 2-14: E-T curve of generic 60Wp poly crystal PV-module. [37]

We can subsitute these values into the above equation and solve it for $\tau.\alpha / U_L$ to yield the following equation: [9]

$$\frac{\tau\alpha}{U_L} = \frac{T_{c,NOCT} - T_{a,NOCT}}{G_{T,NOCT}} \qquad (2.18)$$

Where:

$T_{c, NOCT}$ is the nominal operating cell temperature [°C]

$T_{a, NOCT}$ is the ambient temperature at which the NOCT is defined [20°C]

$G_{T,NOCT}$ is the solar radiation at which the NOCT is defined [0.8 kW/m^2]

If we assume that $\tau.\alpha/U_L$ is constant, we can subsitute this equation into the cell temperature equation to yield:

$$T_C = T_a + G_T\left(\frac{T_{c,NOCT} - T_{a,NOCT}}{G_{T,NOCT}}\right)\left(1 - \frac{\eta_c}{\tau\alpha}\right) \quad (2.19)$$

2.3.3. PV System Installation

The tilt angle of a PV array can be adjusted to optimize various system objectives, such as maximizing annual, summer or winter energy production. Using adjustable fixed mounts and adjusting the title angle periodically through the year can further increase energy production [20]. Fixed amount of PV array, lower in cost than tracking mounts. For best year round power output with the least amount of maintenance, we should set the solar array facing true south at a tilt angle equal to the latitude with respect to the horizontal position. If we plan to adjust the solar array tilt angle seasonally, a good rule of thumb is:

To capture the maximum amount of solar radiation over a year, the solar array should be tilted at an angle approximately equal to a site's latitude, and facing within 15º of due south. To optimize winter performance, the solar array can be tilted 15º more than the latitude angle, and to optimize summer performance, 15º less than the latitude angle. At any given instant, the array will output maximum available power when pointed directly at the sun [38].

When installing PV panels the tracks are mounted on a roof or pole and then the panels are mounted on tracks. Care must be taken to ensure the panels will not shaded during the day as even partial shading of a panel will often reduce its power output to near zero. The PV array can then be connected to DC loads, directly or via battery and / or regulator. DC appliances can be slightly more expensive than AC appliances for which also DC/AC inverter need to be installed. When the PV modules are installed in parallel they can be segregated into separate sets to fine-tune the battery charging current. However, this is only feasible for big systems. Because one PV module is not working properly any more can take out a whole string, PV panels need to be kept clean, free overshadowing, and electrical connections need periodic inspection for loose connections and corrosion.

2.3.4. Solar Energy Resource of Ethiopia

Ethiopia receives 4.55 to 6.5 kWh/m2/day annual average of solar insolation throughout the country [1, 9, 39]. This varies significantly during the year, ranging from a minimum of 4.55kWh/m2/day in July to a maximum of 6.55kWh/m2/day in February and March. Other literatures describe the yearly average radiation to be in the range from 4.25 kWh/m2 in the

areas of Itang in the Gambella regional state (western Ethiopia), to 6.25 kWh/m2 around Adigrat in the Tigray regional state (northern Ethiopia) [27, 40, 41].

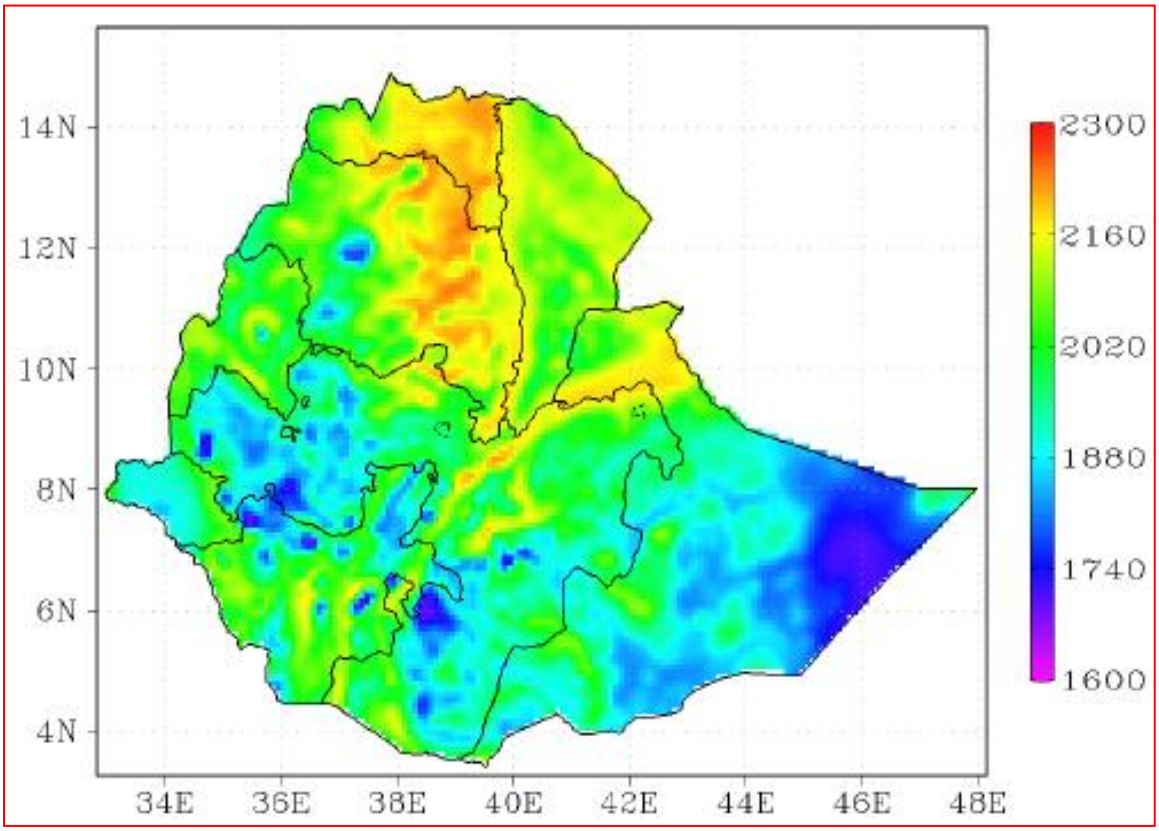

Figure 2-15: Distribution of Average Annual Total Solar Radiation of Ethiopia, kWh/ (m2·a) (1980~2009). [30]

2.3.5. Solar Energy Resource of Study Area

Like wind resource assessment of the study area, a comparison study was done between NASA, SWERA and Meteonorm to assess the solar energy potential. Since the data in SWERA is very much lower than the country average solar radiation (4.55 to 6.5 kWh/m2/day) and, Meteonorm (data base software) may consider nearby stations but its physical distances were much far from the study area to interpolate the solar resource data, therefore, NASA was taken as a source of solar and wind data for simulation since the data in NASA more or less agrees with the national average solar radiation data and the data in Meteonorm. NASA has estimated the 22 years annual average solar radiation incidence to a horizontal surface of the site to be 6.13kWh/m2/day [31].

Table 2-5: Solar radiation potential comparation of the study area.

Month	NASA (kWh/ m2/d)	Meteonorm (kWh/ m2/d)	SWERA(kWh/ m2/d)	% NASA Vs SWERA	% NASA Vs Meteonorm	% SWERA Vs Meteonorm
January	6.24	6.37	2.86	54.2%	-2.1%	-122.7%
February	6.50	6.81	2.61	59.8%	-4.8%	-160.0%
March	6.66	7.45	2.20	67.0%	-11.9%	-238.6%
April	6.56	7.73	2.70	58.8%	-17.8%	-186.3%
May	6.51	7.40	2.29	64.8%	-13.5%	-223.1%
June	5.88	6.78	1.08	81.6%	-15.3%	-527.8%
July	5.30	6.02	1.31	75.3%	-13.6%	-359.5%
August	5.31	5.98	1.72	67.6%	-12.6%	-247.7%
September	5.90	6.26	2.08	64.7%	-6.1%	-200.9%
October	6.41	6.46	3.06	52.3%	-0.8%	-111.1%
November	6.28	6.31	3.03	51.8%	-0.5%	-108.3%
December	6.07	6.24	2.40	60.5%	-2.8%	-160.0%
Average	6.13	6.65	2.28	62.8%	-8.5%	-191.7%

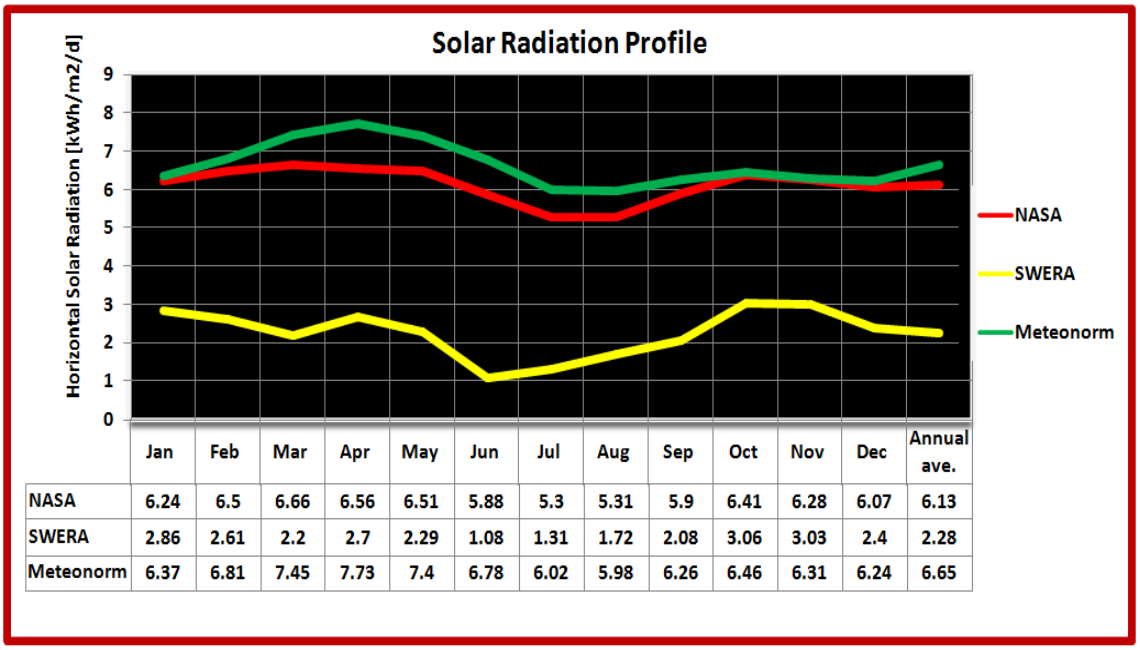

Figure 2-16: Solar radiation data of the study area

2.4. Biogas Energy

Biogas is a fuel gas consisting of a mixture of methane (CH4) and carbon dioxide (CO2), produced through microbial processes under anaerobic conditions from a variety of organic material like animal, agricultural, industrial and domestic wastes. Production of biogas from cattle dung, piggery waste, human excreta, etc, using simple anaerobic digesters has been in use in several developing countries [42]. The gases formed are the waste products of the

respiration of these decomposer microorganisms and the composition of the gases depends on the substance that is being decomposed. If the material consists of mainly carbohydrates, such as glucose and other simple sugars and high-molecular compounds (polymers) such as cellulose and hemicelluloses, the methane production is low. However, if the fat content is high, the methane production is likewise high [43].

Table 2-6: Biogas composition

Gas	%
Methane (CH_4)	55 – 70
Carbon dioxide (CO_2)	30 – 45
Hydrogen sulphide (H_2S)	1 – 2
Hydrogen (H_2)	
Ammonia (NH_3)	
Carbon monoxide (CO)	trace
Nitrogen (N_2)	trace
Oxygen (O_2)	trace

Methane and whatever additional hydrogen there may be – makes up the combustible part of biogas. Methane is a colorless and odorless gas with a boiling point of -162°C and it burns with a blue flame. At normal temperature and pressure, methane has a density of approximately 0.75 kg/m3. Due to carbon dioxide being somewhat heavier, biogas has a slightly higher density of 1.15-1.25kg/m3. Pure methane has an upper calorific value of 39.8 MJ/m3 (11.06 kWh/m3) [43].

Table 2-7: Potential biogas production from various biomass feedstocks on VS based.

Substrate	HRT (days)	Solid concentration (%)	Temperature (^{o}c)	Biogas yield (m3/kg VS)	Methane (%)
Sewage sludge	25	6	35	0.52	68
Domestic garbage	30	5	35	0.47	-
Piggery waste	20	6.5	35	0.43	69
Poultry waste	15	6	35	0.5	69
Cattle waste	30	10	35	0.3	58
Canteen waste	20	10	30	0.6	50
Food-market waste	20	4	35	0.75	62
Mango processing waste	20	10	35	0.45	52
Tomato-processing waste	24	4.5	35	0.63	65
Lemon waste	30	4	37	0.72	53
Citrus waste	32	4	37	0.63	62
Banana peel	25	10	37	0.60	55
Pineapple waste	30	4	37	0.37	60
Mixed feed of fruit waste	20	4	37	0.62	50

2.4.1. The Biogas Production Process

Anaerobic digestion (AD) is a biochemical process during which complex organic matter is decomposed in absence of oxygen, by various types of anaerobic microorganisms. The result of the AD process is the biogas and the digestate. Biogas is a combustible gas, consisting primarily of methane and carbon dioxide. Digestate is the decomposed substrate, resulted from the production of biogas. If the substrate for AD is a homogenous mixture of two or more feedstock types (e.g. animal slurries and organic wastes from food industries), the process is called "co– digestion" and is common to most biogas applications today.

The process of biogas formation is a result of linked process steps, in which the initial material is continuously broken down into smaller units. Specific groups of micro-organisms are involved in each individual step. The simplified diagram of the AD process, shown in Figure 2.17, highlights the four main process steps: hydrolysis, acidogenesis, acetogenesis, and methanogenesis. The process steps quoted in Figure 2.17 run parallel in time and space, in the digester tank. During hydrolysis, relatively small amounts of biogas are produced. Biogas production reaches its peak during methanogenesis. [44]

A. Hydrolysis

Hydrolysis is theoretically the first step of AD, during which the complex organic matter (polymers) is decomposed into smaller units (mono- and oligomers). During hydrolysis, polymers like carbohydrates, lipids, nucleic acids and proteins are converted into glucose, glycerol, purines and amino acids. Hydrolytic microorganisms excrete hydrolytic enzymes, converting biopolymers into simpler and soluble compounds as it is shown below:

$$\text{Lipids} \xrightarrow{\text{lipase}} \text{fatty acids, glycerol}$$

$$\text{Polysaccharide} \xrightarrow{\text{cellulose, cellobiase, amylase}} \text{monosaccharide}$$

$$\text{Proteins} \xrightarrow{\text{protease}} \text{amino acids}$$

B. Acidogenesis

During acidogenesis, the products of hydrolysis are converted by acidogenic (fermentative) bacteria into methanogenic substrates. Simple sugars, amino acids and fatty acids are degraded into acetate, carbon dioxide and hydrogen (70%) as well as into volatile fatty acids (VFA) and alcohols (30%). [44]

C. Acetogenesis

Products from acidogenesis, which cannot be directly converted to methane by methanogenic bacteria, are converted into methanogenic substrates during acetogenesis. VFA and alcohols are oxidised into methanogenic substrates like acetate, hydrogen and carbon dioxide. VFA, with carbon chains longer than two units and alcohols, with carbon chains longer than one unit, are oxidized into acetate and hydrogen. During methanogenesis, hydrogen is converted

into methane. Acetogenesis and methanogenesis run parallel, as symbiosis of two groups of organisms [44].

D. Methanogenesis

The production of methane and carbon dioxide from intermediate products is carried out by methanogenic bacteria. 70% of the formed methane originates from acetate, while the remaining 30% is produced from conversion of hydrogen (H) and carbon dioxide (CO2), according to the following equations:

$$\text{Acetic acid} \xrightarrow{\text{methanogenic bacteri}} \text{methane + carbon dioxide}$$

$$\text{Hydrogen + carbon dioxide} \xrightarrow{\text{methanogenic bacteria}} \text{methane + water}$$

Methanogenesis is a critical step in the entire anaerobic digestion process, as it is the slowest biochemical reaction of the process. Methanogenesis is severely influenced by operation conditions. Composition of feedstock, feeding rate, temperature, water content, NH3 concentration and pH are examples of factors influencing the methanogenesis process.

Temperature for fermentation will greatly affect biogas production. The AD process can take place at different temperatures, divided into three temperature ranges: psychrophilic (below 20^{o}C), mesophilic (30^{o}C – 42^{o}C), and thermophilic (43^{o}C – 55^{o}C). There is a direct relation between the process temperature and the HRT. The biogas production rate increases with increase the process temperature.

Table 2-8: Biogas production thermal stage and their corresponding retention time [47]

Thermal stage	Process Temperature	Minimum HRT
Psychrophilic	< 20^{o}c	70-80 days
Mesophilic	30-42^{o}c	30-40 days
Thermophilic	43-55^{o}c	15-20 days

Many modern biogas plants operate at thermophilic process temperatures as the thermophilic process provides many advantages, compared to mesophilic and psychrophilic processes:

- Effective destruction of pathogens
- Higher grow rate of methanogenic bacteria at higher temperature
- Reduced retention time, making the process faster and more efficient
- Improve digestibility and availability of substrates
- better degradation of solid substrates and better substrate utilization
- better possibility for separating liquid and solid fractions

In this study thermophilic biogas temperature process is chosen in order to get higher biogas output and to achieve this target flat plate collector can be used to maintain digester process temperature at 55^{o}c. See details of it from flat plate collector design in Chapter-3.

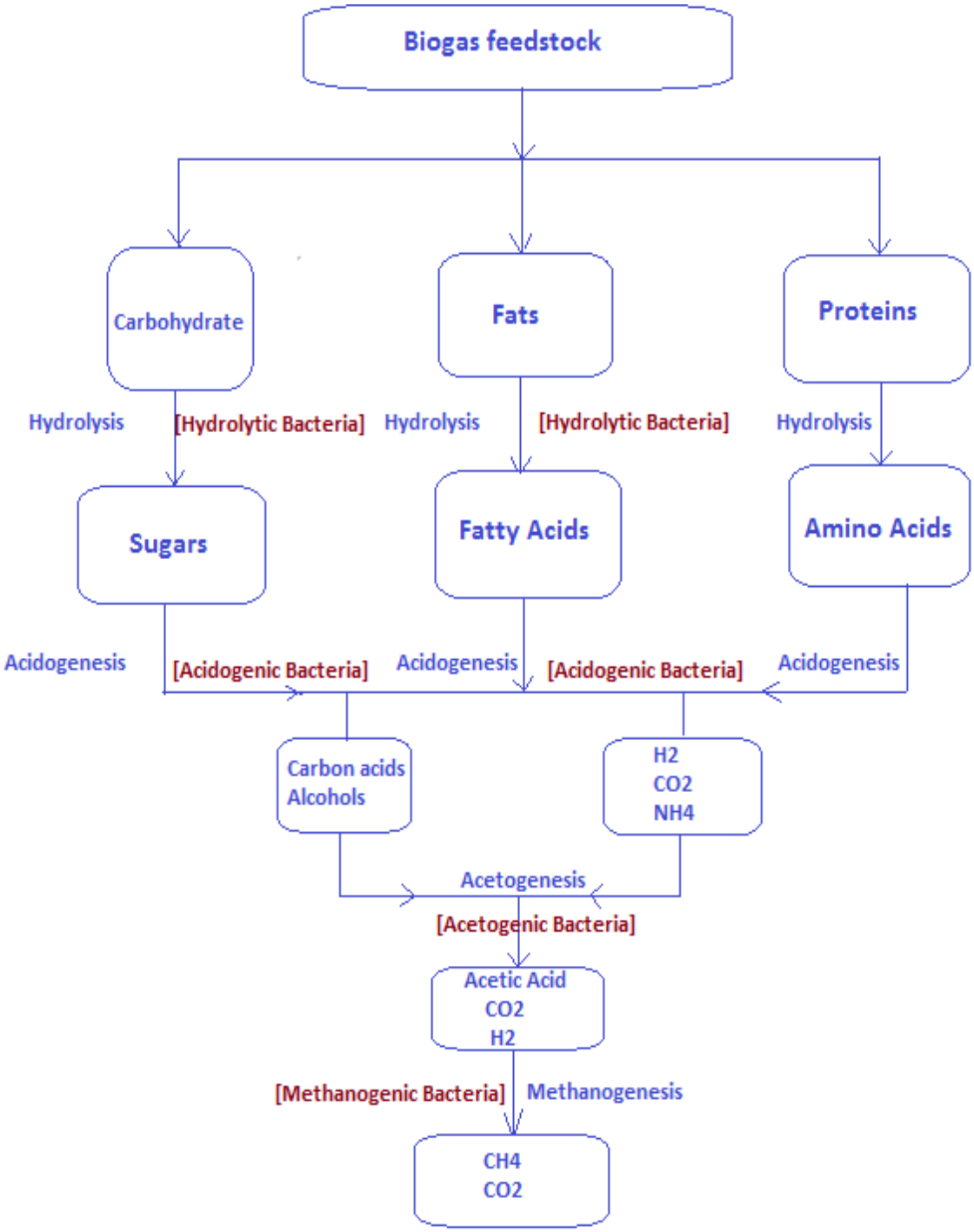

Figure 2-17: The main process steps of biogas production by AD.

2.4.2. Biogas Plant

A biogas plant is a complex installation, consisting of a variety of elements. The layout of such a plant depends to a large extent on the types and amounts of feedstock supplied. As there are many different feedstock types suitable for digestion in biogas plants, there are, correspondingly, various techniques for treating these feedstock types and different digester

constructions and systems of operation. Furthermore, depending on the type, size and operational conditions of each biogas plant, various technologies for conditioning, storage and utilization of biogas are possible to implement. As for storage and utilisation of digestate, this is primarily oriented towards its utilization as fertilizer and the necessary environmental protection measures related to it.

The construction and operation of a biogas plant is a combination of economical and technical considerations. Obtaining the maximum biogas yield, by complete digestion of the substrate, would require a long retention time of the substrate inside the digester and a correspondingly large digester size. In practice, the choice of system design (digester size and type) or of applicable retention time is always based on a compromise between getting the highest possible biogas yield and having justifiable plant economy.

Biogas plants have the following main components and operate with four different process stages. [44]

Process stages of biogas production:

- ✓ Transport, Delivery, storage and pre-treatment of feedstocks
- ✓ Biogas production
- ✓ Storage of digestate, conditioning and utilization
- ✓ Storage of biogas, conditioning and utilization

Main components of biogas plant:

- ✓ Feedstock pre-storage tank
- ✓ Substrate mixing Tank
- ✓ Biogas digester
- ✓ Post storage tank
- ✓ Gas holder tank and
- ✓ CHP system

When building a biogas plant, the choice of type and the design of the plant are mainly determined by the amount and type of available feedstock. The amount of feedstock determines the dimensioning of the digester size, storage capacities and CHP unit. The feedstock types and quality (DM-content, structure, origin etc.) determines the process technology.

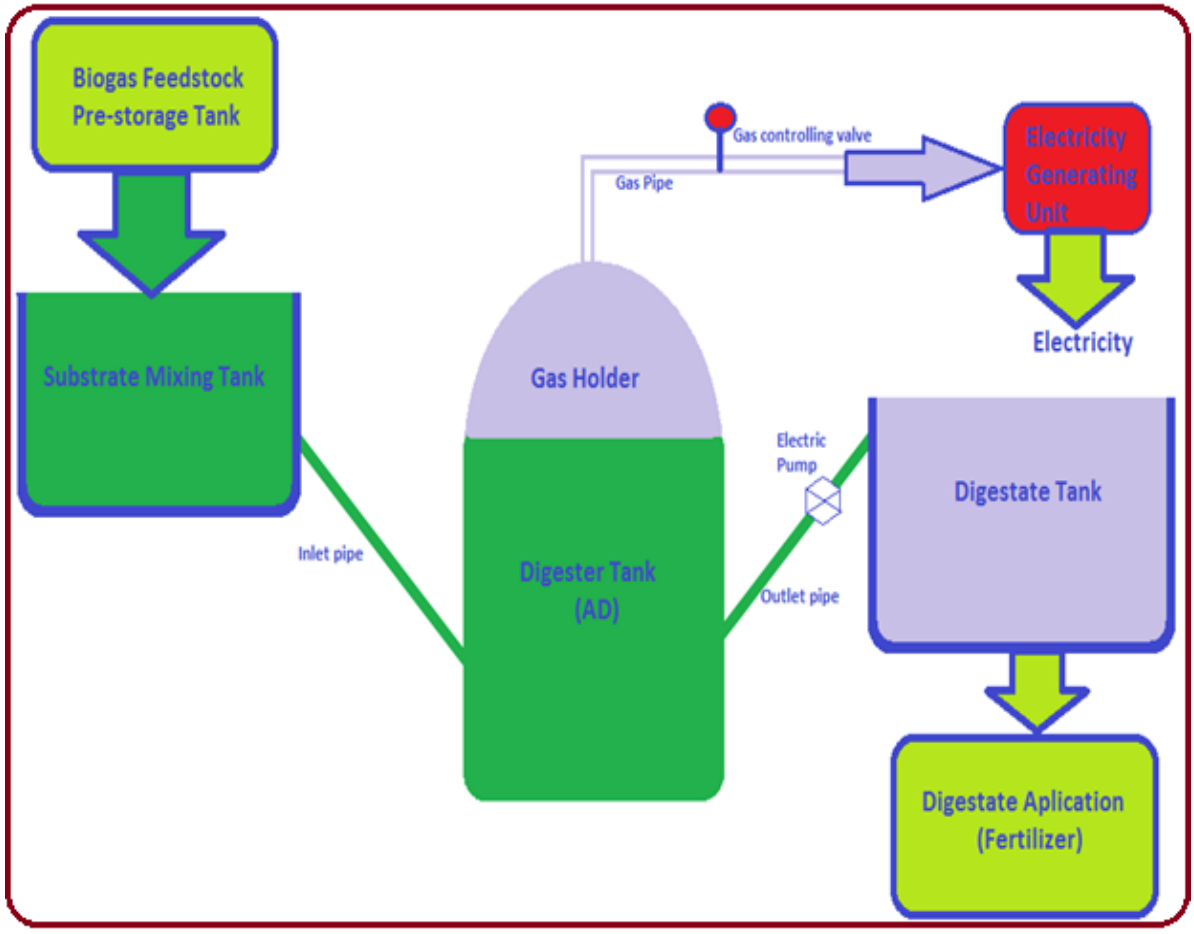

Figure 2-18: Main components and general process flow of biogas production

Table 2-9: Biogas minimum requirement used in an electric engine [44]

No.	Parameter	Symbol	Value
1.	Lower heat value	LHV	≥4kWh/m3
2.	Sulphur content	S	≤2.2g/m3 CH4
3.	Hydrogen sulphide	H_2S	≤0.15 Vol. %
4.	Chlorine content	Cl	≤100mg/m3 CH4
5.	Fluoride content	F	≤50mg/m3 CH4
6.	Dust(3-10µm)	-	≤10mg/m3 CH4
7.	Relative humidity	ϕ	<90%
8.	Flow pressure	P_{gas}	20-100mbar
9.	Gas pressure fluctuation	-	<±10% of set value
10.	Gas temperature	T	10-50^{o}c
11.	Hydro carbon	HC	<0.4 mg/m3 CH4
12.	Silicon	Si	<10mg/CH4

The CHP system utilizes the biogas either in heat or electrical energy. The manufacturers of CHP units have minimum requirements for the properties of the combustible gas (Table 2.9). The combustion properties must be guaranteed, to prevent damage to the engines. This also applies to the use of biogas. For other utilizations of biogas (e.g. as vehicle fuel or in fuel cells), further gas up-grading and conditioning measures are necessary.

2.4.3. Design of the Biogas Plant

The design of the biogas plant includes the design of:

- The digester
- The gas Holder
- Digester heat maintaining system
- Siting of biogas plant

To calculate the scale of a biogas plant, certain characteristic parameters are used. These are:

- **Daily fermentation slurry feeding (Sd**), which is an equal mixture of biogas feedstock (animal dung, human feces, poultry waste and jatropha byproduct) with water feed in to the biogas digester.
- **Retention time (RT),** the time by which the fermentation slurry stays in the digester. It is about 2-5 weeks.
- **Digester loading (R).** The digester loading indicates how much organic material per day has to be supplied to the digester or has to be digested. The digester loading is calculated in kilograms of organic dry matter per cubic meter of digester volume per day (kg/m3/day).
- **Specific gas production per day (Gd),** which depends on the retention time, the digestion temperature and the feed material.

A. Sizing of Biogas Digester and Gasholder

The size of the digester - the digester volume (V_D) - is determined by the length of the retention time (RT) and by the amount of fermentation slurry supplied daily (S_D). The amount of fermentation slurry consists of the feed material considered in this study (e.g., cattle dung) and the mixing water.

I. Sizing of Site-A Biogas Digester and Gasholder

Daily average collectable biogas feedstock potential from cow dung, oxen dung, donkey, mule, and horse waste, chicken waste, human feces and jatropha byproduct in this study in tonnes/day is 10.867=10867kg/day=15.53m3/day. Since the average density of animal slurry mix is 700kg/m3.

Additional 15.53m 3/day water is required for proper digestion of biogas feedstock material to enhance biogas production.

HRT=20day, under thermophilic digestion temperature (55^{o}c) the hydraulic retention time of the digestion process becomes short.

The volume of digester should be, V_D =HRT *x* S_D

=20 day *x* (15.53 *x* 2m3/day) = 621m3.

Therefore the size of the digester for site A could be 621m3.

Where, V_D= the size of the digester, HRT= hydraulic retention time, and S_D is the amount of fermentation slurry (water + feedstock) feed in to the digester per day.

Biogas yield in m3/kg of fresh biogas feedstock mix is 1736.4m3/31850kg=0.054m3/kg; the biogas production rate is 10867kg/day x 0.054m3/kg=588m3/day. Therefore the size of gasholder should account this daily biogas production.

II. Sizing of Site-B Biogas Digester and Gasholder

Daily average collectable biogas feedstock potential from cow dung, oxen dung, donkey, mule, and horse waste, chicken waste, human feces and jatropha byproduct of Site-B in tonnes/day is 9.253=9253kg/day=13.22m^3/day. Since the average density of animal slurry mix is 700kg/m^3.

Additional 13.22 m^3/day water is required for proper digestion process of biogas feedstock material to enhance biogas production.

HRT=20day, under thermophilic digestion temperature the hydraulic retention time of the digestion process becomes short.

The volume of digester should be, V_D=HRT *x* S_D

=20 day x (13.22 x 2m3/day) = 529m3. Therefore the size of the digester for **site-B** is 529m3. The biogas gas production rate is 9253kg/day *x* 0.054m3/kg=501m3/day. Therefore the size of gasholder should account this daily biogas production.

III. Sizing of Site-C Biogas Digester and Gasholder

Daily average collectable biogas feedstock potential from cattle dung, donkey, mule, and horse waste, chicken waste, human feces and jatropha byproduct of Site-C in tonnes/day is 8.82=8820kg/day=12.6m3/day, Since the average density of animal slurry mix is 700kg/m3.

Additional 12.6 m3/day water is required for proper digestion of biogas feedstock material to enhance biogas production.

The volume of digester should be, V_D =HRT x S_D, HRT=20day

=20 day x (12.6 x 2m3/day) = 504m3.

Therefore the size of the digester for **site-C** is 504m3.

The gas production rate is 8820kg/day x 0.054m3/kg=477m3/day. Therefore the size of gasholder should account this daily biogas production also.

IV. Sizing of Site-D Biogas Digester and Gasholder

Daily average collectable biogas feedstock potential of Site-D in tonnes/day is 3.091=3091kg/day=4.42m3/day, since the average density of animal slurry mix is taken as 700kg/m3.

Additional 4.42 m3/day water is required.

The volume of digester should be, V_D=HRT x S_D, HRT=20day

=20 day x (4.42 x 2m3/day) = 179m3.

Therefore the size of the digester for **site-D** is 179m3.
The gas production rate is 3091kg/day x 0.054m3/kg=168m3/day. Therefore the size of gasholder should account this daily biogas production.

B. Location of Biogas Plant

The next planning step in a biogas plant project idea is to find a suitable site for the establishment of the plant. The list below shows some important considerations to be made, before choosing the location of the plant: [44]

- The site should be located at suitable distance from residential areas in order to avoid inconveniences, nuisance and thereby conflicts related to odours and increased traffic to and from the biogas plant.
- The direction of the dominating winds must be considered in order to avoid wind born odours reaching residential areas.
- The site should have easy access to infrastructure such as to the electricity grid, in order to facilitate the sale of electricity and to the transport roads in order to facilitate transport of feedstock and digestate.
- The soil of the site should be investigated before starting the construction.
- The chosen site should not be located in a potential flood affected area.
- The size of the site must be suitable for the activities performed and for the amount of biomass supplied.
- The site should be located relatively close (central) to the agricultural feedstock production (manure, slurry, energy crops) aiming to minimize distances, time and costs of feedstock transportation.
- For cost efficiency reasons, the biogas plant should be located as close as possible to potential users of the produced heat and electricity.

The required site space for a biogas plant cannot be estimated in a simple way. Experience shows that for example a biogas plant of 500 kW_{el} needs an area of approximate 8,000m².

This figure can be used as a guiding value only, as the actual area also depends on the chosen technology [44]. Based on the above criteria of site selection of biogas plant, the location of the biogas plant for each site of the study area is chosen and the detail of it is found in the economic analysis section of the biogas plant in this paper (see Chapter 4).

2.5. Biodiesel Energy from Jatropha

2.5.1. Characteristics of Jatropha Plant

Jatropha is a plant that produces seeds with high oil content. The seeds are toxic and in principle non-edible. Jatropha grows under (sub) tropical conditions and can withstand conditions of severe drought and low soil fertility. Because jatropha is capable of growing in marginal soil, it can also help to reclaim problematic lands and restore eroded areas.

Current interest by investors, farmers and NGOs in jatropha is mainly due to its potential as an energy crop. Jatropha seeds can be pressed into bio-oil that has good characteristics for direct combustion in compressed ignition engines or for the production of biodiesel. The bio-oil can also be the basis for soap-making. The pressed residue of the seeds (presscake) is a good biogas source and can also be used for fertilizer production [45]. Jatropha seeds look like black beans and are on average 18 mm long and 12 mm wide and 10 mm thick. These dimensions vary within seeds from the same plant or provenance and between seeds from different provenances. Seed weigh between 0.5 and 0.8 gram, with an average of 1333 seeds per kilogram. Seeds contain various toxic components (phorbol esters, curcin, trypsin inhibitors, lectins and phytates) and are non-edible. Seeds consist of a hard shell that makes up around 37% by weight on average and soft white kernel that makes up 63% by weight. The dry seeds have a moisture content of around 7% and contain between 32 and 40% of oil, with an average of 34%. Virtually all the oil is present in the kernel. [45]

Figure 2-19: Jatropha Plant and Seed

2.5.2. Application of Jatropha Products

Jatropha has many potential applications. However, until now only a few have been realized on a reasonable and large scale. Jatropha is primarily cultivated for its oil application. However, this oil is not the only usable product from the plant. During the process of extracting the oil, many useful by-products are created, as well. Here, first the oil applications are discussed, followed by the applications of by-products.

Applications of oil: Jatropha oil can be used in several ways. The pure (untreated) oil can be used as fuel or for soap production. Jatropha oil can also serve as a resource for the production of biodiesel.

Applications of other jatropha products: When the seeds are pressed to oil, about 20%-30% of oil by weight is obtained [45]. The rest remains as presscake. Not only are all the minerals still inside this cake but due to the oil content the presscake still contains a considerable amount of energy, With 20-25 MJ/kg, about half as energy-rich as the oil that contains 40 MJ/kg – but the fact that there is two to four times more presscake, compensates for this [45]. Theoretically, the best use of the presscake is for energy purposes first, and then as a fertilizer next.

- **Presscake as a biogas feedstock**

Results from lab test on behalf of FACT proved that jatropha presscake alone, when started with fermentation bacteria to start the process, showed a fairly good production of biogas. Based on these tests a prediction for real life productions was made as follows: biogas yield of $1m^3$/kg, CH4 content of 50%-60% and LHV between 18-22 MJ/kg. [46]

- **Jatropha as a fertilizer**

Jatropha presscake contains high amounts of nitrogen (3.8-6.4% by wt), phosphorus (0.9-2.8% by wt) and potassium (0.9-1.8% by wt). It also contains trace amounts of calcium, magnesium, sulphur, zinc, iron, copper, manganese and sodium. Reviewing various literatures shows that an application of 1 tone of Jatropha byproduct (Presscake and fruit hull) is equivalent to 200 kg of mineral fertilizer [47]. Presscake and fruit hull have to be composted before they can be used as fertilizer.

In this study the average jatropha digestate used as a fertilizer from Presscake and fruit hull after biogas generation and biodiesel production is estimated to be 92.1tone/year in the study area and this is equivalent with 18,420kg chemical fertilizer.

- **Insecticide from oil and/or press cake**

Jatropha oil has also proven to be an effective pesticide. In one study 1.4 liters of jatropha oil was mixed with 16 liters of water and sprayed on cotton and acted efficiently [48]. An

organization in Tanzania promotes the following process for obtaining insecticide out of jatropha seeds: grind some jatropha seeds, soak them in water for 24 hours, filter the particles from this mixture, and dilute the mixture in a 1:10 ratio with water.

2.5.3. Biodiesel Potential from Jatropha

In the study area more than 20 hectare free land for jatropha cultivation is available and this land is only suitable for jatropha farming, its fertility is low and highly inclined (exposed to soil erosion) as compared with other edible crop farming areas found in the site.

Figure 2-20: Sample Photo of land suitable for jatropha plantation in the study area.

Table 2.10 contains jatropha data's that are used for potential estimation of biogas and biodiesel from jatropha plant.

Table 2-10: Jatropha fact sheet

Parameter	Unit	Minimum	Average	Maximum	Source
Seed yield	dry tone/ hectare/year	0.3	3.15	6	Position Paper on Jatropha Large Scale Project Development, FACT 2007
Fruit hull yield	dry tone/ hectare/year	0.2	2.1	4	
Rainfall requirements for seed production	mm/year	600	1000	1500	Position Paper on Jatropha Large Scale Project Development, FACT 2007
Oil content of seeds	% of mass	_	34%	40%	Jatropha bio-diesel production and use, W. Achten et al, 2008
Oil yield after pressing	% of mass of seed input	20%	25%	30%	Jatropha handbook, 2010
Presscake yield after pressing	% of mass of seed input	70	75	80	
Energy content of Seed	MJ/kg	-	37	-	

Biofuels are considered in part, a solution to such issues as sustainable development, energy security and a reduction of greenhouse gas emissions. Biodiesel, an environmental friendly diesel fuel similar to petro-diesel in combustion properties, has received considerable attention in the recent past worldwide. Biodiesel is a methyl or ethyl ester of fatty acid made from renewable biological resources such as vegetable oils (Jatropha), recycled waste vegetable oil and animal fats [49, 50, 51]. The use of vegetable oils as alternative fuels has been around since 1900 when the inventor of the diesel engine Rudolph Diesel first tested peanut oil in his compression ignition engine [52].

Various researches show that jatropha seeds contain an average of 34 % of oil by weight. With mechanic oil expellers up to 70 - 80 % of the oil can be extracted (1 kg of seeds give about 0.255-0.298 liter of oil) [47]. The soil fertility and annual rain fall (~1000mm) is sufficient for jatropha cultivation in the study area [53]. So we can consider the average jatropha biomass and its biogas yield given in Table 3.5 above for analysis in HOMER. The study area have a potential of 3150kg/hectare * 20 hectare=63000kg jatropha seed yield per annum. The equivalent oil yield of the area is 16,090-18,774 liter annually. Therefore the Jatropha oil potential of the site is in the range of 16.09-18.774m^3 annually.

The oil can also be chemically treated to produce biodiesel. Properties of biodiesel are very similar to those of fossil diesel, and hence it can be used in any diesel engine without adaptations. Clean, well-produced and refined biodiesel is at least as good an engine fuel as regular fossil diesel. It gives better ignition and combustion and emits fewer harmful components like smoke and sulphur.

Table 2-11: Fuel properties of *Jatropha* oil, *Jatropha* biodiesel and fossil diesel [54-56]

Property	J. oil	J. biodiesel	Diesel	Biodiesel Standard	
				AST D6751-02	DIN EN 14214
Density (15°c, kg/m3)	940	880	850	-	860-900
Viscosity (mm2/s)	24.5	4.8	2.6	1.9-6.0	3.5-5.0
Flash point (°c)	225	135	68	>130	>120
Pour point (°c)	4	2	-20	-	-
Ash content (%)	0.8	0.012	0.01	<0.02	<0.02
Water content (%)	1.4	0.025	0.02	<0.03	<0.05
Carbone residue (%)	1	0.2	0.17	-	<0.3
Acid value (mg KOH/g)	28	0.4	-	<0.80	<0.50
Calorific value (MJ/kg)	38.65	39.23	42	-	-

2.5.4. Biogas Potential from Jatropha

Various literatures show that, Methane yield of jatropha fruit hull is 0.438m^3/kg VS, and the VS is 76% of the TS of the jatropha fruit hull. Methane is 50% of the total biogas yield (1.153m3/kg). The biogas yield of Jatropha seed presscake is approximately 1m3/kg of presscake. The biogas yield of jatropha fruit hull is better than the seedcake [57]. Based on

the Jatropha fact sheet given in Table 2.10, the biomass, biogas and methane yield potential of the jatropha byproduct is estimated in Table 2.12 & 2.13

Table 2-12: Jatropha byproduct biomass potential in the study area.

Biogas feedstock	Jatropha biomass, tones/year	Average Jatropha biomass, tones/year	Biogas yield, m^3/kg	Methane yield, m^3/kg	Total biogas yield, m^3	Average biogas yield, m^3/year	Average methane yield, m^3/year
1. Presscake	4.2 -96	50.1	1	0.5-0.6	4200 - 96,000	50,100	25,050-30,060
2. Fruit hull	4-80	42	1.153	0.576-0.69	4,612-92,240	48,426	27894-33414
Total	8.2-176	92.1	1.07	0.575-0.689	8812-188,240	98,526	52944-63474

- ✓ ***Jatropha biomass (from presscake) = seed yield (tone/hectare) * % of presscake yield during oil production * total land for Jatropha farming (hectare)***
- ✓ ***Jatropha biomass (from fruit hull) = hull yield (tone/hectare) * total land for Jatropha farming (hectare).***

Table 2-13: Jatropha biogas potential of the study area

Profile	Jatropha biomass, tones	Biogas yield, m^3/kg	Biogas yield, m^3	Methane yield, m^3/kg	Methane yield, m^3
Yearly average	92.1	1.07	98,526	0.575-0.689	52944-63474
Daily average	0.253	1.07	270	0.575-0.689	145-174

Table 2-14: Summary of Jatropha potential of the study area.

Jatropha product	Jatropha oil (liter/year)	Jatropha biogas (m3/year)	Jatropha fertilizer (kg/year)	Jatropha biomass (tone/year)
Product yield	16,090-18,774	98,526	18,420	92.1

2.5.5. Biogas energy potential of the study area from animal dung

A wide range of biomass types can be used as substrates (feedstock) for the production of biogas from AD. The most common biomass categories used in biogas production are listed in Table 2.15 for this thesis work. To produce biogas from animal manure first we have to check whether we have animal livestock potential sufficient for biogas feedstock production or not. The following Table demonstrates the animal livestock potential for each sites of the study area.

Table 2-15: Jama Woreda, Kebele-8 districts Animal livestock Potential

Animal livestock's	Site-A	Site-B	Site-C	Site-D	Ave. no. of animal/HH	Total livestock in the study area
Cows	666	566	535	172	1.7	1935
Oxen	719	612	577	184	1.85	2092
Goats	163	139	131	43	0.42	476
Sheep	1841	1567	1477	472	4.72	5350
Mule	12	10	9	3	0.03	29
Chickens	2340	1992	1878	600	6	6810
Pigs	0	0	0	0	0	0
Horse	48	40	37	12	0.12	133
Donkey	345	295	278	89	0.89	1007

(Source: Jama Woreda rural development and Kebele-8 administration office, Nov - 2012)

The average fresh manure obtained from, cattle is 4.5kg/day/head [42, 58, 59], donkey, horse and mule is 10kg/day/head [58, 59], sheep and goat 1kg/day/head [58, 59], and chicken is 0.08kg/day/head [58, 59]. The average biogas yield of cattle, horse, mule, and donkey manure is 0.24m3/kg DM [43, 44, 60] and pigs, sheep and goat is 0.37m3/kg DM where as chicken is 0.4m3/kg of DM [43, 44, 60]. The dry matter content from the total mass of fresh animal manure and the proportion of methane from the total biogas production is summarized in Table 2.16. [43, 44, 61]

Table 2-16: Summary of fresh manure, biogas and methane yield of animal livestock's.

Biomass source	Average Fresh manure, kg/day/head	m^3 biogas/kg DM	DM % Fresh manure	Methane % Biogas
Cattle	4.5	0.24	16.7	65
Pigs	2	0.37	4.4	65
Sheep, goats	1	0.37	30.7	65
Chickens	0.08	0.40	30.7	65
Horse, mule	10	0.24	7	65
Donkey	10	0.24	15	65

- ✓ Total Fresh manure potential of the study area (tonnes/day) = Average Fresh manure (kg/day/head) * Total no. of livestock in study area.
- ✓ Total dry mater (DM) from fresh manure = DM % of Fresh manure * Total Fresh manure potential of the study area (tonnes/day).
- ✓ Total biogas production, m^3/day = Biogas m3/kg of DM * Total dry mater (DM) from fresh manure in kg/day.
- ✓ Total electricity production in kWh/day= electricity production by biogas generator from 1 m3 biogas in kWh * total biogas production in m3/day.
- ✓ By using biogas generator it is possible to generate 1kWh electricity from 0.7m3 biogas [42].

Table 2-17: Summary of expected animal manure potential of the study area.

Animal livestock	Ave. Fresh manure, kg/day/ head	Total no.of livestock in study area	Total Fresh manure (ton/day)	Total DM (kg/day)	Biogas, m3/kg of DM	Total biogas, m^3/day	Electricity production, kWh/day
Cows	4.5	1935	8.708	1455	0.24	350	500
Oxen	4.5	2092	9.414	1573	0.24	378	540
Goats	1	476	0.476	147	0.37	55	79
Sheep	1	5350	5.350	1643	0.37	608	869
Mule	10	29	0.290	24	0.24	6	9
Chicken	0.08	6810	0.545	168	0.40	68	98
Pigs	2	0	0.000	0.00	0.37	0.0	0.0
Horse	10	133	1.330	92	0.24	22	32
Donkey	10	1007	10.070	1511	0.24	363	519
Total animal manure biomass			**36.183**	**6613**	**0.28**	**1850**	**2646**

For a given size of plant (rated gas production capacity per day) the amount of feedstock required can be estimated using the biogas yield data provided. The specific biogas consumption in biogas engines is 0.6-0.8 m3/kWh [42]. This specific fuel consumption value can be used to calculate the requirement for biogas for power generation purposes. The expected biomass potential from animal manure of the case study area is 36.2tonnes/day and its biogas production capacity is 1850m3/day. Various literatures show that the collection efficiency of animal manure varies from country to country and region to region.

Most significantly the collection efficiency varies from 50%-100% [62]. Let as consider collection efficiency of 90% for cattle, donkey, mule, horse, pig and chicken manure, 50% for goat and sheep manure and 100% for human feces based on their difficulty of collecting it. Therefore the biomass potential available for biogas generation is estimated as follows.

Table 2-18: Summary of collectable animal manure potential of the study area.

Animal livestock	Ave. Fresh manure, kg/day/ head	Total no. of livestock in study area	Total collectable Fresh manure, tonnes/day	Total collectable DM, kg/day	Biogas, m3/kg of DM	Total biogas, m^3/day	Electricity production , kWh/day
Cows	4.5	1935	7.837	1309.5	0.24	315	450
Oxen	4.5	2092	8.473	1415.7	0.24	340	486
Goats	1	476	0.238	73.5	0.37	27.3	39
Sheep	1	5350	2.675	821.5	0.37	304	434.3
Mule	10	29	0.261	21.6	0.24	5.2	7.43
Chicken	0.08	6810	0.491	151.2	0.40	60.5	86.43
Pigs	2	0	0.000	0.00	0.37	0.0	0.0
Horse	10	133	1.197	82.8	0.24	19.9	28.43
Donkey	10	1007	9.063	1360	0.24	326.4	466.3
Total animal manure Biomass			30.235	5235.8	0.27	1398.3	1998

The total collectable fresh animal manure biomass potential of the study area is estimated to be 30.235tonnes/day and its biogas production capacity is 1398.3m3/day.

2.5.6. Biogas potential of the study area from human feces

Human feces are another feedstock for biogas production in the study area and the potential biogas production from human feces is discussed in this section. Feces are mostly made of water (about 75%). The rest is made of dead bacteria that helped us digest our food, living bacteria, protein, undigested food residue (known as fiber), waste material from food, cellular linings, fats, salts, and substances released from the intestines (such as mucus) and the liver.

Table 2-19: Jama Woreda, Kebele-8 districts population data

Population	Site-A	Site-B	Site-C	Site-D	Total
Number of household	390	332	313	100	1135
Average Family per household	4.39(5)	4.39(5)	4.39(5)	4.39 (5)	4.39(5)
Total population	1950	1660	1565	500	5675

One person produces on average 100–140 g of feces per day, the dry matter content of which is about 25% and its biogas yield of about 0.2m3/kg DM [5]. The total collectable fresh manure biomass potential of the case study area from humans is estimated to be 0.681tonnes/day and its biogas production capacity is 34.05m3/day. This figure accounts the collection efficiency of human excreta.
Table 2.20 demonstrates the biogas potential of the study area from human feces.

Table 2-20: Biogas Potential of study area from human feces

Live stock	Ave. Fresh manure, kg/day/ head	Total no. of population	Total Fresh manure potential (tone/day)	Total DM (kg/day)	Biogas, m3/kg DM	Total biogas, m^3/day	Electricity production, kWh/day
Human	0.12	5675	0.681	170.25	0.2	34.05	48.7

2.5.7. Total biogas potential of the study area

The total biogas potential from Jatropha byproduct, Animal waste and human feces discussed above can be summarized in this section.

Taking the density of biogas 1.15kg/m3 and calculating the gasification ratio (the mass of biogas produced per unit mass of feed stock consumed) of the biogas system. From table 3.16 the mass of biogas feedstock consumed is 31850kg/day and the gas produced is 1736.4m3/day. Therefore the gasification ratio of biogas feedstock mix is 1736.4m3/31850kg=0.0545m3/kg=**0.0626kg/kg**.

Table 2-21: The total biogas and collectable feedstock potential of the study area

Animal Livestock	Ave. Fresh manure, kg/day/ head	Total no. of live stock	Total collectable Fresh manure (tone/day)	Total collectable DM (kg/day)	Biogas, m3/kg DM	Total biogas production, m^3/day	Electricity yield, kWh/ day
Cows	4.5	1935	7.837	1309.5	0.24	315	450
Oxen	4.5	2092	8.473	1415.7	0.24	340	486
Goats	1	476	0.238	73.5	0.37	27.3	39
Sheep	1	5350	2.675	821.5	0.37	304	434.3
Mule	10	29	0.261	21.6	0.24	5.2	7.43
Chicken	0.08	6810	0.491	151.2	0.40	60.5	86.43
Pigs	2	0	0.000	0.00	0.37	0.0	0.0
Horse	10	133	1.197	82.8	0.24	19.9	28.43
Donkey	10	1007	9.063	1360	0.24	326.4	466.3
Human	0.12	5675	0.681	170.25	0.2	34.05	48.7
Jatropha Byproduct biomass			0.253	253	1.07	270	386
Total			31.85	5829.3	0.3	1736.4	2481.4

As we have seen from Table 2.21, animal manure is the major biogas feedstock constitutes which accounts 97% from the total biogas feedstock potential where as jatropha byproducts and human excreta constitute 1% and 2% of the total biogas feedstock potential of the study area respectively. However, the share of biogas production from, animal manure is 82%, and human excreta is 2% but biogas production from jatropha byproduct is increase to 16% regardless of its low contribution to the biomass potential since the biogas yield of jatropha byproduct is high as compared to both animal and human manure and this can be summarized in Figure 2.21 given below.

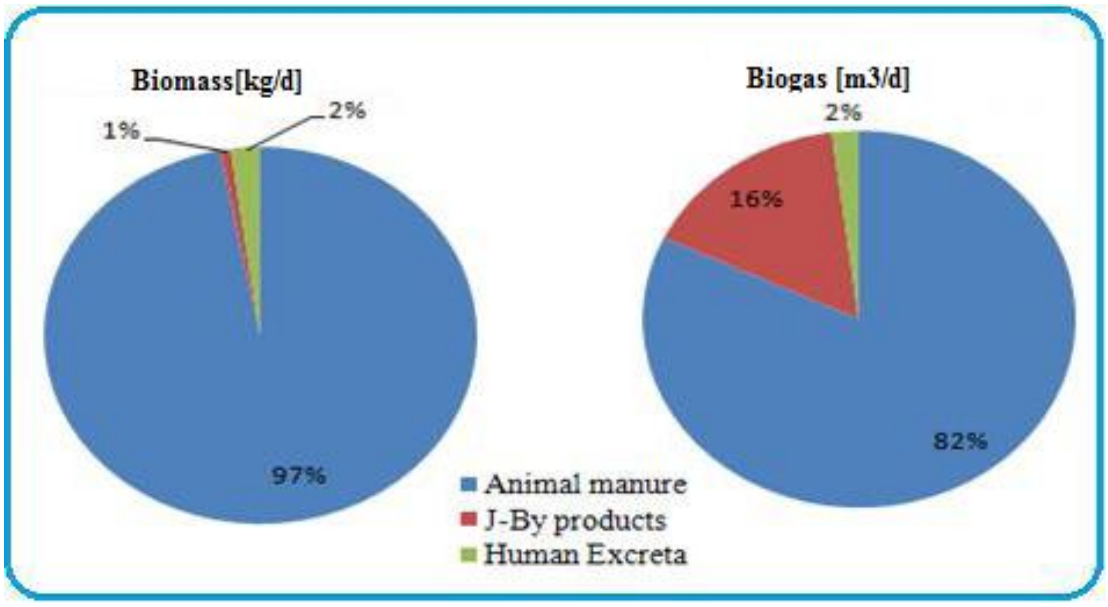

Figure 2-21: Biogas feedstock contributions for biogas production in the study area.

2.5.8. Monthly Variation of the Biogas Feed Stock Potential

The variation of jatropha byproduct feedstocks is assumed to be constant throughout the year and the potential biomass obtained from it was divided to each site regardless of the total house hold in each of the study area.

However, the biomass obtained from animal is highly depending on the availability and type of the animal feeding material. The animal feeding materials are varying in type and amount from month to month in the study area. In June and July there is enough root grass in addition to the usual animal food, let as consider this value as the annual average in tonne/day (the data obtained by multiplying the biomass obtained per animal live stock in tonne/day with the total number of animal live stock for each animal group in the district), as a reference frame. In January, February, and December there is excess dry agricultural farm grass for the animal food in the study area and assuming a 5% biomass resource increment is expected from the reference. March and April is a dry season and there is no enough food for the animal so considering a 5% biomass resource decrement from the reference. May, extremely drought month and August, animal grazing area are not permitted for animal food assuming a 10% animal based biomass resource drop is expected. From September to November there is excess animal food and a 10% biomass growth is assumed. Also assuming chicken manure and human feces are constant throughout the year. Taking in to account the assumption listed above the biogas feedstock potential month to month variation is presented in Table 2.22, 2.23, 2.24, and 2.25.

Table 2-22: Biomass resource of Site-A - 390 families

Month	Biomass, tonnes/day										
	Cow	Oxen	Mule	Horse	Donkey	Sheep	Goats	Chicken	Jatroph	Human	Total
Jan	2.82	3.069	0.114	0.4536	3.28	0.967	0.086	0.17	0.0633	0.234	11.257
Feb	2.82	3.069	0.114	0.4536	3.28	0.967	0.086	0.17	0.0633	0.234	11.257
Mar	2.552	2.775	0.1031	0.4104	2.97	0.875	0.08	0.17	0.0633	0.234	10.233
Apr	2.552	2.775	0.1031	0.4104	2.97	0.875	0.08	0.17	0.0633	0.234	10.233
May	2.417	2.63	0.0972	0.3654	2.811	0.83	0.074	0.17	0.0633	0.234	9.693
Jun	2.686	2.921	0.108	0.432	3.123	0.921	0.082	0.17	0.0633	0.234	10.740
Jul	2.686	2.921	0.108	0.432	3.123	0.921	0.082	0.17	0.0633	0.234	10.740
Aug	2.417	2.63	0.0972	0.3654	2.811	0.83	0.074	0.17	0.0633	0.234	9.6912
Sep	2.954	3.213	0.119	0.475	3.4353	1.013	0.09	0.17	0.0633	0.234	11.767
Oct	2.954	3.213	0.119	0.475	3.4353	1.013	0.09	0.17	0.0633	0.234	11.767
Nov	2.954	3.213	0.119	0.475	3.4353	1.013	0.09	0.17	0.0633	0.234	11.767
Dec	2.82	3.069	0.114	0.4536	3.28	0.967	0.086	0.17	0.0633	0.234	11.257
Average	2.693	2.958	0.1096	0.4335	3.1628	0.9327	0.083	0.17	0.0633	0.234	10.867

Table 2-23: Biomass resource of Site-B - 332 families

Month	Biomass, tonnes/day										
	Cow	Oxen	Mule	Horse	Donkey	Sheep	Goats	Chicken	Jatropha	Human	Total
Jan	2.40	2.614	0.095	0.378	2.788	0.823	0.073	0.144	0.0633	0.183	9.56
Feb	2.40	2.614	0.095	0.378	2.788	0.823	0.073	0.144	0.0633	0.183	9.56
Mar	2.17	2.364	0.086	0.342	2.523	0.744	0.066	0.144	0.0633	0.183	8.69
Apr	2.17	2.364	0.086	0.342	2.523	0.744	0.066	0.144	0.0633	0.183	8.69
May	2.056	2.240	0.081	0.324	2.390	0.706	0.062	0.144	0.0633	0.183	8.25
Jun	2.284	2.489	0.09	0.36	2.655	0.784	0.070	0.144	0.0633	0.183	9.12
Jul	2.284	2.489	0.09	0.36	2.655	0.784	0.070	0.144	0.0633	0.183	9.12
Aug	2.056	2.240	0.081	0.324	2.38	0.706	0.062	0.144	0.0633	0.183	8.24
Sep	2.513	2.737	0.099	0.469	2.921	0.862	0.077	0.144	0.0633	0.183	10.07
Oct	2.513	2.737	0.099	0.469	2.921	0.862	0.077	0.144	0.0633	0.183	10.07
Nov	2.513	2.737	0.099	0.469	2.921	0.862	0.077	0.144	0.0633	0.183	10.07
Dec	2.40	2.614	0.095	0.378	2.788	0.823	0.073	0.144	0.0633	0.183	9.56
Average	2.313	2.52	0.09	0.383	2.69	0.794	0.071	0.144	0.0633	0.183	9.25

Table 2-24: Biomass resource of Site-C - 313 families

Month	Biomass, tonnes/day										
	Cow	Oxen	Mule	Horse	Donkey	Sheep	Goats	Chicken	Jatropha	Human	Total
Jan	2.263	2.46	0.085	0.755	2.637	0.776	0.069	0.136	0.0633	0.188	9.434
Feb	2.263	2.46	0.085	0.755	2.637	0.776	0.069	0.136	0.0633	0.188	9.431
Mar	2.048	2.23	0.077	0.316	2.385	0.702	0.062	0.136	0.0633	0.188	8.206
Apr	2.048	2.23	0.077	0.316	2.385	0.702	0.062	0.136	0.0633	0.188	8.206
May	1.94	2.13	0.073	0.30	2.26	0.665	0.059	0.136	0.0633	0.188	7.812
Jun	2.156	2.35	0.081	0.333	2.511	0.739	0.066	0.136	0.0633	0.188	8.618
Jul	2.156	2.35	0.081	0.333	2.511	0.739	0.066	0.136	0.0633	0.188	8.618
Aug	1.94	2.123	0.073	0.30	2.26	0.665	0.059	0.136	0.0633	0.188	7.812
Sep	2.37	2.556	0.089	0.41	2.76	0.813	0.072	0.136	0.0633	0.188	9.457
Oct	2.37	2.556	0.089	0.41	2.76	0.813	0.072	0.136	0.0633	0.188	9.457
Nov	2.37	2.556	0.089	0.418	2.76	0.813	0.072	0.136	0.0633	0.188	9.457
Dec	2.263	2.463	0.085	0.755	2.637	0.669	0.069	0.136	0.0633	0.188	9.328
Average	2.183	2.372	0.082	0.449	2.542	0.739	0.067	0.136	0.0633	0.188	8.820

Table 2-25: Biomass resource of Site-D - 100 families

Month	Biomass, tonnes/day										
	Cow	Oxen	Mule	Horse	Donkey	Sheep	Goats	Chicken	Jatropha	Human	Total
Jan	0.723	0.787	0.029	0.1134	0.841	0.496	0.044	0.0432	0.0633	0.06	3.199
Feb	0.723	0.787	0.029	0.1134	0.841	0.496	0.044	0.0432	0.0633	0.06	3.199
Mar	0.654	0.712	0.026	0.1026	0.761	0.448	0.04	0.0432	0.0633	0.06	2.910
Apr	0.654	0.712	0.026	0.1026	0.761	0.448	0.04	0.0432	0.0633	0.06	2.910
May	0.620	0.674	0.024	0.0972	0.721	0.425	0.038	0.0432	0.0633	0.06	2.766
Jun	0.689	0.750	0.027	0.108	0.801	0.472	0.043	0.0432	0.0633	0.06	3.056
Jul	0.689	0.750	0.027	0.108	0.801	0.472	0.043	0.0432	0.0633	0.06	3.056
Aug	0.620	0.675	0.024	0.0972	0.721	0.425	0.038	0.0432	0.0633	0.06	2.766
Sep	0.757	0.825	0.03	0.1188	0.881	0.519	0.046	0.0432	0.0633	0.06	3.344
Oct	0.757	0.825	0.03	0.1188	0.881	0.519	0.046	0.0432	0.0633	0.06	3.344
Nov	0.757	0.825	0.03	0.1188	0.881	0.519	0.046	0.0432	0.0633	0.06	3.344
Dec	0.723	0.787	0.028	0.1134	0.841	0.496	0.044	0.0432	0.0633	0.06	3.199
Average	0.697	0.759	0.027	0.1094	0.811	0.478	0.043	0.0432	0.0633	0.06	3.091

CHAPTER 3

3. ENERGY SAVING MECHANISM

3.1. Introduction

Energy saving mechanisms for residential application considered under this study are efficient cooking stoves and design of flat plate solar collector. In this study cooking and water heating loads of the communities are not considered to supply them from the hybrid electric power supply system. So, Self contained flat plate solar collector is design for the community hot water requirement and efficient cooking stoves are suggested to the community by assessing various literatures. These are good solution for poor rural community to save their energy consumption and allowed to use clean and renewable energy.

The utilization of solar energy covers a large area of multiple applications. The solar installations for house water heating are the most frequently used. These installations have as primary component of the flat plate solar collector that makes the conversion of solar radiation into thermal energy. Flat plate solar collector gather the sun's energy, transform its radiation into heat, and then transfer that heat to a fluid (usually water or air). There are a large number of solar collector designs that have shown to be functional. These designs are classified in two general types:

- ✓ **Flat-plate collectors** – the absorbing surface is approximately as large as the overall collector area that intercepts the sun's rays.
- ✓ **Concentrating collectors** – large areas of mirrors or lenses focus the sunlight onto a smaller absorber. – Costy and complicated design.

This paper presents a simplified methodology that allows designing of the flat plate solar collector. A software based design and modeling using KOLEKTOR was used with the possibility of a report generating in the software, with the unit values calculated.

Improved stoves dissemination in Ethiopia in the past already showed to involve over 25,000 individuals mostly women, creating jobs and business opportunities for both urban and rural poor, boosting involvement of the local supply chain. To reach 80% of the household in rural cities and villages with improved cooking stoves, the government plan to disseminate 9 million efficient cooking stoves up to 2015 and additional 25.2 million in 2016-2030 [3]. In order to match with this plan, research on the area should be conducted and interpret the study with the country context is necessary.

3.2. Design of Flat Plate Solar Collector

3.2.1. Mathematical Model of Collector

The core of the design tool KOLEKTOR 2.2 is a mathematical model of solar flat plate liquid collector solving one-dimensional heat transfer balances. Detailed geometrical,

thermal and optical properties of individual elements of solar collector, climatic and operation conditions are the input parameters of the model. Basic outputs of the model are:

- ✓ Usable heat gain Q_u ,
- ✓ Efficiency, η with respect to reference collector area (aperture area A_a)
- ✓ Output heat transfer fluid temperature t_e.
- ✓ And the advanced outputs as heat transfer coefficients, temperatures of main surfaces in collector layout.

The mathematical model of solar collector consists of external energy balance of absorber (heat transfer from absorber surface to ambient environment) and internal energy balance of absorber (heat transfer from absorber surface into heat transfer fluid). The model solves the energy balance of the solar collector under steady-state conditions according to principle Hottel-Whillier equation for usable thermal power, Qu.

$$Qu=A_a.F_R\,[\tau\alpha G-U\,(T_{in}-T_a)] \qquad (3.1)$$

Through the external energy balance of absorber the heat transfer by radiation and by natural convection in the air gap between absorber surface and glazing, heat conduction through glazing and heat transfer by convection and radiation from exterior glazing surface to ambient is solved. To calculate the heat transfer coefficients properly, temperatures for principal collector levels (surfaces) should be known, but on the other side the temperature distribution in the collector is dependent on the heat transfer coefficients values.

3.2.1.1. External energy balance of the absorber

General external energy balance of the absorber can be described by Eq^{n} 3.2 given in differential form.

$$\frac{dQ}{dt}=G_i-P_{op}-P_{hl}-P_u \qquad (3.2)$$

Where

$\frac{dQ}{dt}$ - is change of heat content in collector;

G_i - solar irradiation incident on collector area, in W;

P_{op} - optical loss, in W;

P_{hl} - heat loss, in W;

P_u - useful thermal power from collector, W.

The model and design tool KOLEKTOR is developed primary for evaluation of collector performance, comparable with experimental testing under steady state conditions (term dQ/dt=0). By expanding the individual terms from the Equation above, a detailed balance is obtained in Equation below.

$$Q_u=G.A_a\,(\tau\alpha)_{ef}-U_pA_G(t_{abs}-t_a)-U_zA_G(t_{abs}-t_a)-U_bA_b(t_{abs}-t_a) \qquad (3.3)$$

Where
G-is solar irradiation, in W/m2;
t_{abs}-absorber temperature, in °C;
t_a-ambient temperature, in °C
τ-solar radiation transmittances of collector cover glazing;
A_a-collector aperture area, in m2;
A_b-collector edge area, in m^2;
α-solar radiation absorptance of absorber;
U_p-heat loss coefficient for front side of the collector, in W/m2K;
U_z-heat loss coefficient for back side of the collector, in W/m2K;
U_b-heat loss coefficient for edge side of the collector, in W/m2K;
A_G-collector gross area, in m^2.

The model solves the heat transfer coefficients from absorber to ambient through front side (gas layer and cover), through back and edge side (gas layer and insulation frame). Solar collector is defined by means of main levels: glazing exterior surface (p1), glazing interior surface (p2), absorber (abs), frame interior surface (z2) and frame exterior surface (z1). Ambient environment is labeled with (a). These levels are schematically outlined in Figure 3.1. In KOLEKTOR 2.2, the edge side is considered the identical construction as for back side.

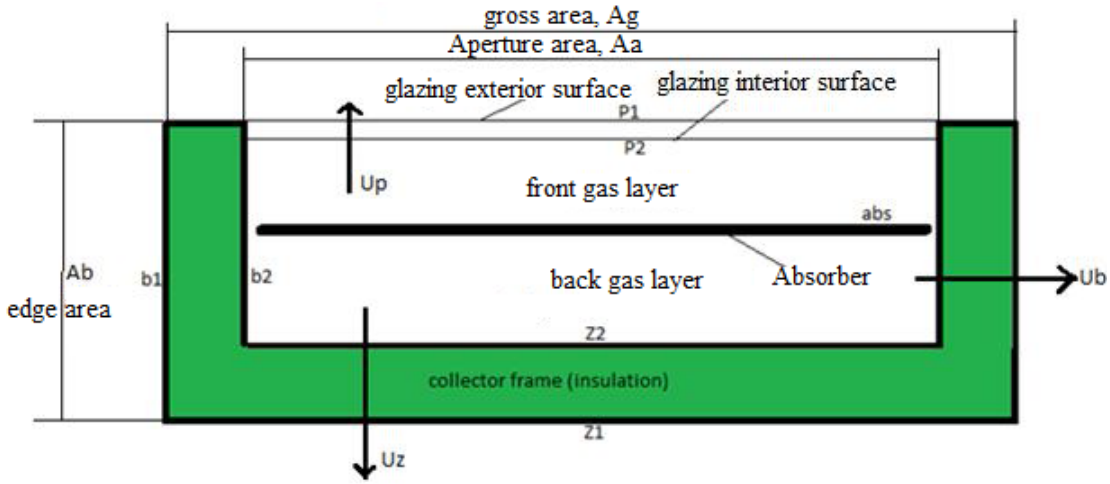

Figure 3-1: Main temperature levels (surfaces) in solar collector model.

The heat transfer in collector can be described by:

- Radiation between absorber and interior surface of cover glazing and interior surface of collector frame (back and edge side);
- Natural convection between absorber and interior surface of cover glazing, interior surface of collector frame.
- Heat conduction through cover glazing and collector frame (insulation).

- Radiation between exterior surface of cover glazing and sky dome, and exterior surface of collector frame and adjacent surfaces.
- Natural and forced convection at exterior surface of cover glazing, and exterior surface of collector frame.

The collector element, the calculated heat transfer coefficient is appropriate to, is defined by pair of indices designating the boundary surfaces (main levels of collector), e.g. gas layer (air gap) between absorber and interior surface of glazing is designated by index $p_{2\text{-}abs}$. The principle regimes of heat transfer are designated as: *v*–conduction; *p* – convection; *s* – radiation.

I. Radiation between glazing and sky ($h_{s,p1\text{-}a}$)

To describe the heat exchange between glazing exterior surface and sky, the sky area is considered as a black body of equivalent temperature T_o. T_o be defined based on absolute ambient temperature T_a [K] as given in Equation below.

$$T_o^4 = \varepsilon_o T_a^4 \qquad (3.4)$$

Where, ε_o-is sky emittance

Radiation heat exchange between exterior surface of glazing and sky is given by: [63]

$$Q_{p1\text{-}a} = \varepsilon_{p1}\sigma(T^4_{p1} - T^4_o) = h_{s,\,p1\text{-}a}\,(T_{p1} - T_a)$$

$$h_{s,p1-a} = \varepsilon_{p1}\sigma\frac{T_{p1}^4 - T_o^4}{T_{p1} - T_a} \qquad (3.5)$$

Where

ε_{p1}–is emittance of exterior surface of cover glazing;

σ–Stefan-Boltzmann constant, σ = 5.67x10^{-8} W/m^{2}K^4;

*T*p1 -absolute temperature of exterior surface of cover glazing, in K;

*T*a- absolute ambient temperature, in K.

$h_{s,p1-a}$ – Radiation heat transfer coefficient.

II. Wind convection from glazing to ambient ($h_{p,p1\text{-}a}$)

A large number of relationships and correlations derived from experiments, more or less reproducing the boundary conditions of solar collector installation, can be found in literature. The most of authors keep the correlation as simple as possible resulting in Equation below in the form of linear function:

$$h_w = a + b.w \qquad (3.6)$$

Where *w* is wind velocity, in m/s.

In the solar collector theory, the most used wind convection model is correlation according to McAdams, [64] as given in Equation below:

$$h_{p,\ p1\text{-}a} = h_w = 5.7 + 3.8w \qquad (3.7)$$

III. Radiation between absorber and cover glazing ($h_{s,abs\text{-}p2}$)

Radiation heat transfer between absorber front surface and interior surface of glazing is given by Stefan-Boltzmann law: [63]

$$q_{s,abs-p2} = \sigma \frac{T_{abs}^4 - T_{p2}^4}{\frac{1}{\varepsilon_{p2}} + \frac{1}{\varepsilon_{abs,p}} - 1} = h_{s,abs-p2}(T_{abs} - T_{p2}) \qquad (3.8)$$

T_{abs} absorber surface temperature, in K;

ε_{p2} emittance of glazing interior surface;

$\varepsilon_{abs,\ p}$ emittance of front absorber surface

Radiation heat transfer coefficient is given by:

$$h_{s,abs-p2} = \frac{q_{s,abs-p2}}{T_{abs} - T_{p2}} = \sigma \frac{T_{abs}^4 - T_{p2}^4}{\frac{1}{\varepsilon_{p2}} + \frac{1}{\varepsilon_{abs,p}} - 1} \cdot \frac{1}{T_{abs} - T_{p2}} \qquad (3.9)$$

IV. Radiation between absorber and back frame ($h_{s,z2\text{-}abs}$)

Radiation heat transfer coefficient between back surface of absorber and interior surface of collector frame (back side of collector) is given by Stefan-Boltzmann law similarly as in part-III.

$$h_{s,z2-abs} = \sigma \frac{T_{abs}^2 + T_{z2}^2}{\frac{1}{\varepsilon_{z2}} + \frac{1}{\varepsilon_{abs,z}} - 1} (T_{abs} + T_{z2}) \qquad (3.10)$$

Where

T_{z2} is frame interior surface temperature, K;

T_{abs} absorber surface temperature, in K;

ε_{z2} emittance of frame interior surface;

$\varepsilon_{abs,z}$ emittance of back absorber surface.

Distinction between front and back absorber surface emittance is necessary since most of solar flat-plate collectors is equipped with spectrally selective coating at front absorber surface (low emittance in IR region) while back surface is left without any treatment (oxidized, dirty, etc.).

V. Conduction heat transfer through frame ($h_{v,z1\text{-}z2}$)

Thermal conductance of collector back frame (thermal insulation) is given by equation below:

$$h_{v,z1-z2} = \frac{\lambda_{z1-z2}}{L_{z1-z2}} \qquad (3.11)$$

Where

$\lambda_{z1\text{-}z2}$ is thermal conductivity of back frame material (mostly insulation), in W/mK;

$L_{z1\text{-}z2}$ thickness of back frame material, in m.

VI. Radiation heat exchange between frame and adjacent ambient surfaces ($h_{s,z1\text{-}a}$)

Radiation heat transfer coefficient between exterior surface of collector back frame and adjacent surfaces in ambient environment (roof) related to ambient temperature $\boldsymbol{T_a}$ can be expressed as:

$$h_{s,z1-a} = \sigma \frac{T_{z1}^4 - T_{as}^4}{\frac{1}{\varepsilon_{z1}} + \frac{1}{\varepsilon_{as}} - 1} \cdot \frac{1}{T_{z1} - T_a} \qquad (3.12)$$

Where

$\boldsymbol{T_{z1}}$ is temperature of frame exterior, K;

$\boldsymbol{T_{as}}$ is temperature of adjacent surface,

$\boldsymbol{T_a}$ absolute ambient temperature, in K;

$\boldsymbol{\varepsilon_{z1}}$ emittance of frame exterior surface;

$\boldsymbol{\varepsilon_{as}}$ emittance of adjacent surface.

For most cases in ambient environment, $\boldsymbol{T_{as}}$ can be considered as equal to T_a.

VII. Wind convection heat transfer from back frame to ambient ($h_{p,z1\text{-}a}$)

Wind convection heat transfer coefficient from back side of collector frame to ambient can be determined using Eqn. 3-7.

VIII. Conduction through glazing ($h_{v,p1\text{-}p2}$)

Thermal conductance of cover glazing is given by

$$h_{v,p1-p2} = \frac{\lambda_{p1-p2}}{L_{p1-p2}} \qquad (3.13)$$

Where

$\lambda_{p1\text{-}p2}$ is thermal conductivity of cover glazing, in W/mK;

$L_{p1\text{-}p2}$ thickness of cover glazing or transparent cover structure, in m.

IX. Collector heat loss coefficient (*U*-value)

Overall heat loss coefficient, U of the collector can be determined as follows: [63]
Heat loss coefficient for front side of the collector $\mathbf{U_p}$ can be determined as

$$U_p = \frac{1}{\frac{1}{h_{s,p1-a} + h_{p,p1-p2}} + \frac{1}{h_{v,p1-p2}} + \frac{1}{h_{s,abs-p2} + h_{p,abs-p2}}} \qquad (3.14)$$

By analogy, heat loss coefficient for back side of the collector $\mathbf{U_z}$ can be determined as:

$$U_z = \frac{1}{\frac{1}{h_{s,z1-a}+h_{p,z1-a}} + \frac{1}{h_{v,z1-z2}} + \frac{1}{h_{s,abs-z2}+h_{p,abs-z2}}} \qquad (3.15)$$

Heat transfer coefficients for edge side of the collector frame can be determined in similar way as for the back side. On the other side, the usable heat output of the collector refers to aperture area A_a. From the balance of specific heat loss overall collector heat loss coefficient U used in the internal energy balance calculations should be: [63]

$$U_G A_G = U_p A_G + U_z A_G + U_b A_b = U A_a \qquad (3.16)$$

The overall heat loss coefficient U based on aperture area can be obtained as

$$U = (U_p + U_z + U_z \frac{A_b}{A_G}) \frac{A_G}{A_a} \qquad (3.17)$$

3.2.1.2. Internal energy balance of the absorber

Heat transfer from absorber to liquid flowing through the pipe register of absorber can be described by internal energy balance of the absorber. Schematic outline of absorber balance and temperature profile at the fin cross section is shown below:

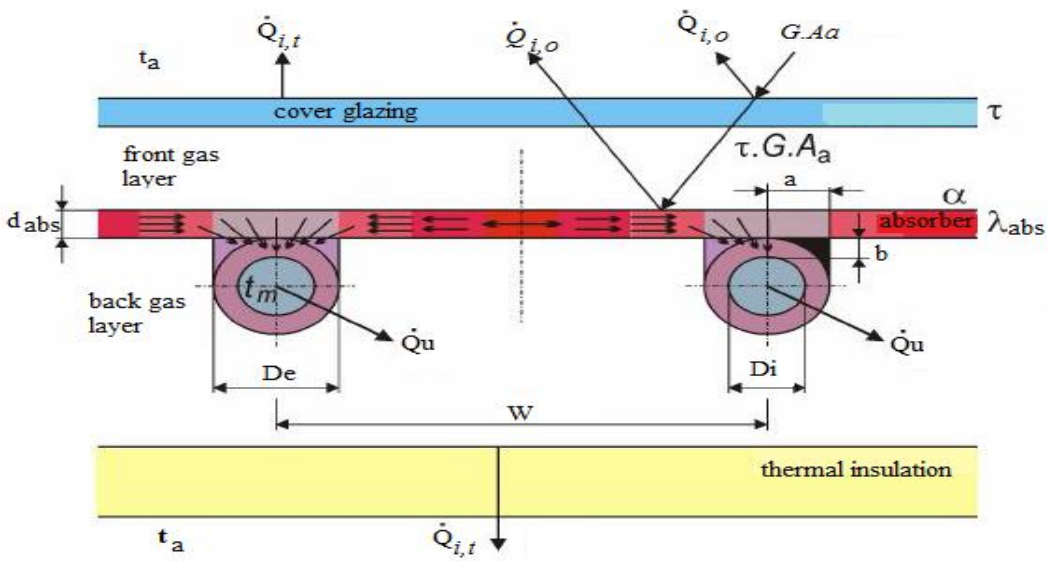

Figure 3-2: Energy balance schematics of FP solar collector.

I. Absorber efficiency factor, *F'*

Not only the conduction heat transfer by the fin (absorber), but also conduction through the bond fin-pipe and heat transfer from pipe to liquid by forced convection influence the overall heat transfer from absorber surface to heat transfer liquid. The parameter describing how efficient is heat transfer from absorber surface to heat transfer fluid is called collector or absorber efficiency factor F′. It can be regarded as a ratio of two heat loss coefficients. It is a

measure of how much of the heat energy absorbed by the collector absorber surface is transferred to heat transfer fluid.

$$F' = \frac{U_o}{U} \qquad (3.18)$$

Where

U_o is heat loss coefficient from liquid to ambient, in W/m^{2}K;

U solar collector heat loss coefficient from absorber to ambient, in W/m^{2}K.

Different absorber configurations (see *Fig. 3.3a-c*) result in appropriate equations.

✓ For upper bond of absorber to riser pipes the efficiency factor is given as:

$$F' = \frac{1/U}{W[\frac{1}{U[D_e+(W-D_e)F]} + \frac{1}{C_{sp}} + \frac{1}{h_i \pi D_i}]} \qquad (3.19)$$

Where, $C_{sp} = \frac{\lambda_{sp} a}{b}$

λ_{sp} is bond thermal conductivity, W/mK

a average bond width, in m;

b average bond thickness, in m

C_{sp} is bond thermal conductance, W/mK

F fin efficiency

D_i internal diameter of riser pipe, in m;

h_i forced convection heat transfer coefficient in riser pipe, in W/m^{2}K

De riser external diameter

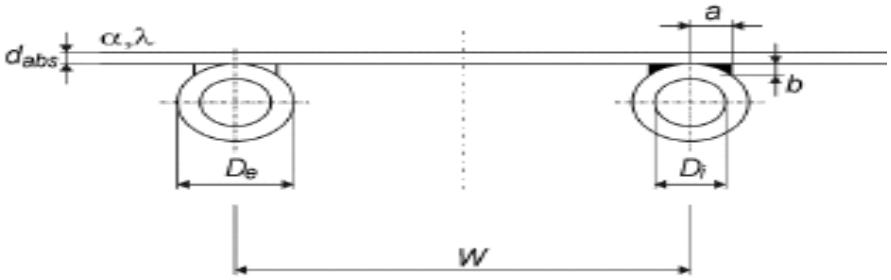

Figure 3-3a: Absorber–pipe upper bond configuration

✓ For side(middle) bond of absorber to riser pipes the efficiency factor is given as

$$F' = \frac{1/U}{W[\frac{1}{U[D_e+(W-D_e)F]} + \frac{1}{h_i \pi D_i}]} \qquad (3.20)$$

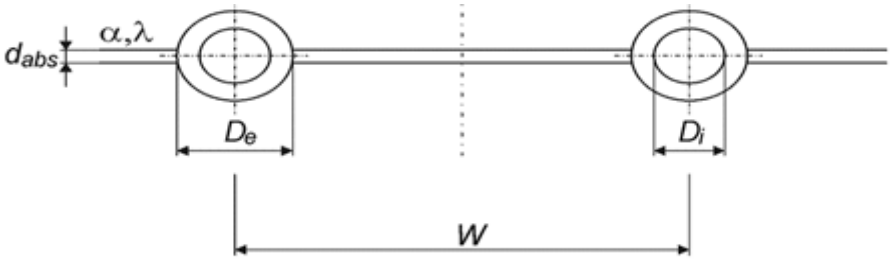

Figure 3-3b: Absorber–pipe side bond configuration

✓ For lower bond of absorber to riser pipes the efficiency factor is given as

$$F' = \frac{1}{\frac{W.U}{h_i \pi D_i} + \frac{1}{\frac{D_e}{W} + \frac{1}{\frac{WU}{C_{sp}} + \frac{W}{(W-D_e)F}}}} \qquad (3.21)$$

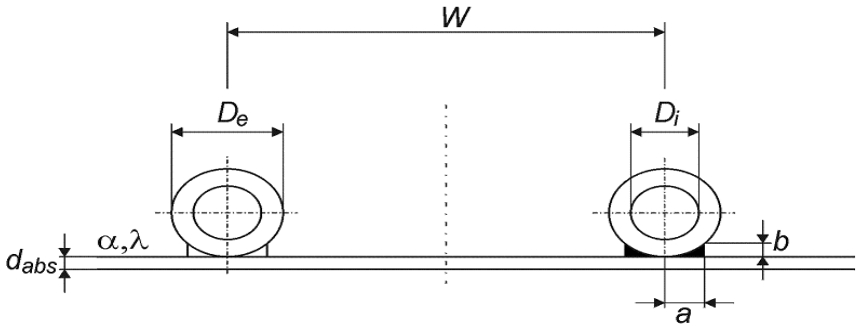

Figure 3-3c: Absorber–pipe lower bond configuration

II. Collector heat removal factor, F_R

Collector heat removal factor *F*R is defined as actual useful energy gain of collector to useful gain if the absorber surface was at the fluid temperature. By introduction of fluid temperature distribution the heat removal factor can be expressed as:

$$F_R = \frac{\dot{M}.C}{A_a.U}[1 - \exp(-\frac{A_a.U.F\prime}{\dot{M}.C})] \qquad (3.22)$$

Where

$\dot{M}$ is total mass flow rate of fluid through solar collector, in kg/s;

C specific thermal capacity of fluid, in J/kgK;

A_a aperture area of solar collector, in m^2.

F' efficiency factor

Collector heat removal factor F_R is equivalent to the effectiveness of a conventional heat exchanger, which is defined as ratio of the actual heat transfer to the maximum possible heat transfer.

III. Useful heat output of solar collector

Useful thermal power output from solar collector can be defined in three different ways, based on given reference collector temperature. From external balance of absorber, the usable thermal power output results as: [63]

$$Q_U = A_a[\tau\alpha_{ef}.G - U(t_{abs} - t_a)] \qquad (3.23)$$

Where,

$(\tau\alpha)_{ef}$ is effective product of transmittance of cover glazing and absorptance of absorber;

U collector heat loss coefficient related to aperture area, in W/m2K;

G solar irradiation incident on aperture, in W/m2;
A_a aperture area of solar collector, in m^2.

The evaluation of thermal power output based on mean absorber temperature t_{abs} is not very practical due to difficulty of identifying t_{abs} by experimental measurements. Expressing the thermal power output based on mean fluid temperature t_m is more practical, because it corresponds with results from experimental testing of solar collectors. Mean fluid temperature can be easily obtained from measured input and output temperatures as:

$$T_{m=\frac{T_{in}+T_{out}}{2}}$$

Where
T_{in} is collector input temperature, in °C;
T_{out} collector output temperature, in °C.

Usable thermal power output from collector based on mean fluid temperature is defined by introduction of efficiency factor F' as

$$Q_U = A_a F'[\tau\alpha_{ef}.G - U(T_m - T_a)] \quad (3.24)$$

For mathematical modeling of solar systems, calculation of heat output and output temperature from collector based on input temperature is needed. Usable heat output based on input temperature can be given as:

$$Q_U = A_a F_R[\tau\alpha_{ef}.G - U(t_{in} - t_a)] \quad (3.25)$$

IV. Efficiency of solar collector

Collector efficiency is defined as usable thermal power output from the collector related to solar radiation input incident on front part of collector (defined by reference collector area = aperture area, A_a). Similarly to usable thermal power output of collector, also efficiency can be related to:

$$\eta = \frac{Q_U}{A_a.G} \quad (3.26)$$

Mean absorber temperature, $\eta = \tau\alpha_{ef} - U(\frac{t_{abs}-t_a}{G})$ (3.27)

Mean fluid temperature, $\eta = F'[\tau\alpha_{ef} - U(\frac{t_m-t_a}{G})]$ (3.28)

Mean input temperature, $\eta = F_R[\tau\alpha_{ef} - U(\frac{t_{in}-t_a}{G})]$ (3.29)

3.2.2. KOLEKTOR Model and Design Output

3.2.2.1.Design and Sensitivity Analysis of Collector

For the design and construction of flat plate solar collector low cost and easily available materials are selected and mathematical modeling and sensitivity analysis of the collector has been done using KOLLEKTOR software.

The climatic parameters of the study area given in Table 3.1 to design the collector are taken from NASA, Meteonorm and various sites. A self contained flat plate solar collector has been designed for each house hold of 60 liter/day hot water demand to heat the water up to 65^{o}c. The collector dimension and riser pipe parameter specified in Table 3.1 is carefully selected to optimize collector cost and loss to deliver the required hot water demand by family. Copper is chosen for construction of the collector absorber surface due to relatively low cost and its good thermal conductivity which provides high heat transfer to fluid (water) and black coating is a must to enhance the solar absorptance of the absorber surface. A glass having good transmittance, low absorptance and reflective property is selected for collector glazing. For collector frame/insulation construction wood is chosen from cost perspective and good insulation property.

Sensitivity analysis was done to identify which collector design parameter greatly affect the output of the collector (fluid output temperature, collector efficiency and collector use full heat output) and to choose the value and type of design parameter for the construction of the collector. The collector design sensitivity values are presented in Table 3.1 given below. For the design, modeling and construction of flat plate solar collector in residential application the following sensitivity input parameters were considered.

- Specific mass flow rate of fluid, M' ($kg/s/m^2$)
- Wind speed, w(m/s)
- Slope of collector, $\beta(^0)$
- The number of pipes, n_{tp}
- Bond type (upper, lower and middle bonding)
- Frame thickness, d_{fr} (mm)
- Glassing thickness, d_{gl} (mm)

The corresponding output variables from the result of the simulation are:

- Output fluid temperature, T_{out} (^{o}c)
- Absorber surface temperature, T_{abs} (^{o}c)
- Mean fluid temperature, T_m(^{o}c)
- Fin efficiency (F'),
- Collector heat removal factor (F_R),
- Collector over all heat loss (U),
- Collector use full thermal power output (Q_u),

Table 3-1: Collector design parameter, values and sensitivity input summary.

Operation and Climatic Condition		Collector Dimension		Absorber Parameter		Pipe register		Glazing parameter		Frame parameter	
Parameter	**Value**	**Parameter**	**Value**	**Parameter**	**Value**	**Parameter**	**Value**	**Parameter**	**Value**	**Parameter**	**Value**
Input fluid temperature	20.4^{o}c	Collector gross height	1m	Material	copper	Material	Steel	Material	glass	Material	wood
						Length of riser pipe	0.94m				
Global solar radiation	832 W/m2	gross width	1m	Material thickness	0.2 mm	Number of riser pipe (sensitivity)	10, 30, 50	Thickness (sensitivity)	4mm, 2mm	Thermal conductivity	0.055 W/mK
Ambient temperature	20.3^{o}c	gross area	1m^2	Material solar absorptance	0.98	Distance between riser pipe	___	Normal solar transmittance	0.95	Thickness (sensitivity)	10, 60 mm
		aperture width	0.94m								
Ambient relative humidity	54%	aperture height	0.94m			Pipe external diameter	10mm	Normal solar reflectance	0.06	External frame surface emissivity	0.95
		Aperture area	0.88 m^2	Material thermal conductivity	390W/ mK						
Wind velocity (sensitivity)	0, 3m/s	Collector depth	0.1m			Pipe internal diameter	8mm	Thermal conductivity	0.8W/ mK		
Collector slope (sensitivity)	0, 12, 45^{o}	Edge sides area	0.42 m^2								
Specific mass flow rate (sensitivity)	0.001, 0.004, 0.01 Kg/s/ m2	Absorber – glazing gap thickness	20mm	Front surface emissivity	0.05	Average bond width	3mm	External glazing surface emissivity	0.85	Internal frame surface emissivity	0.95
						Average bond thickness	3mm				
		Absorber-back frame gap thickness	20mm					Internal glazing surface emissivity	0.85		
Adjacent frontal surface emissivity	0.8			Back surface emissivity	0.5	Bond thermal conductivity	300W /mK				

3.2.2.2. Summary of KOLEKTOR Model

From the sensitivity analysis result of KOLEKTOR shown in Appendix B, we can observe that:

- Wind speed, flow rate and frame thickness are greatly influence the output of the collector
- The effect of collector slope has negligiable effect on collector output
- Middle and lower pipe bonding of the riser give relatively good collector output.
- Low fluid flow rate gives higher fluid output temperature but lower collector efficency.

Wind convection heat loss can be minimized by putting wind shatter that made the wind speed on the collector is zero with out affecting the solar irradiance reached on the collector. Where as the collector slope is associated with the fluid flow rate so that the collector should be sloped to give low flow rate but satisfied family hot water demand. The collector efficency and usefull thermal power output for each sensitivity case can be determined using Equation 3.24 and 3.28 (see Appendix B). The sensitivity analysis result shows that a collector of efficency ranges from 42.7%-88.4%. a higher collector efficency associated with more number of riser pipe which increase the cost of the collector so that a collector having good efficency and deliver a fluid temperature of 63 ^{o}c is selected for impelmentation. Sensitivity number 14 and 19 satisfies this condition but no.-19 increase system cost due to large number of pipe requirment so sensitivity no. 14 is chosen for impelmentation and the simulation result report of this system is shown below.

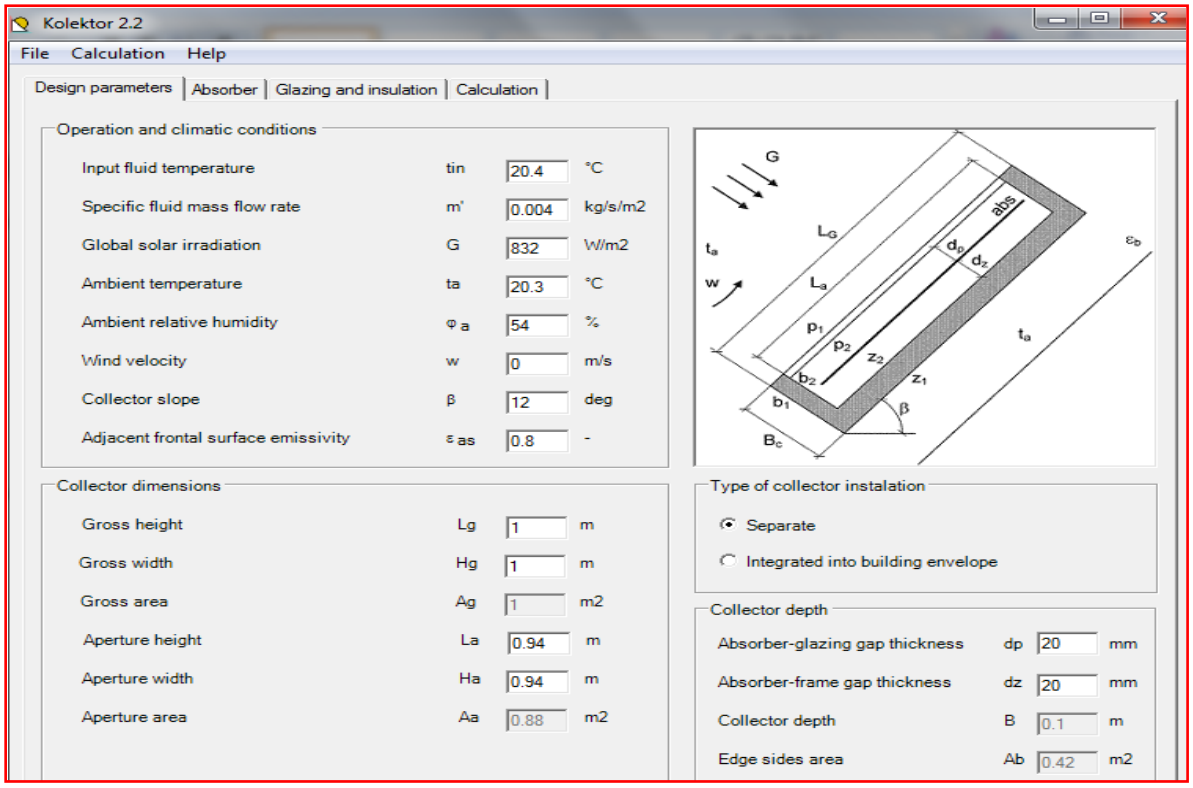

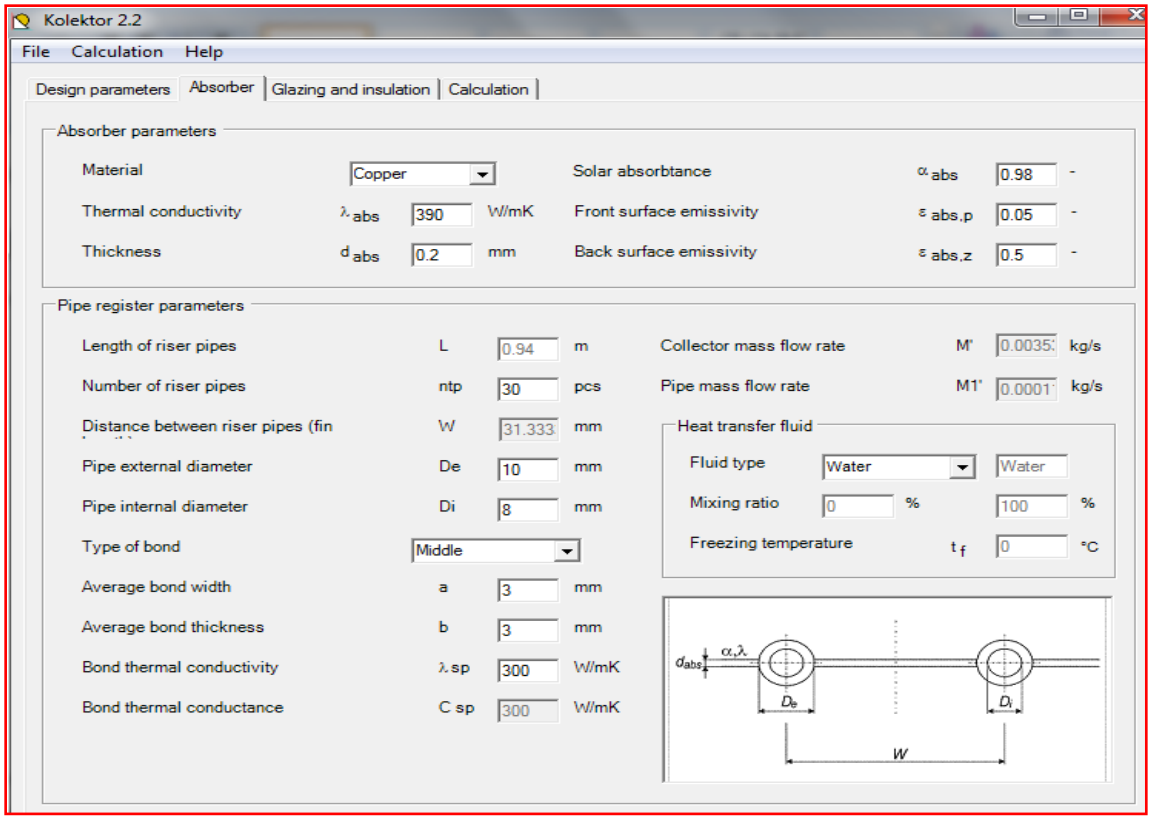
Kolektor 2.2
File Calculation Help
Design parameters Absorber Glazing and insulation Calculation
Absorber parameters
Material Copper
Thermal conductivity λ abs 390 W/mK
Thickness d abs 0.2 mm
Solar absorbtance α abs 0.98 -
Front surface emissivity ε abs,p 0.05 -
Back surface emissivity ε abs,z 0.5 -
Pipe register parameters
Length of riser pipes L 0.94 m
Number of riser pipes ntp 30 pcs
Distance between riser pipes (fin W 31.333 mm
Pipe external diameter De 10 mm
Pipe internal diameter Di 8 mm
Type of bond Middle
Average bond width a 3 mm
Average bond thickness b 3 mm
Bond thermal conductivity λ sp 300 W/mK
Bond thermal conductance C sp 300 W/mK
Collector mass flow rate M' 0.0035 kg/s
Pipe mass flow rate M1' 0.0001 kg/s
Heat transfer fluid
Fluid type Water
Mixing ratio 0 % 100 %
Freezing temperature t f 0 °C
dabs
α,λ
De
Di
W

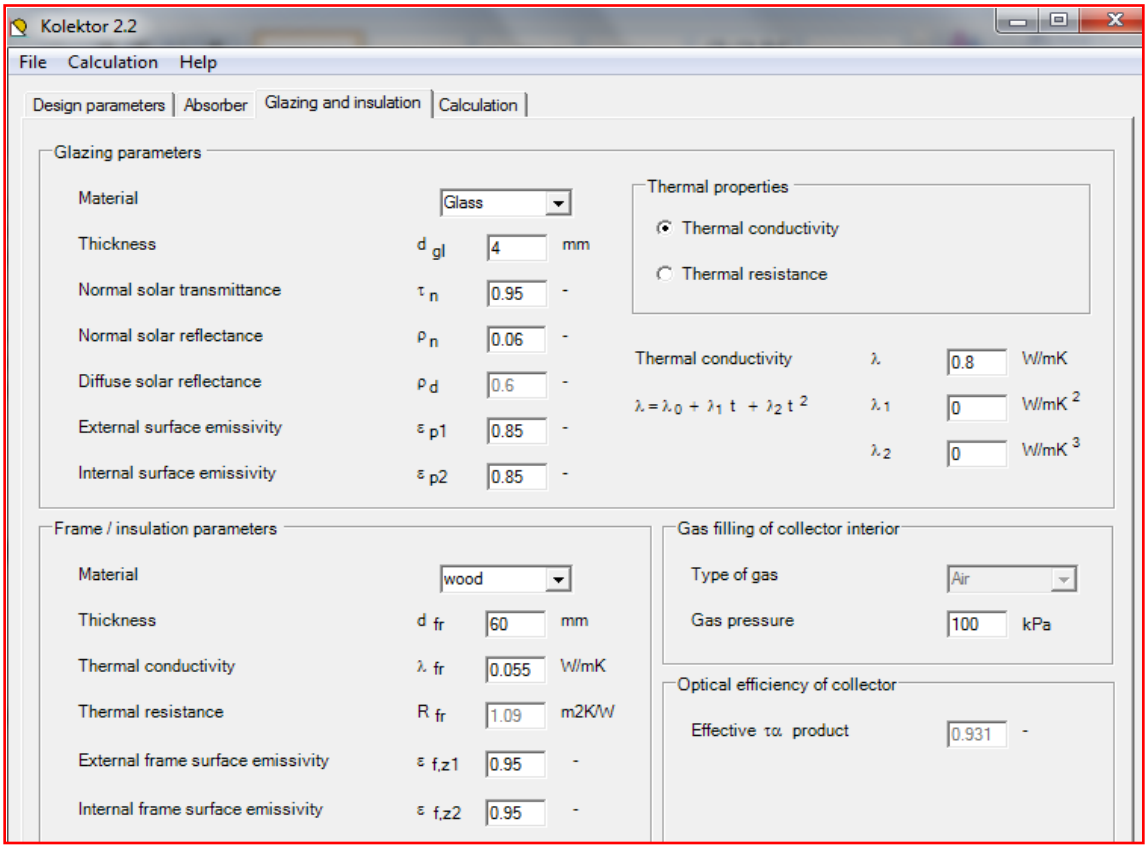
Kolektor 2.2
File Calculation Help
Design parameters Absorber Glazing and insulation Calculation
Glazing parameters
Material Glass
Thickness d gl 4 mm
Normal solar transmittance τ n 0.95 -
Normal solar reflectance ρ n 0.06 -
Diffuse solar reflectance ρ d 0.6 -
External surface emissivity ε p1 0.85 -
Internal surface emissivity ε p2 0.85 -
Thermal properties
Thermal conductivity
Thermal resistance
Thermal conductivity λ 0.8 W/mK
λ = λ0 + λ1 t + λ2 t 2
λ1 0 W/mK 2
λ2 0 W/mK 3
Frame / insulation parameters
Material wood
Thickness d fr 60 mm
Thermal conductivity λ fr 0.055 W/mK
Thermal resistance R fr 1.09 m2K/W
External frame surface emissivity ε f,z1 0.95 -
Internal frame surface emissivity ε f,z2 0.95 -
Gas filling of collector interior
Type of gas Air
Gas pressure 100 kPa
Optical efficiency of collector
Effective τα product 0.931 -

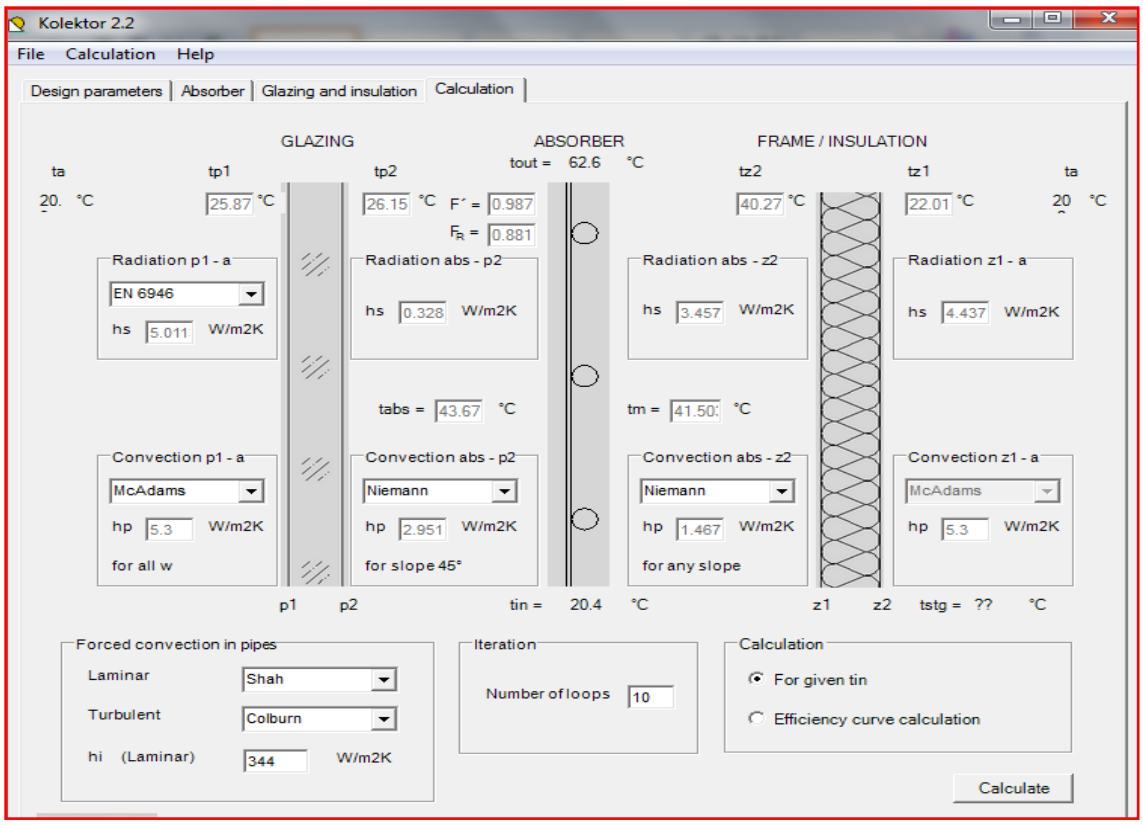

3.3. Improved Cooking Stoves

Various biomass cooking stove technologies are reviewed around the world and stoves which are efficient but applicable for developing countries are suggested to the community under this study. These are good solution for poor rural community to save their energy consumption and allowed to use clean and renewable energy.

3.3.1. Stove Technologies

Various stove technologies, using primarily biomass, and potentially suitable for further of East Africa were picked for a closer look. These are grouped under the main categories of mud-stoves, metal stoves and fired clay stoves.

3.3.1.1. Mud-Stoves

Mud-stove is used here to describe any improved form of stove compared to traditional "three-stone-fireplace". Mud stoves are usually easy to build with simple training, and material is available locally.

I. Traditional Single-pot mud stove

The traditional mud stove is made by using earthen mixture of sand and clay. Some fixed models also use bricks to form the base of the stove, but for example Aprovecho has developed a portable model using only sand, clay and sawdust. It weighs approximately 6 kg

[65]. It uses wood as fuel but can be adapted to charcoal. Most of the traditional models do not have chimney. It is easy to make locally through set of instruction and cost for making the stove is normally free or very low. Mud stoves can be built in big sizes, however compared to fired clay stoves they are not very durable and they suit best for indoors, where they are not affected by rain [66][67]. Energy savings of about 20% over three-stone fireplaces are achievable with basic mud-stoves. [68]

Figure 3-4 a). Single pot mud stove. [69] b). Traditional 3-stone stove

II. Rocket mud stoves

The rocket stove principles were developed about 10 years ago by Dr. Larry Winiarski at the Aprovecho Research Center in Oregon [70]. Very often rocket mud stoves have external chimneys to remove smoke from the kitchen [71]. The stove is designed for household use and is suitable for both large and small families.

Figure 3-5: schematics of Rocket Mud Stove

How is it made?

- **Materials:** The rocket mud stove is made from mud (clay or sand and cement), sometimes mixed with straw or anthill soil (for better efficiency).

- **Skills and tools:** stoves can be produced by local artisans and no special tools are needed
- **Instructions** to build rocket mud stove: (http://www.appropedia.org/Rocket_Lorena_Stove)

3.3.1.2.Metal Stoves

Metal stoves can be built simply by using scrap metal, however construction requires semi-skilled artisans. Simple models use firewood, but metal stoves can also be adapted to use charcoal. Even if the production costs are fairly low, the metal body radiates heat so the energy savings are relatively low (25 % at most). Also the metal stoves usually do not last very long. [72]

I. The Metal Rocket Stoves

Compared to rocket mud stoves (see 3.3.1.1-II), metal rocket stoves are usually 1-pot solutions, lightweight and thus portable. Like the rocket mud stove it also uses small pieces of wood, branches and brushwood. Most common models do not have external chimneys.

How is it made?

- **Materials:** Scrap metal (such as tin cans). Insulation material (for combustion chamber) should be as light as possible and full of air pockets, such as ashes, pumice rock or perlite. However, if these are not available, sand and clay can be used, but it reduces the efficiency and makes the stove heavier.
- **Skills and tools:** A tool to cut thin metal sheet. Building of a metal rocket stove is estimated to take one day.
- **Instructions** how to build a metal rocket stove: [73]

Aprovecho has evaluated the price varying between 100 – 200 Rand ($9.7-$19.4) depending on which material is used [74].

Figure 3-6: The metal Rocket Stoves. [75]

II. VITA Metal Stove

VITA stove was designed by Sam Baldwin and it is a single pot stove that can be constructed easily from sheet metal. It is inexpensive to build and is suitable for cooking outdoors and in refugee situations. it is a simple metal cylinder that surrounds a dedicated pot. The increased heat transfer efficiency improves fuel used, time to boil, etc. compared to the three stone fire place. The air inlets and size of the opening into the fire are scientifically designed.[76, 77]

How is it made?

- **Materials:** sheet metal
- **Skills and tools:** hammer and chisel, but also special tools such as a press for forming the pot support can be used to reduce time. Can be produced by unskilled workers, with supervision and a few days of training.
- **Instructional video:** Building a VITA stove: http://www.aprovecho.org/web-content/media/vita/vita.html.

The main arguments for using the VITA stove are that it is relatively low cost stove which is easy to build. It also cooks rapidly, and as with all metal stoves, fire is contained, which reduces risk of burns.

Figure 3-7: The metal VITA stoves.

III. KSG Metal Stove

This stove was introduced by Kisangani Smith Group in Tanzania in 2005. The stove is designed to burn wood more efficiently and has a sheet metal exterior, lined with clay and bricks to form the combustion chamber. The stove burns firewood and is portable. The stove is lit by inserting burning wood in the inlet port and setting light to it. Once the fire is established, a cooking pot is put in place. Due to the high thermal mass, this stove takes some time to heat up but once the bricks and clay are hot, they retain their heat well. Pieces of wood are continually inserted to keep the fire burning. The expected life of these stoves is three to five years [78].

How is it made?

- **Materials:** sheet metal, clay and bricks
- **Skills and tools:** needs trained artesian.
- **How to construct a KSG stove**: The wood stove has a cylindrical body about 400 mm tall and 400 mm in diameter, with feet to raise it off the ground. At one side an entry port at the base serves as the air inlet. The lid has a pot stand, and a heat spreader. Stove parts are cut from sheet metal according to eight templates and then fastened by folding and riveting. Once the metal body and entry port have been made, the floor of the stove is covered with clay. Insulating bricks are fitted around the sides and held in with clay, making sure that the air inlet is kept free. The bricks help to form an internal chimney and direct the combustion gases towards the hole in the centre of the lid. A steel tube is used to pack the clay and smooth the top surface. The stove lid normally remains in place once it has been attached, but it can be removed for maintenance.

Various performance measurement of this stove suggests that it uses 75% less wood than an open fire. It costs around USD 27 in 2005.

Figure 3-8: KSG metal stove

IV. The Vesto Metal stove

The stove was developed by New Dawn Engineering in Swaziland. It has been designed for mass production, and the prices are set so that it would be in the reach of low income households. The Vesto (the variable energy stove) is a one-pot stove based on modified 25 liter paint can. In addition of firewood, the Vesto can use a variety of biomass. It weighs about 5 kg and is portable [79]. The efficiency of the Vesto is 70 – 75 % savings of combustion material compared to three-stone fireplace could be achieved and its cost has been tried to keep the same as large size pot, in the region of USD 20 – 30. [80]

Figure 3-9: The metal Vesto Stove

When the food is boiling you can turn down the fire with the control lever to save fuel as shown on the figure.

3.3.1.3. Fired Clay Stoves

Producing fired clay stoves requires quite high expertise and it needs very high quality ingredients (clay) compared to traditional method of making clay pots. However, if made properly, they can be more effective than metal stoves (up to 40 % compared to the traditional three-stone stove).

I. The Maendeleo Stove

The Maendeleo is a one-pot stove with no chimney. It is made of a pottery cylinder (known as the stove liner), built into a mud surround in the kitchen. It can be used to burn wood or farm waste such as maize stalks and animal dung. It has low cost and it can be built locally. It can use firewood, animal dung, maize husks or cane stalks. It appears to have a life span of 4 years. It has portable and non- portable version. It saves 43% of the fuel as compared with traditional 3-stone stove. [81]

Figure 3-10: The Maendeleo fired clay stove

CHAPTER 4

4. HYBRID SYSTEM FEASIBILITY STUDY AND GRID COMPARISION USING HOMER

4.1. Introduction

Hybrid power supply system is an alternate solution for electrification of remote rural areas where the grid extension is difficult and not economical. Such system incorporates energy producing components that provide a constant flow of uninterrupted power. It is a combination of one or several renewable energy sources such as solar photovoltaic, biogas system, biodiesel system, diesel generator, battery, wind energy system and some other components like power conditioning devices. Hybrid, biogas system, biodiesel generator, wind turbine and photovoltaic modules, offer greater reliability and increase system efficiency than any one of them alone because the energy supply does not depend entirely on any one source alone. For example, when the day of the time is night, power output from PV module is null where as the system load get power from other power supply system like biogas, biodiesel and wind turbine.

For optimal combination of different renewable resource and technology, various types of hybrid systems and methods of techno economic analysis are used. Hybrid2, linear programming, LINGO and HOMER are the most commonly used tools of hybrid system optimization techniques [82-86]. For this study **HOMER** is chosen as an optimization tool for hybrid system feasibility study and grid comparison analysis.

4.2. Hybrid System Setup

The Biogas/PV/Wind/Biodiesel hybrid power supply system makes use of the biogas generator, biodiesel generator, solar PV, and wind turbine to produce electricity as the primary source to supply the load. The configuration of Biogas-Biodiesel-PV-Wind hybrid system is analyzed for various biogas generators, PV array, wind turbine and biodiesel generator sizes with the battery system. The power conditioning units will determine the ac conversion of the dc power following the load profile. The charge controller will charge the batteries with energy from biogas generator, PV modules, and wind turbines as well as from the biodiesel generator. The main objective of Biogas, PV, wind and Biodiesel hybrid system is to reduce the cost of operation and maintenance and cost of logistic by canceling the runtime of each individual component alone. A schematic of a typical Biogas/PV/Wind and Biodiesel hybrid system is shown in Figure 4.1. The main components of the hybrid system are the Wind turbine, Biogas system, Biodiesel and the PV panel. Battery bank and a converter module are auxiliary parts of the system. The details of biogas, wind, PV and biodiesel systems were discussed in the previous section, and now the remaining components of the hybrid system are discussed in this section.

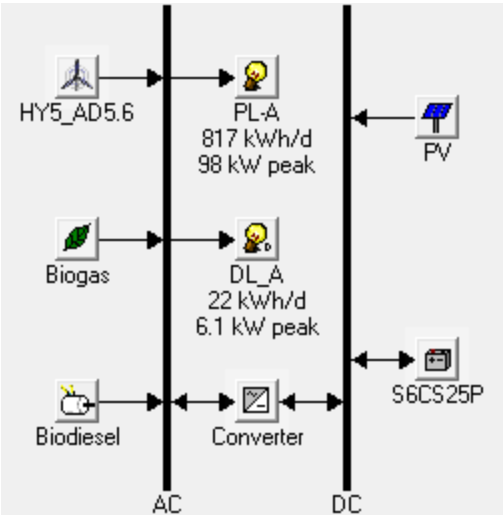

Figure 4-1: Block Diagram of Biogas/Wind/PV/Biodiesel Hybrid System.

4.3. Community Load Assessment

4.3.1. Load Estimation

To minimize power distribution loss, power transmission cost (cable and tower) and man power needed to collect and transport biogas feedstock, the study area that have 11 clusters can be merged in to four sites (Site-A: Amayo, Jarso and Gillu), (Site-B: Meserbo, Kersa and G-mender), (Site-C: Gebrelo, Gendera, and Metabele) and (Site-D: Diguguru and Yegira) based on the distance between them and the geographic layout. According to Bekele, G. electric load in the rural village of Ethiopia can be assumed to be composed of lighting, radio receiver, television set, water pump and loads in health post and primary school [10]. Tamrat, B. considers only lighting, radio and TV as a rural community load [87]. Also Gelma B. and Tadesse, G. considered electricity for flour mill and cooking in addition to the above listed loads [17, 88]. In this study in addition to the above loads, electricity for the animal clinic, electric pump for waste digestate of the biogas plant, electric siren for school, electric stove, printer, desktop computer and copy machine are considered for the school and health center. Water pump and digestate pumps are considered to be deferrable loads while the others as primary loads.

There are about 5675 people without electricity in the study area. An average of 4.39 (5) members in a family, there would be a total of 1135 families [89]. Therefore a total of 4 flour mill, 4 primary schools, 4 human health clinics and one animal clinic centered at Amayo cluster are suggested for the community. Meserbo, Kersa and Gibatmender (332 families); Amayo, Jarso and Gillu (390 families); Metabele, Gendera and Gebrelo (313 families); and Diguguru-Yegira (100 families) clusters are very close each other with a short distance; they can share flour mill, school and clinic service together.

The electric loads for the community contains lighting, water pump, radio receiver, TV set and flour mill. School loads contain electric stoves, water pump, computer, printer, copy

machine, lighting, radio receiver, microphone, electric siren whereas health clinic loads consists of lighting, electric stove, water pump, radio receiver, computer, printer, TV set and electric supply needed for some medical equipment. In the calculation of the load or, in general, the design of hybrid system includes those components which are locally available without considering their efficiencies. This is done for both load and power generation sides.

From 5 family members per household in the area three of them are most probably children if two of them go to school out of three, 13 class rooms for Site-A (390 families); 10 class room for Site-B(332 families); 10 class rooms for Site-C (313 families); and 4 class rooms for Site-D (100 families) are assumed for an average of 60 students per class and also 2 additional classes are suggested for staff member in each school and one class for tea club. Evening classes are conducted from 18:00 to 21:00 and each classroom will be installed with five 11W fluorescent lamps. Additional six 11W fluorescent lamp for Site-B district; eight 11W fluorescent lamp for Site-A; six 11W fluorescent lamp for Site-C; and four 11W fluorescent lamp for Site-D districts, for external lighting are also considered. Two radio receivers of 10W operated 8hours per day (8:00-17:00) are considered for radio lessons of each school. Also one 330W printer operated for 8 hour per day (2hour printing; 6hour standby) (power consumption is 330W during printing and 14W when it is standby) [90], one desktop computer of 300W operated for 10 hour per day and one 0.9kW copy machine operated for 8 hour (2hour copying and 6 hour standby)/day (power consumption is 0.4kW during copying and 1.2W when it is standby) are suggested [91]. For each school one tea club uses a 1.5kW electric stove operating 7:00-8:00, 10:00-10:30, 12:30-13:30 and 14:30-15:00 and two 11W CFL lamps for internal and one 11W CFL lamp for external lighting is considered for staffs and tea house. A 40W electric siren operating 13hours per day for a regular shift class and night class is suggested for each school. Two ceiling fan (100W) per room is also to be installed for air conditioning purpose between 12:00 and 16:00.

Similarly for the four health centers, having 4 rooms each, one 11W CFL per room and two 11W fluorescent lamp for external lighting operating 18:00-6:00 are considered. A vaccine refrigerator of 100W working for 24 hours; a 20W capacity microscope and a 10W radio receiver for the office hours; one 300W desktop computer operated for 8 office hours per day; one 330W printer operated for 8 office hours (2 hour printing; 6hour standby) per day; one 100W television operated for 18 hour per day (6:00-24:00) are also suggested for each health centers. One ceiling fan (75W) per room is also to be installed for air conditioning purpose between 12:00 and 16:00. For each health center one coffee house requires one 1.5kW electric stove operating 7:00-8:30, 10:00-10:30 and 12:30-15:00, two 11W CFL lamp for the house and one 11W CFL lamp for external lighting operating 18:00-22:00 is also considered.

For the community a total of 4 flour mills of 12.5 kW each working from 6:00 to 20:00 is assumed. One 11W florescent lamp for internal and one for external lighting from 18:00 to 21:00 and two 75W ceiling fans in each flour mill is also considered for the flour mill

operation period and each household is to be installed with 3 CFLs of 11W rating to be lit from 18:00 to 24:00. Additionally a CFL of 11W is also considered for external lighting from 19:00-23:00. A radio receiver (10W), a 15W DVD player and a TV set (100W) are to be used in the time 12:00-14:00 and 18:00 to 24:00.

For the central animal clinic located at Amayo Cluster, having 3 rooms, one 11W CFL per room and two 11W fluorescent for external lighting are considered. A vaccine refrigerator of 100W operating for 24 hours of a day; a 20W capacity microscope and a 10 W radio receiver operating for 8 hours; one 300W desktop computer operating for 8 hour per day; one 330W printer operating for 8 (1 hour printing, 7 hour standby) hour per day; and a 1 kW water heater operating for 3 hours per day are also suggested for the clinic. One ceiling fan (75W) per room is also installed for air conditioning purpose between 12:00 and 16:00. Coffee house requires a 1.5kW electric stove operating 7:00-8:30, 10:00-10:30 and 12:30-15:00, two 11W CFL lamps for the house is also considered.

Water pumping system is required for the households, the schools and health care centers. A minimum of 100 L of water per day per family and 2400 L/day for each pair of one health center and one primary school is suggested [10, 17]. To accomplish this, 7 pump operating 9.03 hour/day for site-A, 6 pumps operating 8.6hour/day for site-B, 6 pumps operating 8.455hours/day for site-C and 2 pumps operating 8.104hour/day for site-D of 320 W (with a nominal flow rate of 0.617m3/h, and a head of 10-100m, nominal head is 70m) are to be installed to supply water for the community [92]. Another one pump of 320W operating for 4 hours/day for each districts school and health center are assumed. And also 1200 L/day water requirement for the animal clinic is suggested. For this one 320W electric pump operating 2 hours/day is considered.

Four digestate pumps of 800W (A flow rate capacity of 13.6m3/h) operating 13 hour/day for site-A, 11hour/day for site-B, 10hour/day for site-C, and one pump of 800W operates 13hour/day for site-D at every end of HRT (20 day) for all biogas plant is considered.

A water storage capacity of 2 days is suggested for each district requiring a storage capacity of 40.5kWh (for site-A), 33kWh (for site-B), 32.5kWh (for site-C) and 10.4kWh (for site-D) for the community and 2.56kWh for primary school and health centers in each district and 1.28kWh for animal clinic. The peak deferrable load is 0.32 kW for primary school-health center in each district, 0.32kW for animal clinic and 2.24kW (site-A), 1.92kW (site-B), 1.92kW (site-C), and 0.64kW (site-D) for the community.

The total storage capacity of Site-A 44.3kWh, Site-B 35.6 kWh, Site-C 35.03 kWh and Site-D is 12.9kWh and the total peak deferrable load for site-A 6.08kW, for site-B 5.44kW, for site-C 5.44kW and for site-D is 1.76 kW.

Special Considerations: The following conditions are considered for the statement discussed above for weekend days and, January, June, July, and August. Because of religious concern, peoples are not on their regular activities in the weekend (i.e. religious holydays)

and school works are not conducted, school loads are shutdown. On the other hand, TV and radio may be enjoyed from 10:00 to 18:00 (all the day after church, in addition to 18:00 to 24:00 as stated above). Up to 30% deferrable load decrement can be expected in the rainy season (June-July-august) [10, 17]. Also no water is required by school in January, July and August and a 75 % school–clinic deferrable load decrement is assumed. The school primary loads such as fans, radio, lightings, stoves and siren are not operated and a 50% decrement of remain school loads are assumed for school break.

Based on the above analysis, the community will have a primary peak demand of Site-A 98.4kW, Site-B 86kW, Site-C 82kW and Site-D 39kW and average primary load of Site-A 34kW, Site-B 30kW, Site-C 29.2kW and Site-D 15.3kW. Annual average primary energy demand of Site-A 817kWh/day, Site-B 714kWh/day, Site-C 700kWh/day and Site-D 367kWh/day. A load factor of Site-A 0.346, Site-B 0.347, Site-C 0.356 and Site-D 0.392 is found.

A Primary Load is the electrical demand that the power system designed by HOMER must serve at a specific time while deferrable load is electrical load that must be met within some time period, but the exact timing is not important. Loads are normally classified as deferrable because they have some storage associated with them. Water pumping is a common example - there is some flexibility as to when the pump actually operates, provided the water tank does not run dry. Deferrable loads are loads from water pump in the school, clinic and the community and digestate pump of the biogas plant. Primary load, consisting of domestic, health centre and school load in this study. The load type served is AC and varies during week and weekend days. A 5% both day to day and hour to hour random variability of the primary load is assumed for all sites. The daily pattern and the seasonal profile are shown in Figure 4.2-4.9.

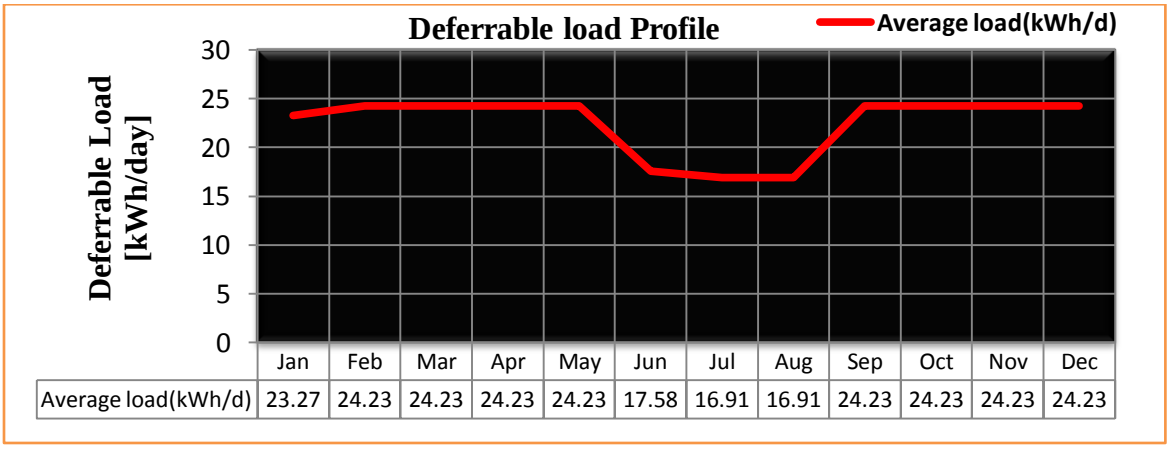

Figure 4-2: Site-A deferrable load profile.

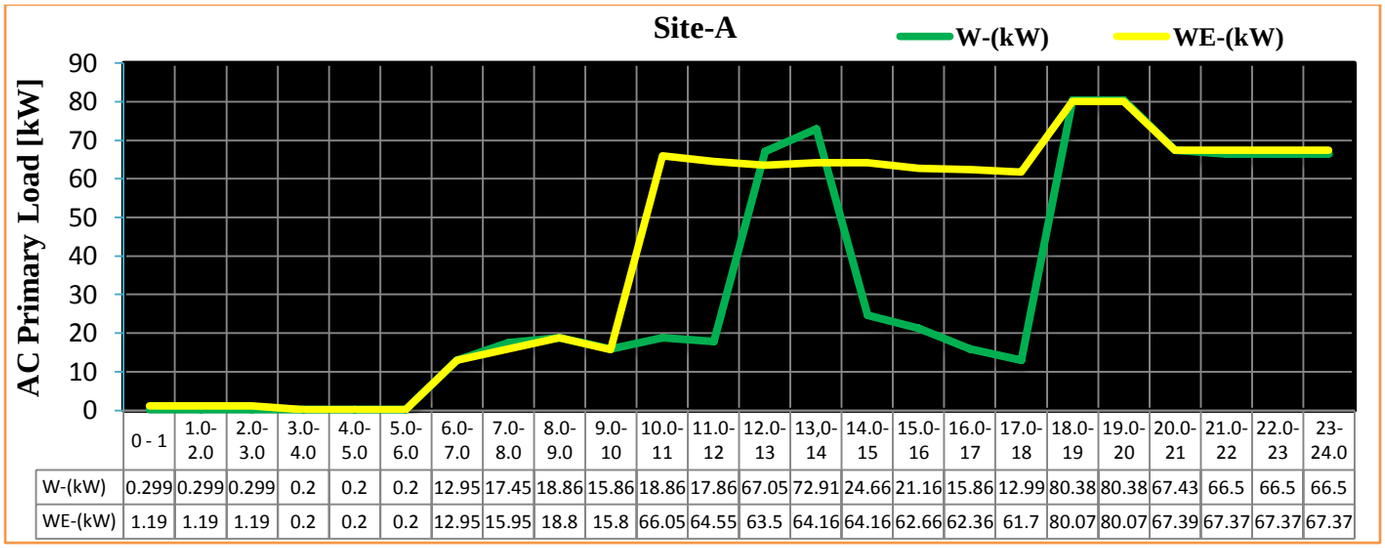

	0 - 1	1.0-2.0	2.0-3.0	3.0-4.0	4.0-5.0	5.0-6.0	6.0-7.0	7.0-8.0	8.0-9.0	9.0-10	10.0-11	11.0-12	12.0-13	13,0-14	14.0-15	15.0-16	16.0-17	17.0-18	18.0-19	19.0-20	20.0-21	21.0-22	22.0-23	23-24.0
W-(kW)	0.299	0.299	0.299	0.2	0.2	0.2	12.95	17.45	18.86	15.86	18.86	17.86	67.05	72.91	24.66	21.16	15.86	12.99	80.38	80.38	67.43	66.5	66.5	66.5
WE-(kW)	1.19	1.19	1.19	0.2	0.2	0.2	12.95	15.95	18.8	15.8	66.05	64.55	63.5	64.16	64.16	62.66	62.36	61.7	80.07	80.07	67.39	67.37	67.37	67.37

Figure 4-3: AC primary Load Profile of Site-A.

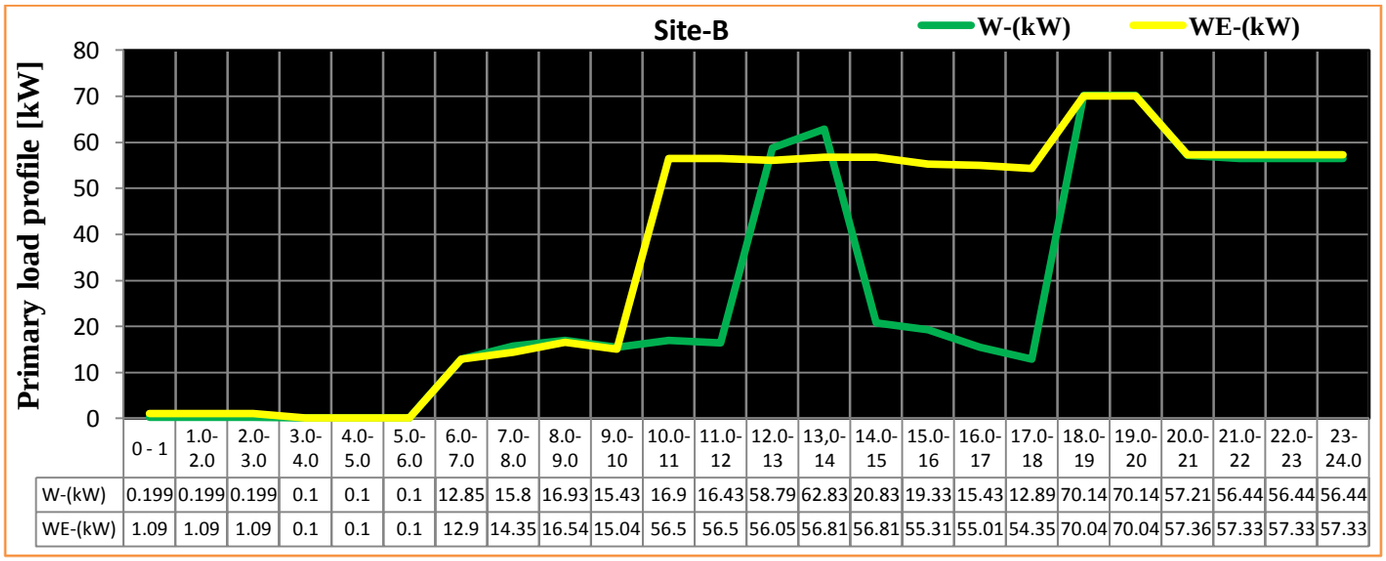

	0 - 1	1.0-2.0	2.0-3.0	3.0-4.0	4.0-5.0	5.0-6.0	6.0-7.0	7.0-8.0	8.0-9.0	9.0-10	10.0-11	11.0-12	12.0-13	13,0-14	14.0-15	15.0-16	16.0-17	17.0-18	18.0-19	19.0-20	20.0-21	21.0-22	22.0-23	23-24.0
W-(kW)	0.199	0.199	0.199	0.1	0.1	0.1	12.85	15.8	16.93	15.43	16.9	16.43	58.79	62.83	20.83	19.33	15.43	12.89	70.14	70.14	57.21	56.44	56.44	56.44
WE-(kW)	1.09	1.09	1.09	0.1	0.1	0.1	12.9	14.35	16.54	15.04	56.5	56.5	56.05	56.81	56.81	55.31	55.01	54.35	70.04	70.04	57.36	57.33	57.33	57.33

Figure 4-4: AC primary Load Profile of Site-B.

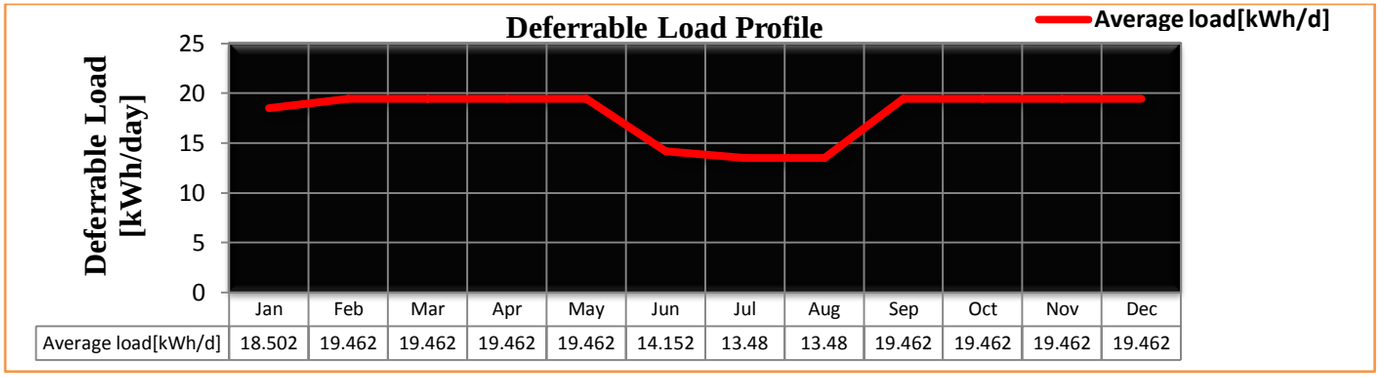

	Jan	Feb	Mar	Apr	May	Jun	Jul	Aug	Sep	Oct	Nov	Dec
Average load[kWh/d]	18.502	19.462	19.462	19.462	19.462	14.152	13.48	13.48	19.462	19.462	19.462	19.462

Figure 4-5: Deferrable load profile of Site-B.

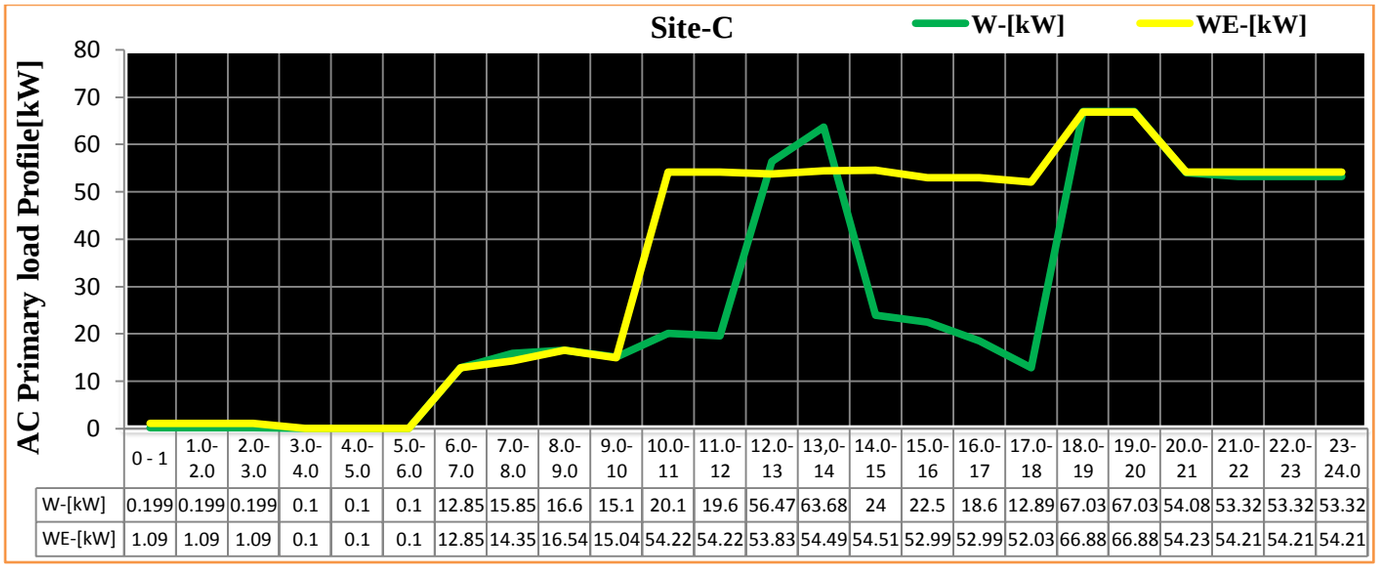

	0 - 1	1.0-2.0	2.0-3.0	3.0-4.0	4.0-5.0	5.0-6.0	6.0-7.0	7.0-8.0	8.0-9.0	9.0-10	10.0-11	11.0-12	12.0-13	13,0-14	14.0-15	15.0-16	16.0-17	17.0-18	18.0-19	19.0-20	20.0-21	21.0-22	22.0-23	23-24.0
W-[kW]	0.199	0.199	0.199	0.1	0.1	0.1	12.85	15.85	16.6	15.1	20.1	19.6	56.47	63.68	24	22.5	18.6	12.89	67.03	67.03	54.08	53.32	53.32	53.32
WE-[kW]	1.09	1.09	1.09	0.1	0.1	0.1	12.85	14.35	16.54	15.04	54.22	54.22	53.83	54.49	54.51	52.99	52.99	52.03	66.88	66.88	54.23	54.21	54.21	54.21

Figure 4-6: AC primary Load Profile of Site-C.

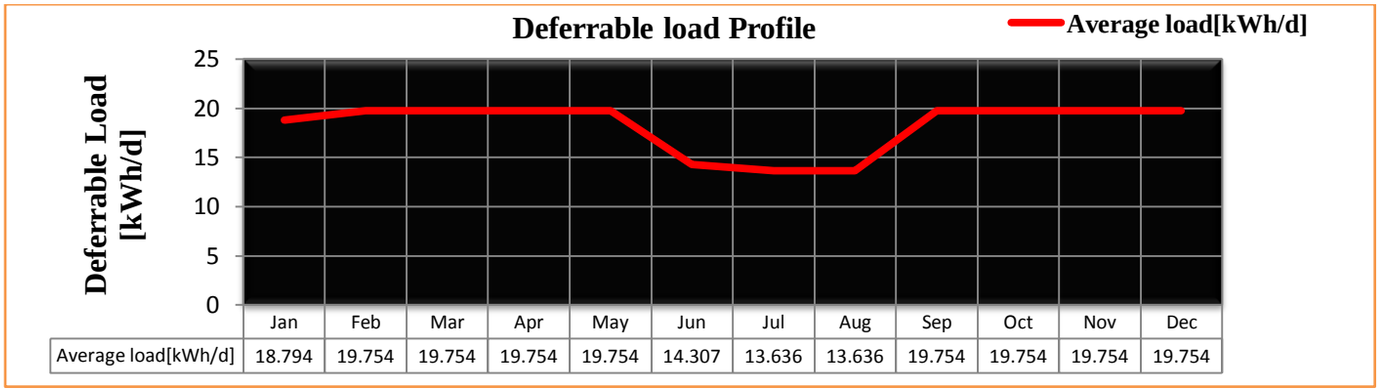

	Jan	Feb	Mar	Apr	May	Jun	Jul	Aug	Sep	Oct	Nov	Dec
Average load[kWh/d]	18.794	19.754	19.754	19.754	19.754	14.307	13.636	13.636	19.754	19.754	19.754	19.754

Figure 4-7: Deferrable load profile of Site-C.

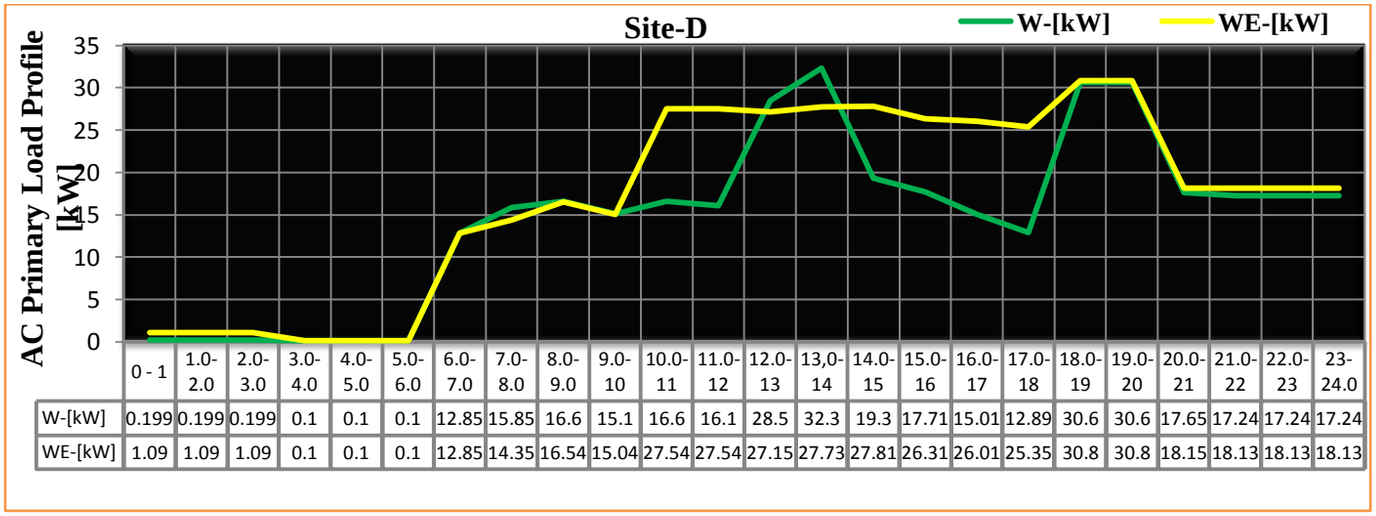

	0 - 1	1.0-2.0	2.0-3.0	3.0-4.0	4.0-5.0	5.0-6.0	6.0-7.0	7.0-8.0	8.0-9.0	9.0-10	10.0-11	11.0-12	12.0-13	13,0-14	14.0-15	15.0-16	16.0-17	17.0-18	18.0-19	19.0-20	20.0-21	21.0-22	22.0-23	23-24.0
W-[kW]	0.199	0.199	0.199	0.1	0.1	0.1	12.85	15.85	16.6	15.1	16.6	16.1	28.5	32.3	19.3	17.71	15.01	12.89	30.6	30.6	17.65	17.24	17.24	17.24
WE-[kW]	1.09	1.09	1.09	0.1	0.1	0.1	12.85	14.35	16.54	15.04	27.54	27.54	27.15	27.73	27.81	26.31	26.01	25.35	30.8	30.8	18.15	18.13	18.13	18.13

Figure 4-8: AC primary Load Profile of Site-D.

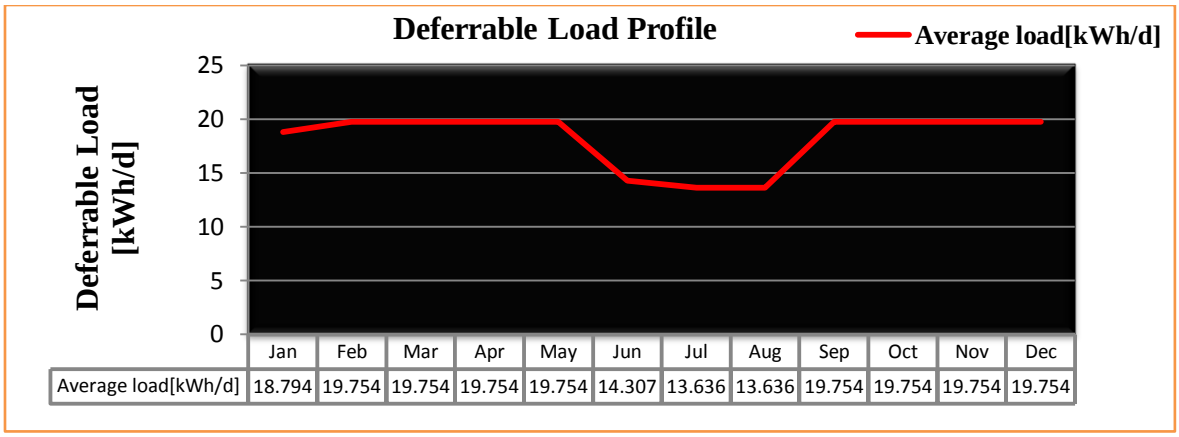

Figure 4-9: Deferrable load profile of Site-D.

Each of the four sites, four hybrid systems, is separately treated since they have different inputs (load, biogas resource and biodiesel resource) for HOMER even if there is some common input like solar and wind resource, and hybrid system component cost.

Table 4-1: Load Summary of the Study Area.

Study Area	AC Primary Load				Deferrable Load		
	Annual average [kWh/day]	Average [kW]	Peak [kW]	Load factor	Annual average [kWh/day]	Storage capacity [kWh]	Peak load [kW]
Site-A	817	34	98.4	0.346	22.4	44.3	6.08
Site-B	714	29.8	85.8	0.347	17.9	35.6	5.44
Site-C	700	29.2	82	0.356	18.2	35.03	5.44
Site-D	367	15.3	39	0.392	7.0	12.93	1.76
Total	2598	108.3	305.2	0.355	65.5	126.39	18.72

4.3.2. Electric Demand Forecasting

An energy demand forecast is a measurement and estimate of historic, current and projected patterns of energy demand. Accurate models for electric power load forecasting are essential to the operation and planning of a utility company. Load forecasting helps an electric utility to make important decisions including decisions on generating electric power, load switching, and infrastructure development. Forecasting is one major work in hybrid electric supply system planning. [93,94]

In this study an end use analysis approach is used to forecast a load growth of a remote area supplied by a hybrid renewable system. This methodology implies the current energy demand of the community is first estimated based on customer's end device energy consumption and the energy demand is projected throughout the project life time based on the household growth due to population growth rate and the penetration of them to the system. The following relation defines the end use methodology:

$$E_i = E_o + S*(H_i - H_o)*E \quad (4.1)$$

Where,

E_i= the i^{th} year annual average energy demand in kWh/day

E= annual average energy consumption in kWh/day/household

S= Customer penetration rate

E_o= the annual average estimated electricity demand, in kWh/day, in 2013.

H_o= the number of household on which E_o is estimated, 2013 base year.

Hi=the number of household in the i^{th} year.

I. Population and Energy Demand

Undoubtedly, population growth has strong ties with energy demand. As population increase, total energy consumption will increase. The end use analysis in this thesis work considered the number of households and household growth, because electricity demand is satisfied and supplied for households not for individual population. The average rural population growth rate of Ethiopia is 1.8% [World Bank, 2012]. This figure is assumed constant throughout the project life time and used to determine the population of the study area in the next 20year. The population size of Site-A is 1950(390HH), Site-B is 1660(332HH), Site-C is 1565(313HH) and Site-D is 500(100HH) in 2013 which is 5 occupant per household. This population figure is projected by an annual growth rate of 1.8% until the end of the forecast period and converted to total number of household using a given number of occupants per household (see appendix A).

II. Customer Penetration

This refers to how many of the newly growing households are connected to the hybrid system annually to be electrified. Assuming 90% of them is electrified annually and this figure is constant up to the project life time or the forecast horizon.

III. Average electricity consumption

As we have discussed in Section 4.1 the annual average, primary energy consumption estimated are 817, 714, 700 and 367kWh/day and deferrable load energy consumption are 22.4,18, 18 and 7kWh/day for Site-A, Site-B, Site-C and Site-D respectively. This energy demand is taken as the demand in the first year of the forecast period (2013). The annual average, primary energy consumption per household should becomes 2.095, 2.151, 2.24 and 3.67 kWh/day and deferrable load energy consumption per household are 0.06,0.06,0.06 and 0.07kWh/day for Site-A, Site-B, Site-C and Site-D respectively. Assuming this annual average energy consumption (Primary + Deferrable) per household is constant throughout the forecasting horizon. Based on the above discussion the energy consumption profiles of the study area for the next 20 years are presented in Figure 4.10-4.13 and in Appendix A.

IV. Forecast Result

The result of load forecast, Annual average energy demand [kWh/day] and Peak load of a standalone hybrid power supply system is summarized in Appendix-A. However it can be presented here in Figure 4.10 -4.13.

Figure 4-10: Load forecast result of Site -A (D=deferrable, P=primary)

Figure 4-11: Load forecast result of Site-B (D=deferrable, P=primary)

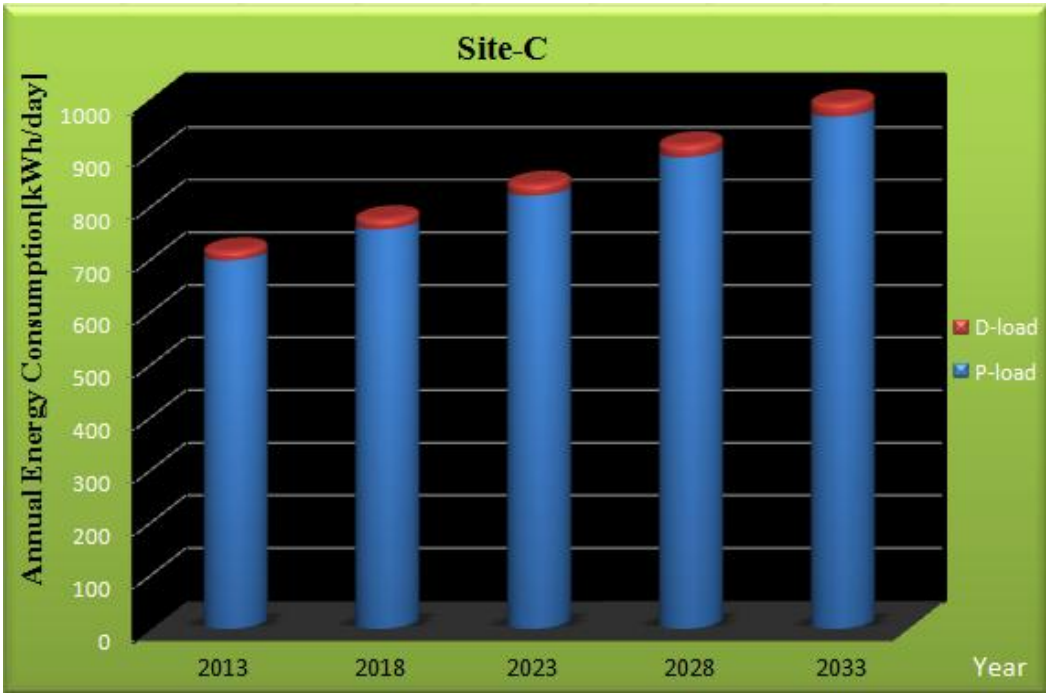

Figure 4-12: Load forecast result of Site-C (D=deferrable, P=primary)

Figure 4-13: Load forecast result of Site-D (D=deferrable, P=primary)

4.4. HOMER Resource Input

In the system designed by HOMER, resource is anything that can be used to generate electricity and comes from outside the system. RE resources available at a location can differ considerably from site to site and this is a vital aspect in developing the hybrid system. In the previous Chapters, the wind, Solar, Biogas and, Biodiesel potential resource are discussed briefly and their potential is estimated and studied for each sites of the study area. As we see the previous section of this study the wind and solar resource is common for all districts of the study area while the biogas and biodiesel resources are not the same.

4.4.1. Common input to all Sites

Wind and solar radiation variations for such small range in the study areas can be neglected [9, 10, 31]. Solar and Wind Resources are Common input for all districts of the study area. The 22 years average solar resource data used for the study area at a location of 10°33' N latitude and 39°20' E longitude was taken from NASA Surface Metrology and Solar Energy.

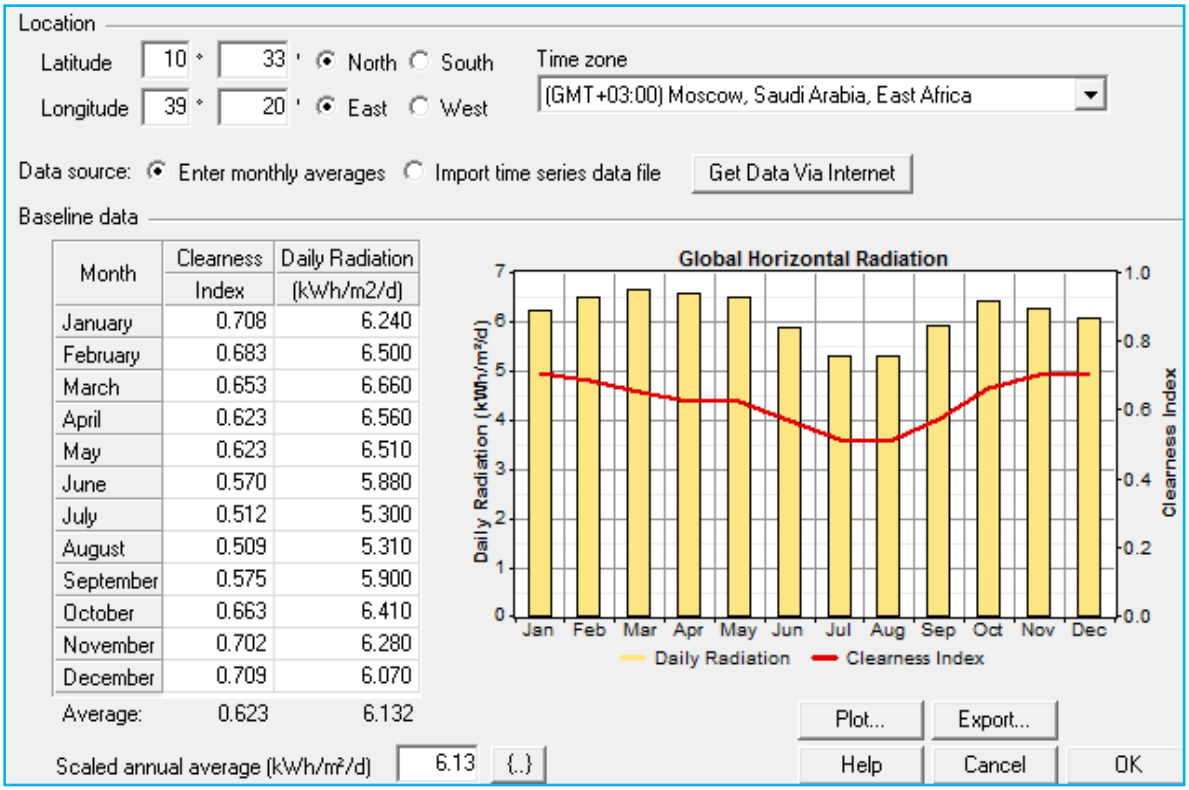

Month	Clearness Index	Daily Radiation (kWh/m2/d)
January	0.708	6.240
February	0.683	6.500
March	0.653	6.660
April	0.623	6.560
May	0.623	6.510
June	0.570	5.880
July	0.512	5.300
August	0.509	5.310
September	0.575	5.900
October	0.663	6.410
November	0.702	6.280
December	0.709	6.070
Average:	0.623	6.132

Figure 4-14: Solar energy resource (Source: NASA, 2012)

A 10 years average wind speed data for hybrid system optimization is also taken from NASA based on the latitude, longitude and elevation of the Site. The 10 years average wind speed at a 10m anemometer height of the site is 3.1m/s.

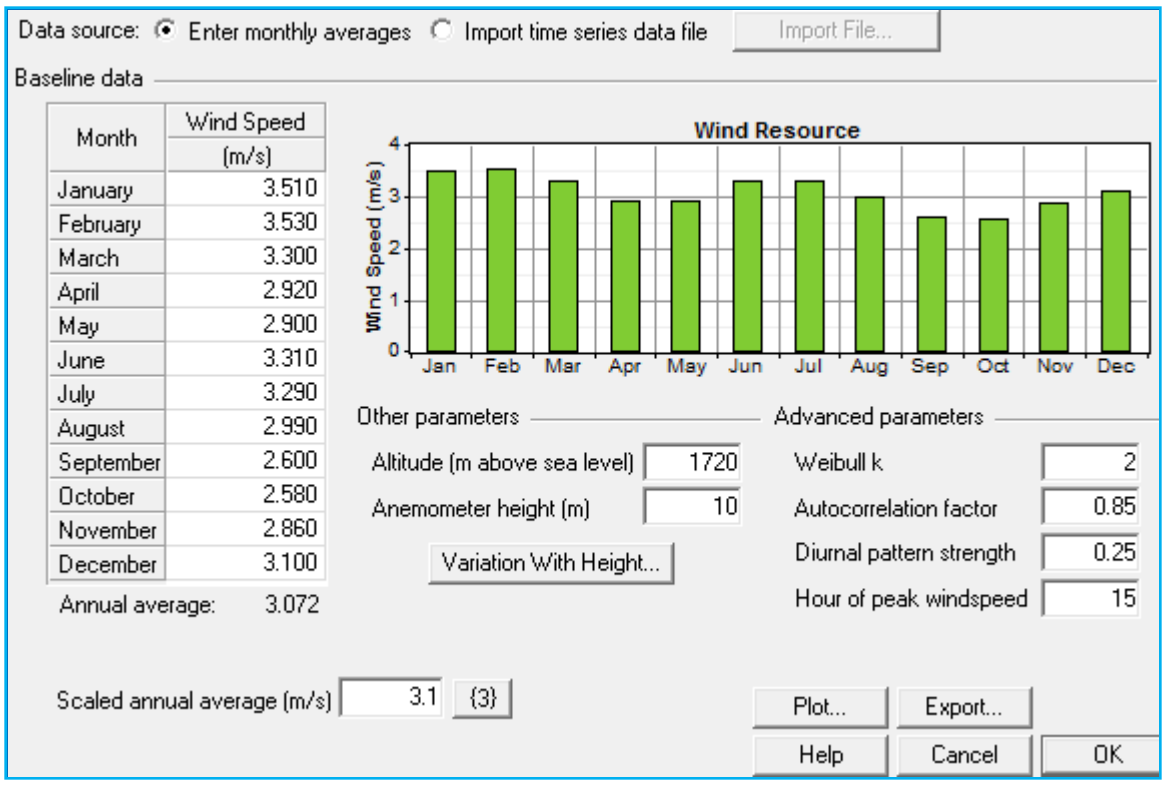

Figure 4-15: Wind energy resource data (NASA, 2012)

4.4.2. Specific input to Site-A, Site-B, Site-C and Site-D

The specific inputs of Site-A, Site-B, Site-C and Site-D in the resource windows of HOMER are the biogas and biodiesel resources.

The biogas feedstock (in this study: manure from cattle, human, horse, donkey, mule, chicken, and jatropha by products) are analyzed and prepared in away suitable for HOMER input and feed in to the biogas resource window (refer Table 2.22-2.25 of Chapter-2). The annual average daily biogas feedstock potential of Site-A, Site-B, Site-C and Site-D are 10.86tones/day, 9.25tones/day, 8.81tones/day and 3.09tones/day respectively. The price of the biogas feedstock is assumed to be equivalent with the current price of the dry animal dung in the study area which lies between 10 to 20 $/tonne as per the information obtained from the community through direct interview (note: the price obtained is in terms of ETB, it can be converted in to USD by a conversion factor of 1USD=18.6ETB) and this price is common for all sites of the study area.

The gasification ratio of a mixture of those biogas feedstocks mentioned above is calculated to be 0.0626kg/kg, which means 0.0626kg biogas is generated by 1kg biogas feedstock mixture of the above listed resources consumed. Refer Chapter 2 of this paper to get more detail information. The carbon content of biogas is taken to be 5% of the total feedstock consumed during the biogas generation process and the LHV of biogas is also 20.2MJ/kg.

The cost of biomass, biogas gasification, carbon content and LHV input of HOMER is also common for all districts. Sample biogas resource window is given in Figure 4.16.

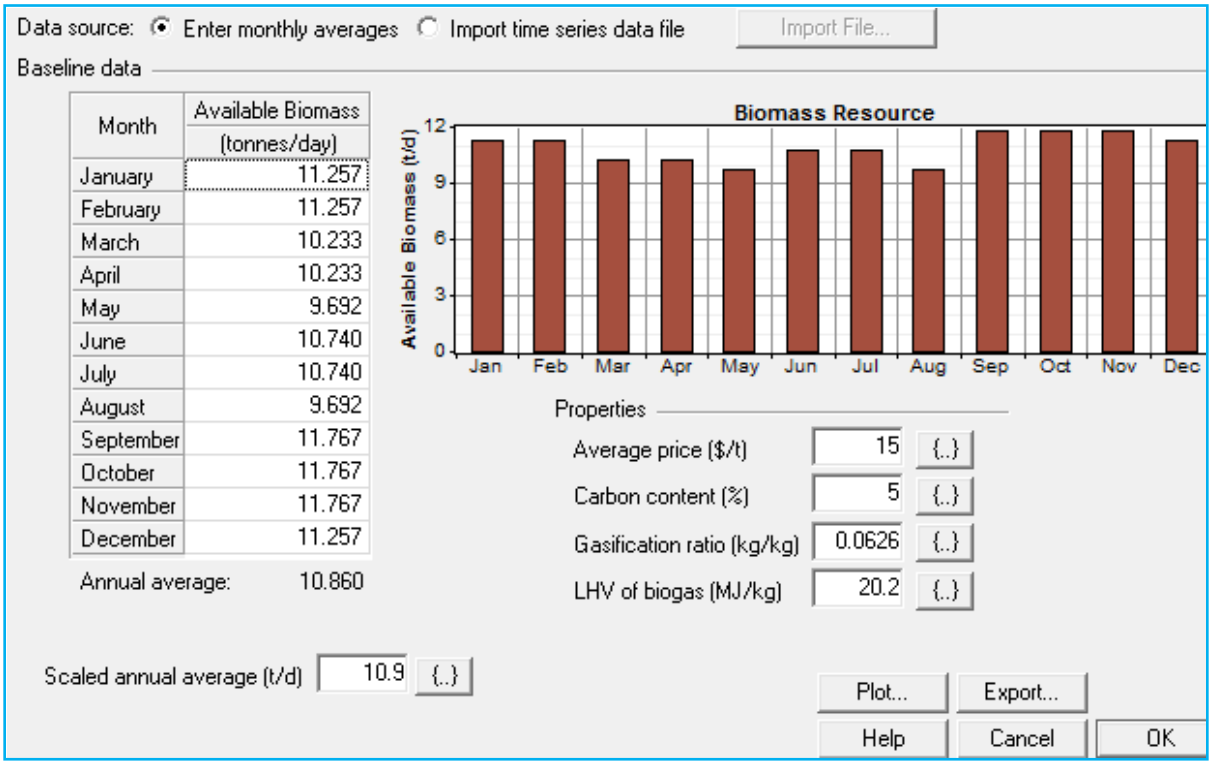

Figure 4-16: Biogas Feedstock resource of Site-A, and some technical parameters.

The source of biodiesel is Jatropha. Its seed is pressed and processed to yield biodiesel and it is used as a fuel for a biodiesel generator operated as a backup for the hybrid system. 20 hectare farming land which was suitable for Jatropha cultivation is identified in the study area and its potential yield of biogas feedstock and biodiesel is estimated. The biodiesel potential of the study area from jatropha seed is estimated to be 18.5m^3/year (refer biodiesel potential estimation from jatropha in Chapter 2 of this paper) and the resource is divided to each sites roughly based on their load share in the community. Therefore 5.5m^3 for Site-A, 5m^3 for Site-B and Site-C each and 3m^3 for Site-D biodiesel fuel amount is considered. The fuel properties of a jatropha biodiesel are lower heating value of 39.23MJ/kg, density of 880kg/m^3 [54] and the carbon and sulfur content of 77% and 0 .0024% respectively [7].

4.5. HOMER Sensitivity Input

HOMER sensitivity inputs help to perform sensitivity analysis in order to optimize resource, load and hybrid system component size and cost variability and to observe their effect on feasibility analysis of the hybrid system. In this study wind speed, PV module price, primary and deferrable loads are selected as a sensitivity input. The wind speed is taken as sensitivity input to show the effect of wind resource variation on the system feasibility result. The present and forecasted primary and deferrable loads are also considered as sensitivity input to

determine hybrid system component combination size and the related NPC of the system. Homer performs a separate optimization procedure for each specified value.

Table 4-2: Homer sensitivity values of all districts

Districts	Sensitivity Variable	Sensitivity Value		
Common input for all districts	PV module capital and replacement multiplier	0.4, 0.6, 0.8, 1.0, 1.2, 1.4		
	Wind speed [m/s]	2	3.1	6.0
Site-A	Primary load[kWh/day]	817	1132	
	Deferrable load[kWh/day]	22	31	
Site-B	Primary load[kWh/day]	714	1000	
	Deferrable load[kWh/day]	18	26	
Site-C	Primary load[kWh/day]	700	973	
	Deferrable load[kWh/day]	18	26	
Site-D	Primary load[kWh/day]	367	510	
	Deferrable load[kWh/day]	7	10	

4.6. Comparison of Grid Extention with Standalone Hybrid System

Grid extension is another option to electrify remote loads. Grid comparison with off grid hybrid system is done to select the most economical system. For each stand-alone system configuration, HOMER calculates the breakeven grid extension distance, which is the distance from the grid at which the total net present cost of the grid extension is equal to the total net present cost of the stand-alone hybrid system.

4.6.1. Grid Extension System

The main grid extension system components that should be considered to compare grid extensions with standalone hybrid system are:

- MV system components
- LV system component
- Transformer assembly

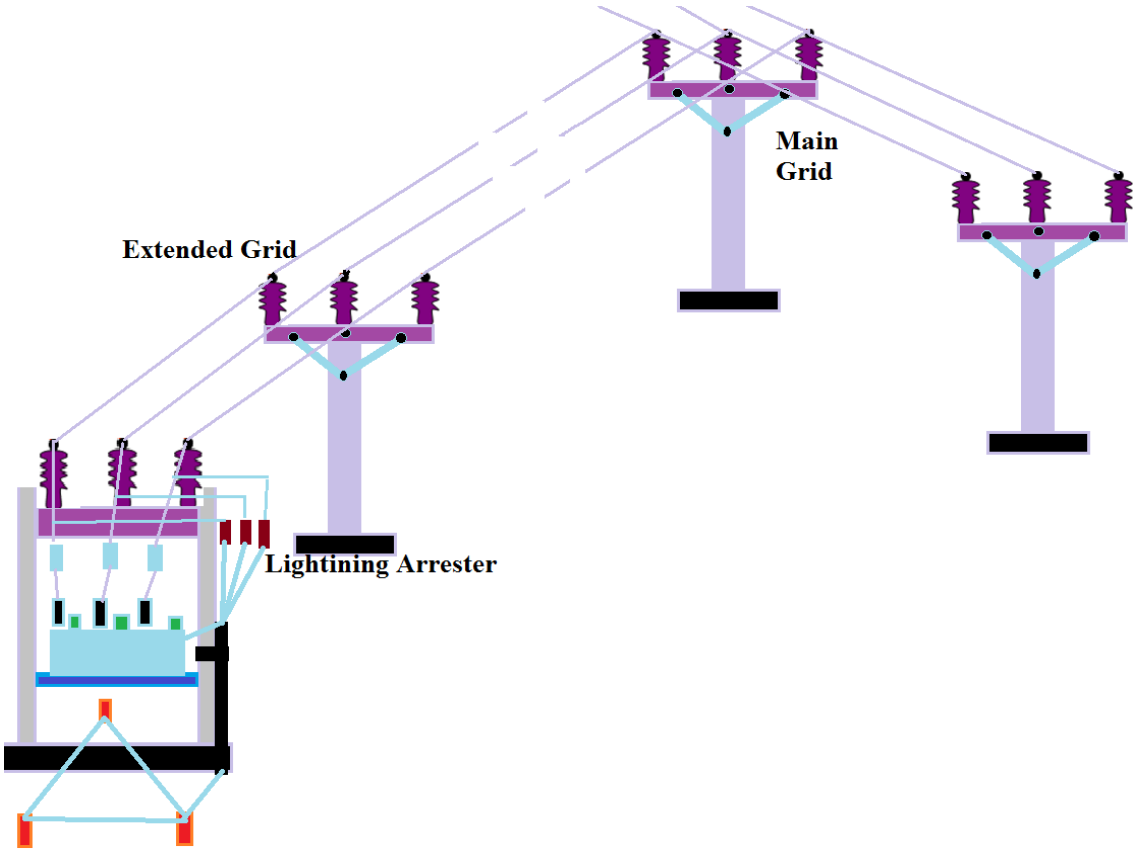

Figure 4-17: The extended grid system from the tapping point of the main grid.

A. MV-System Components

In the study area, the near grid voltage level to be extended is 33kV. The main components of MV systems are electric pole assembly and medium voltage transmission line. The MV-line routes should approximately follow roads, to make the line construction and maintenance works easier. However, angles should be avoided when reasonably possible. Based on the geographic location and nature of the area to be electrified, suspension assembly line route for the medium voltage network extension is selected.

Concrete pole is the first choice for the construction of the network provided that the road is all weather road type, good for transportation of concrete poles and transformer, comfortable landscape for transportation and pole erection. Concrete poles cannot be affected by insects, it's durable, and have good resistance to wind, fire and moist. Therefore concrete poles are the most preferred for rural electrification. Type of concrete poles available for distribution construction of rural towns and village are 8m, 10m and 11m. Some time for special cases 12m may also be used. 8m concrete poles are used for low voltage lines where as 10m, 11m and 12m are used for medium voltage lines. Each type of poles is further classified according to their strength. That is 300daN, 500daN, 800daN and 1250daN which are applicable for different angle conditions. In Ethiopia rural electrification using grid expansion done by

UEAP, uses 10/11m 300danN concrete pole with 100m spacing for medium voltage. The most common accessories of MV electric pole assembly are 33kV pin insulator, 33kV pin, 2.5m U-cross arm, tie wire, tie strap, pole and transmission line. [95]

The location of MV/LV transformer substations must also be re-considered in view of accessibility by the MV -line. The main MV -line shall be constructed with AAAC 95 mm^2. The MV distance from their tapping point to the transformer location for Site-A, Site-B, Site-C and Site-D are 11km, 6km, 2km and 12km respectively.

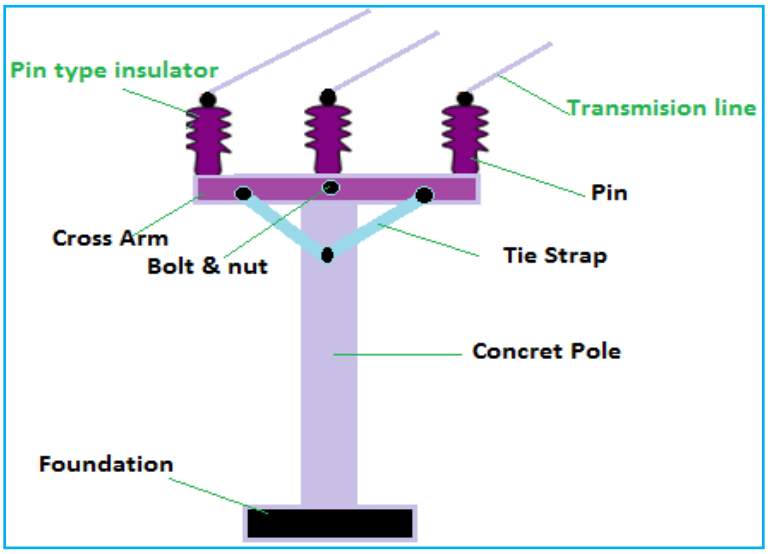

Figure 4-18: Electric pole assemblies

B. Transformer Assembly

The main transformer assembly components are:

- Transformer
- Dead end cross arm insulator cross arm
- Pins
- Pin type insulator
- Bolt and nuts
- Earthing system
- Lightening arrester and drop out fuse
- Pole

The distribution transformer steps down the 33kv grid voltage to 0.4kv (3-phase) customer voltage level. Lightening arrester protects the transformer from high lightening surge voltage while the drop out fuse protects the transformer from high fault current. The line distance from the MV/LV transformer to the furthest consumer should not be longer than 750m, to avoid problems in protection and voltage level. In special cases upto 900m distance may be approved after detailed analyses of the short-circuit currents, voltage drops and functionality of fuse protection. [95]

The peak power demand of Site-A, Site-B, Site-C and Site-D are 142.1kW, 125.4kW, 119.4kW, 55.5kW respectively and the size of transformer selected for Site-A, B, and C are 200kVA while for site-D is 100kVA. The size of the transformer considered here accounts the future demand growth of the community in the study areas and system power loss.

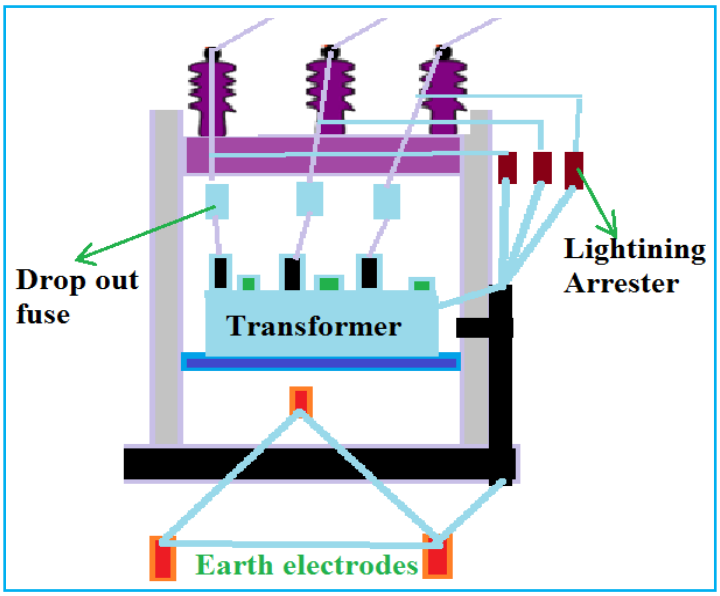

Figure 4-19: Transformer assembly

C. LV System Components

The LV-line routes should be defined so that all consumers requiring electricity are considered. The straightest routes are preferred in order to save cable and facilitate the installation work. A light angle assembly network route for low voltage system is reasonable since the route is not followed straight line rather multidirectional for each customer. A concrete 8/9m 300daN pole is most commonly used for LV distribution in rural area by grid extention and the spacing between two consecutive poles is 50m. ABC 3x50+25mm2 transmission cables is the most frequently used cable by UEAP in rural area electrification for LV side [95]. And 3km total LV route is assumed for each site (site-A, Site-B, Site-C and Site-D).

4.6.2. Grid extension cost analysis

The grid extension cost analysis is based on the cost of material, transportation and construction cost data obtained from UEAP of Ethiopia. It contains the costs of all electrical and mechanical components of the grid system discussed in the previous section. The cost includes:

- The material cost of MV system components, LV system components, transformer assembly, and load break switch assembly
- Construction (labor) cost of all the above system assemblies
- Transport cost of all the above system assemblies.

In addition to the above listed costs 10% of the total capital cost is considered for administration and control and also include 15% VAT for labor and transport costs of all the above system assemblies.

Table 4-3: 33kV (MV) transmission system Materials and their cost

No.	Material	Unit	Unit Price[ETB]
1.	Concrete pole 300dan 10/11m	Pcs	2677.75
2.	2.5mt U-cross arm	pcs	729.62
3.	Big collar for 300dan(long bolt)	pcs	13.42
4.	Tie strap	pcs	31.41
5.	Bolt and nut	pcs	2.74
6.	Long bolt for tie strap to pole	pcs	13.93
7.	33kV pin type insulator	Pcs	134.79
8.	33 kV pin	pcs	64.36
9.	AAAC95mm2 cable	km	14976.34
10.	Tie wire 6AWG	kg	41.71
11.	Cement	kg	2.6
12.	Sand	M3	200
13.	Stone	M3	150

Table 4-4: Materials Cost of Transformer Assembly

No.	Material	Unit	Unit Price[ETB]
1.	Concrete pole 300dan 10/11m	Pcs	2677.75
2.	cross arm for transformer fixture	pcs	806.24
3.	Suspension cross arm	pcs	431.25
4.	Big collar for 300dan(long bolt)	pcs	14.36
5.	Dropout fuse	pcs	848.1
6.	Bolt and nut	pcs	0.89
7.	33kV lighting arrester	pcs	739.87
8.	33kV pin type insulator	Pcs	134.79
9.	33 kV pin	pcs	59.14
10.	Transformer 200kVA	pcs	64795
11.	Tie wire 6AWG	kg	41.71
12.	Cu wire stranded 35mm2 earthing	kg	57.21
13.	Earthing rod 50mmx3mm, 4mt	pcs	194.08
14.	ABC conductor(3*50+25mm2)	mt	32.56
15.	Tie strap	pcs	38.98
16.	AAAC50mm2	mt	6.25
17.	Cement	kg	2.6
18.	Sand	M3	200
19.	Stone	M3	150

Table 4-5: 0.4kV low voltage distribution system materials and their costs

No.	Material	Unit	Unit Price[ETB]
1.	Concrete pole 300dan 8/9m	Pcs	2501.65
2.	Guy wire	kg	30.96
3.	2.5mt U cross arm	pcs	729.62
4.	Pin type insulator	pcs	134.79
5.	0.4kV pin	pcs	64.36
6.	Tie strap	pcs	31.41
7.	Long bolt with nut for pole to cross arm and tie	pcs	8.1
8.	Bolt and nut for tie and pins with cross arm	pcs	0.89
9.	ABC3x50+25mm2	km	47936
10.	Cu wire stranded 35mm2 for earthing	kg	57.21
11.	Earthing road 50x5x3mm, 4mt	pcs	194.08
12.	Cement	kg	2.6
13.	Sand	M3	200
14.	Stone	M3	150

Table 4-6: Load break switch assembly materials and their costs

No.	Material	Unit	Unit Price[ETB]
1.	Concrete pole 300dan 10/11m	Pcs	2677.75
2.	Load break switch	pcs	7615.87
3.	Long bolt with nut for pole to cross arm and tie	pcs	8.1
4.	Bolt and nut for tie and pins with cross arm	pcs	0.89
5.	Cu wire stranded 35mm2 for earthing	kg	57.21
6.	Earth rod 50mmx3mm, 4mt	each	194.08
7.	Dead end cross arm	each	229.82
8.	Guy wire	kg	43.34
9.	Cement	kg	2.6
10.	Sand	M^3	200
11.	Stone	M^3	150

Table 4-7: 33kV MV system Construction cost

No.	Material	Unit	Unit Price[ETB]
1.	Surveying of MV routes , profile drawing and detail design calculation	km	944.16
2.	Suspension assembly	ass	1440.49
3.	Load break switch assembly	ass	3499
4.	Transmission line Pole Foundation	ass	561.53
5.	Transformer pole foundation (2x300dan)	ass	1123.06
6.	Load break switch foundation (2*300dan)	ass	1123.06
7.	Conductor stringing (3-phase)	km	2025.08
8.	Tapping point arrangement	Per site	805.74
9.	Test and commissioning	km	264.95
10.	Transformer erection with earthing	ass	4794.63

Table 4-8: 0.4kV low voltage system construction cost

No.	Material	Unit	Unit Price[ETB]
1.	Surveying of LV routes , profile drawing and detail design calculation	km	944.16
2.	Light angle assembly with guy wire	ass	1238.91
3.	Distribution pole foundation	ass	561.53
4.	Conductor stringing (3-phase)	km	919.79
5.	Test and commissioning	km	264.95
6.	Earthing installation	set	107.04

Table 4-9: Grid extension accessories transportation cost of 33kV MV assembly

No.	Material	Unit	Unit Price[ETB]
1.	Suspension assembly	ass	692.11
2.	Load break switch assembly	ass	692.11
3.	AAAC95mm2 conductor	km	637
4.	Tie wire needed for stringing of 1km 3phase	km	478.8
5.	Transformer with all accessories	set	719.6
6.	Transformer pole transportation	pair	1384.22

Table 4-10: Grid extension accessories transportation cost of 0.4 kV LV assembly

No.	Material	Unit	Unit Price[ETB]
1.	Light angle assembly with all accessories	ass	692.11
2.	Earthing accessories	set	12.6
3.	ABC conductor	km	824.6

To analyze the grid extension cost of the power system an excel spread sheet software taken from UEAP (universal electricity access program) is used. The software contains the following features:

- All necessary components of the distribution system (tower, transmission cable, various insulators, Cross arms, drop out fuses, cements, sands, stones, e.t.c.)
- The cost of materials, Labors and Transportation
- Also MV, Transformer and LV systems are analyzed separately

Finally, based on the above cost consideration of grid extension system, the analyzing tool calculates the breakeven grid extension distance using eq^{n} 4.2 to compare grid extension system with a standalone hybrid power supply system. Breakeven grid extension distance is the distance from the grid which makes the net present cost of extending the grid equal to the net present cost of the stand-alone system. Farther away from the grid, the stand-alone system is optimal. Nearer to the grid, grid extension is optimal. [32]

$$D_{grid} = \frac{C_{NPC}.CRF\left(i,R_{proj}\right) - C_{power}.L_{tot}}{C_{cap}\,CRF\left(i,R_{proj}\right) + C_{OM}} \qquad (4.2)$$

Where:

C_{NPC}=total net present cost of the standalone power system ($)

CRF=capital recovery factor

i=interest rate (%)

R_{proj}=project life time (yr)

L_{tot}=total primary and deferrable load (kWh/yr)

C_{power}=cost of power from the grid ($/kWh)

C_{cap}=capital cost of grid extension ($/km)

C_{om}=O&M cost of grid extension ($/km/yr)

The software is analyzed and summarized in Table 4.11 given below.

Table 4-11: Grid Extension Cost of Site-A, Site-B, Site-C and Site-D.

Study Area	Grid Voltage level	Distance from Grid	Unit capital cost, $/km	Unit O&M cost, $/km/yr	Total Capital Cost of grid extension	Grid power price, $/kWh
Site-A	33kV	11km	13432	267	147752	0.04
Site-B	33kV	6km	17454	349	104724	0.04
Site-C	33kV	2km	35792	716	71584	0.04
Site-D	33kV	12km	11741	235	140892	0.04

The total capital costs of grid extension are $147752, $104724, $71584 and $140892, for Site-A, Site-B, Site-C and Site-D respectively. Moreover, the breakeven distances from the extended grid tapping point are 42.3km, 28.1km, 13.2km and 21.8km for Site-A, Site-B, Site-C and Site-D respectively.

4.6.3. Cost analysis of hybrid system

A. Cost of Biogas Plant

The cost of the biogas plant includes the cost of Biogas digester and biogas generator elements. Based on Ethiopia national biogas program report in 2008, the average investment cost for a 6 m^3 biogas plants is ETB 7500 [58]. According to the estimations of local experts in USA, the capital costs of small-scale (up to 6-8 m^3) thermophilic bioreactors can be reduced by 25 - 35% in case of mass production (about 50 units per year). The annual O&M cost of thermophilic bioreactors is about 2% of capital costs [96]. The capital, replacement and O&M cost of a biogas generator is $500, $400, and $0.05/hr respectively [20].The capital cost includes all components of the biogas plant plus biogas land cost, administrative and transport costs and consultancy fees.

Site-A

The size of the biogas digester for site-A is 621m3 (refer Chapter 2). Assuming 30% capital cost decrement due to large size of the digester, it is more than 50, 6m3 biogas digester units. The capital and O&M cost of the biogas system can be estimated as follows:

- ✓ Capital cost = 621m3 * 7500ETB/6m3 -0.3*621m3*7500ETB/6m3= 776250ETB - 0.3 * 776250ETB = 543375ETB = USD 29,276.7
- ✓ Operation and maintenance cost is 2% of the capital cost =0.020*543375=10867.5ETB/year=USD585.5/year

Site-B

The size of biogas digester for Site-B is 529m3 (refer Chapter 2). Assuming 30% capital cost decrement due to large size of the digester, it is more than 50, 6m3 biogas digester units.

- ✓ Capital cost=529m3*7500ETB/6m3-0.3*529m3*7500ETB/6m3 = 661250ETB-0.3 * 661250ETB=462875ETB= USD24,939
- ✓ Operation and maintenance cost is 2% of the capital cost =0.020*462875=9257.5ETB/year=USD 499/year

Site-C

The size of biogas digester for Site-C is 504m3 (refer Chapter 2). Assuming 30% capital cost decrement due to large size of the digester, it is more than 50, 6m3 biogas digester units.

- ✓ Capital cost = 504m3 * 7500ETB/6m3- 0.3*504m3 * 7500ETB/6m3 = 630000ETB - 0.3 * 630000ETB = 441000ETB =USD 23,761
- ✓ Operation and maintenance cost is 2% of the capital cost =0.020*441000=8820ETB/year=USD 475/year

Site-D:

The size of biogas digester for Site-D is 177m3. 30% capital cost decrement is not considered here due to small size of the digester, because it is less than 50, 6m3 biogas digester units.

- ✓ Capital cost=177m3*7500ETB/6m3=221,250ETB=USD 11,921
- ✓ Operation and maintenance cost=0.020*USD11921=USD238.4/year

The corresponding biogas generator capital cost for all sites is added to the biogas digester cost based on the capacity of the gas to generate electricity. But, O&M costs of the biogas system and generator are not summed together because one is in $/year while the other is in $/hr. So the O&M cost of the biogas digester is put in to the fixed O&M cost in the economic wind together with other fixed O&M cost of the system and the generator O&M cost is put in to the biogas generator input window.

B. Solar PV System

The solar PV panels are connected in series or/and parallel to generate the required power output. When the sunlight is incident on a PV panel it produces electricity. The capital cost and replacement cost for a 1kW SPV is taken as $2200. As there is very little maintenance required for PV, only $10/year is taken for O&M costs [4]. Like for all other hybrid system components the per kW costs considered includes installation, logistics and some other costs. The derating factor considered is 95% for each panel to approximate the varying affects of temperature and dust on the panels with a life time of 20 years. The panels have no tracking system and are tilted at 10.55^{o} (latitude of the site) facing to south.

C. Wind turbine system

A wind turbine type, Huaying 5kW horizontal-axes wind turbines, is considered for this hybrid system. The HY5-AD5.6 wind turbine gives 5kW of AC output. The capital cost of one unit is taken as $5130 and its replacement cost is two third of the capital cost while the operation and maintenance cost is considered to be 2% of the capital cost [20][97-99]. This wind turbine has a hub height of 20m and a lifetime of 20 years.

D. Biodiesel system

The biodiesel system consists of jatropha oil expeller and biodiesel generator. As there is a variety of diesel generators available from various manufacturers and distributors, it is difficult to compare all the different information. The capital cost, replacement cost, O&M costs of a 25kW biodiesel generator are taken as $7875, $5875, and $0.1/hr respectively. The per kW costs of BDG include the costs of jatropha oil expeller, installation, logistics and other costs in addition to the generator. [100][101]

E. Battery

Batteries are used as a backup in the system and to maintain a constant voltage during peak loads or a shortfall in generation capacity. To model the hybrid system, Surrette 6CS25P rechargeable battery is chosen. It is a 6V battery with a nominal capacity of 1,156 Ah (6.94 kWh). Two batteries per string are chosen in order to get a nominal battery terminal voltage of 12V. It has a lifetime throughput of 9,645kWh. The capital cost, replacement cost and O&M costs for one unit of this battery were considered as $833, $555, and $15/year respectively. [10]

F. Converter

A converter is an electronic power device that is required in a hybrid system to maintain the energy flow between AC and DC electrical components. The AC output of the biogas, biodiesel and wind turbine generator are integrated and controlled in such a way that the output can be directly supplied to the connected AC load. When there is excess of energy (mainly from the wind, PV and biogas), it is directed to the battery through the converter and DC center. Similarly, the DC output of the PV panel is connected to the system via the DC center. The DC center is integrated with the system through DC/AC and AC/DC converters, As well as, it is connected to PV and battery components [17]. The capital cost, replacement cost and O&M costs for 1kW converter were considered as $700, $550, and $100/year respectively and also the lifetime of the converter of 15 years, inverter efficiency of 95% and rectifier efficiency of 95% is considered. [102]

Table 4-12: Hybrid system cost, size and technical parameter summary of all districts.

District	System Parameters	PV-panel	Wind turbine HY5-AD5.6	Biogas system	Biodiesel system	Battery	Converter
Site-A	Size (kW)	1	5	85	25	1156Ah	1
	Capital cost($)	2200	5130	71776	7875	833	700
	Replacement cost ($)	2200	3420	71776	5875	555	550
	O&M ($/yr)	10	103	0.05$/h	0.1$/h	15	100
	Size (kW) considered	0,30,35,40,45,50, 60,80,130,200	---	0,30,85, 125,500	15	---	0,25, 45,200
	Quantities considered	---	0,4,6,10,11,13,15,16,17, 18,19,26,27, 28, 40, 100	---	---	0,20,30, 70,120	---
	Life time	20yr	20yr	120000hr	15000hr	---	15
Site-B	Size (kW)	1	5	75	25	1156Ah	1
	Capita cost($)	2200	5130	62439	7875	833	700
	Replacement cost ($)	2200	3420	62439	5875	555	550
	O&M ($)	10	103	0.05$/h	0.1$/h	15	100
	Size (kW) considered	0,30,35,40,45,50, 55,70,100,200	---	0,30,75, 110,500	15	---	0,25, 30,120
	Quantities considered	---	0,6,7,8,9,10,11,13, 14,15,16,25,35,100	`---	---	0,20,35,5 0,70,100	---
	Life time	20yr	20yr	120000hr	15000hr	---	15
Site-C	Size (kW)	1	5	75	25	1156Ah	1
	Capita cost($)	2200	5130	61261	7875	833	700
	Replacement cost ($)	2200	3420	61261	5875	555	550
	O&M ($)	10	103	0.05$/h	0.1$/h	15	100
	Size (kW) considered	0,30,33,35,40,45, 50,70,120,150	---	0,30,75, 100,500	15	---	0,25,30 45,120
	Quantities considered	---	0,6,8,9,10,12,13,14,15,1 8,19,20,23,25, 100	---	---	0,20,35, 70,100	---
	Life time	20yr	20yr	120000hr	15000hr	---	15
Site-D	Size (kW)	1	5	30	25	1156Ah	1
	Capital cost($)	2200	5130	26919	7875	833	700
	Replacement cost ($)	2200	3420	26919	5875	555	550
	O&M ($)	10	103	0.05$/h	0.1$/h	15	100
	Size (kW) considered	0,20,22,25,30,35, 45,60,120	---	0,25,30, 45,500	10	---	0,20, 80,120
	Quantities considered	---	0,2,5,6,7,8,9,10,11, 12,14,15,20,50,	---	---	0,20, 40,70	---
	Life time	20yr	20yr	120000hr	15000hr	---	15

G. Power Distribution Cost of the Hybrid System

These costs are the cost of the distribution part of the hybrid system to reach electrical energy from the hybrid center to the customer side. The cost includes;

- Material costs of low voltage system assemblies discussed in Section 4.6.2
- Transport cost of all low voltage assemblies and,
- Construction cost of the system

The operation and maintenance cost of the biogas digester together with the hybrid system power distribution O&M cost are considered as the system fixed O&M cost and put into the HOMER economic window. To analyze the power distribution cost of the hybrid system an excel spread sheet software taken from UEAP (universal electricity access program) is used.

The power distribution cost of the hybrid system depends on its location. The following hybrid system site selection criteria are used to select the hybrid system location.

- The site should consider the wind resource obstacles
- Avoid bad smell from biogas plant
- Infrastructure facility, roads are available
- As possible the site should be center for all cluster

Site-A

Figure 4-20: The proposed location of the hybrid system for Site-A.

The hybrid system should be located at the appropriate location which has equal distance from all the clusters (Jarso, Gillu and Amayo) connected to it and in a way that haven't social impact on the community (e.g: community water contamination and bad smell from biogas plant), and suitable location for wind turbine site.

Inputs to the software:

- 3*1.2=3.6km three phases LV distribution line.
- 3*1km=3km single phase LV distribution line (assuming a 1km inter distribution distance to reach every ones house for each cluster is considered).
- The cost of material, material transport, and Labor to estimate the power distribution cost of the hybrid system is based on the above listed cost used by UEAP.
- Distance from study area to UEAP store is 140km (which is Kombolcha)

So, based on the above input data feed into the software and the types of pole, cable, insulator, switching device, height of pole, e.t.c. selected in the software; the estimated capital cost of the distribution system of **site A** is 994,317.69 ETB=$53,458 and its O&M cost is 2% of the capital cost, $1069/year.

Site-B

Inputs to the software:

- 3*0.75km=2.25km three phases LV distribution line.
- 3*1km=3km single phase LV distribution line (a 1km inter distribution distance to reach every ones house for each cluster is considered).

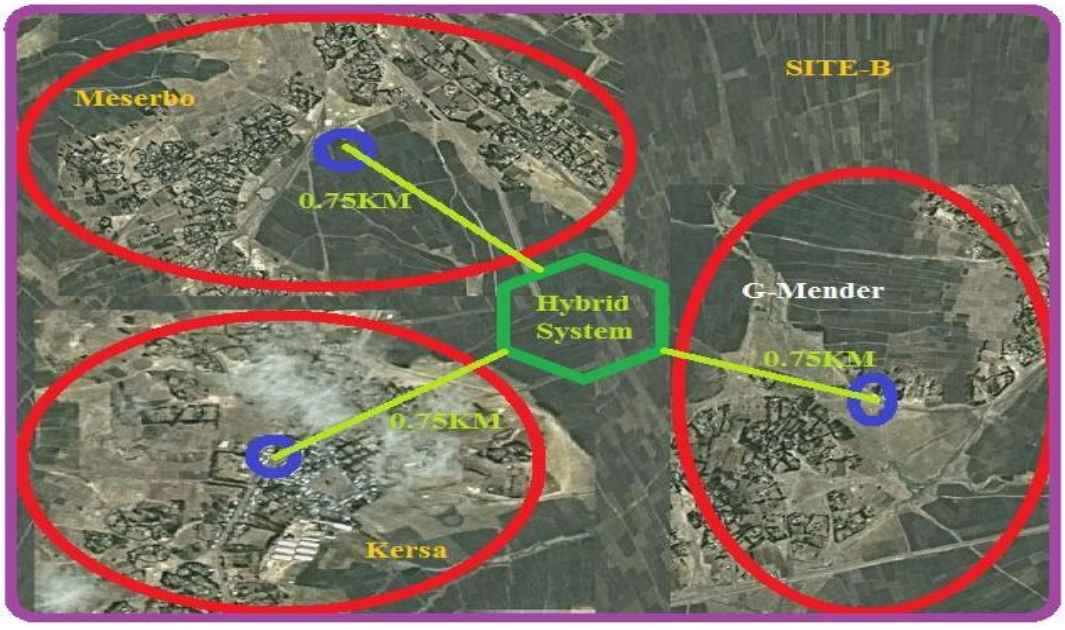

Figure 4-21: The proposed location of the hybrid system for Site-B.

The results of the simulation give us capital cost of the distribution system of site B is $40,785 and its O&M cost is $816/year.

Site-C:

Inputs to the software:

- (0.4km+0.5km+0.5km)=1.4km three phases LV distribution line.

- 3*1km=3km single phase LV distribution line (assuming a 1km inter distribution distance to reach every ones house for each cluster is considered).

So, based on the above input data feed into the software and the types of pole, cable, insulator, switching device, height of pole, e.t.c. selected in the software; the estimated capital cost of the distribution system of **site C** is $34,990 and its O&M cost is 2% of the capital cost, $670/year.

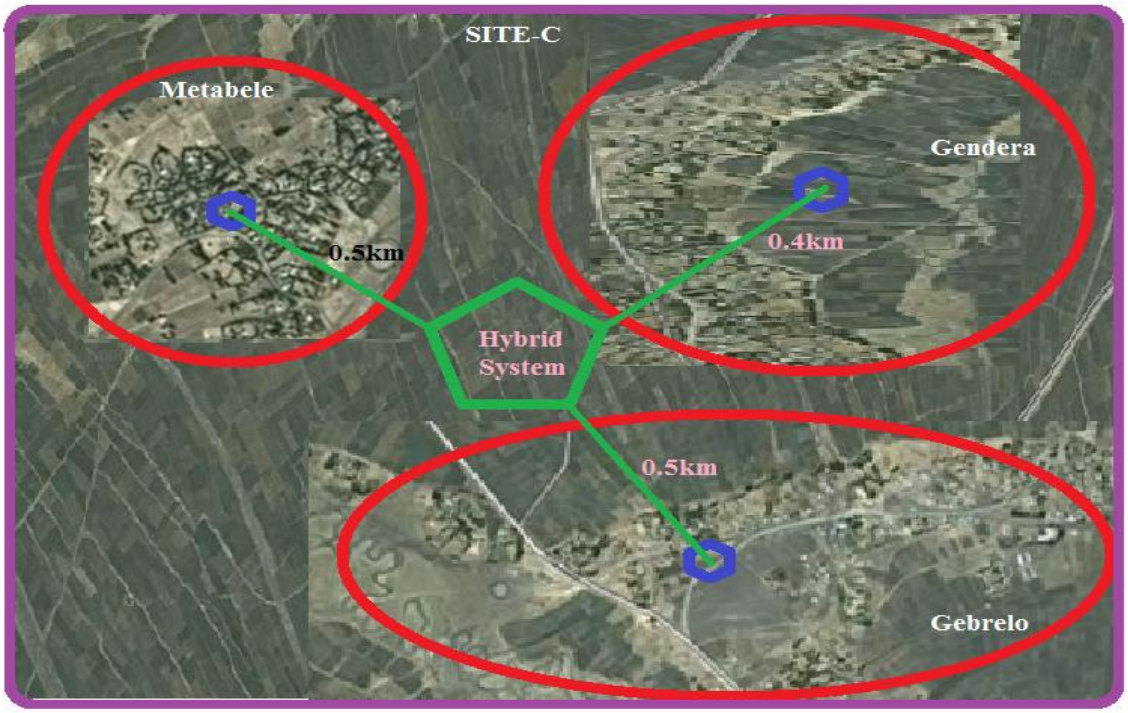

Figure 4-22: The proposed location of the hybrid system for Site-C.

Site-D

Inputs to the software:

- 2*0.8km=1.6km three phases LV distribution line.
- 2*1km=2km single phase LV distribution line (assuming a 1km inter distribution distance to reach every ones house for each cluster is considered).
- Distance from study area to UEAP store is 140km (which is Kombolcha)
- The cost of material, material transport, and Labor cost to estimate the power distribution cost of the hybrid system is based on the current costs of the above listed cost used by UEAP.

The software generates a capital cost of the distribution system of site D is $28,128 and its O&M cost is $563/year.

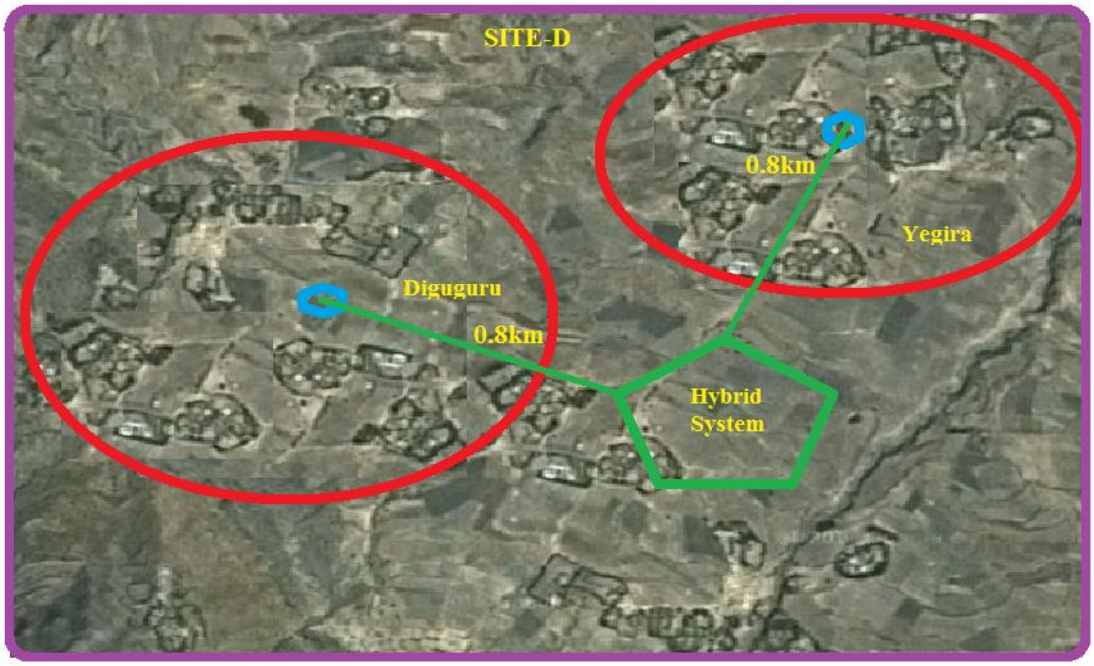

Figure 4-23: The proposed location of the hybrid system for Site-D.

Table 4-13: Cost summary of Hybrid system component feed in to HOMER.

System component	Cost type	Site-A	Site-B	Site-C	Site-D
Biogas digester	Capital cost, $	29276	24939	23761	11921
	O&M cost, $/yr	585.5	499	475	238.4
Hybrid system distribution network cost	Capital cost, $	53457	40785	34990	28128
	O&M cost, $/yr	1069	816	670	563
Grid expansion network cost	Capital cost, $/km	38758.14	42581.3	59726	36939
	O&M cost, $/km/yr	775.16	852	1195	739
Jatropha oil expeller	Capital cost, $	1000	1000	1000	1000
	O&M cost, $/hr	0.05	0.05	0.05	0.05
Gas production rate	m^3/day	597.7	509	485.1	170
Biogas generator size corresponding to the size of the digester.	kW	85kW(10hr)	75kW(10hr)	75kW(10hr)	30kW(8hr)
Economic window input	Hybrid system fixed capital cost ($)	53457	40785	34990	28128
	Hybrid system O&M cost ($/yr)	1069	816	670	563
	Digester O&M cost ($/yr)	585.5	499	475	238
	Total Fixed O&M cost	1654.5	1315	1145	801

CHAPTER 5

5. SIMULATION RESULTS AND DISCUSSION

5.1. Introduction

In this thesis, the RE resource potential and feasibility study of electricity generation from a hybrid system in Jama Woreda, Kebele-8 were performed. HOMER is used as a tool for feasibility study. The wind, solar resource data, biogas and biodiesel feedstock data (see Chapter 2), community load data (see Chapter 4) and the cost of hybrid system component are feed into HOMER by specifying system constraints and system controls to simulate the analysis. To find the optimum solutions, HOMER is run repeatedly by varying parameters that have a controlling effect over the output. The output of the simulation is a list of feasible combinations of solar PV, wind-turbine, biogas generator, biodiesel generator, converter, and battery hybrid system set-up.

The feasibility study is carried out in two ways: optimization and sensitivity analysis. The optimization results are given out in an overall form and in a categorized form which represents feasible system configurations capable of meeting the system load and set of constraints. The results are displayed in an increasing order of total net present cost (NPC). A given system type may have many different configurations based on the size of constituent elements. The categorized table displays only the most cost effective configuration from each system type. The overall optimization table displays all feasible system configurations (for any possible system type) ranked in their cost effectiveness. From the details of the simulation result of the optimal system the following can be observed: system architecture, electrical system characteristics, optimal system cost summary, cash flow, hybrid system component performance characteristics, grid comparison, emission summary, hourly resource and load data, total NPC, operating and maintenance cost of each system and cost of energy (COE).

N.B: Initial capital cost, cost of energy (COE), unmet load and total NPC values can be used as a parameter of selecting a given configuration among the many candidates.

The sensitivity analysis explains how input variables having dynamic nature behave on the hybrid system performance. It takes the most cost effective system configuration for each combination of sensitivity variable values. Since the price for PV panels, community demand and wind resources are more dynamic than other types of parameters. A range of wind speed (2-6m/s) and a PV capital cost multipliers (0.4 to 1.4) are used as sensitivity parameters. The PV capital and replacement cost multipliers; and the community primary and deferrable loads are linked together. HOMER displays the sensitivity analysis both in tabular and graphical form. For each combination of the sensitivity variables, the sensitivity analysis takes the least

cost (ranked 1st) and extrapolates it for the intermediate sensitivity variables. The possibility of other system types can be observed by clicking on the sensitivity graph.

5.2. Optimization Result

For the off-grid electrification of the study area various combinations of hybrid systems with solar PV, wind turbines, biogas generator, biodiesel generator, batteries and convertors have been obtained from the HOMER Optimization simulation.

5.2.1. Result for Site-A

Table 5-1: Top ranked overall optimization result of Site-A

Sensitivity Results | Optimization Results

Sensitivity variables

PL-A (kWh/d) 817 | Wind Speed (m/s) 3.1 | PV Capital Multiplier 1

Double click on a system below for simulation results. | Categorized | Overall | Export... | Details

PV (kW)	HY5AD	BG (kW)	BD (kW)	S6CS25P	Conv. (kW)	Disp. Strgy	Initial Capital	Operating Cost ($/yr)	Total NPC	COE ($/kWh)	Ren. Frac.	Capacity Shortage	Biodiesel (m3)	Biomass (t)	BG (hrs)	BD (hrs)
40	13	85	15	40	25	LF	$ 335,468	43,806	$ 837,915	0.239	0.94	0.00	5	2,351	4,061	1,833
40	11	85	15	40	25	LF	$ 325,208	44,705	$ 837,976	0.239	0.94	0.00	5	2,423	4,104	1,845
45	11	85	15	40	25	LF	$ 336,208	43,779	$ 838,346	0.239	0.94	0.00	5	2,359	4,058	1,841
40	10	85	15	40	25	LF	$ 320,078	45,187	$ 838,369	0.239	0.94	0.00	5	2,462	4,129	1,839
40	15	85	15	40	25	LF	$ 345,728	42,956	$ 838,430	0.239	0.94	0.00	5	2,282	4,008	1,826
40	16	85	15	40	25	LF	$ 350,858	42,550	$ 838,908	0.239	0.94	0.00	5	2,249	3,983	1,820
45	10	85	15	40	25	LF	$ 331,078	44,277	$ 838,926	0.239	0.94	0.00	5	2,399	4,090	1,841
45	13	85	15	40	25	LF	$ 346,468	42,942	$ 839,011	0.239	0.94	0.00	5	2,291	4,022	1,829
40	17	85	15	40	25	LF	$ 355,988	42,191	$ 839,914	0.239	0.94	0.00	5	2,219	3,961	1,817
45	15	85	15	40	25	LF	$ 356,728	42,129	$ 839,947	0.239	0.94	0.00	5	2,225	3,970	1,819
35	15	85	15	40	25	LF	$ 334,728	44,062	$ 840,119	0.239	0.94	0.00	5	2,357	4,067	1,831
35	13	85	15	40	25	LF	$ 324,468	44,961	$ 840,164	0.239	0.94	0.00	5	2,430	4,119	1,838
35	16	85	15	40	25	LF	$ 339,858	43,630	$ 840,293	0.239	0.94	0.00	5	2,323	4,039	1,822
45	16	85	15	40	25	LF	$ 361,858	41,744	$ 840,661	0.239	0.94	0.00	5	2,193	3,944	1,816
40	18	85	15	40	25	LF	$ 361,118	41,821	$ 840,804	0.239	0.94	0.00	5	2,188	3,935	1,822
35	11	85	15	40	25	LF	$ 314,208	45,912	$ 840,820	0.239	0.94	0.00	5	2,506	4,168	1,836
35	17	85	15	40	25	LF	$ 344,988	43,272	$ 841,311	0.240	0.94	0.00	5	2,292	4,021	1,822
35	10	85	15	40	25	LF	$ 309,078	46,405	$ 841,342	0.240	0.94	0.00	5	2,545	4,190	1,835
50	11	85	15	40	25	LF	$ 347,208	43,084	$ 841,377	0.240	0.94	0.00	5	2,311	4,022	1,835
50	10	85	15	40	25	LF	$ 342,078	43,547	$ 841,564	0.240	0.94	0.00	5	2,348	4,047	1,843
45	17	85	15	40	25	LF	$ 366,988	41,404	$ 841,887	0.240	0.94	0.00	5	2,164	3,923	1,819
35	18	85	15	40	25	LF	$ 350,118	42,889	$ 842,054	0.240	0.94	0.00	5	2,261	3,992	1,822
40	19	85	15	40	25	LF	$ 366,248	41,493	$ 842,165	0.240	0.94	0.00	5	2,159	3,919	1,813
50	13	85	15	40	25	LF	$ 357,468	42,276	$ 842,365	0.240	0.94	0.00	5	2,244	3,984	1,822
35	19	85	15	40	25	LF	$ 355,248	42,537	$ 843,141	0.240	0.94	0.00	5	2,231	3,974	1,824
45	18	85	15	40	25	LF	$ 372,118	41,072	$ 843,215	0.240	0.94	0.00	5	2,135	3,905	1,815

Table 5-2: Categorized optimization result of Site-A

Sensitivity Results | Optimization Results

Sensitivity variables

PL-A (kWh/d) 817 | Wind Speed (m/s) 3.1 | PV Capital Multiplier 1

Double click on a system below for simulation results. | Categorized | Overall | Export... | Details

PV (kW)	HY5AD	BG (kW)	BD (kW)	S6CS25P	Conv. (kW)	Disp. Strgy	Initial Capital	Operating Cost ($/yr)	Total NPC	COE ($/kWh)	Ren. Frac.	Capacity Shortage	Biodiesel (m3)	Biomass (t)	BG (hrs)	BD (hrs)
40	13	85	15	40	25	LF	$ 335,468	43,806	$ 837,915	0.239	0.94	0.00	5	2,351	4,061	1,833
45		85	15	40	25	LF	$ 279,778	50,973	$ 864,432	0.246	0.94	0.00	5	2,901	4,522	1,955
	26	85	15	40	25	LF	$ 314,158	50,502	$ 893,411	0.254	0.94	0.00	5	2,722	4,658	1,725
	10	85	15			LF	$ 181,258	64,719	$ 923,580	0.264	0.94	0.01	5	3,978	6,816	1,848
40	13	85	15		25	LF	$ 302,148	55,292	$ 936,347	0.267	0.95	0.00	5	3,163	5,621	2,092
		85	15	40	25	LF	$ 180,778	67,304	$ 952,751	0.273	0.93	0.01	5	3,978	6,195	1,685
60		85	15		45	LF	$ 293,458	62,055	$ 1,005,225	0.286	0.95	0.01	5	3,517	6,258	2,304

The results obtained were based on a wind speed of 3.1 m/s, a primary and deferrable community load of 817kWh/day and 22kWh/day respectively and PV capital cost of $2200/kW. From Table 5-2 and the overall simulation result, the levelized COE was observed to be in the range of $0.239/kWh to $0.286/kWh, initial capital cost ranges from $180,778 to $451,078, operating cost ranges from $36,664 to $67,304 and the total NPC lies

in the range of $837,915 to $1,005,225. Both of LF and CC dispatch strategies are feasible. By any means a hybrid system contain PV, biogas generator, biodiesel generator, wind turbine, converter and battery is the cheapest system with low NPC and small COE. The contribution of the renewable energy resource is indicated by the renewable fraction given in percentages. The renewable fraction in this study is 100% for all feasible system since no conventional energy source is used. Capacity shortage is allowed to go a maximum of 1%.

As seen from the categorized simulation results there are systems which do not contain wind turbine and PV and which do not require battery and converter. But those systems are not as cost effective as a hybrid system contains all system components together. Even if the COE obtained here is higher compared to the current energy tariff of Ethiopia which is below $0.04/kWh but still this is within the range of the global tariff. Due to high transmission power loss and power outage problem of the current system a 100% clean, environmental friendly, green energy, renewable, and reliable hybrid system, was even better than the current system if we think for our future and our planet to be safe. The simulation result in Table 5-1 shows that all feasible system have the same renewable fraction and unmet load (0%). Those systems are compared based on NPC, COE and initial capital cost instead of the above common parameters.

Table 5-3: System report for top (1st) ranked hybrid system for Site-A

System Architecture		Sensitivity case		Annual Electric production[kWh/yr]		Annual Electric Consumption[kWh/yr]		Emission[kg/yr]	
PV	40kW	**PV capital Multiplier**	1	**PV**	82926 [25%]	**AC primary Load**	298156 [97%]	**CO2**	14062
Wind	13	**PV Replacement Multiplier**	1	**Wind**	60082 [18%]	**Deferrable Load**	8016 [3%]	**Unburned hydro carbon**	1.70
Biogas	85kW	**Primary Load[kWh/d]**	817 kWh/d	**Biogas**	171666 [51%]	**Total**	306172 [100%]	**Particulate Matter**	1.715
Biodiesel	15kW			**Biodiesel**	20975 [6%]	**Cost Summary**			
Inverter	25kW	**Deferrable Load[kWh/d]**	22 kWh/d	**Total**	335649 [100%]				
Rectifier	25kW			**Excess Electricity**	20105 [5.99%]	**Total NPC**	$837,915	**SO2**	0.227
Battery	40	**Wind Speed**	3.1m/s	**Unmet demand**	48.8 [0.02%]	**Levelized COE**	$0.239/ kWh	**NOx**	137
Dispatch strategy	LF	**Solar Radiation**	6.13 kWh/d/m2	**Capacity Shortage**	384 [0.13%]	**Operating cost**	$43806/yr	**CO**	15.3

The first ranked system has a NPC of $837,915, an initial capital of $335,468 and a COE of $0.239/kWh. A hybrid system setup ranked second have NPC of $837,976 and the same COE but lower initial capital cost of $325,208. The top (1st) ranked system is better than the lower ranked system in terms of NPC and COE while the remains systems are not selected to implement on ground as compared with the first system in the overall optimization table. Since NPC and COE are effective economic measures than the initial capital cost to compare systems. The system report for this particular setup is summarized in Table 5-3.

The monthly average electric energy production by each individual's hybrid system energy producing component (PV panel, Wind turbine, Biogas and Biodiesel generator) and the NPC of the system given by the capital, replacement, O&M, fuel and salvage cost are summarized in Figures 5.1 & 5.2 given below.

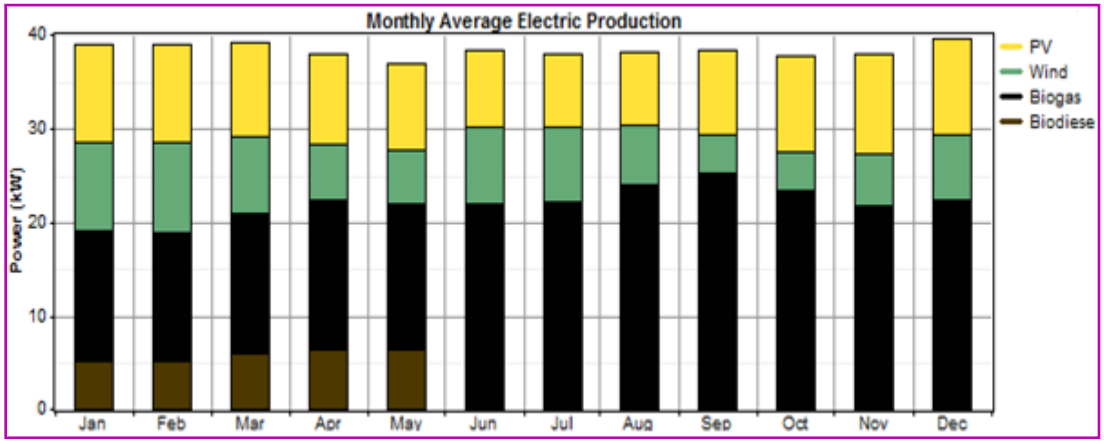

Figure 5-1: Monthly average electric production for Site-A

The electrical power generated by the hybrid system component is highly depend on the nature of the energy resources. The electrical power produced from PV array depends on the time of the day and the strength of solar radiation while electrical energy from the wind turbine depends on the availability of wind resource (wind speed). Wind resource is highly intermittent and this has great impact on the wind turbine output. The electrical power output from biodiesel and biogas generator depends on the availability of the fuel resource. From Figure 5.1 we can observe that biogas system produces more electricity (51%) as compared with, PV (25%), Wind (18%), and Biodiesel (6%).

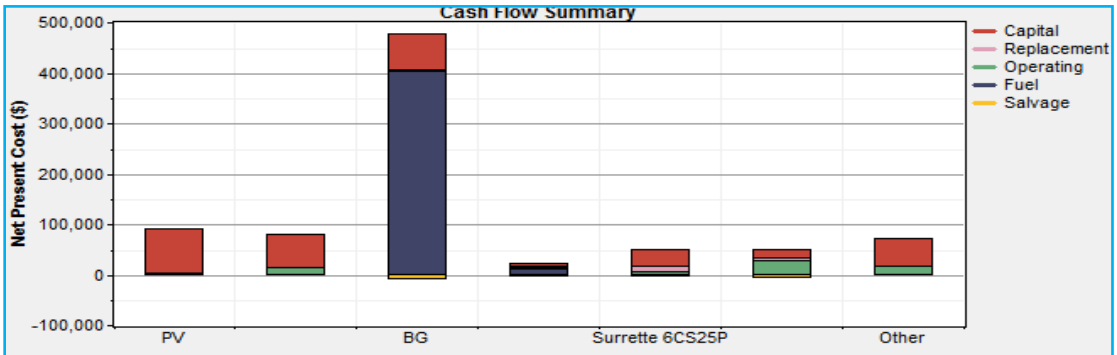

Component	Capital ($)	Replacement ($)	O&M ($)	Fuel ($)	Salvage ($)	Total ($)
PV	88,000	0	4,588	0	0	92,588
HY5_AD5.6	66,690	0	15,358	0	0	82,048
Biogas	71,776	0	2,329	404,456	-7,233	471,328
Biodiesel	4,725	3,546	1,261	12,608	-611	21,530
Surrette 6CS25P	33,320	11,033	6,882	0	-2,307	48,927
Converter	17,500	5,737	28,675	0	-2,858	49,054
Other	53,457	0	18,983	0	0	72,440
System	335,468	20,317	78,076	417,064	-13,009	837,915

Figure 5-2: Cost Summary of the above optimal system for Site-A.

The optimization result in the case of forecasted load demand of the community is presented below in Table 5-4 & 5-5. The result obtained here is based on a wind speed of 3.1 m/s, a primary and deferrable community load of 1,132kWh/day and 31.4kWh/day respectively and PV capital cost of $2200/kW.

Table 5-4: Top ranked overall optimization result under forecasted load scenario.

Sensitivity Results | Optimization Results

Sensitivity variables

PL-A (kWh/d) 1,132 | Wind Speed (m/s) 3.1 | PV Capital Multiplier 1

Double click on a system below for simulation results. ○ Categorized ● Overall Export... Details

PV (kW)	HY5AD	BG (kW)	BD (kW)	S6CS25P	Conv. (kW)	Disp. Strgy	Initial Capital	Operating Cost ($/yr)	Total NPC	COE ($/kWh)	Ren. Frac.	Capacity Shortage	Biodiesel (m3)	Biomass (t)	BG (hrs)	BD (hrs)
60	15	125	15	40	45	LF	$ 437,505	63,409	$ 1,164,797	0.239	0.96	0.00	5	3,494	4,159	1,808
60	16	125	15	40	45	LF	$ 442,635	62,989	$ 1,165,108	0.239	0.96	0.00	5	3,460	4,142	1,806
60	17	125	15	40	45	LF	$ 447,765	62,548	$ 1,165,191	0.239	0.96	0.00	5	3,425	4,119	1,808
60	13	125	15	40	45	LF	$ 427,245	64,342	$ 1,165,240	0.239	0.95	0.00	5	3,569	4,204	1,805
60	11	125	15	40	45	LF	$ 416,985	65,281	$ 1,165,750	0.239	0.95	0.00	5	3,643	4,240	1,819
40	15	125	15	40	25	LF	$ 379,505	68,577	$ 1,166,075	0.241	0.95	0.01	5	3,978	4,730	1,820
60	18	125	15	40	45	LF	$ 452,895	62,185	$ 1,166,156	0.239	0.96	0.00	5	3,394	4,107	1,798
60	10	125	15	40	45	LF	$ 411,855	65,784	$ 1,166,390	0.240	0.95	0.00	5	3,683	4,259	1,830
60	4	125	15	40	45	CC	$ 381,075	68,515	$ 1,166,940	0.240	0.95	0.00	5	3,933	3,667	1,577
35	17	125	15	40	25	LF	$ 378,765	68,725	$ 1,167,041	0.241	0.95	0.01	5	3,978	4,717	1,794
60	19	125	15	40	45	LF	$ 458,025	61,823	$ 1,167,130	0.240	0.96	0.00	5	3,364	4,089	1,794
60	16	125	15	60	45	LF	$ 459,295	61,725	$ 1,167,276	0.240	0.95	0.00	5	3,334	4,047	1,790
60	17	125	15	60	45	LF	$ 464,425	61,281	$ 1,167,312	0.240	0.95	0.00	5	3,298	4,030	1,784
60	18	125	15	60	45	LF	$ 469,555	60,867	$ 1,167,695	0.240	0.96	0.00	5	3,265	4,015	1,778
60	15	125	15	60	45	LF	$ 454,165	62,211	$ 1,167,721	0.240	0.95	0.00	5	3,373	4,069	1,790
30	19	125	15	40	25	LF	$ 378,025	68,861	$ 1,167,856	0.242	0.95	0.01	5	3,977	4,716	1,772
60	19	125	15	60	45	LF	$ 474,685	60,464	$ 1,168,203	0.240	0.96	0.00	5	3,232	3,999	1,780
60	10	125	15	40	45	CC	$ 411,855	65,950	$ 1,168,294	0.240	0.95	0.00	5	3,723	3,615	1,582
60	13	125	15	60	45	LF	$ 443,905	63,206	$ 1,168,871	0.240	0.95	0.00	5	3,451	4,109	1,789
60	6	125	15	40	45	CC	$ 391,335	67,820	$ 1,169,222	0.240	0.95	0.00	5	3,872	3,696	1,583
50	10	125	15	40	45	CC	$ 389,855	67,991	$ 1,169,711	0.240	0.95	0.00	5	3,863	3,677	1,576
50	11	125	15	40	45	CC	$ 394,985	67,558	$ 1,169,865	0.240	0.95	0.00	5	3,828	3,663	1,577
40	19	125	15	40	25	LF	$ 400,025	67,162	$ 1,170,368	0.240	0.96	0.00	5	3,859	4,659	1,805
60	11	125	15	60	45	LF	$ 433,645	64,236	$ 1,170,432	0.240	0.95	0.00	5	3,532	4,148	1,801
40	26	125	15	40	25	LF	$ 435,935	64,045	$ 1,170,525	0.240	0.96	0.00	5	3,610	4,475	1,803
80	13	125	15	60	45	LF	$ 487,905	59,526	$ 1,170,664	0.240	0.96	0.00	5	3,197	3,990	1,798
80	10	125	15	60	45	LF	$ 472,515	60,877	$ 1,170,775	0.240	0.96	0.00	5	3,305	4,041	1,817
80	11	125	15	60	45	LF	$ 477,645	60,436	$ 1,170,846	0.240	0.96	0.00	5	3,270	4,028	1,812

Table 5-5: Categorized optimization result for Site-A under forecasted load scenario.

Sensitivity Results | Optimization Results

Sensitivity variables

PL-A (kWh/d) 1,132 | Wind Speed (m/s) 3.1 | PV Capital Multiplier 1

Double click on a system below for simulation results. ● Categorized ○ Overall Export... Details

PV (kW)	HY5AD	BG (kW)	BD (kW)	S6CS25P	Conv. (kW)	Disp. Strgy	Initial Capital	Operating Cost ($/yr)	Total NPC	COE ($/kWh)	Ren. Frac.	Capacity Shortage	Biodiesel (m3)	Biomass (t)	BG (hrs)	BD (hrs)
60	15	125	15	40	45	LF	$ 437,505	63,409	$ 1,164,797	0.239	0.96	0.00	5	3,494	4,159	1,808
80		125	15	40	45	CC	$ 404,555	68,035	$ 1,184,909	0.243	0.96	0.00	5	3,917	3,608	1,588
	40	125	15	40	25	LF	$ 419,755	69,788	$ 1,220,214	0.251	0.96	0.00	5	3,915	4,783	1,657
80	26	125	15		45	LF	$ 504,615	70,954	$ 1,318,448	0.271	0.96	0.00	5	3,963	5,010	2,034
	100	125	15			LF	$ 676,735	70,275	$ 1,482,780	0.304	0.97	0.00	5	3,787	5,206	1,987
200		125	15		200	LF	$ 743,735	86,540	$ 1,736,347	0.358	0.97	0.01	5	3,978	4,532	2,233

From Table 5-4 & 5-5, the levelized COE of the feasible hybrid system is observed to be in the range of $0.239/kWh to $0.358/kWh, initial capital cost ranges from $378,025 to $743,735, operating cost ranges from $57,209 to $86,540 and the total NPC lies in the range of $1,164,797 to $1,736,347. Both of LF and CC dispatch strategies are feasible. A hybrid system ranked first which contains PV, biogas generator, biodiesel generator, wind turbine, converter and battery is the cheapest system with low NPC and COE under LF dispatch strategy. As seen from the categorized simulation results there are systems which are not contain wind turbine and PV and which do not require battery and converter. But those systems are not as cost effective as a hybrid system contains all system components together.

The simulation result in Table 5-5 shows that all feasible system have the same renewable fraction and unmet load (~0%) those systems are compared based on NPC, COE and initial capital cost instead of the above common parameters. The first ranked system has a NPC of $1,164,797, an initial capital of $378,025 and a COE of $0.239/kWh. From the overall optimization result of the hybrid system, we can observed that the first optimal hybrid system (circled blue) simulated under forecasted load scenario has 39% more NPC, 30.4% more initial capital cost, 44.75% more operating and maintenance cost than that of the first optimal system simulated under the current load scenario shown in Table 5.1, but the two systems have the same COE, renewable fraction, dispatch strategy and capacity shortage.

Table 5-6: 1st ranked hybrid system report for Site-A under forecasted load scenario.

System Architecture		Sensitivity case		Annual Electric production[kWh/yr]		Annual Electric Consumption[kWh/yr]		Emission[kg/yr]	
PV	60kW	**PV capital Multiplier**	1	**PV**	124389 [26%]	**AC primary Load**	413164 [97%]	**CO2**	14269
Wind	15	**PV Replacement Multiplier**	1	**Wind**	69326 [15%]	**Deferrable Load**	11442 [3%]	**Unburned hydro carbon**	2.52
Biogas	125kW	**Primary Load[kWh/d]**	1132 kWh/d	**Biogas**	255134 [54%]	**Total**	424164 [100%]	**Particulate Matter**	1.71
Biodiesel	15kW			**Biodiesel**	20995 [4%]	**Cost Summary**			
Inverter	45kW	**Deferrable Load[kWh/d]**	31.4 kWh/d	**Total**	469843 [100%]				
Rectifier	45kW			**Excess Electricity**	34104 [7.26%]	**Total NPC**	$1,164,797	**SO2**	0.227
Battery	40	**Wind Speed**	3.1m/s	**Unmet demand**	16.7 [0%]	**Levelized COE**	$0.239/ kWh	**NOx**	203
Dispatch strategy	LF	**Solar Radiation**	6.13 kWh/d/m2	**Capacity Shortage**	226 [0.05%]	**Operating cost**	$63409/yr	**CO**	22.7

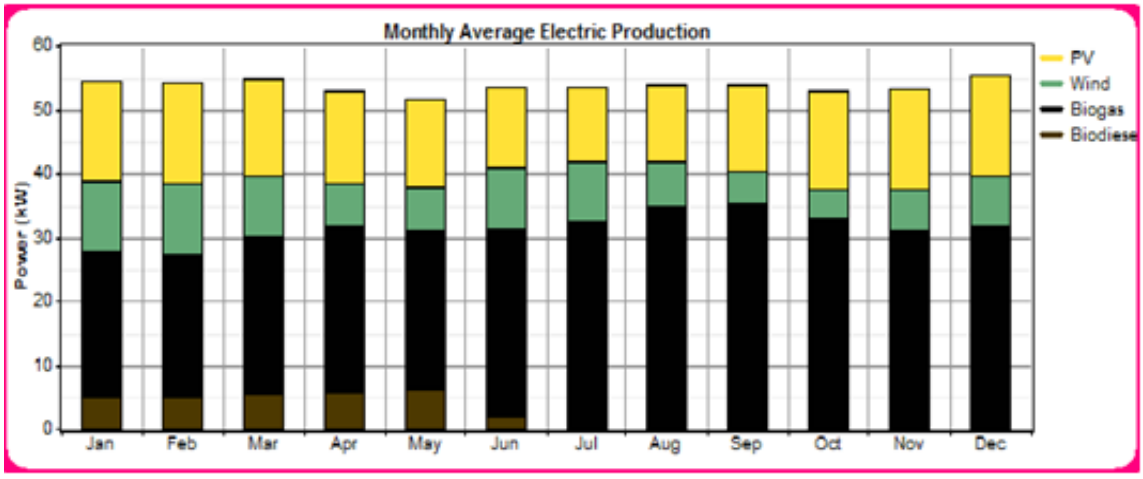

Figure 5-3: Monthly electric production of Site-A under forecasted load scenario.

The monthly average electric energy production by each individual's hybrid system energy producing component; PV panel (26%), Wind turbine (15%), Biogas generator (54%) and Biodiesel generator (4%) and the NPC of the system given by the capital, replacement, O&M, fuel and salvage cost are summarized in Figure 5.4 given below. From the total NPC

of the hybrid system, 60% of the system cost is from biogas system and the remains hybrid system components accounts only 40% of the total NPC of the system.

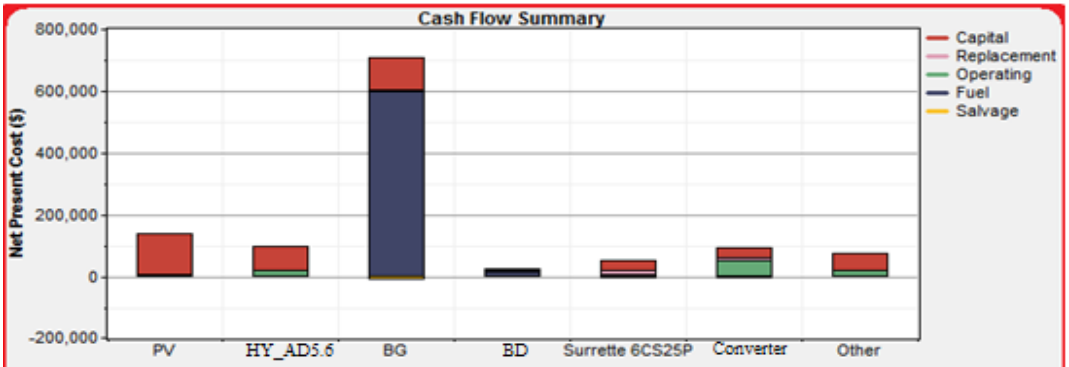

Component	Capital ($)	Replacement ($)	O&M ($)	Fuel ($)	Salvage ($)	Total ($)
PV	132,000	0	6,882	0	0	138,882
HY5_AD5.6	76,950	0	17,721	0	0	94,671
Biogas	105,553	0	3,508	601,165	-10,098	700,127
Biodiesel	4,725	3,514	1,244	12,617	-648	21,452
Surrette 6CS25P	33,320	11,033	6,882	0	-2,307	48,927
Converter	31,500	10,327	51,615	0	-5,145	88,297
Other	53,457	0	18,983	0	0	72,440
System	437,505	24,874	106,834	613,782	-18,198	1,164,797

Figure 5-4: Cost Summary of the above optimal system

5.2.2. Result for Site-B

The results are based on a wind speed of 3.1 m/s, a primary and deferrable community load of 714kWh/day and 18kWh/ day respectively and PV capital cost of $2200/kW. From Table 5.7, the levelized COE is observed to be in the range of $0.237/kWh to $0.285/kWh, capital cost ranges from $164,379 to $386,839, operating cost ranges from $31,520 to $55,190 and the total NPC lies in the range of $725,188 to $873,805. Both of LF and CC dispatch strategies are feasible. By any means a hybrid system contain PV, biogas generator, biodiesel generator, wind turbine, converter and battery is the cheapest system with low NPC and COE. The contribution of the renewable energy resource is indicated by the renewable fraction given in percentages. Capacity shortage is allowed to go a maximum of 1%.

Table 5-7: Categorized optimization result for Site-B

Sensitivity Results | Optimization Results

Sensitivity variables

PL-B (kWh/d) 714 | Wind Speed (m/s) 3.1 | PV Capital Multiplier 1

Double click on a system below for simulation results. Categorized

PV (kW)	HY...	BG (kW)	BD (kW)	S6CS2...	Conv. (kW)	Disp. Strgy	Initial Capital	Operating Cost ($/...	Total NPC	COE $/kWh	Ren. Frac.	Capacit Short...	Biodiese (m3)	Biomass (t)	BG (hrs)	BD (hrs)
40	11	75	15	40	25	LF	$ 303,199	36,791	$ 725,188	0.237	0.93	0.00	5	1,926	3,967	1,669
45		75	15	40	25	LF	$ 257,769	42,378	$ 743,846	0.243	0.93	0.00	5	2,361	4,333	1,773
	25	75	15	40	25	LF	$ 287,019	42,940	$ 779,542	0.254	0.94	0.00	5	2,256	4,538	1,576
	11	75	15			LF	$ 164,379	55,190	$ 797,408	0.261	0.94	0.01	5	3,376	6,738	1,724
40	10	75	15		25	LF	$ 264,749	47,974	$ 815,006	0.266	0.95	0.00	5	2,727	5,628	1,935
55		75	15		30	LF	$ 249,949	54,391	$ 873,805	0.285	0.95	0.01	5	3,146	6,439	2,112

Table 5-8: Top ranked overall optimization result for Site-B.

Sensitivity Results | Optimization Results

Sensitivity variables

PL-B (kWh/d) 714 | Wind Speed (m/s) 3.1 | PV Capital Multiplier 1

Double click on a system below for simulation results. Categorized

PV (kW)	HY...	BG (kW)	BD (kW)	S6CS2...	Conv. (kW)	Disp. Strgy	Initial Capital	Operating Cost ($/..	Total NPC	COE ($/kWh)	Ren. Frac.	Capacit Shortage	Biodiesel (m3)	Biomass (t)	BG (hrs)	BD (hrs)
40	11	75	15	40	25	LF	$ 303,199	36,791	$ 725,188	0.237	0.93	0.00	5	1,926	3,967	1,669
40	10	75	15	40	25	LF	$ 298,069	37,249	$ 725,312	0.237	0.93	0.00	5	1,963	3,994	1,678
40	9	75	15	40	25	LF	$ 292,939	37,721	$ 725,600	0.237	0.93	0.00	5	2,000	4,021	1,683
45	10	75	15	40	25	LF	$ 309,069	36,355	$ 726,060	0.237	0.94	0.00	5	1,901	3,948	1,669
40	13	75	15	40	25	LF	$ 313,459	35,979	$ 726,138	0.237	0.94	0.00	5	1,860	3,917	1,655
45	9	75	15	40	25	LF	$ 303,939	36,814	$ 726,195	0.237	0.94	0.00	5	1,938	3,975	1,682
40	8	75	15	40	25	LF	$ 287,809	38,234	$ 726,355	0.237	0.93	0.00	5	2,041	4,059	1,680
45	11	75	15	40	25	LF	$ 314,199	35,952	$ 726,561	0.237	0.94	0.00	5	1,868	3,927	1,665
45	8	75	15	40	25	LF	$ 298,809	37,317	$ 726,836	0.237	0.94	0.00	5	1,977	4,011	1,685
40	14	75	15	40	25	LF	$ 318,589	35,595	$ 726,861	0.237	0.94	0.00	5	1,828	3,889	1,655
35	11	75	15	40	25	LF	$ 292,199	37,902	$ 726,927	0.237	0.93	0.00	5	2,002	4,020	1,681
40	7	75	15	40	25	LF	$ 282,679	38,732	$ 726,931	0.237	0.93	0.00	5	2,080	4,081	1,687
45	7	75	15	40	25	LF	$ 293,679	37,781	$ 727,024	0.237	0.93	0.00	5	2,015	4,033	1,680
35	13	75	15	40	25	LF	$ 302,459	37,040	$ 727,302	0.237	0.93	0.00	5	1,932	3,970	1,666
35	10	75	15	40	25	LF	$ 287,069	38,385	$ 727,340	0.237	0.93	0.00	5	2,041	4,049	1,683
45	6	75	15	40	25	LF	$ 288,549	38,274	$ 727,553	0.237	0.93	0.00	5	2,054	4,056	1,688
40	15	75	15	40	25	LF	$ 323,719	35,217	$ 727,661	0.237	0.94	0.00	5	1,796	3,856	1,661
35	14	75	15	40	25	LF	$ 307,589	36,640	$ 727,851	0.238	0.94	0.00	5	1,900	3,942	1,662
45	13	75	15	40	25	LF	$ 324,459	35,173	$ 727,886	0.238	0.94	0.00	5	1,804	3,874	1,655
40	6	75	15	40	25	LF	$ 277,549	39,270	$ 727,969	0.238	0.93	0.00	5	2,122	4,112	1,696
35	9	75	15	40	25	LF	$ 281,939	38,909	$ 728,220	0.238	0.93	0.00	5	2,081	4,086	1,685
35	15	75	15	40	25	LF	$ 312,719	36,242	$ 728,416	0.238	0.94	0.00	5	1,867	3,912	1,665
40	16	75	15	40	25	LF	$ 328,849	34,843	$ 728,498	0.238	0.94	0.00	5	1,765	3,823	1,663
35	16	75	15	40	25	LF	$ 317,849	35,833	$ 728,854	0.238	0.94	0.00	5	1,833	3,873	1,672

From the categorized simulation results, there are systems which don't contain wind turbine and PV and which don't require battery and converter also in Table 5-8 shows all feasible system have the same renewable fraction and unmet load (0%) those systems are compared based on NPC, COE and initial capital cost instead of the above common parameters. The system ranked first (circled red) in Table 5.8 has a NPC of $725,188, an initial capital of $303,199 and a COE of $0.237/kWh. A hybrid system setup ranked second have NPC of $725,312 and the same COE but lower initial capital cost of $298,069.

Table 5-9: System report for top (1st) ranked hybrid system for Site-B.

System Architecture		**Sensitivity case**		**Annual Electric production[kWh/yr]**		**Annual Electric Consumption[kWh/yr]**		**Emission[kg/yr]**	
PV	40kW	**PV capital Multiplier**	1	**PV**	82926 [28%]	**AC primary Load**	260573 [98%]	**CO2**	12755
Wind	11	**PV Replacement Multiplier**	1	**Wind**	50984 [17%]	**Deferrable Load**	6558 [2%]	**Unburned hydro carbon**	1.39
Biogas	75kW	**Primary Load[kWh/d]**	714 kWh/d	**Biogas**	140458 [48%]	**Total**	267131 [100%]	**Particulate Matter**	0.946
Biodiesel	15kW			**Biodiesel**	19080 [7%]	**Cost Summary**			
Inverter	25kW	**Deferrable Load[kWh/d]**	18 kWh/d	**Total**	293447 [100%]				
Rectifier	25kW			**Excess Electricity**	17035 [5.81%]	**Total NPC**	$725,188	**SO2**	0.207
Battery	40	**Wind Speed**	3.1m/s	**Unmet demand**	36.6 [0.01%]	**Levelized COE**	$0.237/ kWh	**NOx**	112
Dispatch strategy	LF	**Solar Radiation**	6.13 kWh/d/m2	**Capacity Shortage**	278 [0.1%]	**Operating cost**	$36,791/yr	**CO**	12.6

The top (1st) ranked system is better than the lower ranked system in terms of NPC and COE in the overall optimization table since NPC and COE are an effective economic measures than the initial capital cost to compare systems. The system report for this particular setup is summarized in Table 5-9 given above.

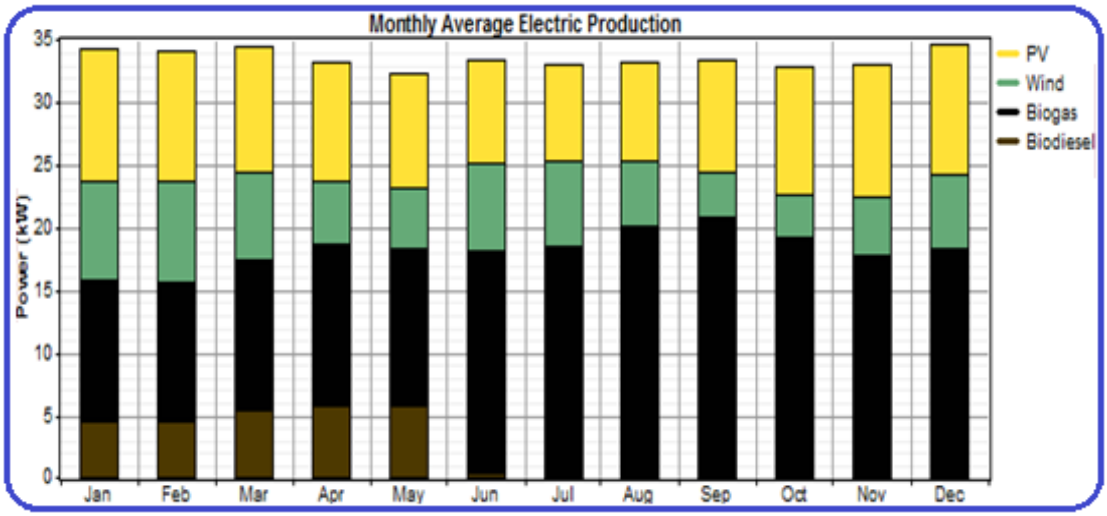

Figure 5-5: Monthly average electric production for Site-B.

The monthly average electric energy production by each individual's hybrid system energy producing component PV panel (28%), Wind turbine (17%), Biogas generator (48%) and Biodiesel generator (7%) and the NPC of the system are summarized in Figure 5-6.

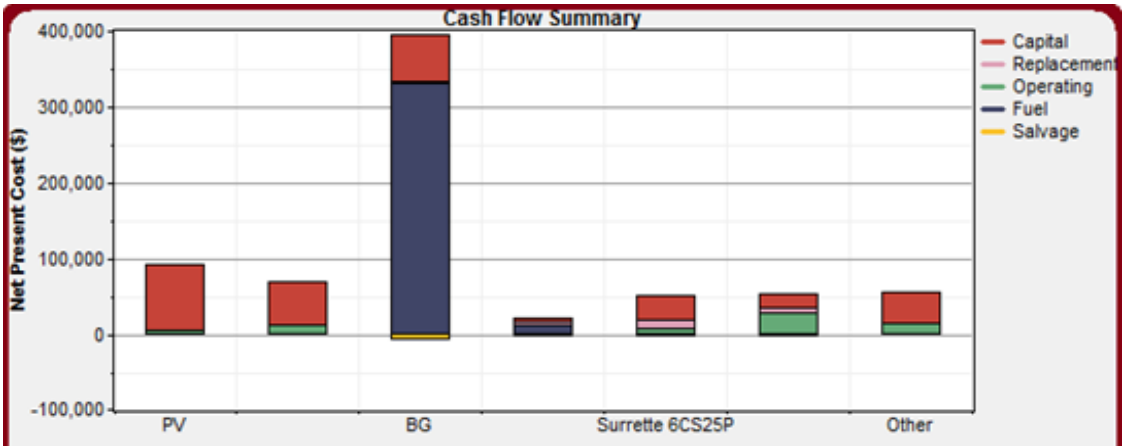

Component	Capital ($)	Replacement ($)	O&M ($)	Fuel ($)	Salvage ($)	Total ($)
PV	88,000	0	4,588	0	0	92,588
HY5-AD5.6	56,430	0	12,995	0	0	69,425
Biogas	62,439	0	2,275	331,392	-6,597	389,509
Biodiesel	4,725	3,325	1,149	11,469	-851	19,816
Surrette 6CS25P	33,320	11,033	6,882	0	-2,307	48,927
Converter	17,500	5,737	28,675	0	-2,858	49,054
Other	40,785	0	15,083	0	0	55,868
System	303,199	20,095	71,647	342,861	-12,614	725,188

Figure 5-6: Cost Summary of the hybrid optimal system of Site-B.

The optimization result in the case of forecasted load of the community is presented below in Table 5-10 & 5-11. The result obtained here is based on a wind speed of 3.1 m/s, a primary and deferrable community load of 1,000kWh/day and 26kWh/day respectively and PV capital cost of $2200/kW.

Table 5-10: Categorized optimization result of Site-B under forecasted load scenario.

Sensitivity Results | Optimization Results

Sensitivity variables

PL-B (kWh/d) 1,000 | Wind Speed (m/s) 3.1 | PV Capital Multiplier 1

Double click on a system below for simulation results. (•) Categorized ( ) Overall Export...

PV (kW)	HY5AD	BG (kW)	BD (kW)	S6CS25P	Conv. (kW)	Disp. Strgy	Initial Capital	Operating Cost ($/yr)	Total NPC	COE ($/kWh)	Ren. Frac.	Capacity Shortage	Biodiesel. (m3)	Biomass (t)	BG (hrs)	BD (hrs)
50	14	110	15	40	30	LF	$ 373,227	55,122	$ 1,005,473	0.234	0.95	0.00	5	3,088	4,241	1,613
70		110	15	70	30	LF	$ 370,397	59,270	$ 1,050,216	0.246	0.95	0.01	5	3,368	4,500	1,751
	35	110	15	40	25	LF	$ 367,457	60,758	$ 1,064,347	0.249	0.96	0.01	5	3,375	4,755	1,510
70	35	110	15		30	LF	$ 491,637	60,359	$ 1,183,952	0.276	0.97	0.00	5	3,342	4,974	1,864
	100	110	15			LF	$ 650,087	60,545	$ 1,344,530	0.313	0.97	0.00	5	3,171	5,059	1,880

Table 5-11: Top ranked overall optimization result of Site-B under load forecasted scenario.

Sensitivity Results | Optimization Results

Sensitivity variables

PL-B (kWh/d) 1,000 | Wind Speed (m/s) 3.1 | PV Capital Multiplier 1

Double click on a system below for simulation results. ( ) Categorized (•) Overall Export...

PV (kW)	HY5AD	BG (kW)	BD (kW)	S6CS25P	Conv. (kW)	Disp. Strgy	Initial Capital	Operating Cost ($/yr)	Total NPC	COE ($/kWh)	Ren. Frac.	Capacity Shortage	Biodiesel. (m3)	Biomass (t)	BG (hrs)	BD (hrs)
50	14	110	15	40	30	LF	$ 373,227	55,122	$ 1,005,473	0.234	0.95	0.00	5	3,088	4,241	1,613
50	15	110	15	40	30	LF	$ 378,357	54,700	$ 1,005,767	0.234	0.95	0.00	5	3,054	4,220	1,610
45	16	110	15	40	30	LF	$ 372,487	55,216	$ 1,005,809	0.234	0.95	0.00	5	3,085	4,234	1,604
50	13	110	15	40	30	LF	$ 368,097	55,600	$ 1,005,820	0.234	0.95	0.00	5	3,126	4,263	1,608
50	16	110	15	40	30	LF	$ 383,487	54,269	$ 1,005,945	0.234	0.95	0.00	5	3,019	4,198	1,610
45	14	110	15	40	30	LF	$ 362,227	56,140	$ 1,006,144	0.234	0.95	0.00	5	3,158	4,283	1,609
45	15	110	15	40	30	LF	$ 367,357	55,696	$ 1,006,188	0.234	0.95	0.00	5	3,122	4,265	1,607
55	13	110	15	40	30	LF	$ 379,097	54,754	$ 1,007,116	0.234	0.95	0.00	5	3,068	4,217	1,612
45	13	110	15	40	30	LF	$ 357,097	56,672	$ 1,007,118	0.234	0.95	0.00	5	3,200	4,312	1,611
50	11	110	15	40	30	LF	$ 357,837	56,620	$ 1,007,270	0.235	0.95	0.00	5	3,206	4,315	1,613
55	14	110	15	40	30	LF	$ 384,227	54,334	$ 1,007,435	0.235	0.95	0.00	5	3,034	4,200	1,612
55	11	110	15	40	30	LF	$ 368,837	55,740	$ 1,008,171	0.235	0.95	0.00	5	3,146	4,269	1,614
55	15	110	15	40	30	LF	$ 389,357	53,952	$ 1,008,178	0.235	0.95	0.00	5	3,002	4,186	1,608
50	10	110	15	40	30	LF	$ 352,707	57,153	$ 1,008,245	0.235	0.95	0.00	5	3,248	4,338	1,624
55	16	110	15	40	30	LF	$ 394,487	53,533	$ 1,008,504	0.235	0.95	0.00	5	2,968	4,164	1,605
55	10	110	15	40	30	LF	$ 363,707	56,230	$ 1,008,658	0.235	0.95	0.00	5	3,185	4,290	1,615
45	11	110	15	40	30	LF	$ 346,837	57,748	$ 1,009,208	0.235	0.95	0.00	5	3,283	4,368	1,612
40	16	110	15	40	30	LF	$ 361,487	56,494	$ 1,009,471	0.235	0.95	0.00	5	3,171	4,301	1,600
40	15	110	15	40	30	LF	$ 356,357	56,972	$ 1,009,819	0.235	0.95	0.00	5	3,209	4,321	1,603
50	9	110	15	40	30	LF	$ 347,577	57,748	$ 1,009,943	0.235	0.95	0.00	5	3,293	4,374	1,625
55	9	110	15	40	30	LF	$ 358,577	56,799	$ 1,010,052	0.235	0.95	0.00	5	3,228	4,320	1,625
45	10	110	15	40	30	LF	$ 341,707	58,306	$ 1,010,471	0.235	0.95	0.00	5	3,326	4,395	1,616
40	14	110	15	40	30	LF	$ 351,227	57,494	$ 1,010,679	0.235	0.95	0.00	5	3,250	4,352	1,605
40	13	110	15	40	30	LF	$ 346,097	58,032	$ 1,011,719	0.236	0.95	0.00	5	3,291	4,382	1,611
50	8	110	15	40	30	LF	$ 342,447	58,367	$ 1,011,915	0.236	0.95	0.00	5	3,340	4,407	1,632
50	7	110	15	40	30	LF	$ 337,317	58,815	$ 1,011,919	0.236	0.95	0.00	5	3,376	4,434	1,647
55	8	110	15	40	30	LF	$ 353,447	57,428	$ 1,012,142	0.236	0.95	0.00	5	3,276	4,358	1,633
35	14	110	15	40	25	LF	$ 336,727	58,892	$ 1,012,218	0.238	0.95	0.01	5	3,375	4,584	1,624

From Table 5-10 & 5-11, the levelized COE is observed to be in the range of $0.234/kWh to $0.313/kWh, initial capital cost ranges from $335,837 to $650,087, operating cost ranges from $48,521 to $60,758 and the total NPC lies in the range of $1,005,473 to $1,344,530. Both of LF and CC dispatch strategies are feasible. A hybrid system contains PV, biogas and biodiesel generator, wind turbine, converter and battery is the cheapest system with low NPC and COE under LF dispatch strategy.

The simulation result in Table 5-11 shows that all feasible system have the same renewable fraction and unmet load (~0%) those systems are compared based on NPC, COE and capital

cost instead of the above common parameters. The system ranked first has a NPC of $1,005,473, an initial capital of $373,227 and a COE of $0.234/kWh. From the overall optimization result of the hybrid system we can observed that the first optimal hybrid system (circled green) simulated under forecasted load scenario has 38.65% more NPC, 23.1% more initial capital cost, 49.8% more operating and maintenance cost but 1.27% less COE, 24.86% less unmeet electric load and 28.8% less capacity shortage than that of the first optimal system simulated under the current load scenario shown in Table 5.8.

Table 5-12: 1st ranked hybrid system report for Site-B under forecasted load scenario.

System Architecture		Sensitivity case		Annual Electric production[kWh/yr]		Annual Electric Consumption[kWh/yr]		Emission[kg/yr]	
PV	50kW	PV capital Multiplier	1	PV	103657 [25%]	AC primary Load	364972 [97%]	CO2	12955
Wind	11	PV Replacement Multiplier	1	Wind	64889 [16%]	Deferrable Load	9473 [3%]	Unburned hydro carbon	2.23
Biogas	110kW	Primary Load[kWh/d]	1000 kWh/d	Biogas	225236 [55%]	Total	374445 [100%]	Particulate Matter	1.52
Biodiesel	15kW			Biodiesel	19091 [5%]	Cost Summary			
Inverter	30kW	Deferrable Load[kWh/d]	26 kWh/d	Total	412873 [100%]				
Rectifier	30kW			Excess Electricity	27767 [6.73%]	Total NPC	$1,005,473	SO2	0.207
Battery	40	Wind Speed	3.1m/s	Unmet demand	27.7 [0.0%]	Levelized COE	$0.234/ kWh	NOx	179
Dispatch strategy	LF	Solar Radiation	6.13 kWh/d/m2	Capacity Shortage	198 [0.05%]	Operating cost	$55,122/yr	CO	20.1

The monthly average electric energy production by each individual's hybrid system energy producing component; PV panel (25%), Wind turbine (16%), Biogas generator (55%) and Biodiesel generator (5%) and the NPC of the system given by the capital, replacement, O&M, fuel and salvage cost are summarized in Figure 5-7 & Figure 5-8 given below.

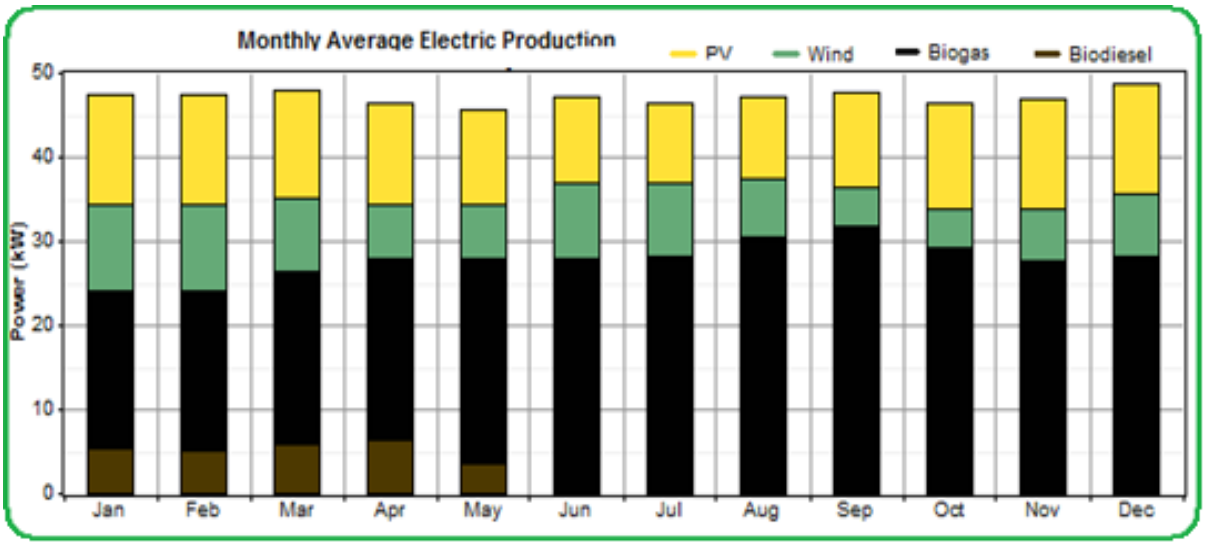

Figure 5-7: Monthly electric production for Site-B under forecasted load scenario.

From the total NPC of the hybrid system given in Figure 5.8, 61.5% of the hybrid system cost is from biogas system and the remains hybrid system components accounts only 39.5% of the total NPC of the system. And also 54% of the total NPC of the hybrid system is associated with the cost of fuel.

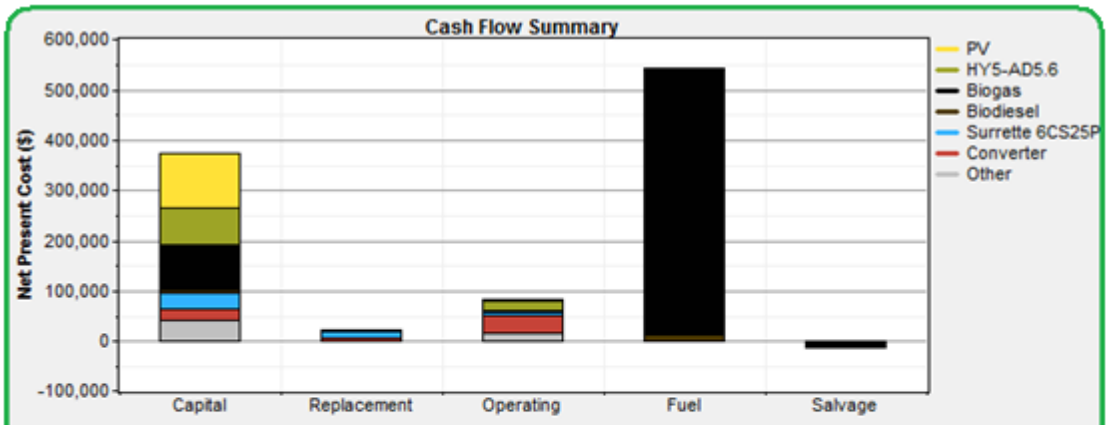

Component	Capital ($)	Replacement ($)	O&M ($)	Fuel ($)	Salvage ($)	Total ($)
PV	110,000	0	5,735	0	0	115,735
HY5-AD5.6	71,820	0	16,540	0	0	88,360
Biogas	91,577	0	3,567	531,333	-8,371	618,106
Biodiesel	4,725	3,243	1,110	11,468	-934	19,612
Surrette 6CS25P	33,320	11,033	6,882	0	-2,307	48,927
Converter	21,000	6,885	34,410	0	-3,430	58,865
Other	40,785	0	15,083	0	0	55,868
System	373,227	21,161	83,327	542,801	-15,042	1,005,473

Figure 5-8: Cost Summary of the above optimal system

5.2.3. Result for Site-C

The optimization results obtained here were based on a wind speed of 3.1 m/s, a primary and deferrable community load of 700kWh/day and 18kWh/ day respectively and PV capital cost of $2200/kW. From Table 5.13, the levelized COE is observed to be in the range of $0.234/kWh to $0.284/kWh, initial capital cost ranges from $162,536 to $379,126, operating cost ranges from $30,178 to $54,088 and the total NPC lies in the range of $703,213 to $852,364. Both of LF and CC dispatch strategies are feasible. A hybrid system contains PV, biogas and biodiesel generator and wind turbine with converter and battery is the cheapest system with low NPC and COE. Capacity shortage is allowed to go a maximum of 1%.

From the categorized simulation results there are systems which do not contain wind turbine and PV and which do not require battery and converter. But those systems are not as cost effective as a hybrid system contains all system components together. Even if the COE obtained here is higher compared to the current energy tariff of Ethiopia which is below $0.04/kWh but still this is within the range of the global tariff. A 100% clean, environmental friendly, green energy, renewable and reliable hybrid system is even better than the current system if we think for our future and our planet to be clean and safe.

Table 5-13: Categorized optimization result for Site-C

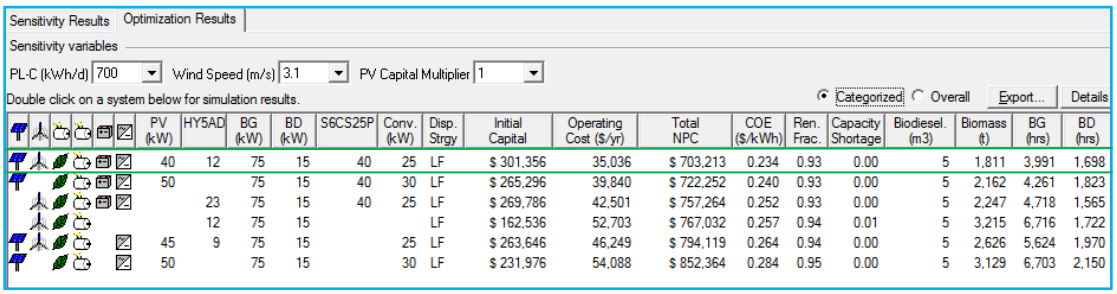

Sensitivity Results | Optimization Results

Sensitivity variables

PL-C (kWh/d) 700 | Wind Speed (m/s) 3.1 | PV Capital Multiplier 1

Double click on a system below for simulation results. ◉ Categorized ○ Overall | Export... | Details

PV (kW)	HY5AD	BG (kW)	BD (kW)	S6CS25P	Conv. (kW)	Disp. Strgy	Initial Capital	Operating Cost ($/yr)	Total NPC	COE ($/kWh)	Ren. Frac.	Capacity Shortage	Biodiesel. (m3)	Biomass (t)	BG (hrs)	BD (hrs)
40	12	75	15	40	25	LF	$ 301,356	35,036	$ 703,213	0.234	0.93	0.00	5	1,811	3,991	1,698
50		75	15	40	30	LF	$ 265,296	39,840	$ 722,252	0.240	0.93	0.00	5	2,162	4,261	1,823
	23	75	15	40	25	LF	$ 269,786	42,501	$ 757,264	0.252	0.93	0.00	5	2,247	4,718	1,565
	12	75	15			LF	$ 162,536	52,703	$ 767,032	0.257	0.94	0.01	5	3,215	6,716	1,722
45	9	75	15		25	LF	$ 263,646	46,249	$ 794,119	0.264	0.94	0.00	5	2,626	5,624	1,970
50		75	15		30	LF	$ 231,976	54,088	$ 852,364	0.284	0.95	0.00	5	3,129	6,703	2,150

Table 5-14: Top ranked overall optimization result for Site-C.

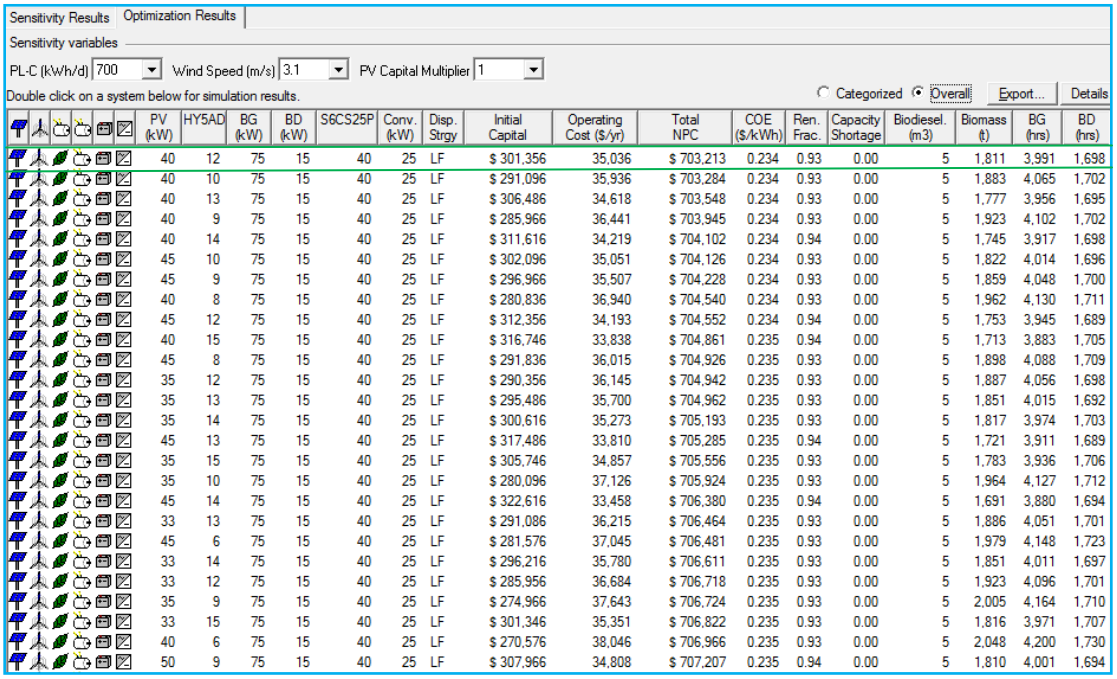

Sensitivity Results | Optimization Results

Sensitivity variables

PL-C (kWh/d) 700 | Wind Speed (m/s) 3.1 | PV Capital Multiplier 1

Double click on a system below for simulation results. ○ Categorized ◉ Overall | Export... | Details

PV (kW)	HY5AD	BG (kW)	BD (kW)	S6CS25P	Conv. (kW)	Disp. Strgy	Initial Capital	Operating Cost ($/yr)	Total NPC	COE ($/kWh)	Ren. Frac.	Capacity Shortage	Biodiesel. (m3)	Biomass (t)	BG (hrs)	BD (hrs)
40	12	75	15	40	25	LF	$ 301,356	35,036	$ 703,213	0.234	0.93	0.00	5	1,811	3,991	1,698
40	10	75	15	40	25	LF	$ 291,096	35,936	$ 703,284	0.234	0.93	0.00	5	1,883	4,065	1,702
40	13	75	15	40	25	LF	$ 306,486	34,618	$ 703,548	0.234	0.93	0.00	5	1,777	3,956	1,695
40	9	75	15	40	25	LF	$ 285,966	36,441	$ 703,945	0.234	0.93	0.00	5	1,923	4,102	1,702
40	14	75	15	40	25	LF	$ 311,616	34,219	$ 704,102	0.234	0.94	0.00	5	1,745	3,917	1,698
45	10	75	15	40	25	LF	$ 302,096	35,051	$ 704,126	0.234	0.93	0.00	5	1,822	4,014	1,696
45	9	75	15	40	25	LF	$ 296,966	35,507	$ 704,228	0.234	0.93	0.00	5	1,859	4,048	1,700
40	8	75	15	40	25	LF	$ 280,836	36,940	$ 704,540	0.234	0.93	0.00	5	1,962	4,130	1,711
45	12	75	15	40	25	LF	$ 312,356	34,193	$ 704,552	0.234	0.94	0.00	5	1,753	3,945	1,689
40	15	75	15	40	25	LF	$ 316,746	33,838	$ 704,861	0.235	0.94	0.00	5	1,713	3,883	1,705
45	8	75	15	40	25	LF	$ 291,836	36,015	$ 704,926	0.235	0.93	0.00	5	1,898	4,088	1,709
35	12	75	15	40	25	LF	$ 290,356	36,145	$ 704,942	0.235	0.93	0.00	5	1,887	4,056	1,698
35	13	75	15	40	25	LF	$ 295,486	35,700	$ 704,962	0.235	0.93	0.00	5	1,851	4,015	1,692
35	14	75	15	40	25	LF	$ 300,616	35,273	$ 705,193	0.235	0.93	0.00	5	1,817	3,974	1,703
45	13	75	15	40	25	LF	$ 317,486	33,810	$ 705,285	0.235	0.94	0.00	5	1,721	3,911	1,689
35	15	75	15	40	25	LF	$ 305,746	34,857	$ 705,556	0.235	0.93	0.00	5	1,783	3,936	1,706
35	10	75	15	40	25	LF	$ 280,096	37,126	$ 705,924	0.235	0.93	0.00	5	1,964	4,127	1,712
45	14	75	15	40	25	LF	$ 322,616	33,458	$ 706,380	0.235	0.94	0.00	5	1,691	3,880	1,694
33	13	75	15	40	25	LF	$ 291,086	36,215	$ 706,464	0.235	0.93	0.00	5	1,886	4,051	1,701
45	6	75	15	40	25	LF	$ 281,576	37,045	$ 706,481	0.235	0.93	0.00	5	1,979	4,148	1,723
33	14	75	15	40	25	LF	$ 296,216	35,780	$ 706,611	0.235	0.93	0.00	5	1,851	4,011	1,697
33	12	75	15	40	25	LF	$ 285,956	36,684	$ 706,718	0.235	0.93	0.00	5	1,923	4,096	1,701
35	9	75	15	40	25	LF	$ 274,966	37,643	$ 706,724	0.235	0.93	0.00	5	2,005	4,164	1,710
33	15	75	15	40	25	LF	$ 301,346	35,351	$ 706,822	0.235	0.93	0.00	5	1,816	3,971	1,707
40	6	75	15	40	25	LF	$ 270,576	38,046	$ 706,966	0.235	0.93	0.00	5	2,048	4,200	1,730
50	9	75	15	40	25	LF	$ 307,966	34,808	$ 707,207	0.235	0.94	0.00	5	1,810	4,001	1,694

The simulation result in Table 5.14 shows that all feasible systems have the same renewable fraction (100%) and unmet load (0%). The system ranked first has a NPC of $703,213, an initial capital of $301,356 and a COE of $0.234/kWh. A hybrid system setup ranked second have NPC of $725,312 and the same COE but lower initial capital cost of $298,069. The top ($1^{st}$) ranked system is better than the lower ranked system in terms of NPC and COE while the remain systems are not selected to implement as compared with the first system in the overall optimization table since NPC and COE are an effective economic measures than the initial capital cost to compare systems. The system report for this particular setup is summarized in Table 5.15.

Table 5-15: System report for top (1st) ranked hybrid system for Site-C.

System Architecture		Sensitivity case		Annual Electric production[kWh/yr]		Annual Electric Consumption[kWh/yr]		Emission[kg/yr]	
PV	40kW	**PV capital Multiplier**	1	**PV**	82926 [29%]	**AC primary Load**	255491 [97%]	**CO2**	12723
Wind	12	**PV Replacement Multiplier**	1	**Wind**	55461 [19%]	**Deferrable Load**	6558 [3%]	**Unburned hydro carbon**	1.31
Biogas	75kW	**Primary Load[kWh/d]**	700 kWh/d	**Biogas**	132000 [46%]	**Total**	262049 [100%]	**Particulate Matter**	0.89
Biodiesel	15kW			**Biodiesel**	19061 [7%]	**Cost Summary**			
Inverter	25kW	**Deferrable Load[kWh/d]**	18 kWh/d	**Total**	289448 [100%]				
Rectifier	25kW			**Excess Electricity**	18071 [6.24%]	**Total NPC**	$703,213	**SO2**	0.206
Battery	40	**Wind Speed**	3.1m/s	**Unmet demand**	10.1 [0.0%]	**Levelized COE**	$0.234/ kWh	**NOx**	105
Dispatch strategy	LF	**Solar Radiation**	6.13 kWh/d/m2	**Capacity Shortage**	94.3 [0.04%]	**Operating cost**	$35,036/yr	**CO**	11.8

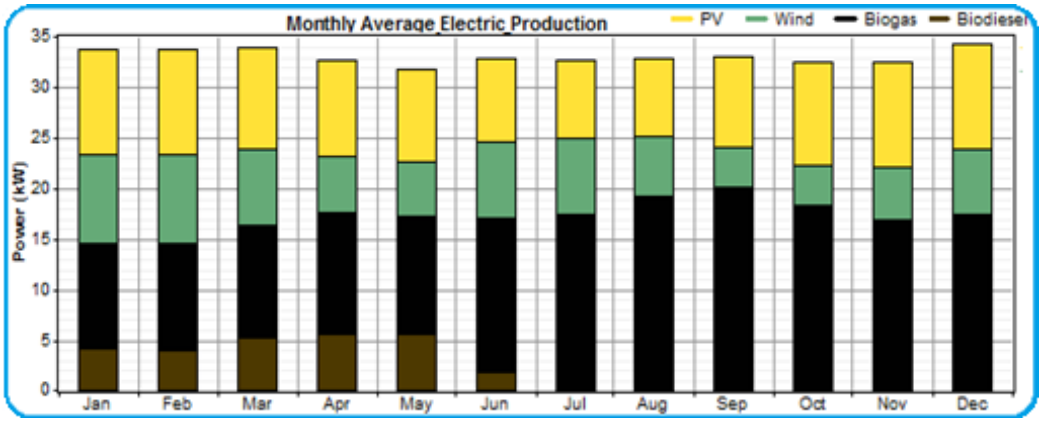

Figure 5-9: Monthly average electric production for Site-C.

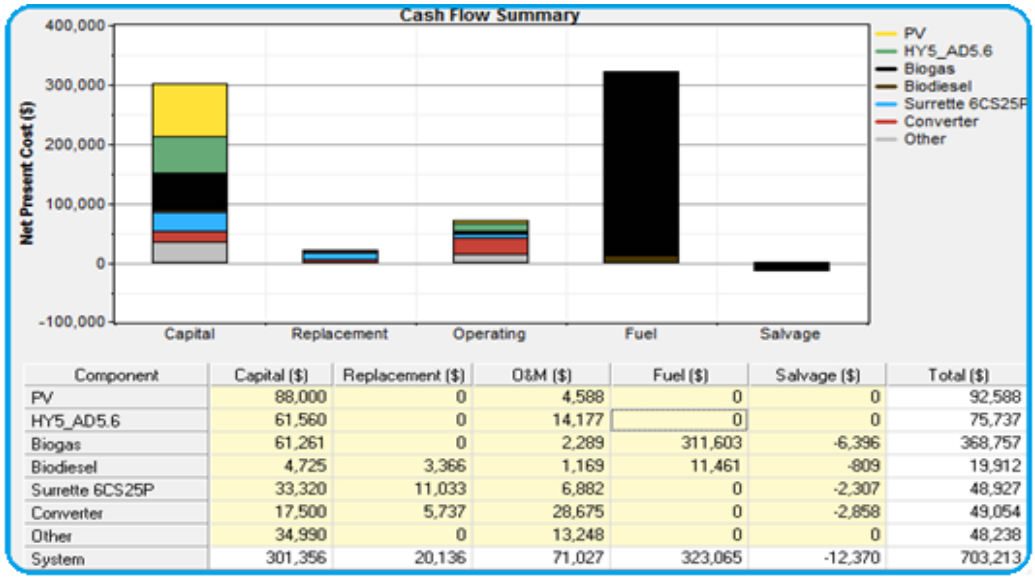

Component	Capital ($)	Replacement ($)	O&M ($)	Fuel ($)	Salvage ($)	Total ($)
PV	88,000	0	4,588	0	0	92,588
HY5_AD5.6	61,560	0	14,177	0	0	75,737
Biogas	61,261	0	2,289	311,603	-6,396	368,757
Biodiesel	4,725	3,366	1,169	11,461	-809	19,912
Surrette 6CS25P	33,320	11,033	6,882	0	-2,307	48,927
Converter	17,500	5,737	28,675	0	-2,858	49,054
Other	34,990	0	13,248	0	0	48,238
System	301,356	20,136	71,027	323,065	-12,370	703,213

Figure 5-10: Cost Summary of the hybrid optimal system of Site-C.

The optimization result in the case of forecasted load of the community is presented below in Table 5.16 & 5.17. The result obtained here is based on a wind speed of 3.1 m/s, a primary and deferrable community load of 973kWh/day and 26kWh/day respectively and PV capital cost of $2200/kW.

Table 5-16: Categorized optimization result of Site-C under forecasted load scenario

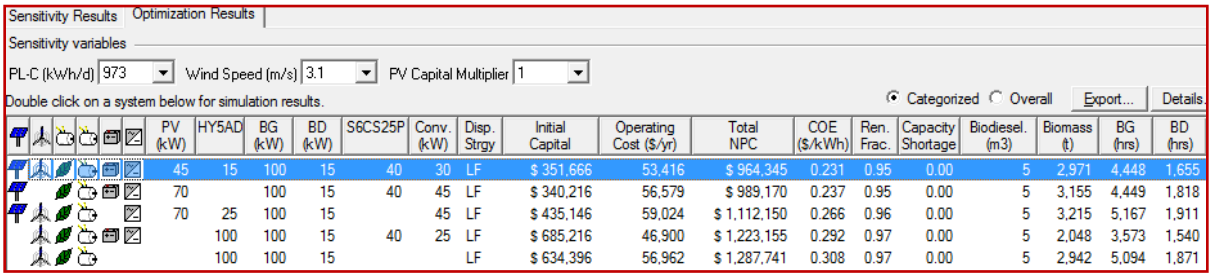

Sensitivity Results | Optimization Results

Sensitivity variables

PL-C (kWh/d) 973 | Wind Speed (m/s) 3.1 | PV Capital Multiplier 1

Double click on a system below for simulation results. ◉ Categorized ○ Overall | Export... | Details

PV (kW)	HY5AD	BG (kW)	BD (kW)	S6CS25P	Conv. (kW)	Disp. Strgy	Initial Capital	Operating Cost ($/yr)	Total NPC	COE ($/kWh)	Ren. Frac.	Capacity Shortage	Biodiesel. (m3)	Biomass (t)	BG (hrs)	BD (hrs)
45	15	100	15	40	30	LF	$ 351,666	53,416	$ 964,345	0.231	0.95	0.00	5	2,971	4,448	1,655
70		100	15	40	45	LF	$ 340,216	56,579	$ 989,170	0.237	0.95	0.00	5	3,155	4,449	1,818
70	25	100	15		45	LF	$ 435,146	59,024	$ 1,112,150	0.266	0.96	0.00	5	3,215	5,167	1,911
	100	100	15	40	25	LF	$ 685,216	46,900	$ 1,223,155	0.292	0.97	0.00	5	2,048	3,573	1,540
	100	100	15			LF	$ 634,396	56,962	$ 1,287,741	0.308	0.97	0.00	5	2,942	5,094	1,871

Table 5-17: Top ranked overall optimization result of Site-C under load forecasted scenario.

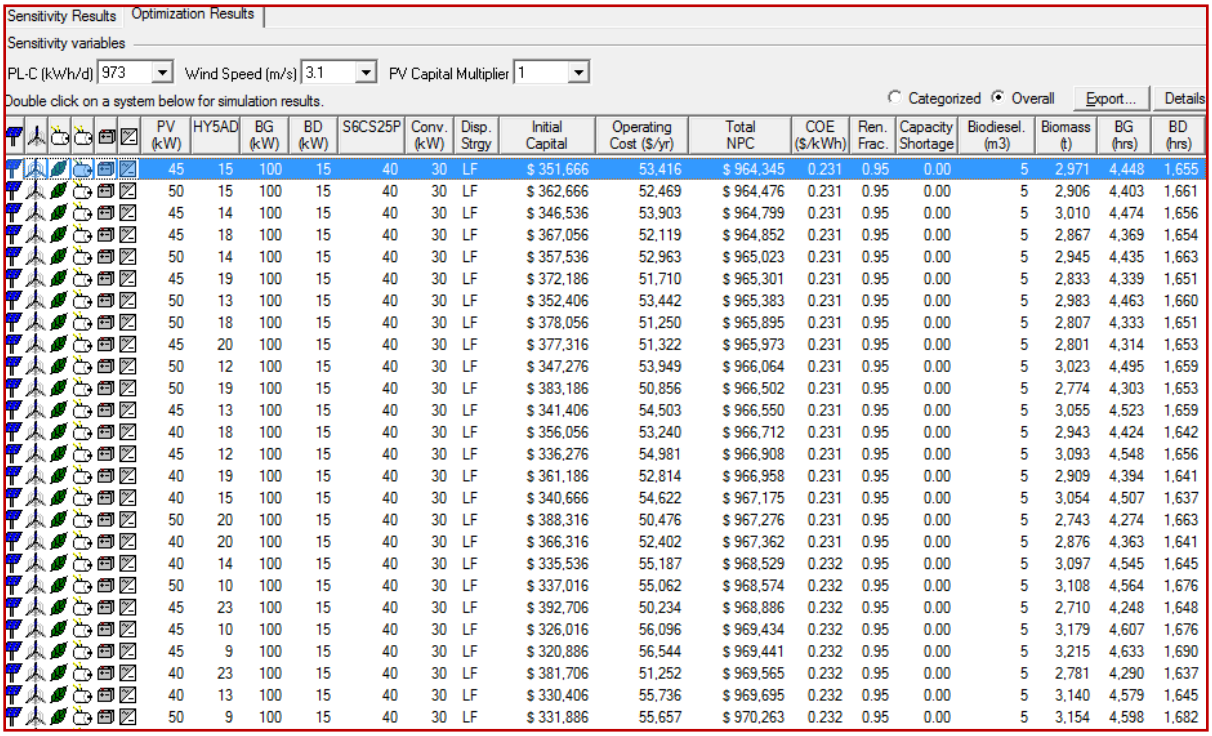

Sensitivity Results | Optimization Results

Sensitivity variables

PL-C (kWh/d) 973 | Wind Speed (m/s) 3.1 | PV Capital Multiplier 1

Double click on a system below for simulation results. ○ Categorized ◉ Overall | Export... | Details

PV (kW)	HY5AD	BG (kW)	BD (kW)	S6CS25P	Conv. (kW)	Disp. Strgy	Initial Capital	Operating Cost ($/yr)	Total NPC	COE ($/kWh)	Ren. Frac.	Capacity Shortage	Biodiesel. (m3)	Biomass (t)	BG (hrs)	BD (hrs)
45	15	100	15	40	30	LF	$ 351,666	53,416	$ 964,345	0.231	0.95	0.00	5	2,971	4,448	1,655
50	15	100	15	40	30	LF	$ 362,666	52,469	$ 964,476	0.231	0.95	0.00	5	2,906	4,403	1,661
45	14	100	15	40	30	LF	$ 346,536	53,903	$ 964,799	0.231	0.95	0.00	5	3,010	4,474	1,656
45	18	100	15	40	30	LF	$ 367,056	52,119	$ 964,852	0.231	0.95	0.00	5	2,867	4,369	1,654
50	14	100	15	40	30	LF	$ 357,536	52,963	$ 965,023	0.231	0.95	0.00	5	2,945	4,435	1,663
45	19	100	15	40	30	LF	$ 372,186	51,710	$ 965,301	0.231	0.95	0.00	5	2,833	4,339	1,651
50	13	100	15	40	30	LF	$ 352,406	53,442	$ 965,383	0.231	0.95	0.00	5	2,983	4,463	1,660
50	18	100	15	40	30	LF	$ 378,056	51,250	$ 965,895	0.231	0.95	0.00	5	2,807	4,333	1,651
45	20	100	15	40	30	LF	$ 377,316	51,322	$ 965,973	0.231	0.95	0.00	5	2,801	4,314	1,653
50	12	100	15	40	30	LF	$ 347,276	53,949	$ 966,064	0.231	0.95	0.00	5	3,023	4,495	1,659
50	19	100	15	40	30	LF	$ 383,186	50,856	$ 966,502	0.231	0.95	0.00	5	2,774	4,303	1,653
45	13	100	15	40	30	LF	$ 341,406	54,503	$ 966,550	0.231	0.95	0.00	5	3,055	4,523	1,659
40	18	100	15	40	30	LF	$ 356,056	53,240	$ 966,712	0.231	0.95	0.00	5	2,943	4,424	1,642
45	12	100	15	40	30	LF	$ 336,276	54,981	$ 966,908	0.231	0.95	0.00	5	3,093	4,548	1,656
40	19	100	15	40	30	LF	$ 361,186	52,814	$ 966,958	0.231	0.95	0.00	5	2,909	4,394	1,641
40	15	100	15	40	30	LF	$ 340,666	54,622	$ 967,175	0.231	0.95	0.00	5	3,054	4,507	1,637
50	20	100	15	40	30	LF	$ 388,316	50,476	$ 967,276	0.231	0.95	0.00	5	2,743	4,274	1,663
40	20	100	15	40	30	LF	$ 366,316	52,402	$ 967,362	0.231	0.95	0.00	5	2,876	4,363	1,641
40	14	100	15	40	30	LF	$ 335,536	55,187	$ 968,529	0.232	0.95	0.00	5	3,097	4,545	1,645
50	10	100	15	40	30	LF	$ 337,016	55,062	$ 968,574	0.232	0.95	0.00	5	3,108	4,564	1,676
45	23	100	15	40	30	LF	$ 392,706	50,234	$ 968,886	0.232	0.95	0.00	5	2,710	4,248	1,648
45	10	100	15	40	30	LF	$ 326,016	56,096	$ 969,434	0.232	0.95	0.00	5	3,179	4,607	1,676
45	9	100	15	40	30	LF	$ 320,886	56,544	$ 969,441	0.232	0.95	0.00	5	3,215	4,633	1,690
40	23	100	15	40	30	LF	$ 381,706	51,252	$ 969,565	0.232	0.95	0.00	5	2,781	4,290	1,637
40	13	100	15	40	30	LF	$ 330,406	55,736	$ 969,695	0.232	0.95	0.00	5	3,140	4,579	1,645
50	9	100	15	40	30	LF	$ 331,886	55,657	$ 970,263	0.232	0.95	0.00	5	3,154	4,598	1,682

From Table 5-16 & 5-17, the levelized COE of the feasible hybrid system is observed to be in the range of $0.231/kWh to $0.308/kWh, capital cost ranges from $319,406 to $685,216, operating cost ranges from $45,626 to $59,024 and the total NPC lies in the range of $964,345 to $1,287,741. Both of LF and CC dispatch strategies are feasible. A hybrid system contains PV, biogas generator, biodiesel generator, wind turbine, converter and battery is the cheapest system with low NPC and small COE under LF dispatch strategy.

The simulation result in Table 5-17 shows that all feasible system has the same renewable fraction and unmet load (~0%). The system ranked first has a NPC of $964,345, an initial

capital of $351,666 and a COE of $0.231/kWh. From the overall optimization result of the hybrid system we can observed that the first optimal hybrid system (circled blue) simulated under forecasted load scenario has 37.14% more NPC, 16.7% more initial capital cost, 338.6% more unmeet load, 346.4% more capacity shortage, 52.5% more operating and maintenance cost but 1.28% less COE, than that of the current optimal system given in Table 5.14.

Table 5-18: 1st ranked hybrid system report for Site-C under forecasted load scenario.

System Architecture		Sensitivity case		Annual Electric production[kWh/yr]		Annual Electric Consumption[kWh/yr]		Emission[kg/yr]	
PV	45kW	**PV capital Multiplier**	1	**PV**	93291 [23%]	**AC primary Load**	355101 [97%]	**CO2**	12936
Wind	15	**PV Replacement Multiplier**	1	**Wind**	69326 [17%]	**Deferrable Load**	9473 [3%]	**Unburned hydro carbon**	2.14
Biogas	100kW	**Primary Load[kWh/d]**	973 kWh/d	**Biogas**	216729 [54%]	**Total**	364574 [100%]	**Particulate Matter**	1.46
Biodiesel	15kW			**Biodiesel**	19084 [5%]	**Cost Summary**			
Inverter	30kW	**Deferrable Load[kWh/d]**	26 kWh/d	**Total**	398430 [100%]				
Rectifier	30kW			**Excess Electricity**	23919 [6%]	**Total NPC**	$964,345	**SO2**	0.207
Battery	40	**Wind Speed**	3.1m/s	**Unmet demand**	44.3 [0.01%]	**Levelized COE**	$0.231/ kWh	**NOx**	173
Dispatch strategy	LF	**Solar Radiation**	6.13 kWh/d/m2	**Capacity Shortage**	421 [0.12%]	**Operating cost**	$53,416/yr	**CO**	19.3

The monthly average electric energy production by each individual's hybrid system energy producing component (PV panel, Wind turbine, Biogas generator and Biodiesel generator) and the NPC of the system given by the capital, replacement, O&M, fuel and salvage cost are summarized in Figure 5-11 & 5-12 given below.

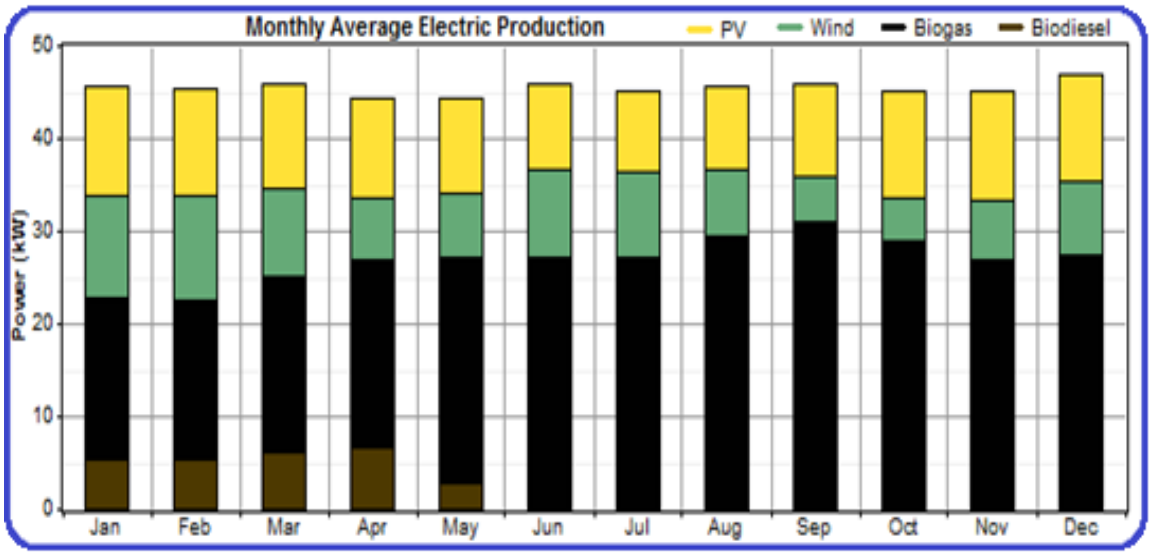

Figure 5-11: Monthly electric production of Site-C under forecasted load scenario

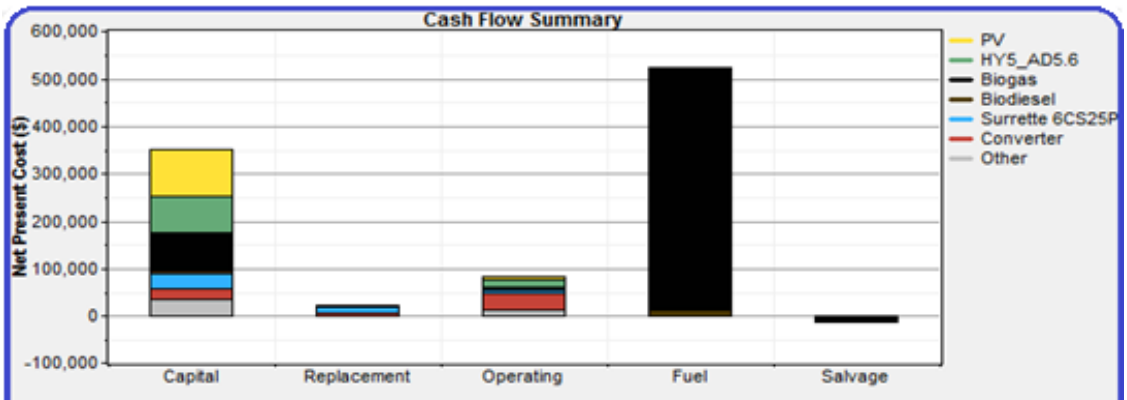

Component	Capital ($)	Replacement ($)	O&M ($)	Fuel ($)	Salvage ($)	Total ($)
PV	99,000	0	5,161	0	0	104,161
HY5_AD5.6	76,950	0	17,721	0	0	94,671
Biogas	81,681	0	3,401	511,222	-6,588	589,717
Biodiesel	4,725	3,305	1,139	11,469	-872	19,766
Surrette 6CS25P	33,320	11,033	6,882	0	-2,307	48,927
Converter	21,000	6,885	34,410	0	-3,430	58,865
Other	34,990	0	13,248	0	0	48,238
System	351,666	21,222	81,962	522,691	-13,197	964,345

Figure 5-12: Cost Summary of the above optimal system

5.2.4. Result for Site-D

The optimization results obtained here were based on a wind speed of 3.1 m/s, a primary and deferrable community load of 367kWh/day and 7kWh/ day respectively and PV capital cost of $2200/kW. From Table 5-19, the levelized COE is observed to be in the range of $0.241/kWh to $0.437/kWh, initial capital cost ranges from $151,377 to $391,657, operating cost ranges from $11,192 to $25,446 and the total NPC lies in the range of $377,669 to $683,516. Both of LF and CC dispatch strategies are feasible. By any means a hybrid system contain PV, biogas generator, biodiesel generator and wind turbine with converter and battery is the cheapest system with low NPC and COE.

Table 5-19: Categorized optimization result of Site-D

Sensitivity Results | Optimization Results

Sensitivity variables

D_Y PL (kWh/d) 367 | Wind Speed (m/s) 3.1 | PV Capital Multiplier 1

Double click on a system below for simulation results. Categorized / Overall | Export... | Details

PV (kW)	HY5AD	BG (kW)	BD (kW)	S6CS25P	Conv. (kW)	Disp. Strgy	Initial Capital	Operating Cost ($/yr)	Total NPC	COE ($/kWh)	Ren. Frac.	Capacity Shortage	Biodiesel. (m3)	Biomass (t)	BG (hrs)	BD (hrs)
35	6	30	10	40	20	LF	$ 213,297	14,331	$ 377,669	0.241	0.93	0.00	3	568	3,546	1,462
45		30	10	40	20	LF	$ 204,517	16,280	$ 391,244	0.250	0.93	0.00	3	722	4,417	1,525
25	5	30	10		20	LF	$ 152,847	21,453	$ 398,917	0.255	0.93	0.01	3	1,111	6,477	2,142
	15	30	10	40	20	LF	$ 182,467	20,809	$ 421,140	0.270	0.92	0.01	3	948	4,747	1,412
	50	30	10			LF	$ 314,697	18,920	$ 531,702	0.340	0.96	0.00	3	814	4,881	2,091
120		45	10		80	LF	$ 391,657	25,446	$ 683,516	0.437	0.97	0.00	3	934	4,088	2,488

From the categorized simulation result in Table 5.19 there are systems which do not contain wind turbine and PV and which do not require battery and converter. But those systems are not as cost effective as a hybrid system contains all system components together. A 100% clean, environmental friendly, green energy, renewable and reliable hybrid system is even better than the current system if we think for our future and our planet to be safe.

Table 5-20: Top ranked overall optimization result of Site-D.

Sensitivity Results | Optimization Results

Sensitivity variables

D_Y PL (kWh/d) 367 | Wind Speed (m/s) 3.1 | PV Capital Multiplier 1

Double click on a system below for simulation results. | Categorized | Overall | Export... | Details

PV (kW)	HY5AD	BG (kW)	BD (kW)	S6CS25P	Conv. (kW)	Disp. Strgy	Initial Capital	Operating Cost ($/yr)	Total NPC	COE ($/kWh)	Ren. Frac.	Capacity Shortage	Biodiesel. (m3)	Biomass (t)	BG (hrs)	BD (hrs)
35	6	30	10	40	20	LF	$ 213,297	14,331	$ 377,669	0.241	0.93	0.00	3	568	3,546	1,462
35	7	30	10	40	20	LF	$ 218,427	13,893	$ 377,782	0.241	0.93	0.00	3	534	3,364	1,441
35	5	30	10	40	20	LF	$ 208,167	14,822	$ 378,169	0.242	0.92	0.00	3	605	3,750	1,481
35	8	30	10	40	20	LF	$ 223,557	13,495	$ 378,348	0.242	0.93	0.00	3	502	3,192	1,418
30	8	30	10	40	20	LF	$ 212,557	14,462	$ 378,437	0.242	0.92	0.00	3	567	3,487	1,473
30	7	30	10	40	20	LF	$ 207,427	14,928	$ 378,655	0.242	0.92	0.00	3	602	3,670	1,500
30	9	30	10	40	20	LF	$ 217,687	14,066	$ 379,018	0.242	0.93	0.00	3	535	3,326	1,452
30	6	30	10	40	20	LF	$ 202,297	15,453	$ 379,537	0.243	0.92	0.00	3	642	3,870	1,522
35	9	30	10	40	20	LF	$ 228,687	13,161	$ 379,640	0.243	0.93	0.00	3	475	3,046	1,404
30	10	30	10	40	20	LF	$ 222,817	13,703	$ 379,994	0.243	0.93	0.00	3	506	3,167	1,435
30	5	30	10	40	20	LF	$ 197,167	16,015	$ 380,858	0.243	0.92	0.00	3	684	4,088	1,543
30	11	30	10	40	20	LF	$ 227,947	13,360	$ 381,181	0.244	0.93	0.00	3	478	3,018	1,426
35	10	30	10	40	20	LF	$ 233,817	12,857	$ 381,291	0.244	0.93	0.00	3	449	2,912	1,398
25	9	30	10	40	20	LF	$ 206,687	15,297	$ 382,137	0.244	0.92	0.00	3	616	3,686	1,507
25	10	30	10	40	20	LF	$ 211,817	14,872	$ 382,396	0.244	0.92	0.00	3	583	3,511	1,479
25	8	30	10	40	20	LF	$ 201,557	15,776	$ 382,511	0.245	0.92	0.00	3	653	3,879	1,529
30	12	30	10	40	20	LF	$ 233,077	13,062	$ 382,893	0.245	0.93	0.00	3	453	2,869	1,427
25	11	30	10	40	20	LF	$ 216,947	14,482	$ 383,055	0.245	0.93	0.00	3	552	3,357	1,470
35	11	30	10	40	20	LF	$ 238,947	12,572	$ 383,151	0.245	0.93	0.00	3	425	2,767	1,400
25	7	30	10	40	20	LF	$ 196,427	16,327	$ 383,696	0.245	0.92	0.00	3	694	4,078	1,552
35	2	30	10	40	20	LF	$ 192,777	16,670	$ 383,985	0.245	0.92	0.00	3	741	4,417	1,550
25	12	30	10	40	20	LF	$ 222,077	14,125	$ 384,087	0.245	0.93	0.00	3	523	3,203	1,452
45	5	30	10	40	20	LF	$ 230,167	13,424	$ 384,143	0.245	0.93	0.00	3	510	3,320	1,419
45	6	30	10	40	20	LF	$ 235,297	13,065	$ 385,152	0.246	0.93	0.00	3	481	3,169	1,411
22	10	30	10	40	20	LF	$ 205,217	15,713	$ 385,441	0.246	0.92	0.00	3	638	3,772	1,488
35	12	30	10	40	20	LF	$ 244,077	12,338	$ 385,590	0.246	0.93	0.00	3	404	2,652	1,397
25	6	30	10	40	20	LF	$ 191,297	16,940	$ 385,598	0.247	0.92	0.00	3	739	4,309	1,606

The first ranked system has a NPC of $377,669, an initial capital of $213,297 and a COE of $0.241/kWh. A hybrid system setup ranked second have NPC of $377,782 and the same COE but relatively higher initial capital cost of $218,427. The top (1st) ranked system is better than the lower ranked system in terms of NPC and capital cost. The system report for this particular setup is summarized in Table 5.21.

Table 5-21: System report for top (1st) ranked hybrid system for Site-D.

System Architecture		Sensitivity case		Annual Electric production[kWh/yr]		Annual Electric Consumption[kWh/yr]		Emission[kg/yr]	
PV	35kW	**PV capital Multiplier**	1	**PV**	72560 [48%]	**AC primary Load**	133891 [98%]	**CO2**	7546
Wind	6	**PV Replacement Multiplier**	1	**Wind**	27730 [18%]	**Deferrable Load**	2549 [2%]	**Unburned hydro carbon**	0.411
Biogas	30kW	**Primary Load[kWh/d]**	367 kWh/d	**Biogas**	40564 [27%]	**Total**	136441 [100%]	**Particulate Matter**	0.28
Biodiesel	10kW			**Biodiesel**	11341 [7%]	**Cost Summary**			
Inverter	20kW	**Deferrable Load[kWh/d]**	7 kWh/d	**Total**	152195 [100%]				
Rectifier	20kW			**Excess Electricity**	8036 [5.28%]	**Total NPC**	$377,669	**SO2**	0.124
Battery	40	**Wind Speed**	3.1m/s	**Unmet demand**	63.8 [0.05%]	**Levelized COE**	$0.241/ kWh	**NOx**	33.1
Dispatch strategy	LF	**Solar Radiation**	6.13 kWh/d/m2	**Capacity Shortage**	289 [0.21%]	**Operating cost**	$14,331/yr	**CO**	3.71

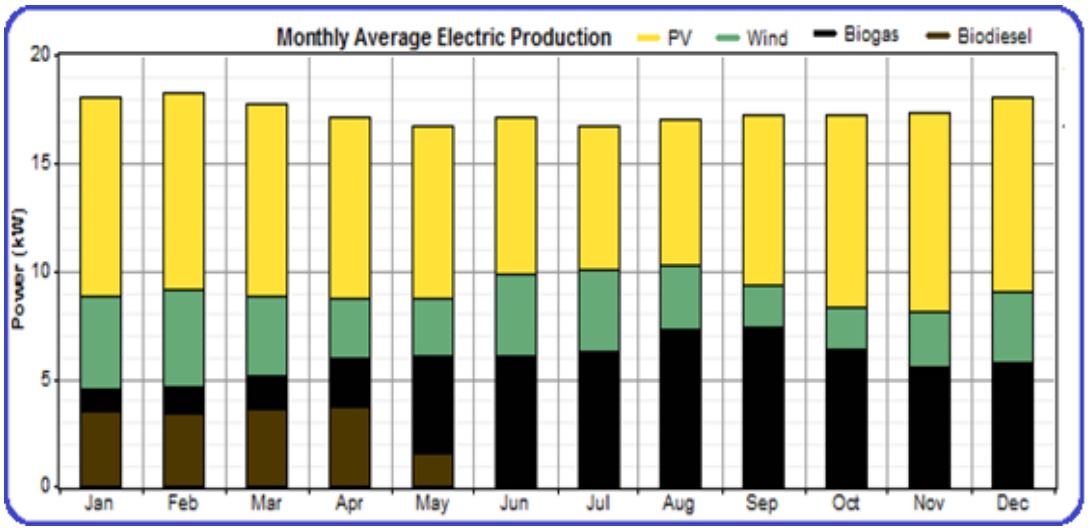

Figure 5-13: Monthly average electric production for Site-D.

The monthly average electric energy production by each individual's hybrid system energy producing component and the NPC of the system given by the capital, replacement, O&M, fuel and salvage cost are summarized in Figure 5.13 & 5.14.

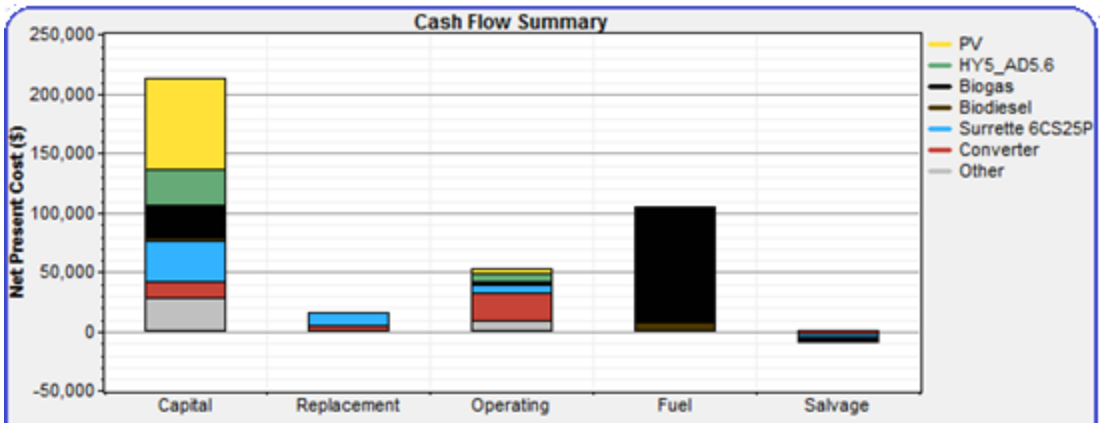

Component	Capital ($)	Replacement ($)	O&M ($)	Fuel ($)	Salvage ($)	Total ($)
PV	77,000	0	4,014	0	0	81,014
HY5_AD5.6	30,780	0	7,088	0	0	37,868
Biogas	26,919	0	2,034	97,662	-3,815	122,800
Biodiesel	3,150	0	671	6,877	-197	10,500
Surrette 6CS25P	33,320	11,033	6,882	0	-2,307	48,927
Converter	14,000	4,590	22,940	0	-2,287	39,243
Other	28,128	0	9,187	0	0	37,315
System	213,297	15,623	52,816	104,538	-8,606	377,669

Figure 5-14: Cost Summary of the hybrid optimal system of Site-D.

The optimization result in the case of forecasted load of the community is presented in Table 5.22 & 5.23. The result obtained here is based on a wind speed of 3.1 m/s, a primary and deferrable community load of 510kWh/day and 10kWh/day respectively and PV capital cost of $2200/kW.

Table 5-22: Top ranked overall optimization result of Site-D under load forecasted scenario.

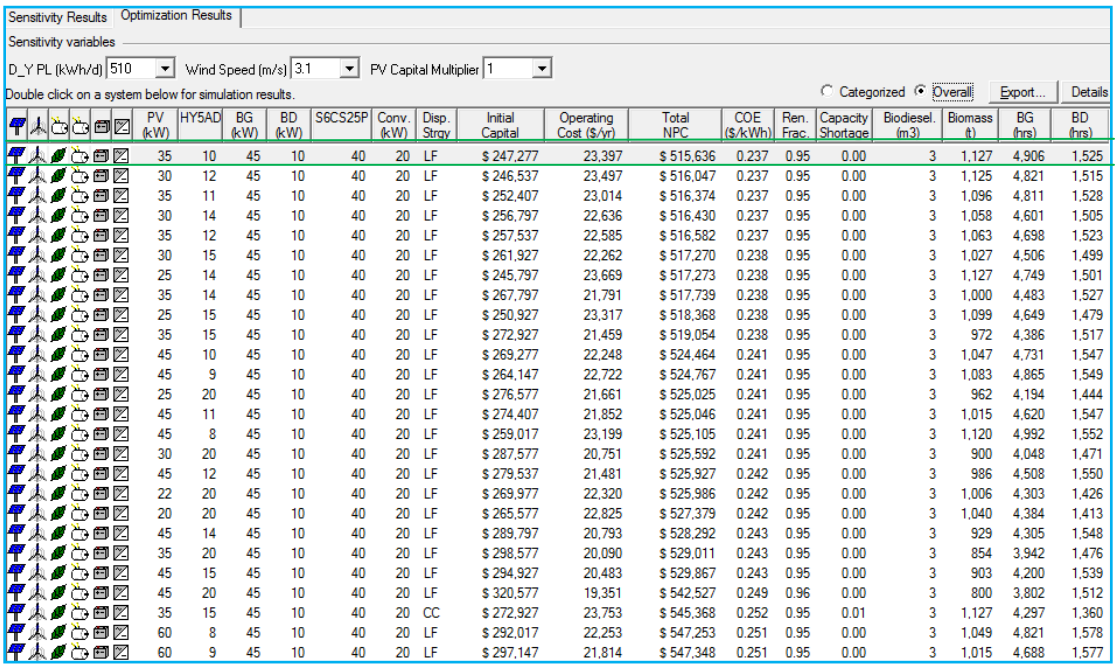

Sensitivity Results | Optimization Results

Sensitivity variables

D_Y PL (kWh/d) 510 | Wind Speed (m/s) 3.1 | PV Capital Multiplier 1

Double click on a system below for simulation results. ○ Categorized ◉ Overall | Export... | Details

PV (kW)	HY5AD	BG (kW)	BD (kW)	S6CS25P	Conv. (kW)	Disp. Strgy	Initial Capital	Operating Cost ($/yr)	Total NPC	COE ($/kWh)	Ren. Frac.	Capacity Shortage	Biodiesel. (m3)	Biomass (t)	BG (hrs)	BD (hrs)
35	10	45	10	40	20	LF	$ 247,277	23,397	$ 515,636	0.237	0.95	0.00	3	1,127	4,906	1,525
30	12	45	10	40	20	LF	$ 246,537	23,497	$ 516,047	0.237	0.95	0.00	3	1,125	4,821	1,515
35	11	45	10	40	20	LF	$ 252,407	23,014	$ 516,374	0.237	0.95	0.00	3	1,096	4,811	1,528
30	14	45	10	40	20	LF	$ 256,797	22,636	$ 516,430	0.237	0.95	0.00	3	1,058	4,601	1,505
35	12	45	10	40	20	LF	$ 257,537	22,585	$ 516,582	0.237	0.95	0.00	3	1,063	4,698	1,523
30	15	45	10	40	20	LF	$ 261,927	22,262	$ 517,270	0.238	0.95	0.00	3	1,027	4,506	1,499
25	14	45	10	40	20	LF	$ 245,797	23,669	$ 517,273	0.238	0.95	0.00	3	1,127	4,749	1,501
35	14	45	10	40	20	LF	$ 267,797	21,791	$ 517,739	0.238	0.95	0.00	3	1,000	4,483	1,527
25	15	45	10	40	20	LF	$ 250,927	23,317	$ 518,368	0.238	0.95	0.00	3	1,099	4,649	1,479
35	15	45	10	40	20	LF	$ 272,927	21,459	$ 519,054	0.238	0.95	0.00	3	972	4,386	1,517
45	10	45	10	40	20	LF	$ 269,277	22,248	$ 524,464	0.241	0.95	0.00	3	1,047	4,731	1,547
45	9	45	10	40	20	LF	$ 264,147	22,722	$ 524,767	0.241	0.95	0.00	3	1,083	4,865	1,549
25	20	45	10	40	20	LF	$ 276,577	21,661	$ 525,025	0.241	0.95	0.00	3	962	4,194	1,444
45	11	45	10	40	20	LF	$ 274,407	21,852	$ 525,046	0.241	0.95	0.00	3	1,015	4,620	1,547
45	8	45	10	40	20	LF	$ 259,017	23,199	$ 525,105	0.241	0.95	0.00	3	1,120	4,992	1,552
30	20	45	10	40	20	LF	$ 287,577	20,751	$ 525,592	0.241	0.95	0.00	3	900	4,048	1,471
45	12	45	10	40	20	LF	$ 279,537	21,481	$ 525,927	0.242	0.95	0.00	3	986	4,508	1,550
22	20	45	10	40	20	LF	$ 269,977	22,320	$ 525,986	0.242	0.95	0.00	3	1,006	4,303	1,426
20	20	45	10	40	20	LF	$ 265,577	22,825	$ 527,379	0.242	0.95	0.00	3	1,040	4,384	1,413
45	14	45	10	40	20	LF	$ 289,797	20,793	$ 528,292	0.243	0.95	0.00	3	929	4,305	1,548
35	20	45	10	40	20	LF	$ 298,577	20,090	$ 529,011	0.243	0.95	0.00	3	854	3,942	1,476
45	15	45	10	40	20	LF	$ 294,927	20,483	$ 529,867	0.243	0.95	0.00	3	903	4,200	1,539
45	20	45	10	40	20	LF	$ 320,577	19,351	$ 542,527	0.249	0.96	0.00	3	800	3,802	1,512
35	15	45	10	40	20	CC	$ 272,927	23,753	$ 545,368	0.252	0.95	0.01	3	1,127	4,297	1,360
60	8	45	10	40	20	LF	$ 292,017	22,253	$ 547,253	0.251	0.95	0.00	3	1,049	4,821	1,578
60	9	45	10	40	20	LF	$ 297,147	21,814	$ 547,348	0.251	0.95	0.00	3	1,015	4,688	1,577

Table 5-23: Categorized optimization result for Site-D under forecasted load scenario.

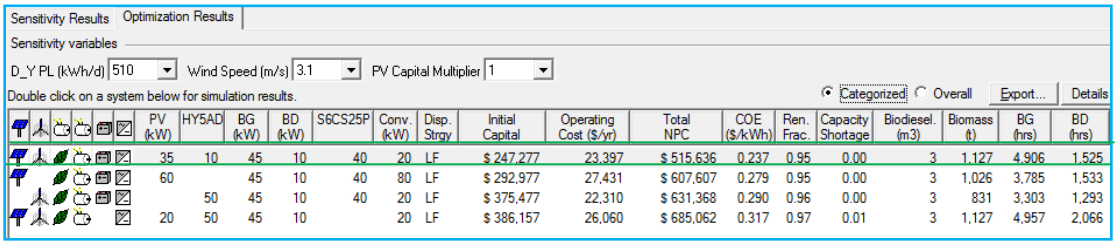

Sensitivity Results | Optimization Results

Sensitivity variables

D_Y PL (kWh/d) 510 | Wind Speed (m/s) 3.1 | PV Capital Multiplier 1

Double click on a system below for simulation results. ◉ Categorized ○ Overall | Export... | Details

PV (kW)	HY5AD	BG (kW)	BD (kW)	S6CS25P	Conv. (kW)	Disp. Strgy	Initial Capital	Operating Cost ($/yr)	Total NPC	COE ($/kWh)	Ren. Frac.	Capacity Shortage	Biodiesel. (m3)	Biomass (t)	BG (hrs)	BD (hrs)
35	10	45	10	40	20	LF	$ 247,277	23,397	$ 515,636	0.237	0.95	0.00	3	1,127	4,906	1,525
60		45	10	40	80	LF	$ 292,977	27,431	$ 607,607	0.279	0.95	0.00	3	1,026	3,785	1,533
	50	45	10	40	20	LF	$ 375,477	22,310	$ 631,368	0.290	0.96	0.00	3	831	3,303	1,293
20	50	45	10		20	LF	$ 386,157	26,060	$ 685,062	0.317	0.97	0.01	3	1,127	4,957	2,066

From Table 5.22 & 5.23, the levelized COE is observed to be in the range of $0.237/kWh to $0.317/kWh, capital cost ranges from $246,537 to $403,247, operating cost ranges from $18,850 to $30,143 and the total NPC lies in the range of $515,636 to $685,062. Both of LF and CC dispatch strategies are feasible. A hybrid system contains PV, biogas generator, biodiesel generator, wind turbine, converter and battery is the cheapest system having low NPC and small COE under LF dispatch strategy. From the categorized simulation results there are systems which do not contain wind turbine and PV and which do not require battery. But those systems are not as cost effective as a hybrid system contains all system components together.

The simulation result in Table 5.23 shows that all feasible system have the same renewable fraction and unmet load (~0%). Those systems are compared based on NPC, COE and capital cost instead of the above common parameters. The first ranked system has a NPC of $515,636, an initial capital of $247,277 and a COE of $0.237/kWh. From the overall optimization result of the hybrid system we can observed that the first optimal hybrid system (circled green) simulated under forecasted load scenario has 36.53% more NPC, 15.93%

more initial capital cost, 57.42% more excess electricity, 284% more unmeet electric load, 35% more capacity shortage, 63.26% more operating and maintenance cost but 1.7% less COE, than that of the current system.

Table 5-24: 1st ranked hybrid system report for Site-D under forecasted load scenario.

System Architecture		Sensitivity case		Annual Electric production[kWh/yr]		Annual Electric Consumption[kWh/yr]		Emission[kg/yr]	
PV	35kW	**PV capital Multiplier**	1	**PV**	72560 [34%]	**AC primary Load**	185905 [98%]	**CO2**	7642
Wind	10	**PV Replacement Multiplier**	1	**Wind**	46217 [22%]	**Deferrable Load**	3643 [2%]	**Unburned hydro carbon**	0.814
Biogas	45kW	**Primary Load[kWh/d]**	510 kWh/d	**Biogas**	80459 [38%]	**Total**	189548 [100%]	**Particulate Matter**	0.554
Biodiesel	10kW			**Biodiesel**	11327 [3%]	**Cost Summary**			
Inverter	20kW	**Deferrable Load[kWh/d]**	10 kWh/d	**Total**	210563 [100%]				
Rectifier	20kW			**Excess Electricity**	12650 [5.28%]	**Total NPC**	$515,636	**SO2**	0.124
Battery	40	**Wind Speed**	3.1m/s	**Unmet demand**	245 [0.13%]	**Levelized COE**	$0.237/ kWh	**NOx**	65.6
Dispatch strategy	LF	**Solar Radiation**	6.13 kWh/d/m2	**Capacity Shortage**	390 [0.21%]	**Operating cost**	$23,397/yr	**CO**	7.35

The monthly average electric energy production by each individual's hybrid system energy producing component (PV panel, Wind turbine, Biogas generator and Biodiesel generator) and the NPC of the system given by the capital, replacement, O&M, fuel and salvage cost are summarized in Figure 5-15 & 5.16 given below.

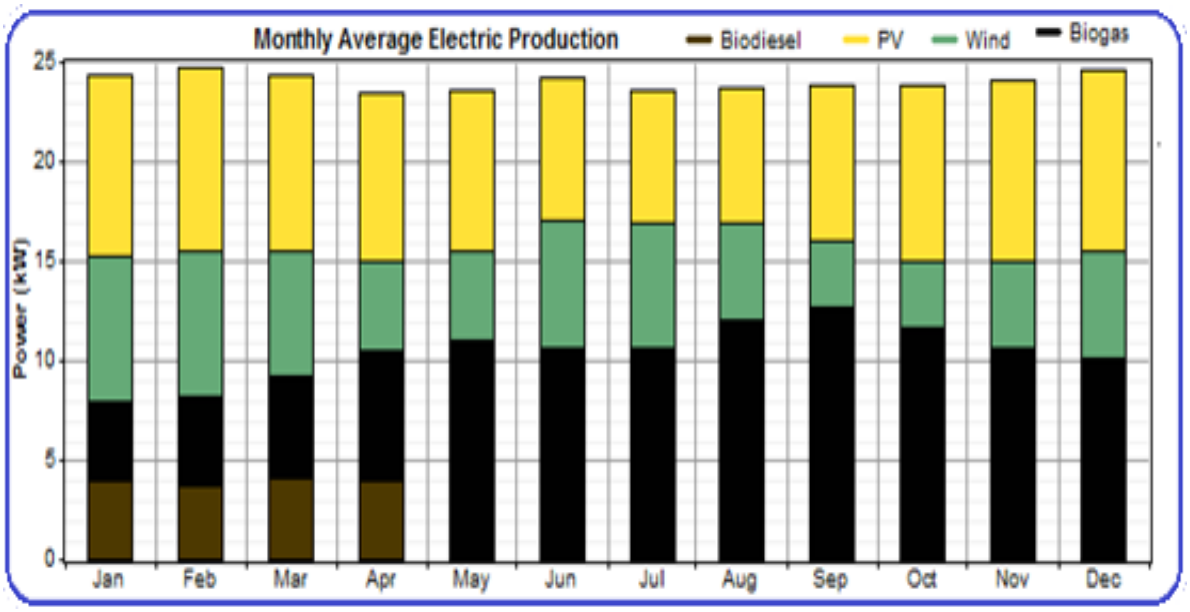

Figure 5-15: Average electric production for Site-D under forecasted load scenario.

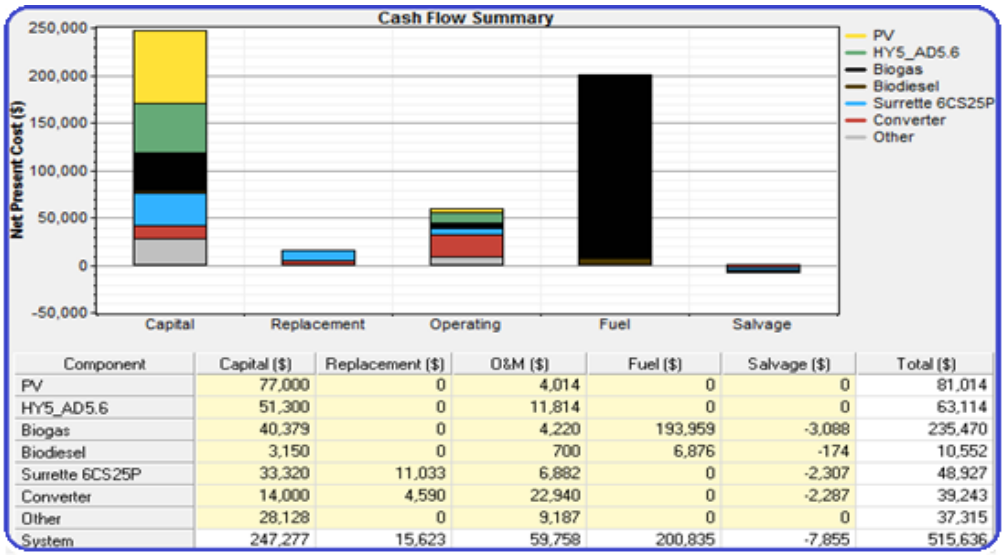

Component	Capital ($)	Replacement ($)	O&M ($)	Fuel ($)	Salvage ($)	Total ($)
PV	77,000	0	4,014	0	0	81,014
HY5_AD5.6	51,300	0	11,814	0	0	63,114
Biogas	40,379	0	4,220	193,959	-3,088	235,470
Biodiesel	3,150	0	700	6,876	-174	10,552
Surrette 6CS25P	33,320	11,033	6,882	0	-2,307	48,927
Converter	14,000	4,590	22,940	0	-2,287	39,243
Other	28,128	0	9,187	0	0	37,315
System	247,277	15,623	59,758	200,835	-7,855	515,636

Figure 5-16: Cost Summary of the above optimal system

5.3. Sensitivity Result

HOMER can also display the optimal system type in a graph and tabular form based on a given sensitivity values, in this case are community Load, wind speed and PV cost. For each combination of the sensitivity variables, the sensitivity analysis takes the least cost (ranked 1st) and extrapolates it for the intermediate sensitivity variables. The possibility of other system types can be observed by clicking on the sensitivity graph.

5.3.1. Result for Site-A

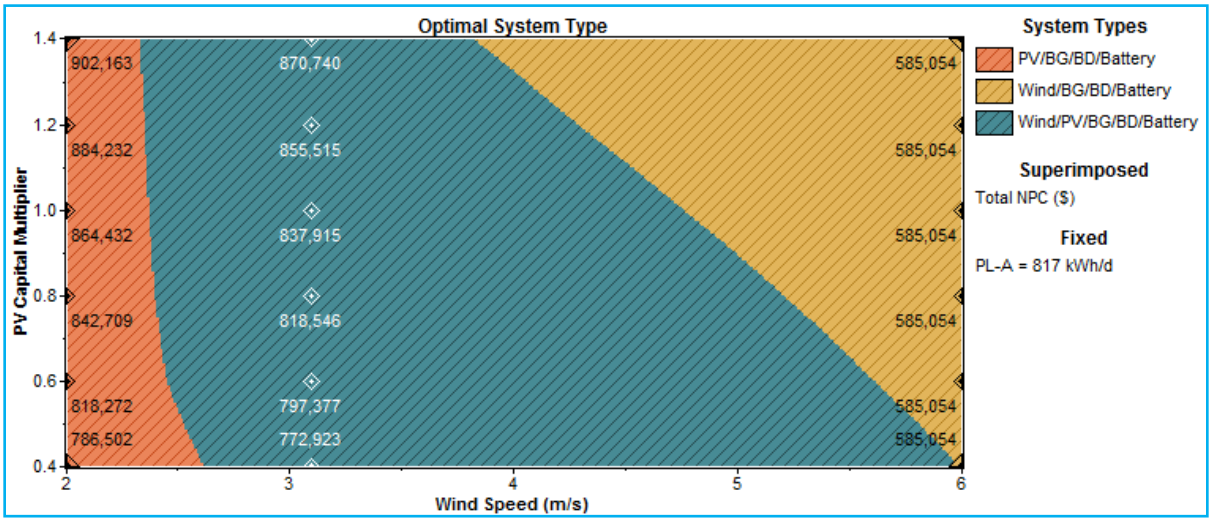

Figure 5-17: Sensitivity of PV cost to wind speed with some important NPCs labeled.

From the sensitivity result graph in Figure 5.17, a hybrid system contain the PV array, biogas generator, biodiesel generator and batteries is optimal when the wind resource (speed) is very low for all PV capital multiplier. But, at higher wind speed and a decreasing PV capital

multiplier a wind turbine, PV array, Biogas generator, Biodiesel generator and battery (blue) combination becomes the preferred system type. The wind, biogas, biodiesel and battery (yellow) system is also optimal when the PV capital multiplier increase beyond 0.4 and the wind speed above the resource potential but below 6m/s under this model. Total net present cost (NPC) is superimposed on the graph at the point where sensitivity values are set, ranging from $585,054 to $902,163.

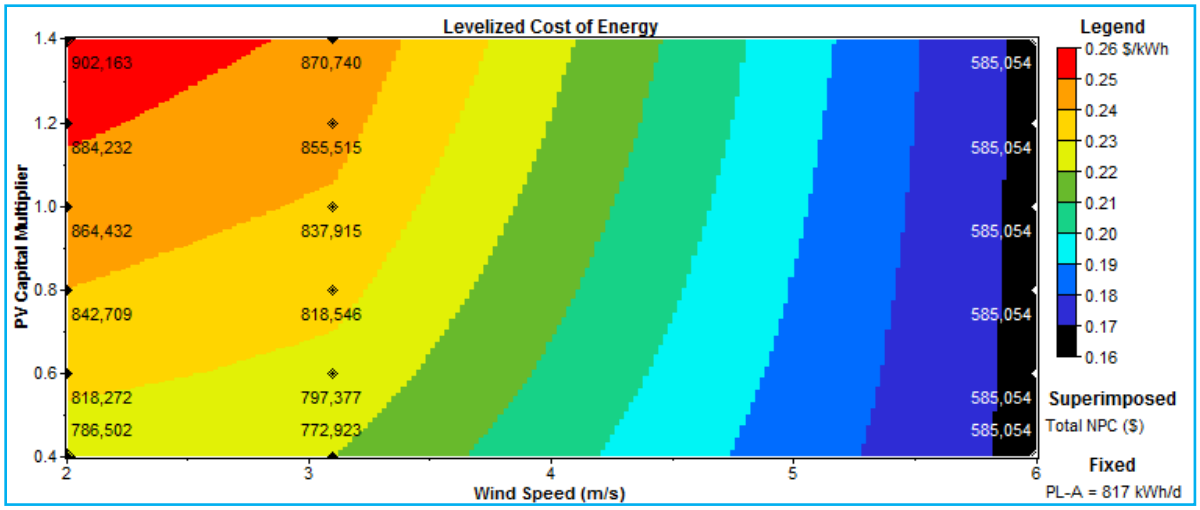

Figure 5-18: Levelized COE for a sensitivity variable of PV capital multiplier and wind speed.

At higher wind speed (black) the wind, biogas, biodiesel and battery optimal system discussed above have low levelized COE. When the wind speed is low and the PV capital multiplier is high (red) the levelized COE of the hybrid system becomes high. Total net present cost (NPC) is superimposed on the graph at the point where sensitivity values are set, ranging from $585,054 to $902,163. If the hybrid system contains PV, its NPC increases with the PV system capital multiplier for all wind speed whereas for all PV capital multiplier the NPC of the hybrid system decrease with an increase of the wind speed.

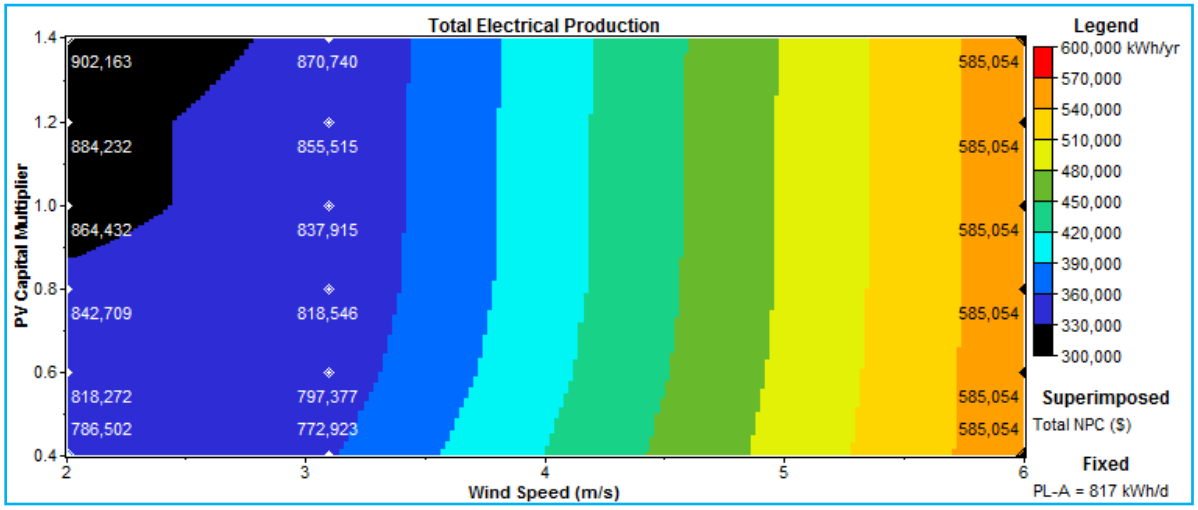

Figure 5-19: Electricity production with sensitivity of PV capital multiplier and wind speed.

At lower wind speed and a PV capital multiplier of greater than 0.9 the hybrid systems have lower electricity production but have higher total system NPC. When the wind speeds near to 6m/s for all PV capital multiplier, the hybrid systems have low total system NPC but the highest electricity production. Also the graph demonstrates a constant electricity production within a small wind speed range of greater than 3.1m/s for all PV capital multipliers.

5.3.2. Result for Site-B

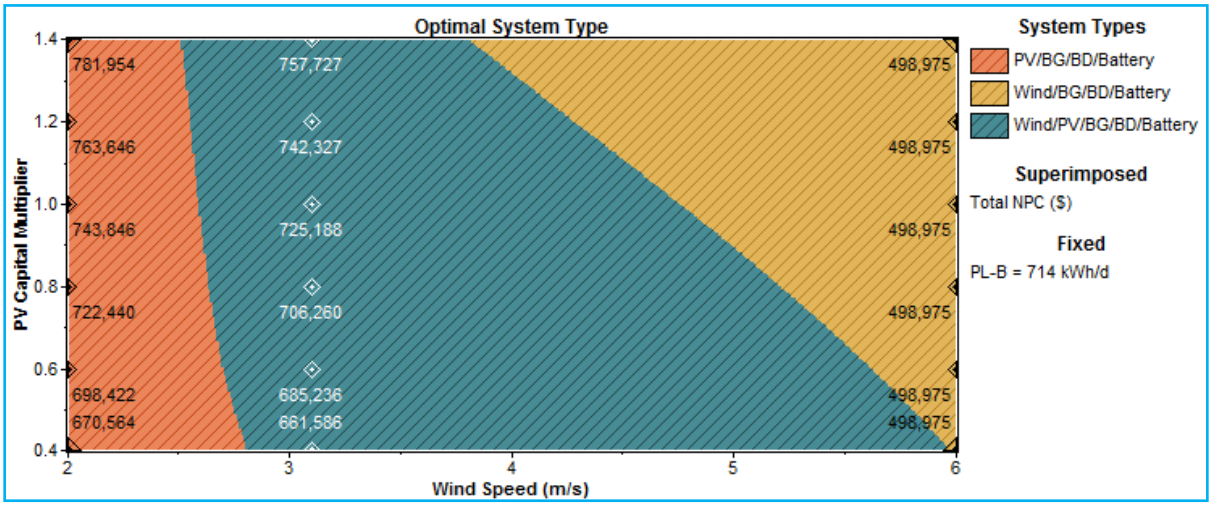

Figure 5-20: Sensitivity of PV cost to wind speed with some important NPCs labeled.

Figure 5.20 demonstrates that the optimal system given by lower wind speed below 2.8m/s is a combination of a PV array, biogas generator, biodiesel generator and batteries (red) without wind turbine, but at higher wind speed and a decreasing PV capital multiplier a wind turbine, PV array, biogas and biodiesel generator and battery (blue) combination becomes the preferred system type. The wind, biogas, biodiesel and battery (yellow) system is also optimal when the PV capital multiplier increase beyond 0.4 and the wind speed above the resource potential but below 6m/s under this model. Total net present cost (NPC) is superimposed on the graph at the point where sensitivity values are set, ranging from $498,975 to $781, 954.

5.3.3. Result for Site-C

Figure 5-21 demonstrates that the optimal system given by lower wind speed below 2.88m/s is a combination of a PV array, biogas generator, biodiesel generator and batteries (red) without wind turbine, but at higher wind speed and a decreasing PV capital multiplier a wind turbine, PV array, biogas generator, biodiesel generator and battery (blue) combination becomes the preferred system type. The wind, biogas, biodiesel and battery (yellow) system is also optimal when the PV capital multiplier increase beyond 0.4 and the wind speed above the resource potential but below 6m/s.

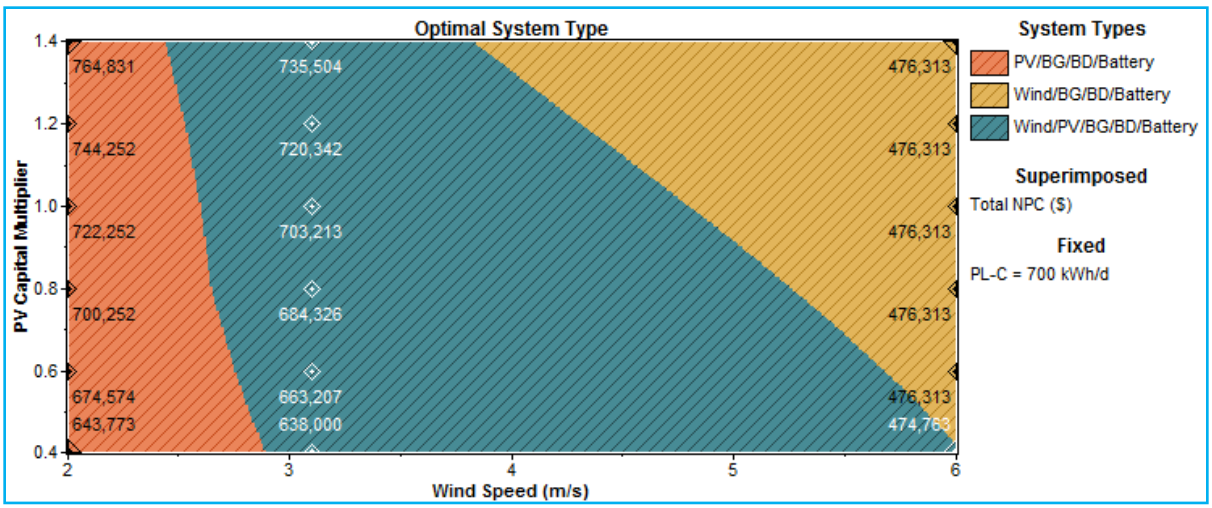

Figure 5-21: Sensitivity of PV cost to wind speed with some important NPCs labeled.

5.3.4. Result for Site-D

Figure 5-22 demonstrates the optimal system given by wind speed below 2.83m/s is a combination of a PV array, biogas and biodiesel generator and batteries (red) without wind turbine, but at higher wind speed and a decreasing PV capital multiplier a wind turbine, PV array, biogas and biodiesel generator and battery (blue) combination becomes the preferred system type. The wind, biogas, biodiesel and battery (yellow) system is also optimal when the PV capital multiplier increase beyond 0.4 and the wind speed above the resource potential but below 6m/s under this model. Also the system contains wind, biogas and biodiesel generator is optimal when the PV capital multiplier greater than 0.64 and a wind speed higher than 5.86m/s.

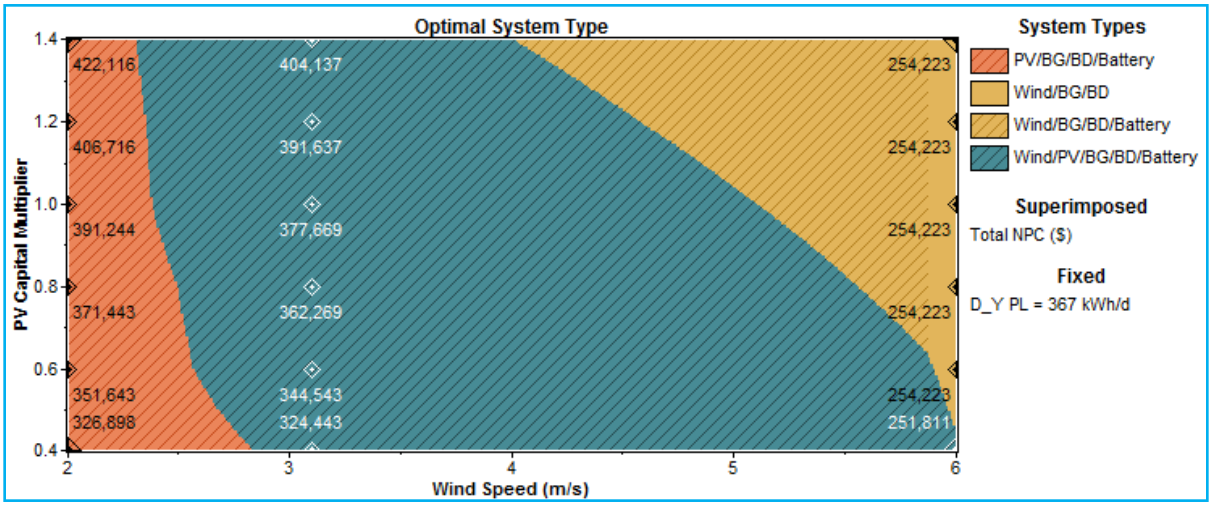

Figure 5-22: Sensitivity of PV cost to wind speed with some important NPCs labeled.

5.4. Grid Comparison Result

Grid extension is another alternative solution to electrify remote loads. In this study grid comparison was done to compare the cost of the grid extension with the cost of each stand-alone system configuration based on the proposed model. For each stand-alone system configuration, HOMER will calculate the breakeven grid extension distance. The grid comparison result discussed here is based on the total NPC of the top ranked optimal system and the grid extended system considered above under non load forecasted scenario (current system).

5.4.1. Result for Site-A

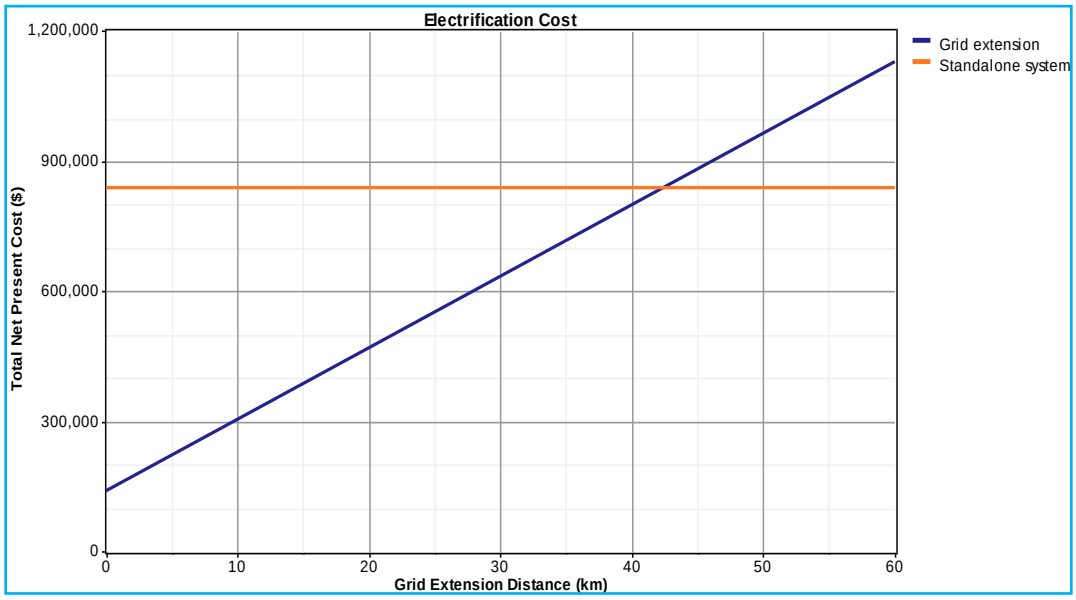

Figure 5-23: Comparison curve of grid extension with standalone hybrid system

The point at which the total NPC curve of grid extension and optimal hybrid system intersect each other is called breakeven grid extension distance (BGD). At the BGD, the optimal hybrid system and the extended grid to electrify the community load have equal total NPC. The BGD from the grid to the point at which the extended grid no further optimal beyond this point is 42.3km. Below BGD extending the grid to electrify the community load is feasible, but beyond this point the hybrid system is feasible to electrify the remote load. At the BGD the total grid extension NPC is $837,915 while at the actual distance of the grid from the community load, total initial capital cost of grid extension is $147,752 and its O&M cost is $2,937/yr. The actual distance of the grid from the location of the community load in Site-A is 11km. The result of the simulation given in Figure 5.23 demonstrates grid extension is feasible over standalone hybrid system to electrify the community load in Site-A, this is because of low grid electricity price in Ethiopia which is less than $0.04/kWh and short grid distance from the community load. While, the problem of rural electrification by grid extension is the power distribution loss due to wide spaced population settlement, the

reliability of the power source and limitation on power supply mix. The above mentioned reason and some special features of the hybrid system made the standalone hybrid system preferable than grid extension. A 100% clean, environmental friendly, green energy, renewable and reliable hybrid system is even better than the current system if we think for our future and our planet to be safe.

5.4.2. Result for Site-B

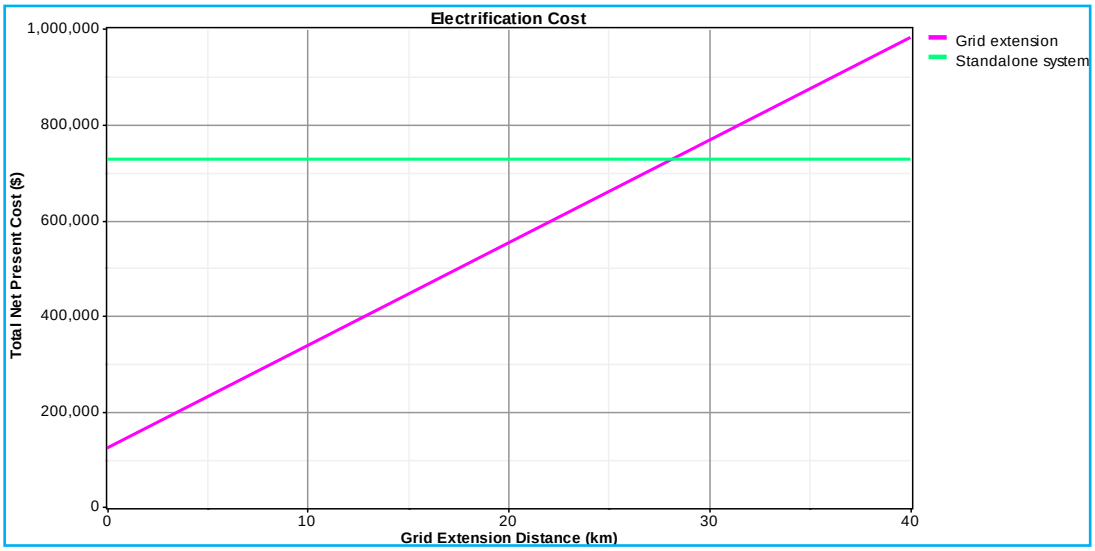

Figure 5-24: Comparison curve of grid extension with standalone hybrid system of Site-B

The BGD of Site-B is 28.1km. But, the actual distance of the grid from the location of the community load in Site-B is 6km. At the BGD the total grid extension NPC is $725,188 while at the actual distance of the grid from the community load total initial capital cost of grid extension is $104,724 and its O&M cost is $2094/yr.

The simulation result given in Figure 5.24 show that grid extension is feasible over standalone hybrid system to electrify the community load in Site-B, this is because of low grid electricity price in Ethiopia.

5.4.3. Result for Site-C

From Figure 5.25, the BGD of Site-C is 13.2km. But, the actual distance of the grid from the location of the community load in Site-C is 2km. At the BGD the total grid extension NPC is $703,213 while at the actual distance of the grid from the community load, total initial capital cost of grid extension is $71,584 and its O&M cost is $1432/yr. The simulation result given in Figure 5.25 show that grid extension is feasible over standalone hybrid system to electrify the community load in Site-C**,** this is because of low grid electricity price in Ethiopia.

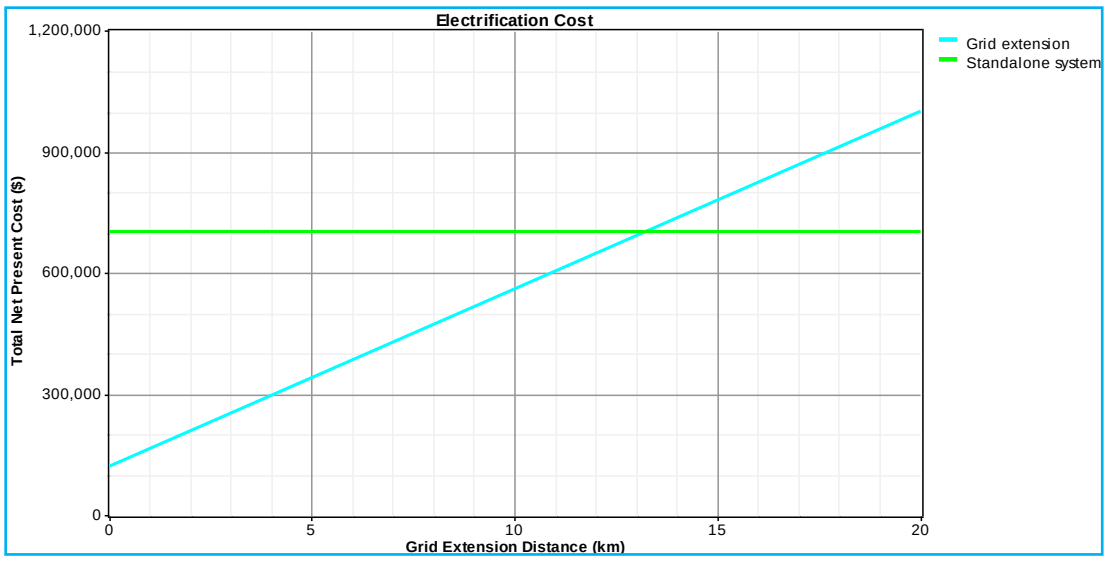

Figure 5-25: Comparison curve of grid extension with standalone hybrid system of Site-C

5.4.4. Result for Site-D

From Figure 5.26, the BGD of this site is 21.8km. But, the actual distance of the grid from the location of the community load is 12km. At the BGD the total grid extension NPC is $377,669 while at the actual distance of the grid from the community load, total initial capital cost of grid extension is $140,892 and its O&M cost is $2820/yr. The simulation result given in Figure 5.26 show that grid extension is still feasible over standalone hybrid system to electrify the community load in **Site-D** also**,** this is because of low grid electricity price in Ethiopia which is below $0.04/kWh.

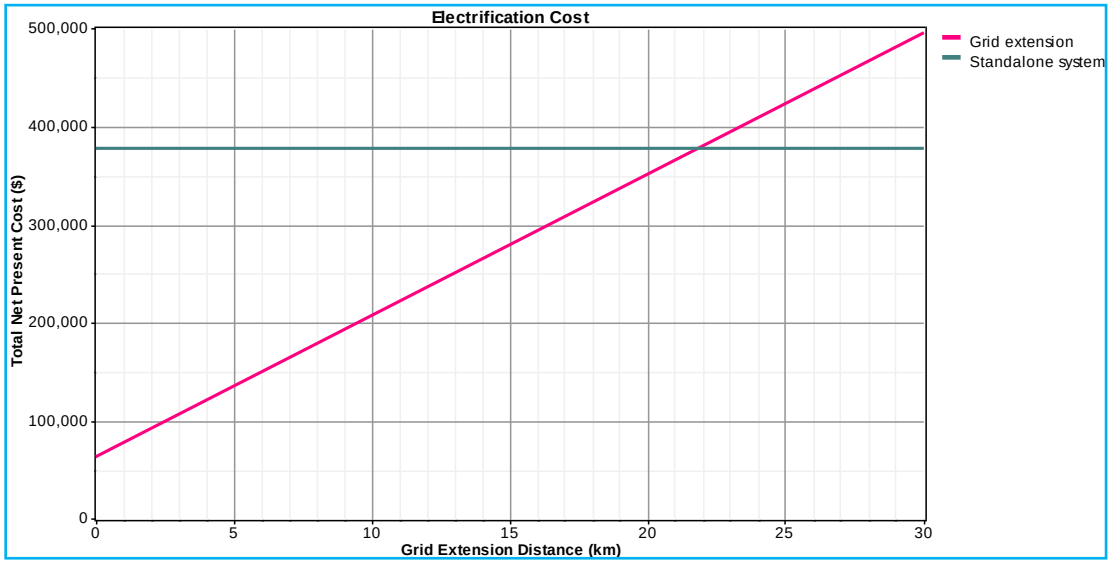

Figure 5-26: Comparison curve of grid extension with standalone hybrid system of Site-D

CHAPTER 6

6. CONCLUSIONS, RECOMMENDATIONS AND SUGGESTIONS FOR FUTURE WORK

6.1. Conclusion

The renewable energy potential of the site is estimated based on the primary data collected directly from the study area and secondary data obtained from various sources. The biogas feedstock mix potential of the study area is found to be 10.9tons/day, 9.25tons/day, 8.81tons/day and 3.09 tons/day for Site-A, Site-B, Site-C and Site-D respectively with a gasification ratio of 0.0626kg/kg. The study result shows that there is a sufficient biogas feedstock potential for all districts of the study area and the HOMER simulation result demonstrates there is an excess biogas after running a biogas generator in a hybrid system. The excess biogas left unused from a hybrid electric generating unit would go to biogas cooking application for the community cooking loads. Also, the biodiesel potential of the study area from Jatropha is estimated to be 18.5m3/year.

The study of the wind and solar resource potentials of the site is based on the data obtained from NASA, SWERA and Meteonorm. Therefore, the results obtained from these sources are compared against each other and through the review of various literatures on the accuracy of the sources. Data from NASA is chosen for simulation. The result shows, all the sites have an average wind speed potential of 3.1m/s at 10m anemometer height and solar radiation potential of 6.13kWh/m2/day.

The design of hybrid power generation system which comprises of PV arrays, wind turbines, biogas and biodiesel generator with battery banks and power conditioning units has been discussed in this thesis. The idea is to achieve a cost effective system configuration which is supposed to supply electricity to a rural community of 1135 households found in four sites equipped with a human clinic and animal clinics, flour mill and schools to improve the life of people in the rural areas where electricity from the main grid has not reached yet. The community load is estimated and forecasted over the project horizon. Electrical primary loads for the community are estimated as 817kWh/day, 714kWh/day, 700kWh/day and 367kWh/day while a deferrable load of 22.4kWh/day, 17.9kWh/day, 18.2kWh/day and 7kWh/day for Site-A, Site-B, Site-C and Site-D respectively. The demand forecast result is given as 1132kWh/day, 1000kWh/day, 973kWh/day, 510kWh/day primary energy and 31.4kWh/day, 26kWh/day, 26kWh/day, and 10kWh/day deferrable energy for Site-A, Site-B, Site-C and Site-D respectively. Two separate simulation, but linked together, is done for both estimated and forecasted community load to observe how much the forecasted load raises the cost of the hybrid system and change the system configuration. In addition to the hybrid system component cost, the distribution cost of electricity from hybrid center to load and the cost of biogas digester and biodiesel oil expeller are considered before running the

simulation. The grid comparison analysis with the hybrid system has been carried out using cost data from UEAP.

The feasibility analysis of the renewable energy resources data has been carried out by HOMER software. From the results, the wind energy potential of the site is found to be considerable, although it may not be sufficient for a large independent wind farm; it is viable option if incorporated into other energy conversion systems such as PV, biodiesel and biogas generator with battery and converter. The results also confirmed the availability of huge utilizable solar and biogas energy at the site. HOMER simulation result also demonstrates grid extension is optimal over standalone hybrid electric supply system and forecasted load would raise the NPC of the hybrid system by 36% to 39% from the current system. Also, the results obtained from the software give numerous alternatives of feasible hybrid systems with high levels of renewable resources penetration which their choice is restricted by changing the net present cost of each system set up. The COE of the feasible setups in this study, which is in the range of $0.234 to $0.437/kWh, are high compared to the tariff in the country (<$0.04/kWh).

6.2. Recommendation

In addition to what are covered in this thesis, there are potential biogas feedstock sources like agricultural residue and municipal solid wastes suitable for biogas production. The potential study and determination of biogas technical parameters of those feedstocks are very difficult and may require more time and finance to study it in detail.

Biodiesel in this study is produced from Jatropha plant. It is a non conventional energy source that replaces the conventional diesel fuel to run diesel engine when it is chemically treated. Unlike biogas, for biodiesel resource assessment there is no separate window in HOMER. But there is a possibility to create new fuel with their chemical and physical property to run a generator in hybrid system feasibility study. The problem is, there is no interface in HOMER to specify whether the fuel that the user defined was conventional or renewable energy source and considering it on renewable fraction computation. The author of this work recommends that HOMER team should develop a user interface in HOMER for the types of energy (renewable or conventional) like creating new fuel and specifying its property to solve the ambiguity on the renewable fraction of HOMER simulation result.

Ethiopia has a huge potential of renewable energy resources which can be used for rural electrification through the off-grid system. There are, however, many challenges like low purchasing power of the rural community, unfavorable conditions towards the utilization of renewable energies, absence of awareness how to use these resources, etc. Thus, the author of this work recommends that the government, non-governmental organizations and the private sectors should make combined efforts to overcome these challenges by using more flexible approaches to improve the current poor rural electrification status in Ethiopia.

6.3. Suggestion for Future Work

This thesis work may be refined and expanded by considering:

1. Exact measurement of biomass obtained from each animal group by classifying with animal age, animal weight and animal feeding material type in the case of Ethiopia.
2. Exact measurement of solar radiation and wind resource data at different local time of the sites.
3. Detailed electrical design and modelling of each component and steady state and dynamic performance of the overall optimal hybrid system.

References

[1] World Bank report of 2012. http://www.worldbank.org/
[2] *Ministry of Water, Irrigation and Energy. www.moie.gov.et*
[3] Gosaye mengstie, 2011 "Ethiopia- The case of small scale Renewable Energy for all financing access for the poor", Oslo Norway, 11 October 2011.
[4] John Furtado (2012), "Analysis of a biomass-based hybrid energy system for rural electrification - A case study in Uganda", Master of Science Thesis, Stockholm 2012.
[5] Celik, A.N. (2002), "Optimization and techno-economic analysis of autonomous photovoltaic wind- hybrid energy systems in comparison to single photovoltaic and wind systems." Energy Conversion and Management, Vol. 43, No. 18.
[6] Timur Gul (2004), "Integrated Analysis of Hybrid Systems for Rural Electrification in Developing Countries". Division of Land and Water and Water Resources Engineering, Stockholm 2004.
[7] Rohit Sen (September, 2011), "Off-Grid Electricity Generation with Renewable Energy Technologies in India; An application of HOMER" Renewable Energy & Environmental Modelling University of Dundee.
[8] Ethiopian Rural Energy Development and Promotion Center, "Country background information of Solar and Wind Energy Utilization and Project Development Scenarios". Final report October, 2007.
[9] Drake F. and, Mulugetta Y., 1996, "Assessment of solar and wind energy in Ethiopia. I. Solar energy", *Solar Energy*, Vol. 57, No. 3, pp. 205-217, 1996.
[10] Bekele G, 'Study into the potential and feasibility of a standalone solar wind hybrid electric energy supply system-for application in Ethiopia', Stockholm, December 2009.
[11] Kanwardeep Singh (July, 2010), "Study of Solar/Biogas Hybrid power generation", MSc thesis. Thapar University, 2010.
[12] *Solar and Wind master plan of Ethiopia by Hydro china, July 2012. www.moie.gov.et*
[13] Wikipedia. (2012, November). Retrieved from http://en.wikipedia.org/wiki/Weibull_distribution.
[14] Patil, Mukind R. (1999), "Wind and Solar Power Systems", CRC pres LLC, USA, 1999
[15] RETSCREEN. *RETSCREEN International, Renewable Energy Project Analysis: RETscreen Engineering and Cases Textbook.* Retrieved from Available: http://www.retscreen.net.
[16] NREL. (2009). Homer user manual: http://www.nrel.gov/homer; Feb 2009.
[17] Tadesse, G. (May, 2011), "Feasibility study of small Hydro/PV/Wind hybrid system for Off – Grid rural electrification in Ethiopia", Addis Ababa Institute of Technology Master Thesis.
[18] Gipe P. (1999), *Wind Energy Basics, a Guide to Small and Micro Wind Systems;* Chelsea Green publishing company**.**
[19] Danish Wind Industry Association (Dec. 2008) http://www.windpower.org/en/tour/wres/index.htm
[20] Tesfaye, B. (January, 2011), "Improved Sustainable Power Supply for Dagahabur and Kebridahar Town of Somalia Region in Ethiopia", Eykjavik Energy Graduate School of Sustainable Systems Master Thesis.
[21] Boyle, G. (1996). "Renewable Energy – Power for a sustainable future".
[22] Masters, G. M. (2004.). . *Renewable and Efficient Electric Power Systems, page 310. John Wiley & Sons, Incorporated. Hoboken*, NJ, USA.
[23] Joliet Wind turbines, Dec. 2008, http://www.joliet-windturbines.com/cyclone_20kw_wind_turbine.html
[24] Wolde-Ghiorgis W., 1988, Wind energy survey in Ethiopia, *Solar Wind Technology*; 5: 341-351
[25] Breyer Ch., Gerlach A., Hlusiak M., Peters C., Adelmann P., Winiecki J., Schützeichel H.,Tsegaye S., Gashie W., 2009 "Electrifying the Poor: Highly Economic Off-Grid PV Systems

in Ethiopia a Basis for Sustainable Development" http://www.arcfinance.org/pdfs/news/EthiopiaPaper2009.pdf
[26] Bekele G. and Palm B.,2009 "Wind energy potential assessment at four typical locations in Ethiopia", *Applied Energy*, Vol. 86, Issue 3, pp. 388–396
[27] Japanese Embassy in Ethiopia, 2008 "Study on the Energy Sector in Ethiopia": http://www.et.emb-japan.go.jp/electric_report_english.pdf
[28] *Aklilu Dalelo, (2001). Rural electrification in Ethiopia: opportunities and bottlenecks. Addis Ababa university college of education, Addis Ababa, Ethiopia, 2001.*
[29] *EEA (Ethiopian Electric Agency), (2002). Rural Electrification Symposium Proceedings, March 1-5, 2002.*
[30] *Solar and Wind Master Plan of Ethiopia by Hydro China, July 2012. www.mowie.gov.et*
[31] NASA World Surface Metrology: 2012: http://eosweb.larc.nasa.gov/cgi-bin/sse/retscreen.cgi?email=rets@nrcan.gc.ca
[32] HOMER-version2.68 beta: www.homerenergy.com
[33] Twidell J. And Weir T, 2006, "Renewable Energy Resources", 2nd Edn, Taylor & Francis, London, 2006.
[34] Patel, M. (2006), "*Wind and Solar Power Systems", Second Edition, Taylor & Francis.*
[35] Luque, A. and Hegedus, S., (Ed) (2003) *Handbook of Photovoltaic Science and Engineering*. West Sussex, England: John Wiley & Sons Ltd.
[36] Duffie, J.A. and Beckman, W.A., (2006) *Solar Engineering of Thermal Processes*. 3rd ed. New Jersey: John Wiley and Sons, Inc.
[37] http://www.pvsyst.com/ (PVsyst V6.06 data base)
[38] *KYOCERA*. (2004). Retrieved from http://www.kyocerasolar.com/learn/modules.html.
[39] Ethiopian Electric Power Corporation (EEPCO),2007, "Excerpts from the Power System Master Plan" http://www.energyethiopia.org/downloads/Event_Pr_EEPCo.pdf
[40] Heimann S., 2007 "Renewable Energy in Ethiopia 13 Months of Sunshine for a sustainable development": http://www.stefanheimann.eu/inhalt/Renewables_Ethiopia.pdf
[41] Hadagu A., 2006 "Status and trends of Ethiopian rural Electrification Fund", http://www.bgr.de/geotherm/ArGeoC1/pdf/07%20A.%20Hadgu%20status%20of%20Ethiopian%20Electrification%20fund.pdf.
[42] Sameer Maithel, (2009). "Biomass Energy Resource Assessment Handbook", prepared for Asian and Pacific Centre for Transfer of Technology of the United Nations – Economic and Social Commission for Asia and the Pacific (ESCAP), September 2009.
[43] Peter Jacob Jørgensen, Plan Energi and Researcher for a Day. 'Biogas – green energy'–Faculty of Agricultural Sciences, Aarhus University 2009, 2nd edition. http://lemvigbiogas.com
[44] Teodorita Al Seadi, Dominik Rutz, Heinz Prassl, Michael Köttner, Tobias Finsterwalder, Silke Volk, Rainer Janssen. 'Biogas handbook' -University of Southern Denmark Esbjerg, Niels Bohrs Vej 9-10, DK-6700 Esbjerg, Denmark 2008.
[45] www.fact-foundation.com
[46] Jatropha literature and perspectives review: Main potential social and environmental impacts arising from large scale plantations, May 2008, proforest ltd.
[47] http://home.t-online.de/home/320033440512-0002/downloads/jcl-manual.pdf
[48] R.E.E. Jongschaap et al. (2007) Claims and Facts on Jatropha curcas L., Global Jatropha curcas evaluation, breeding and propagation programme, Plant Research International, Wageningen UR.
[49] Demirbas A (2000). Conversion of biomass using glycerine to liquid fuel for blending gasoline as alternative engine fuel. Energy Convers. Manage. 41: 1741-1748.
[50] Kinney AJ, Clemente TE (2005). Modifying soybean oil for enhanced performance in biodiesel blends. Fuel Process Technol. 86: 1137-1147.
[51] Wilson SC, Mathews M, Austin G, von Blottnitz H (2005). Review of the status of biodiesel related activities in South Africa. Report for the City of Cape Town, South Africa p. 76.

[52] Shay EG (1993). Diesel fuel from vegetable oil: Status and opportunities. Biomass Bioenerg. 4: 227-242.
[53] METEONORM, Version 7.x 2012, www.meteonorm.com
[54] Kamman Jr KP, Phillip AI (1985). Sulfurized vegetable oil products as lubricants additives. J. Am. Oil Chem. Soc., 65: 883-885.
[55] Matsumoto T, Takahashi S, Kaieda M, Ueda M, Tanaka A, Fakuda H, Kondo A (2001). Yeast whole-cell biocatalysts constructed by intracellular overproduction of Rhizopus oryzae lipase are applicable to biodiesel fuel production. Appl. Microbiol. Biotechnol., 57: 4-11.
[56] Ban K, Kaieda M, Matsumoto T, Kondo A, Fukuda H (2001). Whole cell biocatalyst for biodiesel fuel production utilising Rhizopus oryzae cells immobilised within biomass support particles. Biochem. Eng., 8:39-43.
[57] Salafudin, Hendroko, R. and Marwan, R. (2010) _The effect of organic loading, husk freshness and types of inoculum to the performance Jatropha Curcas Linn husk anaerobic digestion', International Conference on Tehnology for New and Renewable Energy (ICTNRE 2010), Jakarta, December.
[58] Ethiopia Rural Energy Development and Promotion Centre (EREDPC), "national biogas program of Ethiopia Programme Implementation Document", 2008 (www.snvworld.org)
[59] Ludwing Sasse, (1988). "Biogas plant", A Publication of the Deutsches Zentrum für Entwicklungstechnologien - GATE in: Deutsche Gesellschaft für Technische Zusammenarbeit (GTZ) GmbH – 1988.
[60] Anelia Milbrandt, (2009). "Assessment of Biomass Resources in Liberia Prepared for the U.S. Agency for International Development (USAID) under the Liberia Energy Assistance Program (LEAP)", Technical Report, NREL/TP-6A2-44808 April 2009.
[61] F.A. Nicholson, B.J. Chambers, J.R. Williamsb, R.J. Unwin. 'Heavy metal contents of livestock feeds and animal manures in England and Wales'-ADAS Gleadthorpe Research Centre, Meden Vale, Mans®eld, Nottinghamshire, NG20 9PF, UK 1999.
[62] J. Mark Powell, Yanxia Li, Zhonghong Wu, Glen A. Broderick, Brian J. Holmes, "Rapid assessment of feed and manure nutrient management on confinement dairy farms" February, 2008.
[63] Fabio Struckmann, "Analysis of a flat-plate solar collector", Lund University department of energy science-Engineering faculty, Lund-Sweden, 2008.
[64] McAdams, W. H.: Heat Transmission, 3rd edition. McGraw-Hill, New York. pp. 249. 1954.
[65] http://www.repp.org/discussiongroups/resources/stoves/apro/mudstove.html
[66] http://www.hedon.info/ImprovedCookstovesInMalawi
[67] http://practicalaction.org/practicalanswers/product_info.php?products_id=319&osCsid=7cu2kv9ecg2fhqqpu0tresrrq2&osCsid=7cu2kv9ecg2fhqqpu0tresrrq2.
[68] http://www.unhcr.org/protect/PROTECTION/406c368f2.pdf.
[69] www.bioenergylists.org/stovesdoc/LBNL/Darfur_FES.pdf.
[70] www.boingboing.net/2008/06/26/rocket-stoves-use-tw.html.
[71] http://www.paceproject.net/UserFiles/File/Energy/improved%20stoves.pdf.
[72] http://www.unhcr.org/protect/PROTECTION/406c368f2.pdf.
[73] www.repp.org/discussiongroups/resources/stoves/Scott/ugandarocket/Uganda_Household_Rocket.pdf
[74] http://www.bioenergylists.org/stovesdoc/Still/AprovechoPlans/Rocket%20Stove%20Design%20Guide.pdf.
[75] www.bioenergylists.org/stovesdoc/LBNL/Darfur_FES.pdf.
[76] http://listserv.repp.org/pipermail/stoves_listserv.repp.org/2007-July/006902.html
[77] http://www.reapcanada.com/online_library/IntDev/id_mts/MTS%20Performance%20Report%20by%20Aprovecho.pdf
[78] http://www.ashdenawards.org/files/reports/ksg_case_study_2008_0.pdf
[79] http://www.hedon.info/NewDawnEnergySystemsSouthAfrica

[80] http://www.vesto.co.za/vesto/vesto1.htm
[81] http://www.hedon.info/TheUpesiRuralStovesProject
[82] Sopian K., Razak J.A., Nopiah Z.M., Ali Y, 2008, "Optimal Operational Strategies for Pico Hydro Wind Photovoltaic Diesel Hybrid Energy System Using Genetic Algorithms", ISESCO Since and Technology Vision, Vol. 4 No. 5, pp. 55-59.
[83] Kenfack J., Neirac F.P., Tatietse T.T., Mayer D., Fogue M. and Lejeune A., 2009, "Micro hydro-PV-Hybrid System: Sizing a Small Hydro-PV-Hybrid System for Rural Electrification in Developing Countries", Renewable Energy, Vol. 34, pp 2259–2263.
[84] Kanase-Patil A.B., Saini R.P., Sharma M.P., 2010 "Integrated Renewable Energy Systems for Off Grid Rural Electrification of Remote Area", Renewable Energy, Vol. 35, Issue 6, pp. 1342–1349.
[85] Bakos G.C., 2002 "Feasibility study of a hybrid wind/hydropower-system for low cost electricity production", Applied Energy, Vol. 72, Issue 3-4, pp. 599–608
[86] Connolly D., Lund H., Mathiesen B.V. and Leahy M., 2010, "A review of computer tools for analysing the integration of renewable energy into various energy systems", Applied Energy, Vol. 87, Issue 4, pp. 1059-1082.
[87] Tamrat B, 2007 "Comparative Analysis of Feasibility of Solar PV, Wind and Micro Hydropower Generation for Rural Electrification in the Selected Sites of Ethiopia", Addis Ababa University MSc. Thesis, July 2007.
[88] Gelma, B. (July, 2011),"Design of a Photovoltaic-Wind hybrid power generation system for Ethiopian remote area", Addis Ababa University MSc. Thesis, July 2011.
[89] (CSA, 2007), Ethiopia National Census conducted by Central Statistics Agency of Ethiopia.
[90] http://www.hp.com/support/lj3380/LJ3380 (LJ3380 user manual)
[91] http://www.canon.com/NP6512 (NP6512 service manual)
[92] www.allpower.co.za (South Africa).
[93] T.Gone, Modern Power System Analysis. New York: Jhon Wiley & Sons, 1988
[94] IEEE Transactions on Power Systems, Vol. 14, No.3, August 1999.
[95] Universal Electrification Access Program (UEAP), Main Report, Volume II, EEPCO, April 2005.
[96] Gipe, P. (2004). *Wind Power: Renewable Energy for Home, Farm, and Business).*
[97] http://www.wind-energy-the-facts.org/en/home--about-the-project.html
[98] Bolinger, M. and R. Wiser. 2011. Understanding Trends in Wind Turbine Prices Over the Past Decade. LBNL-5119E. Berkeley, Calif.: Lawrence Berkeley National Laboratory.
[99] http://www.allsmallwindturbines.com/turbine_detail.php?turbine_id=299&owner=1015
[100] J. K. Maherchandani, Chitranjan Agarwal, Mukesh Sahi, 'Economic Feasibility of Hybrid Biomass/PV/Wind System for Remote Villages Using HOMER', ISSN 2278 - 8875 Vol. 1, Issue 2, August 2012
[101] http://www.jatropha.pro/jatropha_oil_expellers.htm
[102] O.J.Onojo, G.A. Chukwudebe, E.N.C. Okafor, S.O.E. Ogbogu, 'Feasibility investigation of a hybrid renewable energy system as a backup power supply for an ICT building in Nigeria —a review of literature' ISSN-L: 2223-9553, ISSN: 2223-9944 Vol. 4 No. 3 May 2013.

APPENDIX-A

Load Forecast Result

Table A-1: Primary and deferrable load forecast result of Site-A

YEAR	POPULATION	HH	P-LOAD	D-LOAD	P_{PEAK}
2013	1712	390	817	22.4	98
2014	1743	397	830	23	100
2015	1774	404	843.4	23.2	102
2016	1806	411	856.6	23.6	103
2017	1839	419	871.7	24	105
2018	1872	426	884.9	24.4	107
2019	1906	434	900	25	108
2020	1940	442	915	25.2	110
2021	1975	450	930	25.6	112
2022	2011	458	945.2	26.1	114
2023	2047	466	960.3	26.5	116
2024	2084	475	977.3	27	118
2025	2121	483	992.4	27.4	119
2026	2159	492	1009.3	28	121
2027	2198	501	1026.3	28.4	124
2028	2238	510	1043.3	29	126
2029	2278	519	1060.2	29.4	128
2030	2319	528	1077.2	30	130
2031	2361	538	1096	30.4	132
2031	2403	547	1113	31	134
2033	2446	557	1132	31.4	136

Table A-2: Primary and deferrable load forecast result of Site-B

YEAR	POPULATON	HH	P-LOAD	D-LOAD	PPEAK
2013	1457	332	714	18	86
2014	1484	338	726	18.4	87
2015	1510	344	737	18.8	89
2016	1538	350	749	19.2	90
2017	1565	356	761	19.6	91
2018	1593	363	774	19.8	93
2019	1622	369	786	20	94
2020	1651	376	800	20.4	96
2021	1681	383	814	20.8	98
2022	1711	390	826	21.1	99
2023	1742	397	840	21.5	101
2024	1774	404	854	22	103
2025	1805	411	867	22.3	104
2026	1838	419	882	22.7	106
2027	1871	426	896	23.1	108
2028	1905	434	912	23.5	110
2029	1939	442	927	24	111
2030	1974	450	943	24.4	113
2031	2010	458	958	25	115
2031	2046	466	974	25.4	117
2033	2083	474	1000	26	120

Table A-3: Primary and deferrable load forecast result of Site-C

YEAR	POPULATON	HH	P-LOAD	D-LOAD	PPEAK
2013	1374	313	700	18	82
2014	1399	319	712	18.4	83
2015	1424	324	722	18.8	85
2016	1450	330	734	19.2	86
2017	1476	336	747	19.6	88
2018	1503	342	759	19.8	89
2019	1530	349	773	20	91
2020	1558	355	785	20.4	92
2021	1586	361	797	20.8	93
2022	1615	368	811	21.1	95
2023	1644	374	823	21.5	96
2024	1674	381	837	22	98
2025	1704	388	852	22.3	100
2026	1735	395	866	22.7	101
2027	1766	402	880	23.1	103
2028	1798	410	896	23.5	105
2029	1830	417	910	24	107
2030	1863	424	924	24.4	108
2031	1897	432	940	25	110
2031	1931	440	957	25.4	112
2033	1966	448	973	26	114

Table A-4: Primary and deferrable load forecast result of Site-D

YEAR	POPULATON	HH	P-LOAD	D-LOAD	PPEAK
2013	439	100	367	7	39
2014	447	102	374	7.13	40
2015	455	104	381	7.26	41
2016	463	106	389	7.4	41
2017	471	107	391	7.44	42
2018	479	109	397	7.6	42
2019	488	111	404	7.7	43
2020	497	113	410	7.82	44
2021	506	115	417	8	44
2022	515	117	424	8.1	45
2023	524	119	430	8.2	46
2024	534	122	440	8.4	47
2025	544	124	447	8.5	48
2026	554	126	453	8.7	48
2027	564	129	463	8.83	49
2028	574	131	470	9	50
2029	584	133	476	9.1	51
2030	595	136	486	9.3	52
2031	606	138	493	9.4	52
2031	617	141	503	9.6	54
2033	629	143	510	10	54

APPENDIX-B

KOLLEKTOR Sensitivity Analysis Result

Table B-1: Collector Design report for each Sensitivity input variable.

No.	Input Sensitivity parameters							Output sensitivity variable																
	$M^{\cdot}$	w	β	n_{tp}	Bond type	d_{fr}	D_{gl}	T_{out}	T_{abs}	T_m	$h_{s,p1-a}$	$h_{s,abs-p2}$	$h_{s,abs-z2}$	$h_{s,z1-a}$	$h_{p,p1-a}$	$h_{p,abs-p2}$	$h_{p,abs-z2}$	$h_{p,z1-a}$	$h_{v,p1-p2}$	$h_{v,z1-z2}$	hi	F_R	U	Qu	η
1	0.001	0	0	10	up	10	2	131.2	82.4	75.8	5.3	0.42	4.5	4.72	5.3	3.6	1.44	5.3	400	5.5	362	0.5	6.27	341	46.5
2	0.001	3	0	10	up	10	2	124.9	78.8	72.6	5.1	0.4	4.3	4.6	16.1	3.6	1.4	16.1	400	5.5	360	0.46	6.5	313	42.7
3	0.001	0	12	10	up	10	2	130.8	82	76	5.3	0.42	4.5	4.7	5.3	3.6	1.7	5.3	400	5.5	362	0.5	6.23	341	46.5
4	0.001	0	0	30	up	10	2	137	80.3	78.7	5.3	0.41	4.43	4.71	5.3	3.54	1.43	5.3	400	5.5	360	0.52	5.17	354	48.3
5	0.001	0	0	10	mid	10	2	132	82	76.4	5.3	0.42	4.5	4.72	5.3	3.56	1.44	5.3	400	5.5	362	0.50	6.23	341	46.5
6	0.001	0	0	10	up	10	4	131.2	82.5	75.8	5.3	0.42	4.5	4.72	5.3	3.56	1.44	5.3	400	5.5	362	0.5	6.23	341	46.5
7	0.001	0	45	10	up	10	2	130	81.8	75.3	5.3	0.42	4.52	4.73	5.3	3.6	2.3	5.3	400	5.5	361	0.49	6.35	334	45.6
8	0.001	0	0	50	up	10	2	138	80	79	5.3	0.41	4.42	4.7	5.3	3.5	1.43	5.3	400	5.5	360	0.52	5.17	354	48.3
9	0.001	0	0	10	low	10	2	137.7	80	79	5.3	0.41	4.42	4.7	5.3	3.53	1.43	5.3	400	5.5	363	0.52	5.17	354	48.3
10	0.001	0	0	10	up	60	2	146	91	83	5.4	0.44	5.16	4.52	5.3	3.65	1.49	5.3	400	0.92	365	0.59	3.83	402	54.9
11	0.004	0	0	10	up	60	4	60.4	51.7	40.4	5.07	0.35	3.7	4.45	5.3	3.12	1.36	5.3	200	0.92	355	0.84	4.1	572	77.6
12	0.004	3	0	10	up	60	4	59.7	51	40	5	0.34	3.69	4.4	16.1	3.2	1.36	16.1	200	0.92	355	0.82	3.54	558	76.3
13	0.004	0	12	10	up	60	4	60.4	51.7	40.4	5.07	0.35	3.7	4.45	5.3	3.1	1.5	5.3	200	0.92	355	0.84	4.1	572	77.6
14	0.004	0	0	30	up	60	4	62.5	44.2	41.4	5	0.33	3.47	4.44	5.3	2.96	1.34	5.3	200	0.92	344	0.88	4	600	81.9
15	0.004	0	0	10	mid	60	4	60.8	50.3	40.6	5.1	0.34	3.7	4.45	5.3	3.1	1.36	5.3	200	0.92	356	0.84	4.1	572	77.6
16	0.004	0	0	10	up	10	4	58.3	50	39.4	5.06	0.34	3.52	4.54	5.3	3.09	1.34	5.3	200	0.92	355	0.72	3.46	490	67
17	0.004	0	0	10	up	60	2	60.4	52	40.4	5.1	0.35	3.7	4.45	5.3	3.13	1.36	5.3	400	0.92	355	0.84	4.1	572	77.6
18	0.004	0	45	10	up	60	4	60.4	51.7	40.4	5.1	0.35	3.7	4.45	5.3	3.1	1.83	5.3	200	0.92	355	0.84	4.1	572	77.6
19	0.004	0	0	50	up	60	4	62.8	43	41.6	5	0.33	3.44	4.44	5.3	2.94	1.3	5.3	200	0.92	342	0.88	4	600	81.9
20	0.004	0	0	10	Low	60	4	60.7	50.4	40.6	5.06	0.34	3.67	4.45	5.3	3.1	1.4	5.3	200	0.92	355	0.84	4.1	572	77.6
21	0.01	0	0	50	mid	10	2	38	30.5	29.2	5	0.3	3.0	4.44	5.3	2.54	1.3	5.3	400	5.5	339	0.93	5.19	633	86.5
22	0.01	3	0	50	mid	10	2	38	30.4	29	4.9	0.3	3	4.4	16	2.6	1.3	16	400	5.5	339	0.92	5.54	627	85.6
23	0.01	0	12	50	mid	10	2	38	30.5	29	5	0.3	3	4.45	5.3	2.54	1.44	5.3	400	5.5	339	0.93	5.19	633	86.5
24	0.01	0	0	10	mid	10	2	37	38.4	28.6	5	0.32	3.2	4.5	5.3	2.8	1.31	5.3	400	5.5	374	0.87	5.6	593	80.9
25	0.01	0	0	50	low	10	2	38	30.5	29.2	5	0.3	3.0	4.44	5.3	2.54	1.3	5.3	400	5.5	339	0.93	5.19	633	86.5
26	0.01	0	0	50	mid	60	2	38	30.6	29.3	5	0.3	3.1	4.4	5.3	2.55	1.3	5.3	400	0.92	339	0.95	3.2	647	88.4
27	0.01	0	0	50	mid	10	4	38	30.5	29.2	5	0.3	3	4.44	5.3	2.54	1.3	5.3	200	5.5	339	0.93	5.18	634	86.5
28	0.01	0	45	50	mid	10	2	38	30.5	29.2	5	0.3	3	4.45	5.3	2.54	1.8	5.3	400	5.5	339	0.93	5.19	633	86.5
29	0.01	0	0	30	mid	10	2	37.8	31.4	29.1	5	0.3	3.04	4.45	5.3	2.58	1.3	5.3	400	5.5	345	0.93	5.19	633	86.5
30	0.01	0	0	50	up	10	2	37.9	30.8	29	5	0.3	3.03	4.45	5.3	2.6	1.3	5.3	400	5.5	339	0.93	5.19	633	86.5